

Fall 2005

# Glaciochemical records from the Saint Elias Mountains, Yukon, Canada

Kaplan B. Yalcin

*University of New Hampshire, Durham*

Follow this and additional works at: <https://scholars.unh.edu/dissertation>

---

## Recommended Citation

Yalcin, Kaplan B., "Glaciochemical records from the Saint Elias Mountains, Yukon, Canada" (2005). *Doctoral Dissertations*. 293.  
<https://scholars.unh.edu/dissertation/293>

This Dissertation is brought to you for free and open access by the Student Scholarship at University of New Hampshire Scholars' Repository. It has been accepted for inclusion in Doctoral Dissertations by an authorized administrator of University of New Hampshire Scholars' Repository. For more information, please contact [nicole.hentz@unh.edu](mailto:nicole.hentz@unh.edu).

GLACIOCHEMICAL RECORDS FROM THE ST. ELIAS MOUNTAINS,  
YUKON, CANADA

BY

KAPLAN B. YALCIN

B.S. with honors, University of Missouri, 1998

M.S., University of New Hampshire, 2001

DISSERTATION

Submitted to the University of New Hampshire

In Partial Fulfillment of

The Requirements for the Degree of

Doctor of Philosophy

in

Earth and Environmental Science

September 2005

UMI Number: 3183907

### INFORMATION TO USERS

The quality of this reproduction is dependent upon the quality of the copy submitted. Broken or indistinct print, colored or poor quality illustrations and photographs, print bleed-through, substandard margins, and improper alignment can adversely affect reproduction.

In the unlikely event that the author did not send a complete manuscript and there are missing pages, these will be noted. Also, if unauthorized copyright material had to be removed, a note will indicate the deletion.

**UMI**<sup>®</sup>

---

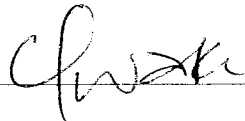
UMI Microform 3183907

Copyright 2005 by ProQuest Information and Learning Company.

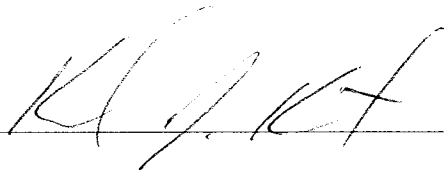
All rights reserved. This microform edition is protected against unauthorized copying under Title 17, United States Code.

ProQuest Information and Learning Company  
300 North Zeeb Road  
P.O. Box 1346  
Ann Arbor, MI 48106-1346

This dissertation has been examined and approved.



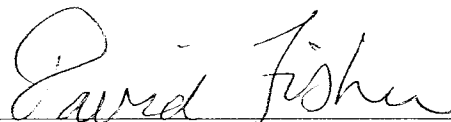
Dissertation Director, Dr. Cameron P. Wake  
Research Associate Professor of Earth Sciences and EOS  
University of New Hampshire



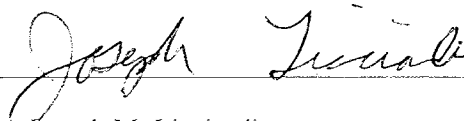
Dr. Karl J. Kreutz  
Assistant Professor of Geological Sciences and Quaternary Studies  
University of Maine



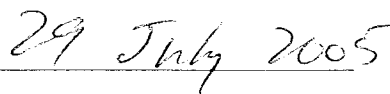
Dr. Jack E. Dibb  
Research Associate Professor of Earth Sciences and EOS  
University of New Hampshire



Dr. David A. Fisher  
Research Scientist  
Geological Survey of Canada



Dr. Joseph M. Licciardi  
Assistant Professor of Earth Sciences  
University of New Hampshire



Date

## ACKNOWLEDGMENTS

There are many people who made invaluable contributions to this project and who deserve my gratitude. First, I would like to thank Erik Blake for drilling the ice cores and the Geological Survey of Canada for logistical support. I am also grateful to Sarah Story and Zach Powers for help in processing the ice core and preparing the samples for analysis. I would also like to thank Sallie Whitlow for ion chromatograph analysis, Karl Kreutz and Doug Introne of the University of Maine for stable isotope analysis, and Mark Germani for electron microprobe analysis of tephra. My thesis advisor, Cameron Wake, has guided me through all stages of my studies at the University of New Hampshire; I would like to thank him for all the opportunities he has opened for me and for believing in my abilities. Committee members Karl Kreutz, Jack Dibb, David Fisher, and Joe Licciardi, as well as Gerry Holdsworth, Karen Von Damm, Fritz Koerner, Kumiko Azuma, Erich Osterberg, and Chris Zdanowicz have provided valuable discussion and input at all stages of the project; I thank all of you for your guidance and insight. Finally, I am indebted to my wife, Rebecca, whose patience and love gave me the drive to see this project through to completion. This research was supported by a grant from the National Science Foundation Office of Polar Programs. My first year at the University of New Hampshire was supported by a Department of Earth Sciences teaching assistantship, and my last year was supported by a Climate Change Research Center assistantship.

## TABLE OF CONTENTS

Acknowledgements.....	iii
List of Tables.....	viii
List of Figures.....	x
Abstract.....	xii

CHAPTER	PAGE
I. INTRODUCTION.....	1
Site Description and Regional Climatology.....	4
Previous Glaciochemical Investigation in the Saint Elias Mountains.....	6
Dissertation Objectives.....	12
II. METHODOLOGY.....	19
Ice Core Recovery.....	19
Major ion and Stable Isotope Analysis.....	20
Dating the Ice Core.....	21
Data Analysis and Interpretation.....	24
Glaciochemical Time Series.....	25

III.	SEASONAL AND SPATIAL VARIABILITY IN SNOW CHEMISTRY AT ECLIPSE ICEFIELD, YUKON, CANADA.....	40
	Abstract.....	40
	Introduction.....	41
	Methods.....	43
	Results and Discussion.....	45
	Snow chemical composition.....	45
	Sea-salt calculations.....	45
	Dependence on accumulation rate.....	47
	Seasonal variations.....	48
	Spatial variations.....	50
	Conclusions.....	52
	Acknowledgements.....	53
	References.....	63
IV.	AEROSOL, SNOW, AND FIRN CORE CHEMISTRY AT KING COL, MT. LOGAN MASSIF, YUKON, CANADA.....	66
	Abstract.....	66
	Introduction.....	68
	Methods.....	69
	Results and Discussion.....	72
	Characterization of King Col aerosol.....	72
	Temporal variations in aerosol concentrations.....	75
	Characterization of fresh and surface snow chemistry.....	78
	Relationships between aerosol and snow chemistry.....	79
	King Col snowpit and firn core chemistry.....	82

Concentrations and fluxes at King Col compared to Eclipse Icefield.....	84
Impact of 2001 Asian dust plume on St. Elias snow chemistry.....	85
Conclusions.....	87
Acknowledgements.....	88
References.....	95

V. A 1000-YEAR RECORD OF FOREST FIRE ACTIVITY FROM ECLISPE ICEFIELD,

YUKON, CANADA.....	100
Abstract.....	100
Introduction.....	101
Ice Core Analysis and Dating.....	104
Identification of Forest Fire Signals.....	106
Validation of the Record.....	108
Reconstruction of Fire Activity.....	110
Fire activity over the last 250 years.....	110
Fire activity over the last 1000 years.....	112
Conclusions.....	114
Acknowledgments.....	116
References.....	125

VI. ICE CORE PALEOVOLCANIC RECORDS FROM THE ST. ELIAS MOUNTAINS,

YUKON, CANADA.....	130
Abstract.....	130
Introduction.....	131
Ice Core Analysis and Dating.....	136
Identification of Volcanic Signals.....	138



Identification of Source Volcanoes.....	145
Correlation with known eruptions.....	145
Tephrochronological evidence.....	149
Climatic Implications.....	163
Conclusions.....	167
Acknowledgments.....	169
References.....	196
VII. ICE CORE EVIDENCE FOR A SECOND VOLCANIC ERUPTION AROUND 1809 IN THE NORTHERN HEMISPHERE.....	207
Abstract.....	207
Introduction.....	208
Evidence from Eclipse Icefield for a Second 1809 Eruption.....	209
Could Cosiguina be the Source of the 1809 Ice Core Tephra?.....	214
Could Eruptions of Cosiguina Affect Global Climate?.....	215
Was Cosiguina the Source of the 1809 Volcanic Signal?.....	217
Conclusions.....	221
Acknowledgments.....	222
References.....	230
VIII. CONCLUSIONS.....	235
Suggestions for Future Research.....	239
LIST OF REFERENCES.....	242

## LIST OF TABLES

Table II.1	Summary of Eclipse 2002 chemical analyses.....	29
Table III.1	Eclipse snowpit composition.....	51
Table III.2	Eclipse snowpit EOF analysis.....	55
Table IV.1	Summary of King Col aerosol composition.....	89
Table IV.2	King Col aerosol correlation matrix.....	89
Table IV.3	Summary of King Col snow composition.....	89
Table IV.4	King Col snow correlation matrix.....	90
Table IV.5	Scavenging ratios.....	90
Table IV.6	Comparison of Eclipse and King Col sites.....	90
Table IV.7	Annual average concentration and fluxes at Eclipse and King Col.....	91
Table IV.8	April 2001 Asian dust plume at King Col.....	91
Table V.1	Eclipse Core 3 EOF analysis.....	117
Table V.2	High fire years in Alaska and the Yukon.....	118
Table V.3	Percentage of high fire years recorded in Eclipse ice cores.....	119
Table VI.1	EOF analysis of Eclipse ice cores.....	170
Table VI.2	Threshold criteria for volcanic signals.....	171
Table VI.3	Mt. Logan EOF analysis.....	171
Table VI.4	Volcanic signals in Eclipse Core 1.....	172
Table VI.5	Volcanic signals in Eclipse Core 2.....	174
Table VI.6	Volcanic signals in Eclipse Core 3.....	178
Table VI.7	Volcanic signals in Mt. Logan Northwest Col ice core.....	180
Table VI.8	Correlation between volcanic sulfate flux records.....	181

Table VI.9	Summary of source volcanoes.....	181
Table VI.10	Twentieth century tephra-bearing layers in Eclipse ice cores.....	182
Table VI.11	Tephrochronology of Eclipse Core 2 ice core.....	184
Table VI.12	Instrumental temperature records.....	185
Table VII.1	Composition of 1809 ice core tephras.....	223
Table VII.2	Comparing 1809 ice core tephras using t-test.....	224
Table VII.3	Ice core volcanic sulfate fluxes from the 1809 eruption.....	225
Table VII.4	Volcanic activity between 1808 and 1810.....	226

## LIST OF FIGURES

Figure I.1	Circum- Arctic ice coring sites.....	16
Figure I.2	Ice coring sites in the St. Elias Mountains.....	17
Figure I.3	Vertical cross-section showing the Eclipse and Logan ice coring sites.....	18
Figure II.1	Annual layer thinning.....	30
Figure II.2	Eclipse Cs-137 profiles compared to Whitehorse aerosol samples.....	31
Figure II.3	Eclipse ice core percent melt.....	32
Figure II.4	Dating the Eclipse ice core via annual layer counting.....	33
Figure II.5	Depth-age relationship.....	34
Figure II.6	Reconstruction of layer thicknesses.....	35
Figure II.7	1000-year $\delta D$ time-series.....	36
Figure II.8	Eclipse $\delta D$ and accumulation time series.....	37
Figure II.9	Eclipse sea salt and dust time series.....	38
Figure II.10	Eclipse $K^+$ , $NH_4^+$ , $NO_3^-$ , and $SO_4^{2-}$ time series.....	39
Figure III.1	Location of Eclipse snowpits with respect to drill site.....	56
Figure III.2	Snowpit stratigraphy.....	57
Figure III.3	Glaciochemical parameters used in snowpit dating.....	58
Figure III.4	Box plot summary of snowpit chemical composition.....	59
Figure III.5	Annual mean concentration versus snow accumulation rate.....	60
Figure III.6	Annual flux versus snow accumulation rate.....	61
Figure III.7	Summary of chemical input seasonal timing.....	62
Figure IV.1	St. Elias location map.....	92
Figure IV.2	King Col aerosol and snow composition, May 17-June 11 2001.....	93

Figure IV.3	Back trajectories for aerosol concentration peaks.....	94
Figure V.1	Location of ice core sites.....	120
Figure V.2	Dating of the Eclipse ice cores.....	121
Figure V.3	Identification of forest fire signals.....	122
Figure V.4	Reconstruction of fire activity since 1750.....	123
Figure V.5	High fire activity in the Medieval Warm Period.....	124
Figure VI.1	Location of Eclipse Icefield with respect to North Pacific volcanic arcs.....	186
Figure VI.2	Eclipse Cs-137 profiles compared to Whitehorse aerosol samples .....	187
Figure VI.3	Seasonal signals in Eclipse ice cores.....	188
Figure VI.4	Identification of volcanic signals.....	189
Figure VI.5	Annual volcanic sulfate flux records.....	190
Figure VI.6	Chemical classification of 20 <sup>th</sup> century glass shards.....	191
Figure VI.7	Chemical classification of glass shards in Eclipse Core 2.....	192
Figure VI.8	Removal of ENSO influence on temperature.....	193
Figure VI.9	Instrumental temperature record.....	194
Figure VI.10	Volcanic temperature signals in Eclipse stable isotope records.....	195
Figure VII.1	Location of Eclipse, South Pole, and Dome C.....	227
Figure VII.2	Dating of Eclipse ice core, 1780-1820.....	228
Figure VII.3	Chemical classification of 1809 ice core tephras.....	229

## ABSTRACT

### GLACIOCHEMICAL RECORDS FROM THE ST. ELIAS MOUNTAINS, YUKON, CANADA

By

Kaplan B. Yalcin

University of New Hampshire, September 2005

While many paleoclimate records have been recovered from the North Atlantic sector of the Arctic, there is a gap in our understanding of climactic and environmental change in the North Pacific. Glaciochemical records from the St. Elias Mountains spanning an elevation range of three to five km provide a three-dimensional view of the paleo-atmosphere in this region. Three ice cores from Eclipse Icefield provide a high-resolution record of precipitation chemistry in the remote northwestern North America mid-troposphere and allow investigation of spatial and temporal variability in glaciochemical signals. Greater spatial variability is observed for species present as coarse mode dust and sea salt particles than for accumulation mode sulfate and ammonium aerosols or gas phase nitrate. Simultaneous sampling of aerosol and snow chemistry at King Col indicates large enrichments of nitrate and chloride in snow relative to aerosol by scavenging of gas phase nitric and hydrochloric acid. Back trajectories document the transport of Asian dust and anthropogenic emissions, the May 22 eruption plume of Sheveluch, Kamchatka, and sea salt from the Gulf of Alaska to King Col during the sampling period. The Eclipse ice cores provide a record of forest fire activity in Alaska and the Yukon that responds to

anthropogenic influences such as the Klondike Gold Rush and natural climate variability such as the Medieval Warm Period. The Eclipse and Mt. Logan ice cores offer a record of regionally significant volcanic eruptions, with at least one-third of the eruptions recorded from Alaskan and Kamchatkan volcanoes. Major tropical eruptions are also recorded. The three Eclipse cores record similar volcanic sulfate fluxes from the largest eruptions such as Katmai, as well as some moderate eruptions. While a bipolar volcanic signal in 1809 is generally attributed to single tropical eruption, dacitic tephra from the Eclipse ice core that is chemically distinct from andesitic 1809 tephra found in Antarctica indicates a second eruption in the Northern Hemisphere at this time. Sulfate flux calculations suggest this eruption contributed little additional sulfate to circum-Arctic ice cores, and therefore had negligible climatic significance.

## CHAPTER I

### INTRODUCTION

The Arctic represents one of the key regions on Earth in our efforts to document and understand global change. The sensitivity of the Arctic to climate perturbations (Houghton *et al.*, 1990; Wigley, 1995; Alley, 1997), model simulations predicting the Arctic to be a precursor to climate change elsewhere (Manabe *et al.*, 1991; Chapman and Walsh, 1993; Rind *et al.*, 1995), and the wealth of paleoenvironmental records available from this region justifies the prominent role the Arctic plays in global change research. Arctic climate feedbacks associated with surface albedo changes and freshwater runoff forcing of ocean thermohaline circulation have global ramifications (Curry *et al.*, 1995; Broecker, 1997). Once considered a pristine environment devoid of anthropogenic contamination and characterized by a relatively stable climate, recent research has revealed that the Arctic is neither chemically pristine nor climatically stable. The Arctic has experienced dramatic increases in a variety of industrial and agricultural contaminants since at least the early portion of this century (Koerner and Fisher, 1982; Barrie *et al.*, 1985; Mayewski *et al.*, 1986; Gregor *et al.*, 1995; Peters *et al.*, 1995; Goto-Azuma and Koerner, 2001). These contaminants are primarily transported to the Arctic from lower latitudes and include acidic species, heavy metals, organic pollutants, and trace gases. The threats (e.g., ecosystem toxicity, bioaccumulation) posed by these contaminants to humans and ecosystems within the Arctic are real and have serious consequences, especially for northern Aboriginal peoples (e.g., Jensen and Shearer, 1997, and references therein).

To further complicate matters the Arctic environment is experiencing changes in atmospheric and oceanic circulation related to natural climate variability or, potentially, to



anthropogenic greenhouse gas forcing (e.g., Huntington and Weller, 2005). These changes extend from the top of the atmosphere to below 1000 m depth in the ocean and include observations of decreased sea ice cover (Cavalieri *et al.*, 1997), a rise in the North Atlantic Oscillation atmospheric circulation index (Hurrell and van Loon, 1997; Ulbrich and Christoph, 1999), reduced formation of North Atlantic Deep Water (Hansen *et al.*, 2001), and strong warming of subpolar land areas in Alaska and northwest Canada, especially in winter and spring (Chapman and Walsh, 2003). Furthermore, the snow-ice albedo feedback mechanism plays a key role in the heat budget of the Arctic (Curry *et al.*, 1995), with decreased snow and ice cover serving to amplify Arctic temperature change over the last century compared to the global average (Huntington and Weller, 2005). Understanding our contemporary environment and predicting future change requires an understanding of changes in the past, providing not only the basis to investigate linkages between the physical climate system and different forcing factors, but also providing boundary conditions for testing and improving global circulation models.

Proxy records developed through physical and chemical analyses of ice cores arguably provide the highest resolution and most direct view of Earth's paleo-atmosphere over time scales ranging from decades to hundreds of thousands of years. The ice cores recovered in the early 1990s from the summit region of the Greenland ice sheet as part of the Greenland Ice Sheet Project 2 (GISP2) and Greenland Ice Core Project (GRIP) have set the standard for documenting changes in precipitation chemistry and climate because they provide a better dated and more detailed record of environmental change than was previously available (e.g., Alley *et al.*, 1993; Dansgaard *et al.*, 1993; Mayewski *et al.*, 1993 a, b; 1995; O'Brien *et al.*, 1995; Hammer *et al.*, 1997). However, no single ice core can provide a complete record of climate change in the Arctic. Documenting natural climate variability in the Arctic on annual to decadal scales, identifying the controls on climate change, determining the environmental response to these changes, and understanding the regional details of Arctic climate change are central themes in

national and international scientific research initiatives (ARCUS, 1993; PAGES, 1995; Ice Core Circum-Arctic Paleoclimate Program (ICCAPP); U.S. Global Change Research Program).

To date, most ice cores recovered from the Arctic basin have been from the North Atlantic sector. Ice core records are already available from sites throughout Greenland (e.g., Mayewski *et al.*, 1986; Hammer *et al.*, 1997; Fischer *et al.*, 1998; Moseley-Thompson *et al.*, 2001) as well as the Agassiz, Devon, and Penny Ice Caps in the eastern Canadian Arctic (e.g., Koerner *et al.*, 1999; Murphy, 2000; Fisher *et al.*, 1998). In the Eurasian Arctic ice cores have been recovered from Svalbard (e.g., Goto-Azuma *et al.*, 1995), Franz Josef Land (Kotlyakov *et al.*, 2004), Akademii Nauk (Fritzsche *et al.*, 2002), and the summit ice cap of Ushkovsky Volcano on the Kamchatka Peninsula (Shiraiwa *et al.*, 1997) (Figure I.1). In the North Pacific sector of the Arctic, ice core paleoclimate records are already available from the Northwest Col of Mt. Logan (Holdsworth *et al.*, 1984) and Eclipse Icefield (Yalcin and Wake, 2001) in the St. Elias Mountains, Yukon, Canada (Figure I.2). These sites, despite their proximity, provide distinct records because of the difference in elevation between the two sites, allowing them to sample different layers of the atmosphere (Figure I.3; Holdsworth *et al.*, 1988; Yalcin and Wake, 2001; Wake *et al.*, 2002; Yalcin *et al.*, 2003).

One means of improving our understanding of regional climate change in the Arctic is to develop a spatial network of ice core records from glaciers and ice caps throughout the Arctic basin. The acquisition of new ice core paleoclimate records from the North Pacific provides a new perspective on climate change in the Arctic that was previously unavailable. These cores will enable a more complete understanding of the altitudinal and temporal variability of climatic and environmental changes in the North Pacific sector of the Arctic. In addition, cores from this region will provide insight into past variability of climate modes such as the Pacific Decadal Oscillation and Pacific-North American Pattern. This insight is unavailable from the comparatively well studied North Atlantic sector of the Arctic, which is influenced by climate modes that characterize the North Atlantic region such as the North Atlantic Oscillation.

### Site Description and Regional Climatology

Bordering the eastern rim of the North Pacific Ocean, the St. Elias Mountains rise to elevations in excess of five km in just 60-180 km from the west coast of North America. In summer, the mountains act as a transition zone between the coastal maritime conditions and the adjacent continental regime to its east while in winter the range acts as a climatic divide separating maritime and polar regimes (Taylor-Barge, 1969). Temperatures are largely modified by the Pacific Ocean on the coastal side of the St. Elias Mountains, while the intra-annual range in temperatures is greater inland. Peak precipitation along the coast occurs in October, with a minimum in June. East of the St. Elias Mountains, precipitation peaks in July with a minimum in April. The west to east movement of cyclonic activity in the region, the orographic effect of the mountains, and convection on the Yukon plains in summer explains this variability. Due to their location, the St. Elias Mountains are under the influence of climate regimes that characterize the North Pacific such as the North Pacific Oscillation (Rogers, 1981; Hameed and Pittalwala, 1991); Pacific Decadal Oscillation (Mantua *et al.*, 1997), Pacific/North American (PNA) pattern (Wallace and Gutzler, 1981; Leathers *et al.*, 1991), and Arctic Oscillation (Thompson and Wallace, 1998). Teleconnections such as the El Nino-Southern Oscillation (ENSO) link regional climate to the climates of the tropics, allowing ice core records from the St. Elias Mountains to reflect climatic conditions in distant regions (Holdsworth *et al.*, 1992; Moore *et al.*, 2001).

Reconstructions of summer and annual temperature variations in the region are available using tree ring chronologies from interior northwest North America (Briffa *et al.*, 1992; D'Arrigo and Jacoby, 1993; Jacoby and D'Arrigo, 1995; Jacoby *et al.*, 1996; Davi *et al.*, 2003; D'Arrigo *et al.*, 2004), coastal Alaska (Wiles *et al.*, 1996; Barclay *et al.*, 1999), and the central Canadian Rockies (Luckman *et al.*, 1997). Records of glacier fluctuations in Alaska and the Canadian Rockies are also available (Wiles *et al.*, 1994, 1998; Calkin *et al.*, 2001). In general, these records show cool periods during the 17<sup>th</sup> and 19<sup>th</sup> centuries and a distinct warming trend beginning in the early 20<sup>th</sup> century, with the strongest warming over the subpolar land areas of

Alaska and northwest Canada. Aside from dramatic cooling in the early 1800s, Gulf of Alaska temperature reconstructions show little resemblance to proxy records from the interior, highlighting the differences between maritime and continental influences on these records. A wealth of new paleoclimatic and paleoenvironmental records has recently been developed from the North Pacific sector of the Arctic, complementing pre-existing records from the North Atlantic sector (Wake and Fisher, 2004).

Large changes in climate have occurred over the past century in northwest North America and elsewhere in the Arctic (Huntington and Weller, 2005). Arctic temperature trends (warming through the mid-1940s, cooling until the mid-1960s, and increasing thereafter) are similar to those observed elsewhere in the Northern Hemisphere, but decadal trends and interannual variability are larger in the Arctic. For example, the average rate of 20<sup>th</sup> century temperature increase is 50% greater north of 60° (0.09 °C per decade) than the global average (0.06 °C per decade). Temperature increases are largest in northwestern North America and Eurasia (exceeding 2°C per decade since the mid-1960s) and in winter and spring, though all seasons show a temperature increase. Precipitation has also increased in the Arctic, while the fraction falling as snow has decreased (Forland and Hanssen-Bauer, 2000; Groisman *et al.*, 2003).

A decrease in sea level pressure in the central Arctic (Walsh *et al.*, 1996) is associated with a positive shift in the Arctic Oscillation since 1970 (Moritz *et al.*, 2002). Model simulations suggest this shift is a response to increased radiative forcing from anthropogenic greenhouse gases (Shindell *et al.*, 1999, 2001; Gillett *et al.*, 2002). Arctic sea-ice extent has decreased by 2.4±0.4% per decade since the mid-1970s (Cavalieri *et al.*, 2003) while sea ice thickness has decreased by 42% (Rothrock *et al.*, 1999). Glaciers (Koerner and Lundgaard, 1995; Arendt *et al.*, 2002), snow cover (Brown, 2000), and permafrost (Nelson, 2003) have also diminished in response to increasing temperatures, while Arctic river discharge has increased (Shiklomanov *et al.*, 2000). Freshwater runoff pulses from increased melting of land ice in a warming Arctic can affect the North Atlantic thermohaline circulation (Belkin *et al.*, 1998). For example, increased

discharge from Arctic rivers during the 1990s is accompanied by a reduction in deepwater formation in the Greenland Sea (Boenisch *et al.*, 1997) and deep-water flow through the Faroe-Shetland Strait (Hansen *et al.*, 2001). Models project continued increases in Arctic temperature and precipitation and decreases in snow and sea ice cover through the 21<sup>st</sup> century (Huntington and Weller, 2005). Increased greenhouse gas concentrations will likely have a larger effect on Arctic climate than elsewhere on the globe (Huntington and Weller, 2005).

### **Previous Glaciochemical Investigations in the St. Elias Mountains**

A 103 m firn and ice core was recovered in 1980 from the Northwest Col (60.35<sup>0</sup> N, 140.30<sup>0</sup> W, 5340 m elevation) on the summit plateau of Mt. Logan (Figures I.1, I.2, and I.3; Holdsworth *et al.*, 1984). Average annual accumulation at this site is 0.3 m water equivalent per year. One of the most interesting features of the Northwest Col record is the absence of an anthropogenic increase in SO<sub>4</sub><sup>2-</sup> and NO<sub>3</sub><sup>-</sup> deposition (Holdsworth and Peake, 1985; Mayewski *et al.*, 1993c); an increase well documented not only in ice cores from Greenland and the eastern Canadian Arctic (Mayewski *et al.*, 1990; Koerner *et al.*, 1999; Goto-Azuma and Koerner, 2001) but also the nearby Eclipse ice core (Yalcin and Wake, 2001). This result suggests there is no detectable input of anthropogenic sulfate aerosols in glaciochemical records from the summit region of Mt. Logan (Monaghan and Holdsworth, 1990). Meanwhile, concentrations of carbon dioxide, methane, and nitrous oxide in bubbles extracted from the Northwest Col core show recent increases (Dibb *et al.*, 1993; Holdsworth *et al.*, 1996) comparable to ice cores from Greenland (Dansgaard and Oeschger, 1989; Dibb *et al.*, 1993) and Antarctica (Etheridge *et al.*, 1992; Machida *et al.*, 1995) due to fossil fuel burning and agricultural land clearing.

Records of episodic events important to the climate system such as volcanic eruptions and forest fires are also available using ice cores from the St. Elias Mountains. Volcanic eruptions are recorded in ice cores as large SO<sub>4</sub><sup>2-</sup> spikes above background levels independent of continental dust (Ca<sup>2+</sup>) or sea salt (Na<sup>+</sup>) deposition, sometimes accompanied by other volcanic

acids (such as HCl and HF) and volcanic glass shards (Herron, 1982; Zielinski *et al.*, 1994). A number of large  $\text{SO}_4^{2-}$  spikes are present in the Northwest Col record (Holdsworth and Peake, 1985; Holdsworth *et al.*, 1992); some of these are unique to the North Pacific region and are not reported in Greenland ice cores. These volcanic horizons have been investigated primarily with respect to their use as dating horizons in the Northwest Col record (Holdsworth *et al.*, 1992), a record of the atmospheric effects of volcanic eruptions has not yet been developed from the Northwest Col ice core.

Biomass burning events such as forest fires are documented in the Northwest Col record by  $\text{NH}_4^+$  concentration spikes that reflect the relative frequency of forest fires in northwest North America and Siberia (Whitlow *et al.*, 1994; Holdsworth *et al.*, 1996). In fact, forest fire plumes from fires burning in Alaska and the Yukon have been directly observed over the Mt. Logan region (Benjey; 1974; Holdsworth *et al.*, 1988). Forest fire plumes are chemically heterogeneous and depositional processes and post-depositional alteration can produce considerable spatial variability in glaciochemical signals. Consequently, there is not, nor should one expect, a one-to-one relationship between forest fire occurrence and ice core forest fire signals (Whitlow *et al.*, 1994). Furthermore, ice cores from different regions record forest fires in different areas; for example, Greenland ice cores preserve a record of the relative frequency of major forest fires in eastern North America (Legrand *et al.*, 1992; Whitlow *et al.*, 1994; Taylor *et al.*, 1996; Savarino and Legrand, 1998).

The oxygen isotope record from the Northwest Col does not cross correlate well with instrumental temperature records or most circum-Arctic paleoclimate records (Holdsworth and Peake, 1985; Holdsworth *et al.*, 1992; Fisher, 2002). Furthermore, the altitudinal variation of  $\delta^{18}\text{O}$  and  $\delta\text{D}$  in the Mt. Logan region and other areas of high relief exhibit a major discontinuity, or step, between 3 and 5 km (Holdsworth *et al.*, 1991; Holdsworth and Krouse, 2002). This step of nearly constant isotopic values separates a fractionation sequence below  $\sim 3$  km from a separate fractionation sequence above  $\sim 5$  km, suggesting two distinct moisture sources at upper and lower

altitudes separated by a mixed layer. This structure indicates the presence of a multi-layered atmosphere during synoptic precipitation, and prevents the interpretation of isotope time series from high elevation sites solely in terms of temperature (Holdsworth and Krouse, 2002).

The Northwest Col record, from an elevation equivalent to the 500-mbar level in the atmosphere, has proven to be uniquely situated for studies of tropospheric circulation and teleconnections. Enhanced dust transport to Mt. Logan, as indicated by ice core non-sea-salt  $Mg^{2+}$  concentrations, is tied to intensification of the Siberian High and Aleutian and Icelandic Lows during spring (Kang *et al.*, 2003). The Northwest Col accumulation time series has been found to strongly correlate with instrumental precipitation records from Japan (Holdsworth *et al.*, 1989) and with indices of the El Niño-Southern Oscillation (ENSO) on both interannual and interdecadal time scales (Moore *et al.*, 2001). The phase relation has shifted from out-of-phase prior to 1900 to in-phase through most of the 20<sup>th</sup> century, implying a nonstationary extratropical response to ENSO. Furthermore, an accelerating increase in accumulation at Mt. Logan since 1850 is observed, and is paralleled by recent warming over northwestern North America (Moore *et al.*, 2002). Over the last 50 years, the increase in accumulation at Mt. Logan is also correlated with an intensification of the Pacific North American (PNA) pattern and the Pacific Decadal Oscillation (PDO). In particular, winters of high accumulation on Mt. Logan are associated with an enhanced trough-ridge structure directing moisture laden air from tropical latitudes into the region (Rupper *et al.*, 2004).

To extend the glaciochemical record from Mt. Logan, the Geological Survey of Canada drilled a 178 m ice core to bedrock at Prospector-Russell Col (5340 m) on Mt. Logan during the 2001 and 2002 field seasons (Fisher *et al.*, 2004). Oxygen isotope analysis suggests the presence of Pleistocene ice in the bottom 3.5 m of the core, indicating that a complete Holocene record may be available from the Prospector-Russell ice core. A 3.5‰ shift at 1843 in the  $\delta^{18}O$  record from Prospector-Russell Col and a 1.6‰ shift in the same direction in the sediment record from nearby Jellybean Lake is associated with a transition from predominately zonal flow prior to 1843

to mixed zonal-meridional flow after 1843 (Fisher *et al.*, 2004). This transition has been interpreted as signaling the end of the Little Ice Age in the North Pacific region. A similar shift at 800 A.D. may mark the regional start of the Medieval Warm Period. Major ion analysis of the Prospector-Russell ice core at the University of Maine is expected to provide a Holocene history of high- elevation precipitation chemistry, including the last glacial-interglacial transition, the first such record from northwest North America.

A 160 m ice core was recovered from Eclipse Icefield (60.51 ° N, 139.47 ° W, 3017 m elevation), 45 km northeast of Mt. Logan (Figures I.1, I.2, and I.3), in the summer of 1996 using a new lightweight electromechanical drill (Blake *et al.*, 1998). The core was continuously sampled in 10 cm segments using clean techniques and analyzed for major ions ( $\text{Na}^+$ ,  $\text{NH}_4^+$ ,  $\text{K}^+$ ,  $\text{Mg}^{2+}$ ,  $\text{Ca}^{2+}$ ,  $\text{Cl}^-$ ,  $\text{NO}_3^-$ ,  $\text{SO}_4^{2-}$ ) with an ion chromatograph at the University of New Hampshire Climate Change Research Center and for oxygen isotopes at the Department of Geophysics, University of Copenhagen, Denmark (Yalcin and Wake, 2001). A section of the core from 50 m to 76 m depth was analyzed for beta activity. Analysis of the beta activity profile indicates that average annual accumulation from 1963 to 1996 was 1.38 meters water equivalent per year. Chronology of the Eclipse ice core is based on multi-parameter annual layer counting, the 1963 and 1961 beta activity reference horizons, and  $\text{SO}_4^{2-}$  reference horizons provided by volcanic eruptions, some of which are supported by major oxide analysis of associated tephra. The resulting time scale indicates that the Eclipse 1996 ice core covers the period 1894 to 1996, with dating error in the core estimated to be  $\pm 1$  year based on the number of independently dated horizons.

The sulfate and nitrate time-series from the Eclipse 1996 ice core provides, for the first time, a record of the anthropogenic influence on precipitation chemistry in the remote northwestern North American mid-troposphere over the last century, in contrast to ice core data from the summit plateau of Mt. Logan (Yalcin and Wake, 2001). The annual  $\text{SO}_4^{2-}$  flux at Eclipse began increasing in the late 1940s and reached peak levels in the 1980s. The  $\text{NO}_3^-$  flux also shows an increasing trend beginning in the late 1940s but peaks later than  $\text{SO}_4^{2-}$  and shows a



less pronounced decrease over the last two decades. Comparison of the Eclipse record with regional emission estimates for total sulfur and nitrogen oxides suggests that Eurasia is the dominant source of pollutants reaching Eclipse.

A preliminary trace metal analysis on the upper 40 m of the Eclipse 1996 ice core provides further evidence of a Eurasian pollution source at Eclipse (C. Wake, pers. comm.). A suite of trace metals were analyzed on 19 samples (each 2 m long) and four processing blanks on a Finnigan Element ICP-MS at Woods Hole Oceanographic Institute (WHOI). While the mean V concentration in the 4 blanks ( $0.14 \pm 0.01$  ppb) was similar to the mean concentration in the 19 samples ( $0.08 \pm 0.03$  ppb), Mn concentrations were significantly greater in the samples ( $1.7 \pm 0.6$  ppb) compared to the blanks ( $0.6 \pm 0.3$  ppb). Noncrustal Mn/V ratios average  $26 (\pm 3.4)$  ppb from 1960-1994. Previous work on trace metal tracers of Arctic haze (Rahn 1981a, b) has shown that an elevated noncrustal Mn/V ratio (i.e. greater than 2) is a tracer for a Eurasian pollution source. The anthropogenic impact on precipitation chemistry in the remote northwestern North America mid-troposphere recorded in the Eclipse ice core provides a historical perspective to contemporary observations of Arctic Haze at Barrow, Alaska and elsewhere in the Arctic.

The Eclipse 1996 ice core also provides a record of regionally significant volcanic eruptions in the North Pacific over the last century (Yalcin *et al.*, 2003). Non-sea-salt  $\text{SO}_4^{2-}$  residuals above a robust spline and an empirical orthogonal function decomposition were used to identify volcanic signatures that are mostly attributable to Alaskan, Aleutian, or Kamchatkan eruptions. Identification of the source volcano responsible for four of these signals is supported by major oxide analysis of associated tephra found in the Eclipse ice core that can be correlated to previously published analyses of tephra from suspected source volcanoes. Applying the same set of statistical analyses to the Northwest Col ice core demonstrates that many more volcanic events are recorded at Eclipse (32 events) than at nearby Mt. Logan (8 events) over the 86 year period of overlap between the two cores. Since most of the signals at Eclipse are attributable to moderate eruptions in the North Pacific, this result suggests that the Eclipse site provides a more sensitive

record of volcanic eruptions in Alaska and Kamchatka that affect primarily the regional troposphere than does the Mt. Logan site. The Eclipse 1996 record of annual volcanic sulfate flux provided by the EOF analysis was used to investigate the effect of volcanic sulfate on instrumental temperature records from the high northern latitudes in general and in the Gulf of Alaska region in particular, with the most pronounced negative temperature anomalies following the exceptionally large 1912 Katmai, Alaska eruption (Yalcin, 2001).

The high accumulation rate and well-detailed chronology of the Eclipse ice core are well suited for comparison of the glaciochemical record with instrumental time series of temperature, precipitation, and sea level pressure (Wake *et al.*, 2002). Results of cross correlation analysis of instrumental temperature records with the Eclipse  $\delta^{18}\text{O}$  time series reveals a significant positive relationship between summertime  $\delta^{18}\text{O}$  at Eclipse and summer (April-September) temperatures at both coastal and interior Alaskan sites. The results indicate that the Eclipse  $\delta^{18}\text{O}$  time series provides a better proxy for regional temperature than does the  $\delta^{18}\text{O}$  time series from Mt. Logan for which only negative correlations were found. However, temperatures recorded at lower-elevation meteorological sites explain on average only 10% of the variability in the Eclipse  $\delta^{18}\text{O}$  record. Summer accumulation at Eclipse is significantly correlated with summer precipitation only at the closest recording station (Haines Junction, Yukon), reflecting substantial regional variability in precipitation. The  $\delta^{18}\text{O}$ , accumulation, and glaciochemical time series also display significant correlations with the Northern Hemisphere sea level pressure data set, especially between annual variability in sulfate and nitrate deposition at Eclipse and the intensity of the wintertime Siberian High and Aleutian and Icelandic Lows. These results suggest that year-to-year variability in the deposition of pollutants at Eclipse can be linked to changes in atmospheric circulation while long-term trends can be explained by changes in source strength.

These findings illustrate that the Eclipse site samples a distinct air mass with different source regions and transport histories, resulting in a glaciochemical record complementary to, yet distinct from, that available from nearby Mt. Logan. This is illustrated by the presence of

anthropogenic sulfate and nitrate signals at Eclipse but not at Mt. Logan, the larger number of volcanic eruptions recorded at Eclipse relative to Mt. Logan, and the significant positive correlations between the Eclipse  $\delta^{18}\text{O}$  record and regional temperature records, while only negative correlations were found with the Mt. Logan  $\delta^{18}\text{O}$  record. This conclusion was also reached by Holdsworth *et al.* (1988) who collected snowpit samples and shallow cores from eight sites in the St. Elias Mountains spanning an elevation range from 1800 to 5630 m, including Eclipse Icefield. Events such as the 1986 Augustine, Alaska volcanic eruption, forest fires, and radioactive fallout from the Chernobyl nuclear power plant accident were observed at lower elevation sites such as Eclipse but were ambiguous or absent at high elevation sites on the Logan Plateau, illustrating that differences in site elevation result in distinct glaciochemical records.

### **Dissertation Objectives**

Two new ice cores, 345 m and 130 m in length, were recovered from Eclipse Icefield in the summer of 2002, along with a suite of samples from four 4 m snowpits. Snowpit and ice core samples have been analyzed for stable isotopes ( $\delta^{18}\text{O}$  and  $\delta\text{D}$ ) and major ions ( $\text{Na}^+$ ,  $\text{NH}_4^+$ ,  $\text{K}^+$ ,  $\text{Mg}^{2+}$ ,  $\text{Ca}^{2+}$ ,  $\text{Cl}^-$ ,  $\text{NO}_3^-$ ,  $\text{SO}_4^{2-}$ ,  $\text{C}_2\text{O}_4^{2-}$ ). In addition, select ice core sections have also been analyzed for  $^{137}\text{Cs}$  activity and volcanic glass composition. Full details of the analyses and methods employed are provided in Chapter II. The resulting database provides a continuous, high-resolution record of precipitation chemistry in the remote northwestern North America mid-troposphere that is used to address the following objectives:

1. Characterize the seasonal and spatial variability in snow chemistry at Eclipse Icefield (Chapter III). In order to fully utilize the glaciochemical records available from Eclipse Icefield, a robust understanding of the controls on snow chemical composition, seasonal input timing, and spatial variability in snow chemistry at the Eclipse site is needed. Snowpit sampling provides a useful tool to investigate these properties (e.g., Mayewski *et al.*, 1990; Kreutz *et al.*, 1999; Wake *et al.*, 2004), with the results potentially improving confidence in the use of ice cores in paleo-

environmental reconstructions. The results of 2002 snowpit survey at Eclipse Icefield allow the characterization of recent snow chemistry, identification of seasonal input timing, delineation of the relative contributions of sea salt versus non-sea-salt sources, and assessment of the spatial variability in glaciochemical signals at Eclipse.

2. Characterize the major ion chemistry of the aerosol, recent snow, and a shallow firn core at King Col (Chapter IV). In support of ice coring efforts on the summit plateau of Mt. Logan, an intermediate elevation climbing camp and research station was established at King Col (60.35° N, 140.36° W, 4135 m elevation; Figure I.2) on the Mt. Logan massif during the 2001 field season. From May 18 to June 11, twice daily aerosol and snow samples were collected. In addition, samples from a 3 m snowpit and a 12 m firn core were also collected. The resulting database provides the information needed to characterize the late spring-early summer aerosol at King Col, examine the relationships between aerosol and snow chemistry on an event basis, and compare major ion concentrations and fluxes at King Col to those at Eclipse Icefield.

3. Develop a record of forest fire activity in Alaska and the Yukon using the multiple ice cores available from Eclipse Icefield (Chapter V). The occurrence of fire in the boreal forest region is highly variable from year to year, responding largely to climatic variations in temperature and precipitation (Hess *et al.*, 2001; Kasischke *et al.*, 2002; Heyerdahl *et al.*, 2002). Boreal forest fires also have important implications for the global carbon cycle, atmospheric chemistry, regional air quality, and climate (Levine, 1991; Kasischke and Bruhwiler, 2003; DeBell *et al.*, 2004). The sensitivity of high northern latitudes to anticipated climatic changes over the 21<sup>st</sup> century is expected to result in a significant increase in forest fire activity in the boreal forest region due to higher summer temperatures and lengthened fire seasons (Wotton and Flannigan, 1993; Stocks *et al.*, 1998), making long-term records of boreal forest fire activity important for evaluating the response of boreal fire regimes to climatic change. The Eclipse ice cores document the response of Alaskan and Yukon fire regimes to natural and anthropogenic forcings, extending historical fire activity records available since 1940 and complementing

existing work on forest fire records from Mt. Logan and Greenland ice cores (Whitlow *et al.*, 1994, Taylor *et al.*, 1996; Savarino and Legrand, 1998).

4. Extend the ice core record of volcanism in the North Pacific beyond the 20<sup>th</sup> century and improve our understanding of the volcanic history of this region (Chapter VI). Previous work on a 160 m ice core recovered from Eclipse in 1996 has demonstrated that lower elevation sites in the St. Elias Mountains record both large and moderate sized eruptions in Alaska, the Aleutian Islands, and Kamchatka and that tephra from both Alaskan and Kamchatkan volcanoes can be identified in ice cores from the St. Elias Mountains (Yalcin *et al.*, 2003). The development of a longer ice-core-based paleovolcanic record for this region from Eclipse Icefield incorporating both volcanic acid ( $\text{SO}_4^{2-}$ , Cl) and volcanic glass characterization offers great potential for improving our understanding of the eruptive history of these very active and poorly-known regions. Furthermore, the availability of multiple ice cores from Eclipse Icefield enables assessment of the variability in volcanic signal preservation at Eclipse as well as the atmospheric sulfate loading and climatic impacts of individual eruptions such as the 1912 Katmai, Alaska eruption. A paleovolcanic record is also developed using the ice core recovered from the Northwest Col of Mt. Logan in 1980 and the results compared to the record from Eclipse Icefield.

5. Present evidence for a second volcanic eruption in the Northern Hemisphere in 1809 from Eclipse Icefield (Chapter VII). A large volcanic sulfate signal of unknown source is seen in ice cores from both polar regions six years prior to Tambora (e.g., Cole-Dai *et al.*, 1991), and may have contributed to strong cooling beginning before the Tambora eruption and culminating afterwards in the “year without a summer” in 1816 (e.g., Harrington, 1992). Identifying the source(s) of the 1809 eruption is an important priority for understanding the history of potential climate forcing volcanic eruptions (e.g., Zielinski, 2000). Recovery of dacitic tephra from the 1809 horizon in the Eclipse ice core with a chemical composition distinct from andesitic 1809 tephra found in Antarctic ice cores (Palais *et al.*, 1990) indicates a second eruption in the Northern Hemisphere at this time. The sulfate contribution from this eruption to the 1809

volcanic signal in circum-Arctic ice cores is examined to assess the atmospheric perturbation and possible climatic significance of this Northern Hemisphere eruption. Andesitic eruptions thought to have taken place from tropical volcanoes between 1808 and 1810 are also examined in an attempt to identify the source volcano responsible for the bipolar 1809 volcanic signal.

These objectives are addressed in this dissertation as five chapters written for publication in peer-reviewed journals as outlined above. These chapters, together with the introduction presented here (Chapter I), the following methods section (Chapter II), and a concluding summary with suggestions for future research (Chapter VIII) constitute this dissertation. The data from Eclipse Icefield will also contribute to the growing suite of ice core records from the St. Elias Mountains spanning an elevation range from 3017 to 5340 m (Figure I.2). These include cores drilled at Prospector-Russell Col (5340 m) and King Col (4135) on Mount Logan (Goto-Azuma *et al.*, 2003; Fisher *et al.*, 2004), as well from the saddle (4400 m) between Mt. Bona and Mt. Churchill (Thompson *et al.*, 2004) and the summit ice cap (4100 m) of Mt. Wrangell (Kanamori *et al.*, 2004). These records will define vertical gradients in precipitation chemistry (e.g., Holdsworth *et al.*, 1991) and the implications for atmospheric structure and dynamics (e.g., Holdsworth and Krouse, 2002); allowing more complete interpretation of the glaciochemical time-series from all three sites and offering an unprecedented opportunity to construct a three-dimensional view of the paleo-atmosphere in the North Pacific region. This represents an area of continuing collaborative research beyond the scope of this dissertation. The Eclipse data will be made available on the NOAA paleoclimatology web site to facilitate continued collaborative research on North Pacific climate variability.

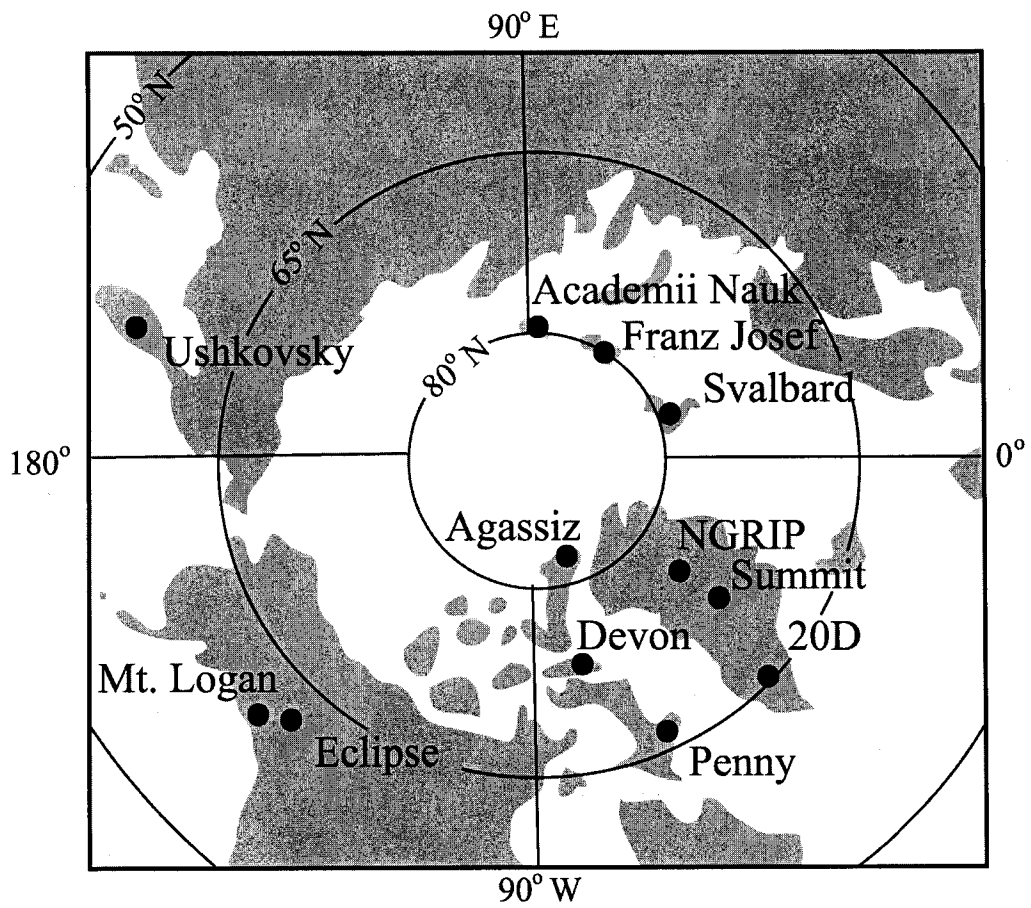


**Figure I.1.** Location of circum- Arctic ice coring sites.

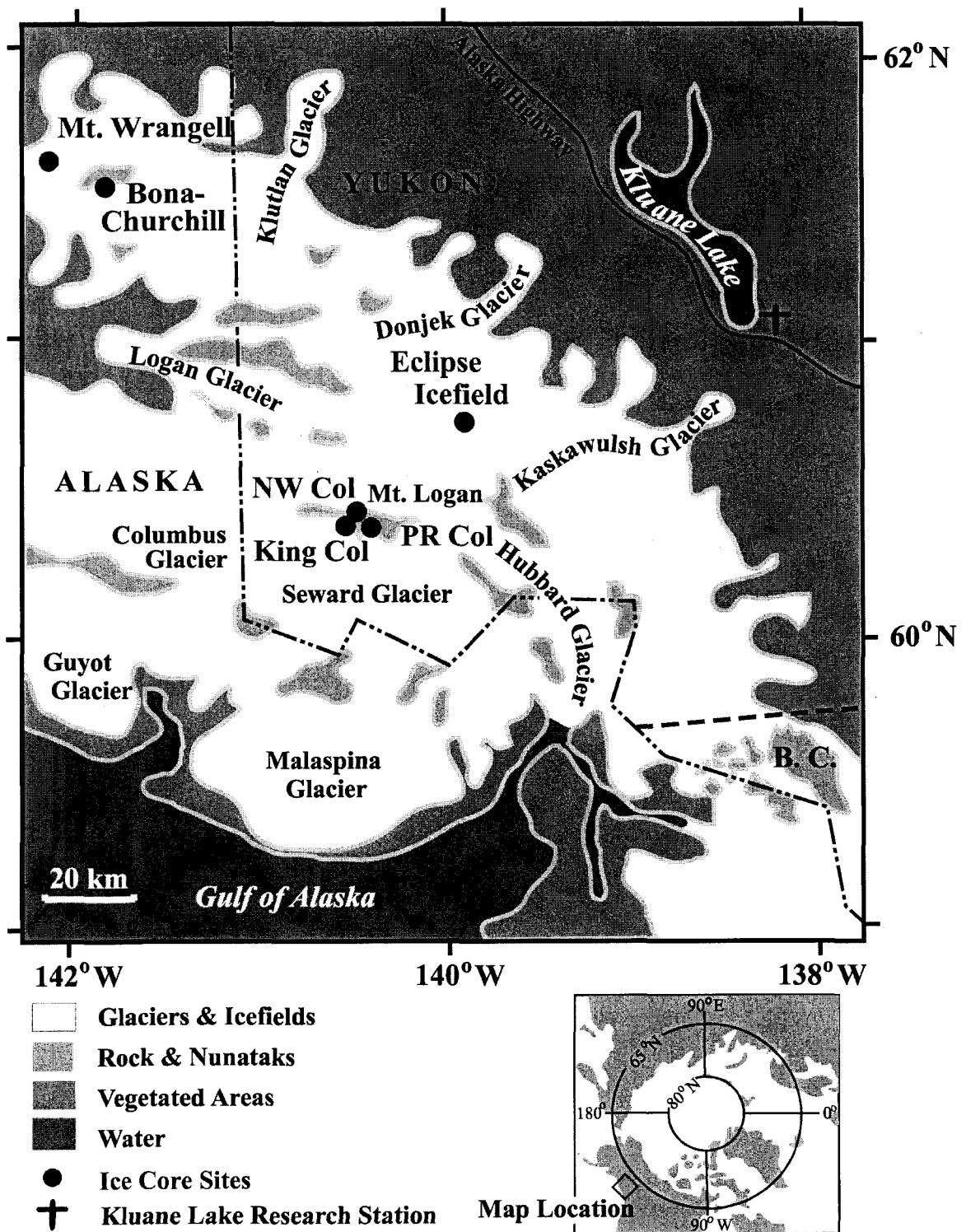


**Figure 1.2.** Eclipse Icefield is located at  $60.51^{\circ}$  N,  $139.47^{\circ}$  W, 3017 m elevation in the St. Elias Mountains, Yukon, Canada; 45 km northeast of Mt. Logan. Also shown are the ice core sites at Northwest Col (5340), Prospector-Russell Col (5340 m), King Col (4135 m), Bona-Churchill (4400 m) and Mt. Wrangell (4100 m).



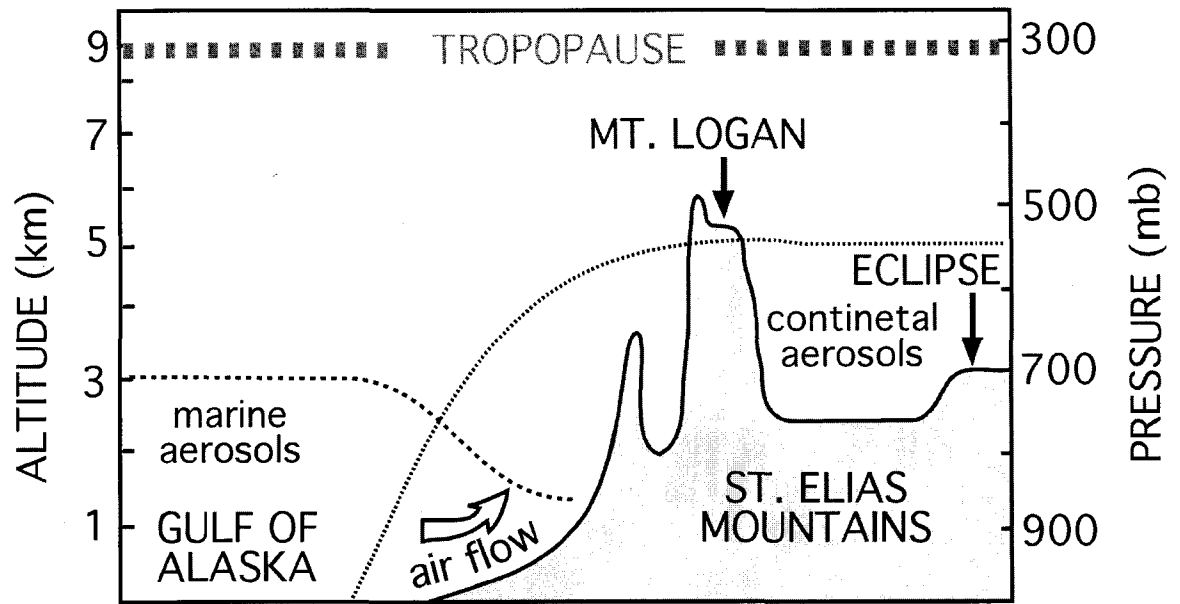


**Figure I.3.** Vertical cross section through the St. Elias Mountains showing the ice coring sites on Mt. Logan (Northwest and Prospector- Russell Cols), and Eclipse Icefield. Also shown are the principal domains of marine and continental aerosols. After Holdsworth *et al.*, 1992.

## CHAPTER II

### METHODOLOGY

#### Ice Core Recovery

Two ice cores 345 m (Core 2) and 130 m (Core 3) in length were collected from Eclipse Icefield in the summer of 2002 using the field portable ECLIPSE ice drill (Blake *et al.*, 1998). The Geological Survey of Canada's ultra-clean titanium drill barrel ("Clean Simon") was used to recover the top 60 m of the 345 m core for ultra clean trace metal analyses, but problems were encountered with auger advance and core quality. The ultra-clean barrel and head made of titanium and carbide was successfully tested on Devon Island, Nunavut in 1998 (Zheng, 2000). The core is drilled directly into a pre-cleaned high-density polyethylene (HDPE) sleeve that is capped when extracted from the core barrel. The sealed HDPE tube then serves as a transport tube, thereby minimizing core handling and exposure. The remainder of the cores was recovered using a conventional stainless steel ice auger and packaged in sealed polyethylene bags. The cores were packed in insulated shipping containers and stored in snow caves. A fixed-wing aircraft was used to evacuate the core directly from the field to freezer trucks at Kluane Lake for shipment to the freezers at the University of New Hampshire. During the drilling season, fresh snow, surface snow, and snowpit samples for major ion and stable isotope analysis were collected from four 4 m snowpits to investigate seasonal signals and spatial variability in all of the chemical species measured in the Eclipse ice cores.

### **Major Ion and Stable Isotope Analysis**

The Eclipse ice cores have been sampled continuously at high resolution for major ions and stable isotopes to establish a detailed chronology for the core. A sampling resolution of 10-15 cm was used for Core 2 from 0-200 m water equivalent (w.e.) depth and all of Core 3, yielding approximately eight samples per year. Annual layer thinning (Figure II.1) required resampling of the lower third of Core 2 at higher resolutions (beginning at 6 cm per sample at 200 m w.e. and decreasing to 2 cm per sample by 254 m w.e. depth) to obtain an annually dated record to 1450 A.D. This portion of the core was resampled continuously for stable isotopes and around select high sulfate horizons for major ions.

Ice core processing was performed in a freezer at the UNH Climate Change Research Center (CCRC) using established techniques for ultra-clean sample preparation. The top 60 m of Core 2 drilled with Clean Simon was sampled at the University of Maine Climate Change Institute. Prior to core sampling, a description of the visible stratigraphy (the location and thickness of ice layers) and density measurements were made on each of the approximately one-meter core sections. Above the firn-ice transition which occurs at 45 m depth, core was scraped on an acrylic lathe system under a laminar flow bench using a titanium scraper so that all surface and sub-surface contamination from the drilling process was removed. Below the firn-ice transition, samples were cut into 3 x 3 cm pieces 10 cm long and the middle of the samples melted out using a custom made melter used to sample the GISP2, Penny, Devon, and Eclipse 1996 ice cores. Blanks (artificial core made by freezing 18m $\Omega$  Milli-Q water) were processed frequently in the same manner as the core to ensure samples are uncontaminated by core processing. All samples were placed in LDPE bottles cleaned by successive soaking and rinsing in 18m $\Omega$  Milli-Q water. Sample aliquots (5 ml) were taken for major ion and stable isotope analysis. The remaining sample volume was archived for future measurements.

Samples were analyzed for major ions ( $\text{Na}^+$ ,  $\text{NH}_4^+$ ,  $\text{K}^+$ ,  $\text{Mg}^{2+}$ ,  $\text{Ca}^{2+}$ ,  $\text{Cl}^-$ ,  $\text{NO}_3^-$ ,  $\text{SO}_4^{2-}$ ,  $\text{C}_2\text{O}_4^{2-}$ ) via ion chromatography using a 0.5 ml sample loop in a dedicated laboratory at the Climate Change Research Center. The cation system used a CS12A column with CSRS-ultra suppressor in auto suppression recycle mode with 20 mM MSA eluent. The anion system used an AS11 column with an ASRS-ultra suppressor in auto suppression recycle mode with 6 mM NaOH eluent. Analytical precision was monitored by analyzing 10% of the samples in duplicate and found to be 11% for  $\text{K}^+$ , 10% for  $\text{NH}_4^+$ , 7% for  $\text{Na}^+$ , and less than 5% for all other species. Stable isotope samples were analyzed at the University of Maine Stable Isotope Laboratory with a Multiprep  $\text{CO}_2$  equilibration system coupled to a VG SIRA mass spectrometer for  $\delta^{18}\text{O}$  (precision  $\pm 0.05\text{‰}$ ) and a Eurovector Cr pyrolysis unit coupled to a GV Isoprime mass spectrometer for  $\delta\text{D}$  (precision  $\pm 0.5\text{‰}$ ).

### **Dating the Ice Core**

The depth-age relationship for the Eclipse core was developed using multi-parameter annual layer counting of seasonal oscillations in the  $\delta^{18}\text{O}$  and major ion records (e.g., Yalcin, 2001) and verified by identification of  $^{137}\text{Cs}$  peaks from atmospheric thermonuclear weapons testing and  $\text{SO}_4^{2-}$  reference horizons from volcanic eruptions (Zielinski *et al.*, 1994; Yalcin *et al.*, 2003). Samples for radionuclide analysis were collected from the outside of the core, and then melted, acidified with 0.33 ml HCl per kg, and gravity filtered twice through cation exchange filters (MN 616-LSA-50, Macherey-Nagel, Germany). Radionuclide concentrations ( $^{137}\text{Cs}$ ) were determined by non-destructive gamma spectrometry using a Canberra gamma spectrometer with a germanium well detector and multi-channel analyzer (Dibb, 1989). The radionuclide concentration profiles were dated by comparison to real-time aerosol samples from Whitehorse, Yukon (Holdsworth *et al.*, 1984). The 130 and 345 m ice cores show nearly identical  $^{137}\text{Cs}$  profiles, with clear identification of the 1963 and 1961 radionuclide peaks from atmospheric

thermonuclear weapons testing (Figure II.2). Radioactive fallout from the 1986 Chernobyl nuclear power plant explosion was also detected, providing an additional stratigraphic marker. Average annual accumulation from 1963 to 2002 was 1.30 m water equivalent, which compares favorably to the value of 1.38 m water equivalent determined for the Eclipse 1996 core (Core 1) for the period 1996 to 1963.

The presence of discrete ice layers in the Eclipse ice cores demonstrate that a limited amount of surface melting occurs at the Eclipse site during summer. These discrete ice layers average less than 5% of the total net accumulation by weight in the Eclipse ice cores prior to 1960 (Figure II.3). Meltwater percolation does not significantly alter the glaciochemical records available from the Eclipse ice core as evidenced by the preservation of clear seasonal signals in the major ion and oxygen isotope records, allowing dating of the core via annual layer counting (Yalcin and Wake, 2001). Annual layers were delineated by seasonal oscillations in the stable isotope and major ion records from the Eclipse ice cores (Figure II.4). Sodium shows the most consistent seasonal oscillation of the major ion species, although seasonal signals in the  $\text{NH}_4^+$ ,  $\text{NO}_3^-$ ,  $\text{SO}_4^{2-}$ ,  $\text{Ca}^{2+}$ , and  $\text{Mg}^{2+}$  records can also be used to count annual layers except where episodic events such as forest fires, volcanic eruptions, and dust storms overwhelm the seasonal signal. Despite layer thinning, high resolution sampling permits annual layer counting in the stable isotope records as far back as 1450 A.D.

The annual cycle of  $\delta^{18}\text{O}$  maxima in summer precipitation and  $\delta^{18}\text{O}$  minima in winter precipitation observed at Eclipse and other ice core sites is related at least in part to the temperature at which evaporation and condensation occurs (Dansgaard *et al.*, 1973). The annual cycle of  $\text{Na}^+$  concentration maxima in winter and minima in summer is related to pronounced seasonal changes in the influx of marine aerosols (e.g., Whitlow *et al.*, 1992). Increased storminess in the Gulf of Alaska during winter results in higher wind speeds, enhanced entrainment of sea salt aerosols, and more frequent advection of marine air masses into the St. Elias Mountains; producing the observed winter peaks in  $\text{Na}^+$  concentrations.

Age control on the chronology established via annual layer counting is provided by the 1986, 1963, and 1961  $^{137}\text{Cs}$  reference horizons as well as volcanic reference horizons developed through statistical analysis of the high-resolution  $\text{SO}_4^{2-}$  record (Zielinski *et al.*, 1994; Yalcin *et al.*, 2003). Identification of high  $\text{SO}_4^{2-}$  horizons from major volcanic eruptions such as the 1912 Katmai, 1815 Tambora, 1783 Laki, and 1453 Kuwae eruptions provides additional age control for the ice core chronology. Additional volcanic reference horizons such as Redoubt 1989, Hekla 1947, and Ksudach 1907 were developed by tephrochronology. Tephra associated with volcanic  $\text{SO}_4^{2-}$  horizons was collected by filtering of melt water through a 0.2-micron polycarbonate membrane filter. Visual inspection of filters under a microscope suggested a significant number of volcanic glass particles on about 10% of the filters. Individual volcanic glass shards from these filters were analyzed for major oxide composition using an automated scanning electron microscope (SEM; Hitachi S-570) at Micromaterials Research (Germani and Buseck, 1991). Individual particles greater than 4 micrometers with glass shard morphology were selected for x-ray microanalysis of major oxide composition because analyzing larger particles minimizes the effect of particle size and shape on quantitative x-ray microanalysis.

In summary, the Eclipse 2002 ice cores have been analyzed continuously for major ions and stable isotopes and along select sections for  $\text{Cs}^{137}$  activity and volcanic glass composition (Table II.1). The chronology of the Eclipse ice cores is based on the counting of annual layers delineated by summer maxima in  $\delta^{18}\text{O}$  and  $\delta\text{D}$  and winter maxima in  $\text{Na}^+$  concentrations. Age control on the chronology established via annual layer counting is provided by the 1986, 1963 and 1961  $^{137}\text{Cs}$  reference horizons as well as volcanic reference horizons (e.g., Katmai 1912; Tambora 1815; Laki 1783, Kuwae 1453) developed through statistical analysis of the high-resolution  $\text{SO}_4^{2-}$  record. In some cases these identifications have been independently verified using tephrochronology. Dating error is estimated based on the number of independently dated reference horizons (radioactivity, volcanic eruptions), and ranges from  $\pm 1$  year between 2002 and 1912 and between 1815 and 1783,  $\pm 2$  years between 1912 and 1815, and up to  $\pm 5$  years (1%)

between 1783 and 1453 due to the lack of independently dated horizons in this interval. Below 1450, chronology is an extension of a polynomial fit to absolutely dated horizons (Figure II.5). It should be noted that this fit is “floating” at its lower end and not constrained by any independently dated horizons prior to Kuwae. Hence, dating error is estimated to progressively increase from 1450 ( $\pm 1\%$ ) to the bottom of the core ( $\pm 10\%$ ).

Annual layers become progressively thinner with depth in the Eclipse ice cores (Figure II.1), requiring reconstruction of original annual layer thicknesses by correcting for ice creep. An empirical approach was used that is based on the observed layer thicknesses from annual layer counting of the Eclipse ice cores because no ice flow or strain rate measurements were made on the Eclipse boreholes, and radar soundings of the ice thickness suggested bedrock should have been reached around 320 m but had not been reached when drilling was stopped at 345 m, which was the limit of the drill cable length. Assuming a constant accumulation rate from identification of the 1963 radioactivity maximum of 1.38 and 1.30 m water equivalent for the 1996 and 2002 cores, respectively, and no creep deformation in the firm section of the cores, we calculated a decompression ratio for each annual layer from a smoothed fit to the observed layer thicknesses (Holdsworth *et al.*, 1992). This ratio was then applied to the observed thickness of each annual layer to reconstruct the original thickness (Figure II.6).

### **Data Analysis and Interpretation**

The evaluation and interpretation of glaciochemical records such as that developed from the Eclipse ice core are complicated by three principle factors. First, there are multiple sources for individual species. For example,  $\text{SO}_4^{2-}$  sources include anthropogenic emissions, volcanic eruptions, oxidation of biogenic reduced gases, sea spray, crustal dust, and evaporate deposits. Second, temporal variability in the accumulation rate and layer thinning with depth results in non-uniform sampling. Third, a combination of non-stationary atmospheric circulation systems and other variable features of the climate system control concentrations of the individual species.

Because the multi-parameter techniques used in the development of the Eclipse glaciochemical record ( $\text{Na}^+$ ,  $\text{NH}_4^+$ ,  $\text{K}^+$ ,  $\text{Mg}^{2+}$ ,  $\text{Ca}^{2+}$ ,  $\text{Cl}^-$ ,  $\text{NO}_3^-$ ,  $\text{SO}_4^{2-}$ ) measure the bulk of the soluble impurities in glacial ice with high temporal resolution, statistical techniques can be used to differentiate sources and transport trajectories by chemical associations and describe a large proportion of the variance in individual time series (e.g., Mayewski *et al.*, 1993 a, b; Meeker *et al.*, 1995; Hammer *et al.*, 1997). Robust smoothing is used to identify trends in background levels; such trends identify changes in circulation patterns, transport efficiency, or source strength. Outlier identification allows separation of volcanic and forest fire signals and identification of individual events. Spectral analysis is used to identify cycles in seasonal and annual loading of dust or sea salt species that can be related to circulation patterns or source strength. Empirical orthogonal function analysis is used to describe the common variance in the ion records; correlation of the ion records is used to identify chemical associations and differences in input timing. These statistical tools allow detailed interpretation of high-resolution, multi-parameter glaciochemical records such as that developed from the Eclipse ice cores.

### **Glaciochemical Time Series**

Annually-averaged time-series of  $\delta\text{D}$ , major ions, and accumulation in Eclipse 2002 Core 2 are presented in Figures II.7 to II.10. Chronology is based on annual layer counting from 1450 to 2002 and verified by independently dated reference horizons (radionuclides, volcanic eruptions). Below 1450, chronology is an extension of a polynomial fit to absolutely dated horizons (1453, 1783, 1912, 1963, etc.) that accounts for annual layer thinning (Figure II.5). It should be noted that this fit is “floating” at its lower end and not constrained by any independently dated horizons prior to Kuwae. Hence, dating error progressively increases from 1450, where dating error is  $\pm 1\%$ , to the bottom of the core, where dating error could be as much as  $\pm 10\%$ . Because annual layers are not resolved prior to 1450, annual accumulations have not been determined for this section of the core. Furthermore, annual averages of species with strong



seasonal variations such as  $\delta D$  are not reliable below 1450 because the core is not annually dated. Instead, annual averages over this interval represent mathematical resampling of the original time series at a constant resolution of one year. Biannual samples are presented for the 1000-year  $\delta D$  time-series in Figure II.7 to minimize seasonal fluctuations. Annualized time series in Figures II.8-II.10 have also been smoothed with a robust spline (tension parameter set to 0.2 resulting in an 85% smooth) to highlight interdecadal variability. A spectral analysis of the uniformly resampled time series with modified Daniell smoothings was used to explore periodicities in the records; all spectral peaks quoted are significant at the 99% level as determined by random noise simulations.

The 1000-year  $\delta D$  time-series shows a “normal” Little Ice Age with more negative  $\delta D$  values (Figure II.7). However, the Little Ice Age period suggested by the  $\delta D$  time series lasts from about 1250 to 1920, somewhat longer than the more frequently quoted dates of 1400 to 1850. The earlier date is in agreement with records of glacier fluctuations in Alaska that show the earliest Little Ice Age advance was centered around 1250 (e.g., Wiles *et al.*, 2004). There is also a tendency towards less negative values in the 20<sup>th</sup> century, especially after about 1920, possibly reflecting 20<sup>th</sup> century warming in the region. The interannual variability post-1450 (Figure II.8) is typically within 30‰ but approaches 40‰ in some sections. A number of interdecadal variations on the order of 5-10‰ are apparent in the record. Spectral analysis shows power in the  $\delta D$  time series at 4 and 11 years. The 11 year periodicity is also seen in Summit, Greenland stable isotope records and could be related to the 11 year sunspot cycle (White *et al.*, 1996). The accumulation time-series (Figure II.8, bottom) also shows a number of interdecadal shifts. The periods of highest annual accumulation are seen from 1470-1500 and 1540-1560. Other intervals of generally higher accumulation are noted from 1560-1680, 1780-1875, and 1925-1975. Periods of low accumulation are observed between 1500-1540, 1680-1780, and 1875-1925. The strongest multi-year drop in accumulation is seen between 1979 and 1984, although there are isolated years

with lower accumulation. It is possible that this drop in accumulation is related to the 1977 regime shift in the Pacific Decadal Oscillation (Mantua *et al.*, 1997), although a causal link has not been established. It is noteworthy that the Eclipse accumulation time series is out of phase with the accumulation time series from Mount Logan on all time scales. Spectral analysis of the Eclipse accumulation time series shows power at 4, 6, 8, 14, and 203 years, though the length of the record limits the significance of the 203 year cycle.

Species associated with sea salt ( $\text{Na}^+$ ,  $\text{Cl}^-$ ) and dust ( $\text{Mg}^{2+}$ ,  $\text{Ca}^{2+}$ ) show greater interannual variability post-1300 and especially post-1400 (Figure II.9). Interannual variability is comparatively subdued between 1000 and 1300, except for higher and more variable  $\text{Cl}^-$  concentrations between 1050 and 1150. Interestingly, this interval is not readily apparent in the  $\text{Na}^+$  record. Interannual variability in sea salt species is less after 1880 and especially after 1940, while variability in dust species remains high. An increase in the  $\text{Na}^+$ ,  $\text{Mg}^{2+}$ , and  $\text{Ca}^{2+}$  baseline over time is observed, while the  $\text{Cl}^-$  record shows no clear trend. For  $\text{Na}^+$ , the increase in interannual variability takes place in two steps, the first around 1250 and the second around 1400. The  $\text{Mg}^{2+}$  and  $\text{Ca}^{2+}$  data show a ramped increase between 1250 and 1400, rather than a two-step shift. The increase in major ion concentrations, especially  $\text{Na}^+$ , at 1400 has been attributed to a strengthening of atmospheric circulation during the Little Ice Age (O'Brien *et al.*, 1995; Kreutz *et al.*, 1997). The timing of the increased interannual variability in the Eclipse sea salt and dust records at 1400 is consistent with the onset of Little Ice Age conditions in the GISP2 and Siple Dome ice cores, however, the shift is not as abrupt at Eclipse. The volcanic  $\text{Cl}^-$  deposition from the 1912 Katmai eruption is readily apparent in annual concentration data as the largest  $\text{Cl}^-$  event to affect the St. Elias Mountains in the last 1000 years. All four species show spectral power at 8 years, while the dust species ( $\text{Ca}^{2+}$ ,  $\text{Mg}^{2+}$ ) also show power at 72 and 130 years.

There is little interannual variability in the  $\text{K}^+$  series, with annual average concentrations less than  $0.1 \text{ ueq l}^{-1}$ , with the exception of about ten outliers (Figure II.10). The  $\text{NH}_4^+$  record shows a number of large spikes that are interpreted as originating from forest fire events. Most of

these events are clustered between 1240 and 1410. Spectral power in the  $\text{NH}_4^+$  time series is seen at 20 and 28 years. The  $\text{NO}_3^-$  time series shows a well-defined anthropogenic increase beginning in the 1940s. The beginning of a return to pre-industrial  $\text{NO}_3^-$  levels is suggested in the last five years of the record. A number of  $\text{NO}_3^-$  concentration peaks are observed around 1400 which are coincident with  $\text{NH}_4^+$  peaks and could also represent forest fire events. Spectral power in the  $\text{NO}_3^-$  time series is observed at 5 years and  $\sim 150$  years. An anthropogenic increase is not as convincing in the  $\text{SO}_4^{2-}$  time series, and is more prominent when annual  $\text{SO}_4^{2-}$  flux data from non-sea-salt and non-volcanic sources is considered. Higher and more variable  $\text{SO}_4^{2-}$  concentrations between 1050 and 1150 are synchronous with a similar shift in  $\text{Cl}^-$  concentrations. A number of large  $\text{SO}_4^{2-}$  spikes from volcanic eruptions are observed; some of the more prominent events are labeled. Spectral power in the  $\text{SO}_4^{2-}$  time-series is seen at 7, 10, and  $\sim 150$  years. The latter periodicity is also evident from the  $\text{NO}_3^-$  time-series.

**Table II.1.** Summary of Eclipse 2002 chemical analyses.

Analysis	Species	Analysis Method	Samples Analyzed	
			Core 2	Core 3
major ions	Na <sup>+</sup> , NH <sub>4</sub> <sup>+</sup> , K <sup>+</sup> , Mg <sup>2+</sup> , Ca <sup>2+</sup> , Cl <sup>-</sup> , NO <sub>3</sub> <sup>-</sup> , SO <sub>4</sub> <sup>2-</sup>	ion chromatography	2764	1052
stable isotopes	δ <sup>18</sup> O and δD	mass spectrometry	4871	1052
radioactivity	<sup>137</sup> Cs	gamma spectrometry	17	45
volcanic glass	SiO <sub>2</sub> , TiO <sub>2</sub> , Al <sub>2</sub> O <sub>3</sub> , Fe <sub>2</sub> O <sub>3</sub> , MgO, CaO, Na <sub>2</sub> O, K <sub>2</sub> O	electron microprobe	7	4

(n) Total number of samples analyzed.

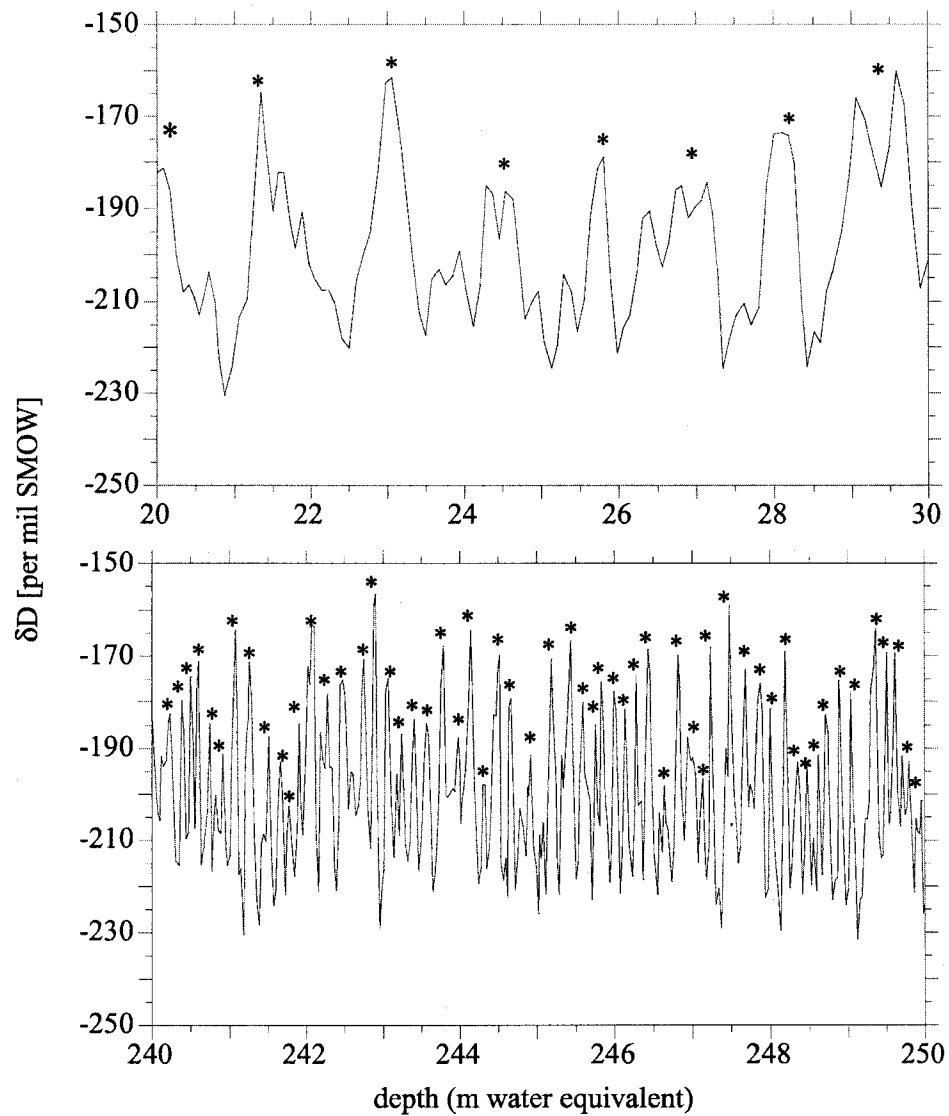


**Figure II.1.** Plots of  $\delta D$  versus water equivalent depth for two 10 m depth ranges in Core 2 illustrate thinning of annual layers with depth. Summers are marked on the  $\delta D$  curve by asterisks. Above the firn-ice transition (e.g., 20-30 m w.e. depth), where annual layer thicknesses are unaffected by layer thinning, annual layers are about 1.3 m thick. Layers get progressively thinner with depth below the firn-ice transition. Between 240-250 m w.e. depth, annual layer thicknesses average 0.15 m thick.

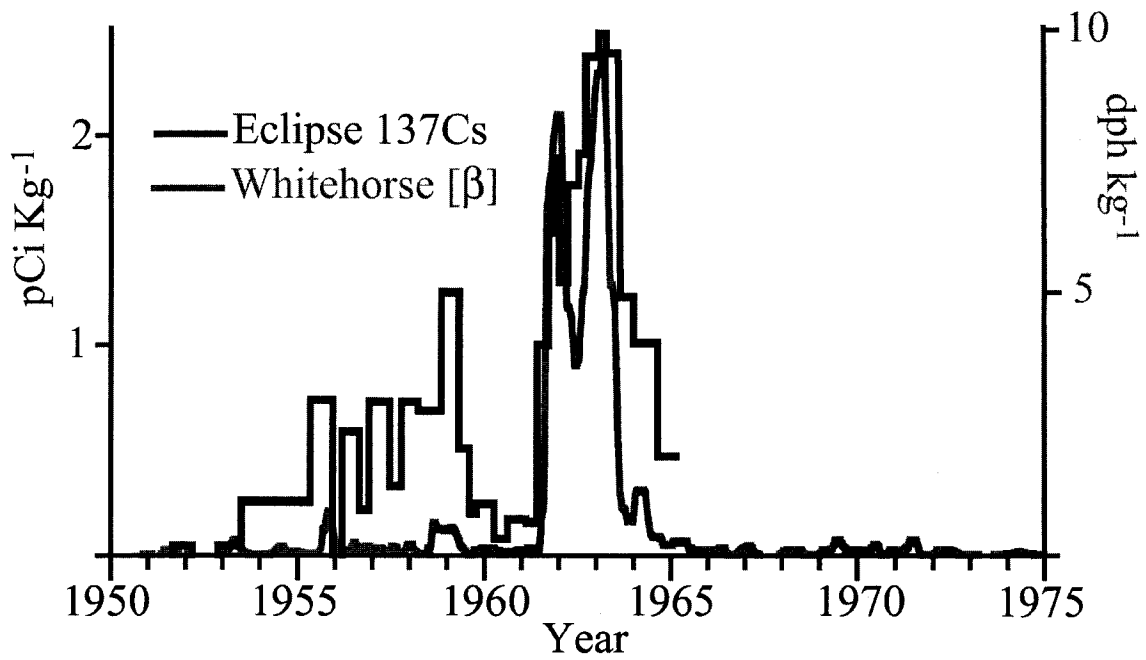


**Figure II.2.** Comparison of Eclipse ice core  $^{137}\text{Cs}$  profiles with real-time aerosol samples from Whitehorse, Yukon, shows clear identification of the 1963 and 1961 radionuclide peaks from atmospheric nuclear weapons testing.

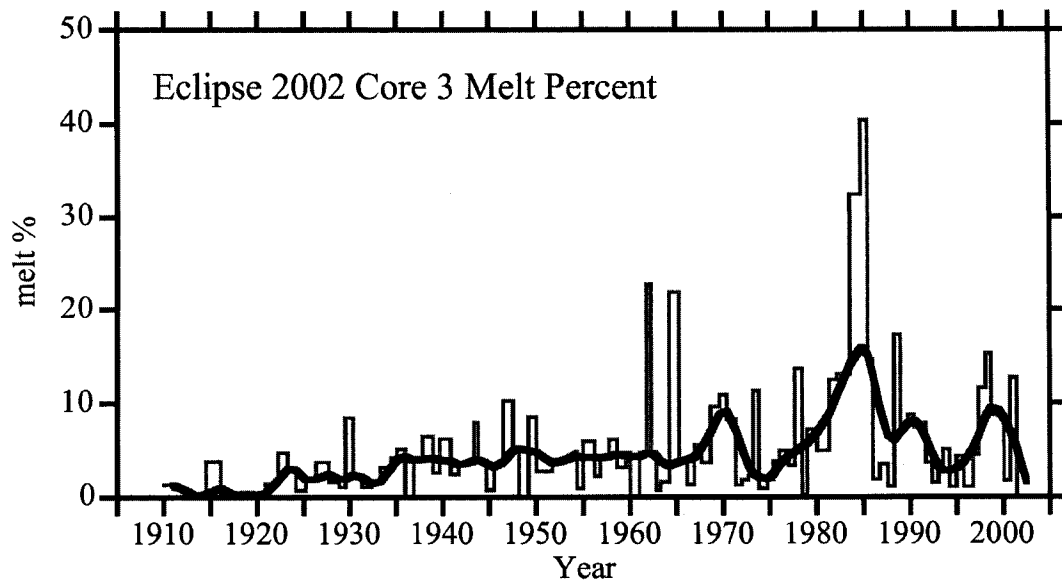


**Figure II.3.** Percent melt as discrete ice layers in Eclipse 2002 Core 3 (2002- 1910). Smoothing with a robust spline (heavy line) highlights the long-term trends in the record.

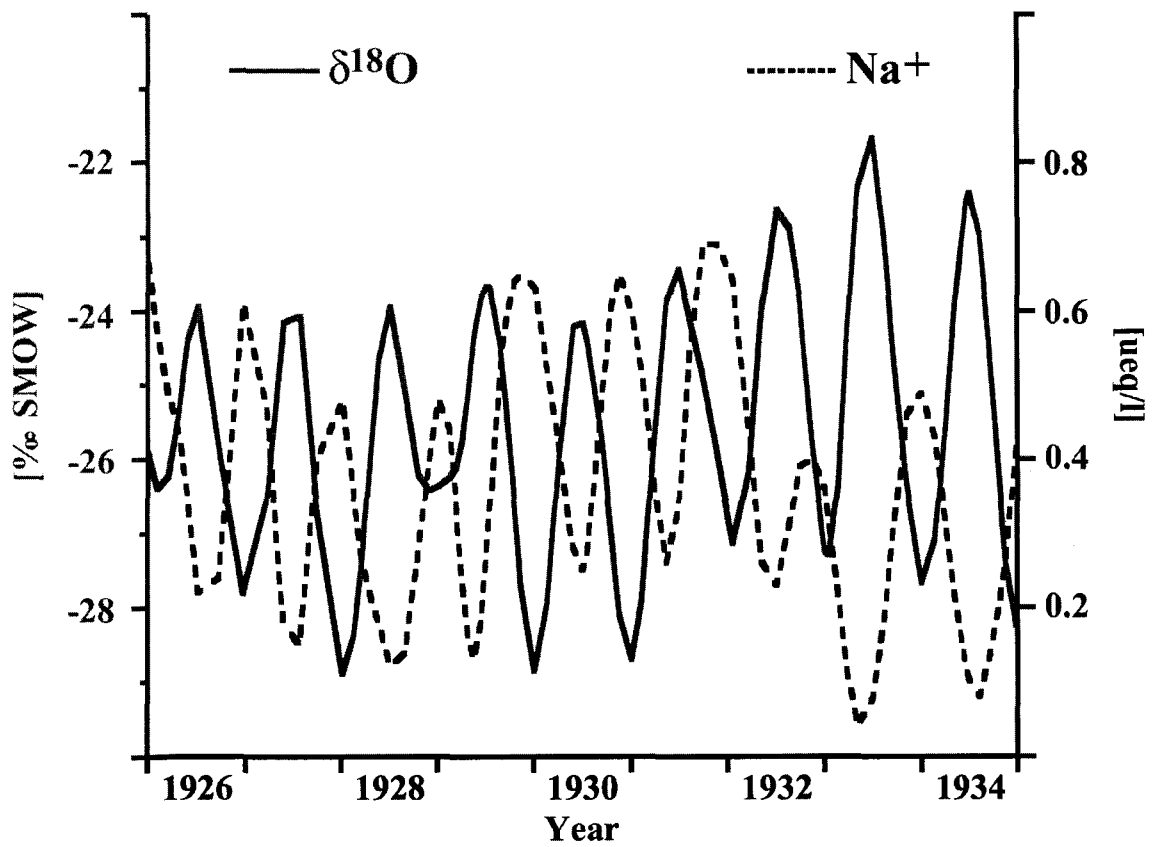


**Figure II.4.** Seasonal signals in the Eclipse 2002 Core 3  $\delta^{18}\text{O}$  and  $\text{Na}^+$  records used to date the core via annual layer counting. Records were smoothed with a robust spline to highlight the seasonal variability.



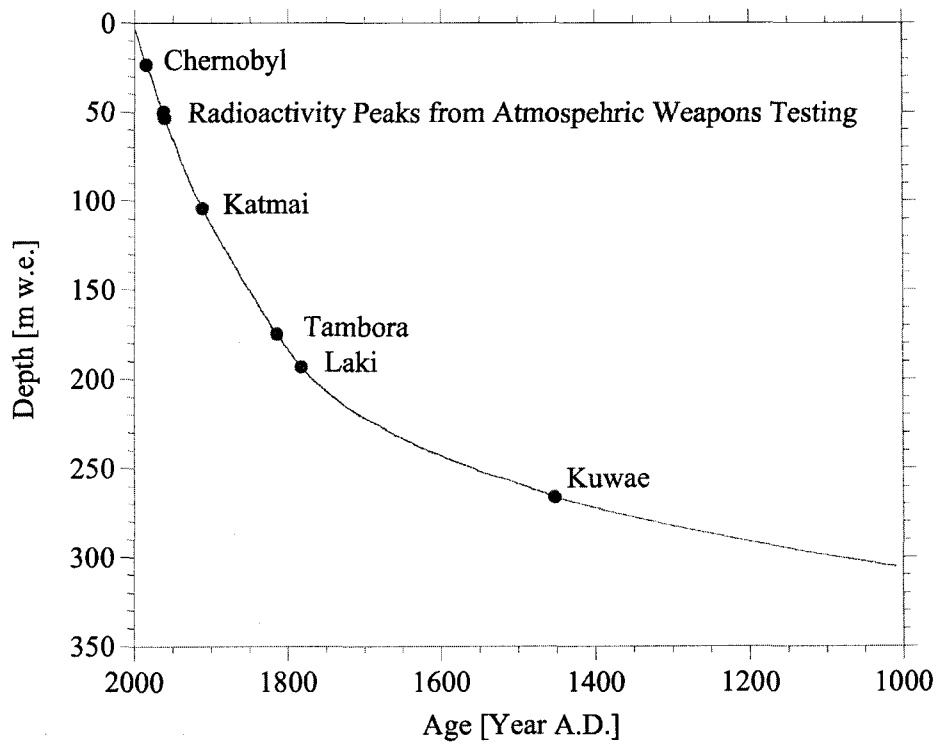


**Figure II.5.** Depth-age relationship for Eclipse 2002 Core 2. Reference horizons used to verify the chronology developed via annual layer counting from 2002 to 1450 are indicated. Below 1450, dating is an extension of a polynomial fit to these reference horizons.

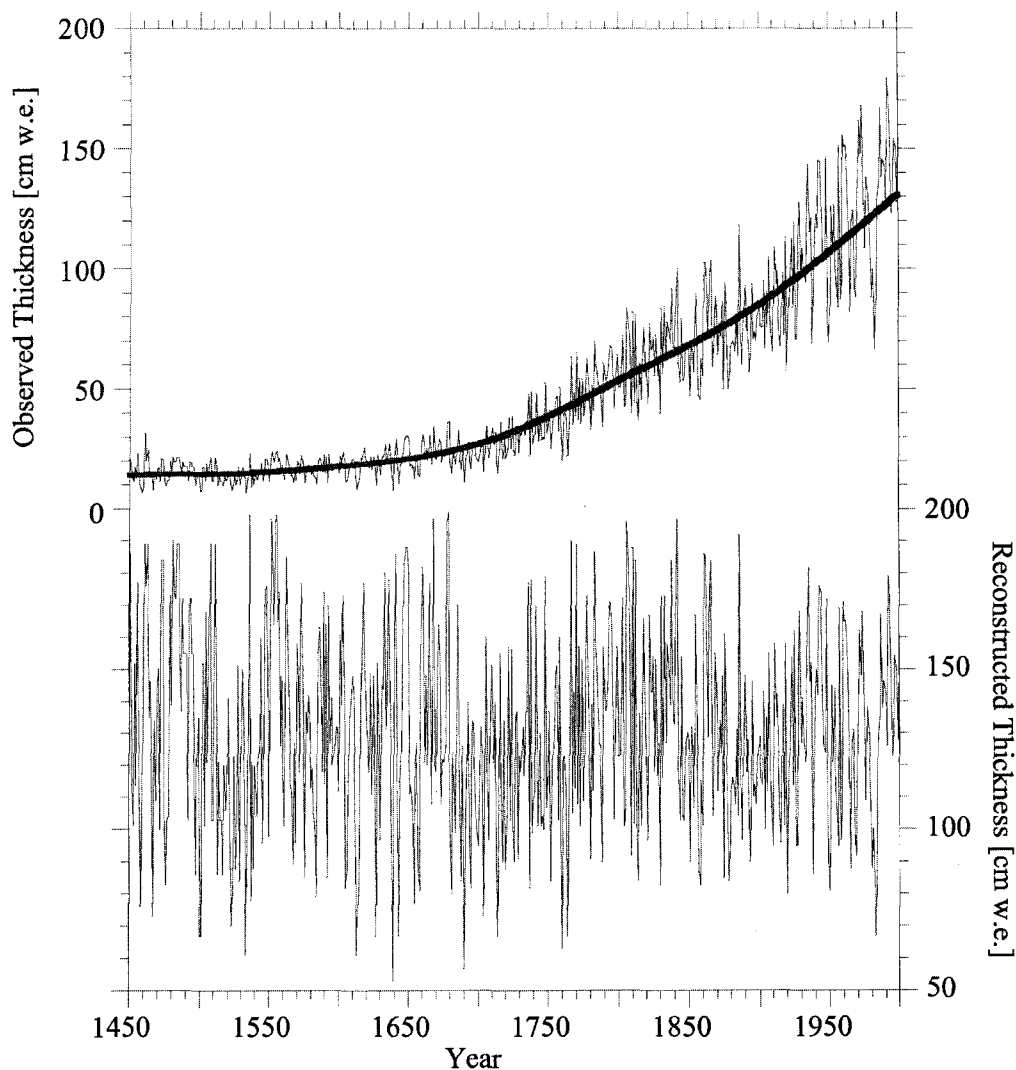


**Figure II.6.** Reconstruction of original annual layer thicknesses by correcting for layer thinning. Observed annual thicknesses derived by dating of the core by annual layer counting of seasonal oscillations in the stable isotope and major ion records shows thinning of annual layers with depth (top). Assuming a constant accumulation rate from identification of the 1963 radioactivity maximum of 1.38 and 1.30 m water equivalent for the 1996 and 2002 cores, respectively, and no creep deformation in the firn section of the cores, a decompression ratio for each annual layer was calculated from a smoothed fit to the observed layer thicknesses (red line). This ratio was then applied to the observed thickness of each annual layer to reconstruct the original thickness (bottom).

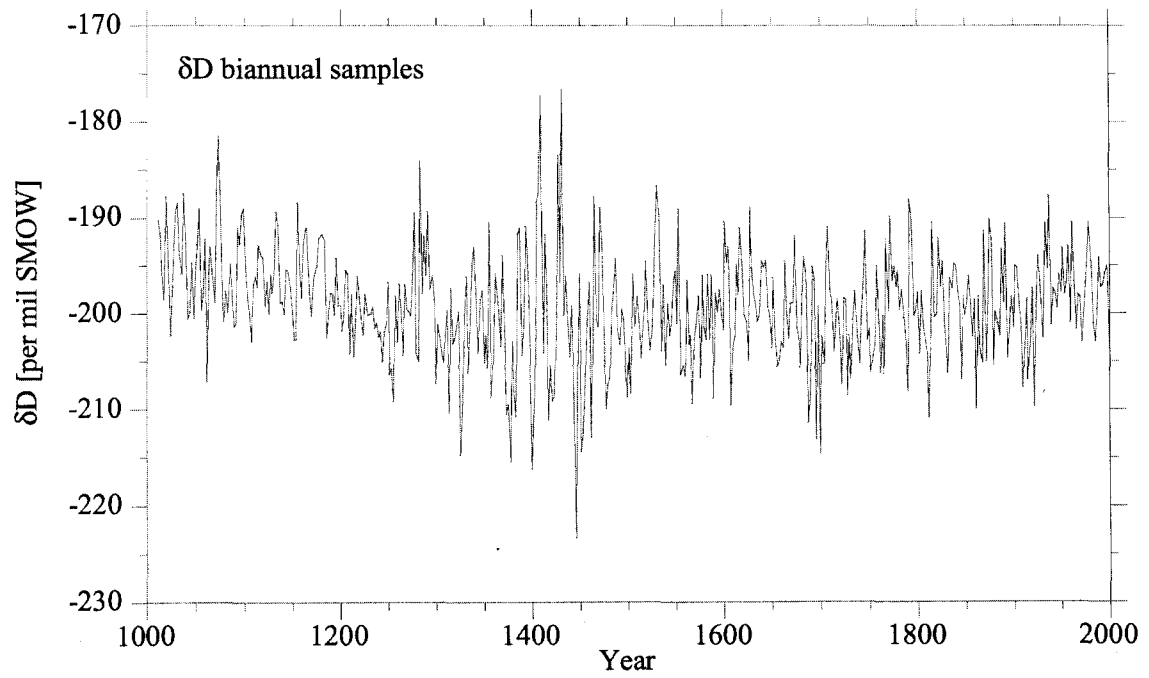


**Figure II.7.** The 1000 year  $\delta D$  time series from Eclipse 2002 Core 2. Biannual samples are shown to minimize seasonal fluctuations.

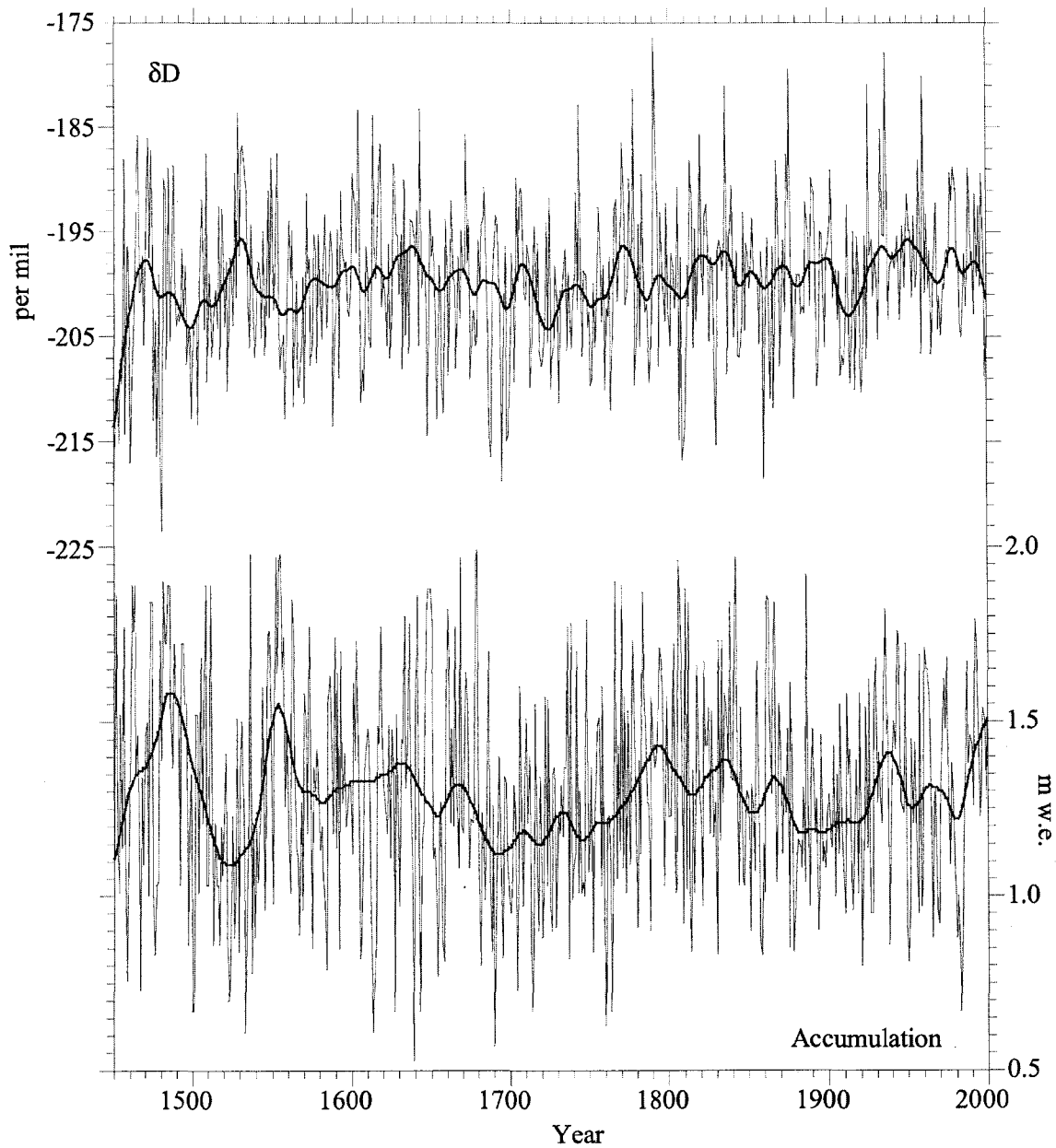


**Figure II.8.** Time-series of annual average  $\delta D$  (top) and annual accumulation (bottom) from the Eclipse 2022 Core 2 ice core. Records were smoothed with a robust spline (red line) to highlight the interdecadal variability.

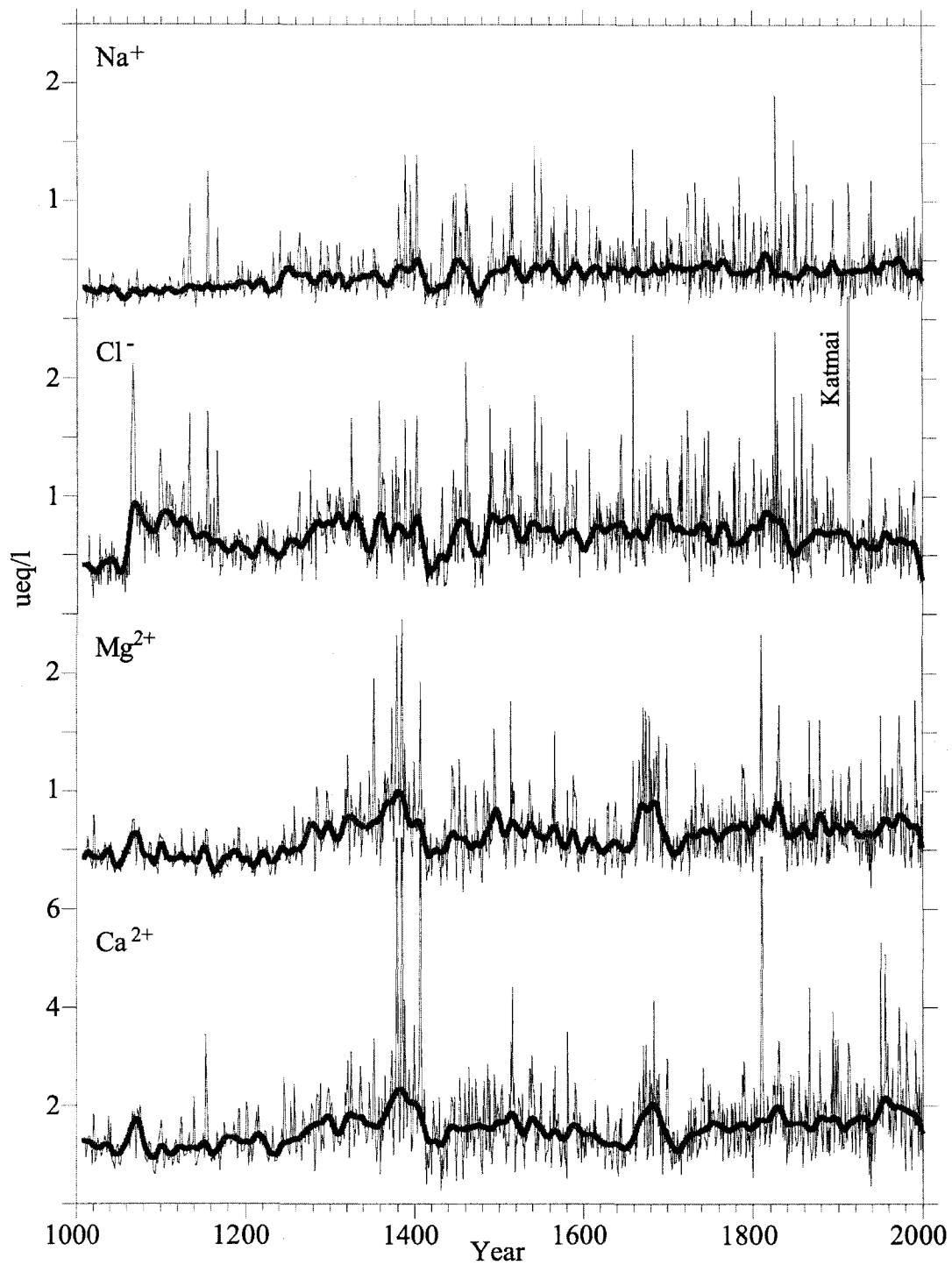


**Figure II.9.** Time-series of annual average  $\text{Na}^+$ ,  $\text{Cl}^-$ ,  $\text{Mg}^{2+}$ , and  $\text{Ca}^{2+}$  concentrations from the Eclipse 2002 Core 2 ice core. Records were smoothed with a robust spline (red line) to highlight the interdecadal variability.

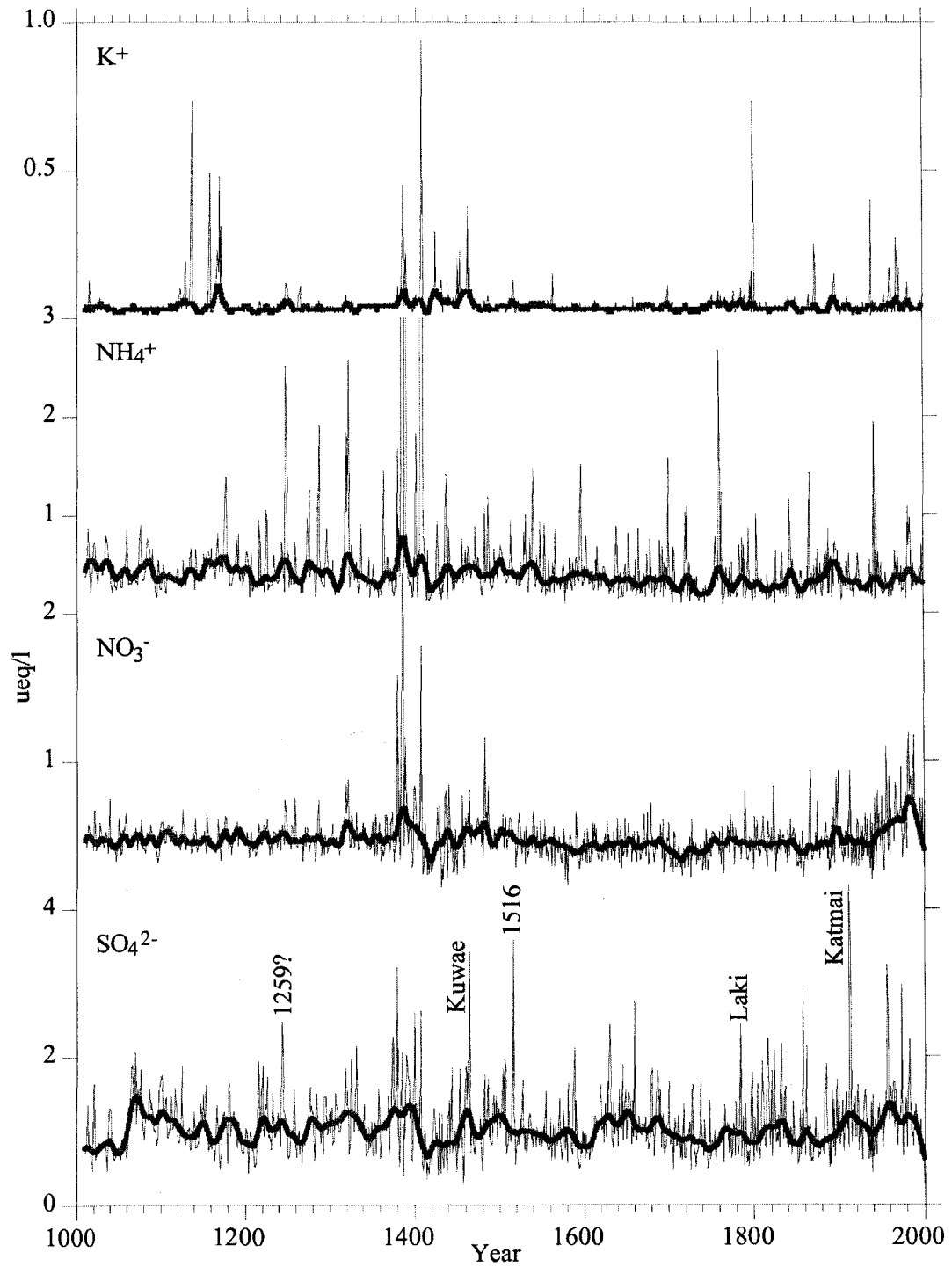


**Figure II.10.** Time-series of annual average  $K^+$ ,  $NH_4^+$ ,  $NO_3^-$ , and  $SO_4^{2-}$  concentrations from the Eclipse 2002 Core 2 ice core. Records were smoothed with a robust spline to highlight the interdecadal variability.

## CHAPTER III

### SEASONAL AND SPATIAL VARIABILITY IN SNOW CHEMISTRY

#### AT ECLIPSE ICEFIELD, YUKON, CANADA

(Annals of Glaciology, in review)

#### Abstract

Samples collected from four snowpits at Eclipse Icefield, Yukon, Canada, were analyzed for stable isotopes and major ions to assess seasonal and spatial variability in snow chemistry. Accumulation since the end of the 2001 summer season over the 0.1 km<sup>2</sup> area sampled ranges from 0.77 to 1.16 m water equivalent, with snowpit stratigraphy and chemical records demonstrating that the low accumulation at Pit 3 is due to an under-representation of winter snow accumulation at that site. For all major ion species, chemical concentrations are independent of snow accumulation rate. Seasonal variations are evident in the major ion records and can be divided between sea-salt species (Na<sup>+</sup>, Cl<sup>-</sup>) that peak in late fall-winter, and dust (Ca<sup>2+</sup>, Mg<sup>2+</sup>, K<sup>+</sup>) and other species (NH<sub>4</sub><sup>+</sup>, NO<sub>3</sub><sup>-</sup>, SO<sub>4</sub><sup>2-</sup>, C<sub>2</sub>O<sub>2</sub><sup>2-</sup>) that peak in late spring-summer. The signal common to all four snowpits identified by empirical orthogonal function analysis ranges from 49% of the total variance for Na<sup>+</sup> and Cl<sup>-</sup> to as high as 80% of the total variance for SO<sub>4</sub><sup>2-</sup>. There is greater spatial variability in species associated with coarse mode particles (Na<sup>+</sup>, Cl<sup>-</sup>, Ca<sup>2+</sup>, Mg<sup>2+</sup>) than in species present mainly in accumulation mode aerosols (SO<sub>4</sub><sup>2-</sup>, NH<sub>4</sub><sup>+</sup>) or in the gas phase (NO<sub>3</sub><sup>-</sup>).

## Introduction

Proxy records developed through physical and chemical analyses of ice cores arguably provide the highest resolution and most direct view of Earth's paleo-atmosphere over time scales ranging from decades to hundreds of thousands of years (e.g., Legrand and Mayewski, 1997). Ice cores spanning the last one hundred to one thousand years have been recovered from Eclipse Icefield (60.51° N, 139.47° W, 3017 m elevation) in the St. Elias Mountains, Yukon, Canada (Yalcin and Wake, 2001; Yalcin *et al.*, 2004). High annual accumulation (averaging 1.38 m water equivalent for the period 1996 to 1963) and limited melting (averaging less than 5% by weight per year) makes the Eclipse Icefield suitable for developing high resolution records of natural and anthropogenic environmental change in the northwest North American Arctic over the last few centuries. Indeed, the Eclipse ice cores have yielded valuable insights into anthropogenic sulfate and nitrate trends in this part of the Arctic (Yalcin and Wake, 2001), the history of volcanism in the North Pacific Rim (Yalcin *et al.*, 2003), and the relationship between ice core proxy records and meteorological variables (Wake *et al.*, 2002).

In order to fully utilize the glaciochemical records available from Eclipse Icefield, a robust understanding of the controls on snow chemical composition, seasonal input timing, and spatial variability in snow chemistry at the Eclipse site is required. Snowpit sampling provides a useful tool to investigate these properties (e.g., Mayewski *et al.*, 1990; Kreutz *et al.*, 1999; Wake *et al.*, 2004). Comparison of snowpack chemistry at Summit, Greenland and the South Pole demonstrates differences in both relative importance and seasonal input timing of crustal and sea salt species (Whitlow *et al.*, 1992). Dust species peak in boreal spring at Summit but in austral fall at the South Pole due to differences in timing of long-range transport from continental source areas. Furthermore, sea-salt is a much more important source of  $Mg^{2+}$  at the South Pole due to much lower dust concentrations. Snowpit studies can be used to assess the spatial representativeness of an ice core record, and investigations at Summit have reported greater spatial variability in snow chemistry for species present as coarse mode particles than for species



found in the accumulation mode or gas phase (e.g., Dibb and Jaffrezo, 1997). Snowpit studies can also help improve ice core dating via a multi-parameter approach identifying seasonal variations in glaciochemical species (e.g., Kreutz *et al.*, 1999).

Likewise, identifying any potential dependence of chemical concentration and flux on snow accumulation can aid the interpretation of ice core data (Yang *et al.*, 1996; Kreutz *et al.*, 2000). For example, if chemical concentration is found to be independent of snow accumulation, concentration changes can be interpreted in terms of changes in source strength and/or atmospheric circulation. On the other hand, if chemical concentration is dependent on snow accumulation, changes in accumulation rate over different time scales could obscure changes in concentration due to source strength or transport mechanisms. Ice core data from Greenland, Mt. Logan (Yukon), and the Himalayas demonstrate that major ion concentrations are independent of snow accumulation over a range of accumulation rates from 0.23 to 0.60 m water equivalent (Yang *et al.*, 1995). However, nitrate flux was found to have a strong linear relationship to accumulation, suggesting the atmospheric supply of nitrate is sufficiently large to remain undepleted by precipitation at these accumulation rates. The 1.38 m water equivalent accumulation rate at Eclipse Icefield offers the opportunity to investigate the relationship between chemical concentration, chemical flux, and accumulation rate with a high accumulation rate site.

In this paper, we present the results of a snowpit survey for stable isotopes and major ions at Eclipse Icefield during the 2002 field season. The results allow us to characterize the chemistry of recent snowfall at Eclipse, define the relative contributions of sea salt versus non-sea-salt sources, investigate the dependence of chemical species concentration and flux on snow accumulation rate, identify the seasonal input timing, and assess the spatial variability in glaciochemical signals at Eclipse.

## Methods

As part of ice core drilling efforts at Eclipse Icefield during May and June 2002, four snowpits were sampled for major ions and stable isotopes. Each 4 m snowpit was located approximately 100 meters to the N, W, S, and E of the drilling site, respectively (Figure III.1). Stringent sampling protocols were used to ensure samples were contamination free at the  $\text{ng g}^{-1}$  level. All sampling equipment and sample containers were pre-cleaned with Milli-Q water at the University of New Hampshire by rinsing three times, soaking at least 24 hours, rinsing three times, and dried in a laminar flow bench in a clean room. Snowpits were sampled continuously at 5 cm resolution by personnel wearing non-particulating suits, plastic gloves, and dripless face masks. A pre-cleaned stainless steel sampling tool was used to pack samples directly into pre-cleaned 60 ml polypropylene containers. Density measurements were made every 10 cm. A stratigraphic description, including the location and thickness of ice layers from surface melting during summer, was made for each pit (Figure III.2).

Samples were transported frozen to the University of New Hampshire where they were melted and 5 ml aliquots taken for major ion and stable isotope analysis. Samples were analyzed for major ions ( $\text{Na}^+$ ,  $\text{NH}_4^+$ ,  $\text{K}^+$ ,  $\text{Mg}^{2+}$ ,  $\text{Ca}^{2+}$ ,  $\text{Cl}^-$ ,  $\text{NO}_3^-$ ,  $\text{SO}_4^{2-}$ ,  $\text{C}_2\text{O}_4^{2-}$ ) via ion chromatography using a 0.5 ml sample loop in a dedicated laboratory at the Climate Change Research Center. The cation system used a CS12A column with CSRS-ultra suppressor in auto suppression recycle mode with 20 mM MSA eluent. The anion system used an AS11 column with an ASRS-ultra suppressor in auto suppression recycle mode with 6 mM NaOH eluent. Analytical precision was monitored by analyzing 10% of the samples in duplicate and found to be 11% for  $\text{K}^+$ , 10% for  $\text{NH}_4^+$ , 7% for  $\text{Na}^+$ , and less than 5% for all other species. Stable isotopes ( $\delta^{18}\text{O}$ ) were analyzed at the University of Maine Stable Isotope Laboratory with a Multiprep  $\text{CO}_2$  equilibration system coupled to a VG SIRA mass spectrometer (precision  $\pm 0.05\text{‰}$ ). Concentrations of  $\text{K}^+$ ,  $\text{Mg}^{2+}$ ,  $\text{Ca}^{2+}$ , and  $\text{SO}_4^{2-}$  were partitioned into sea-salt and non-sea-salt fractions using  $\text{Na}^+$  as the sea salt

indicator and the micro-equivalent ratios of  $\text{Na}^+$  to other ions in seawater, assuming no fractionation of the sea-salt aerosol during transport and deposition (Keene *et al.*, 1986).

Snowpit stratigraphic properties (Figure III.2) and seasonal variations in  $\delta^{18}\text{O}$  (Figure III.3) were used to date the snowpits. Two high  $\text{Ca}^{2+}$  and  $\text{Mg}^{2+}$  dust events in the spring and fall of 2001 provided additional time lines (Figure III.3). The spring 2001  $\text{Ca}^{2+}$  and  $\text{Mg}^{2+}$  event could be the local signature of the April 2001 Asian dust plume that traveled across North America (De Bell *et al.*, 2004; Zdanowicz *et al.*, 2004). Placing the four snowpits on a common depth-age scale allows us to investigate the variability in glaciochemical signals between the four snowpits without variation in accumulation rates influencing our results.

This step was necessary in our analysis because available data indicate that a gradient in accumulation exists across the Icefield. Using the location of ice layers and the  $\delta^{18}\text{O}$  records as the most reliable indicator of summer versus winter snowfall, we found accumulation since the end of the 2001 melt season to range from 0.77 m water equivalent (w.e.) at Pit 3 to 1.02 m w.e. at Pit 4 and 1.16 m w.e. at Pits 2 and 5 (Figure III.1). Inspection of snowpit stratigraphy and oxygen isotope records (Figures III.2 and III.3) demonstrates the low accumulation at Pit 3 is due to an under-representation of winter snowfall at this site. The mountain slope to the east of Pit 3 could produce a funneling effect focusing wind energy along the east side of the Icefield, leading to enhanced wind erosion and removal of low density winter snow at Pit 3. Other snowpit surveys have also reported similar variability in snow accumulation rates over local areas (e.g., Kreutz *et al.*, 1999; Goto- Azuma *et al.*, 1997), and found wind scour and removal particularly important for controlling the accumulation distribution of winter snow (Fisher *et al.*, 1983). The Eclipse ice cores suggest this gradient has remained stable over the last 40+ years because average annual accumulation since 1963 at the 1996 m drill site (one hundred meters down the flow line and further from the mountain slope to the east) is 7% more than at the 2002 drill site.

## **Results and Discussion**

### **Snow Chemical Composition**

The Eclipse snowpit data is summarized on a micro-equivalent per liter ( $\mu\text{eq l}^{-1}$ ) basis in the box plots shown in Figure III.4. Calcium is the predominant cation in our samples (Table III.1), followed by  $\text{Mg}^{2+}$ ,  $\text{Na}^+$ ,  $\text{NH}_4^+$ , and  $\text{K}^+$ , the last of which is present at very low concentrations. Sulfate is the predominant anion in our samples, followed by  $\text{NO}_3^-$  and  $\text{Cl}^-$ . On a per sample basis,  $\text{Ca}^{2+}$  concentrations are the highest of the cations in 82% of the samples, followed by  $\text{Na}^+$  (15%) and  $\text{NH}_4^+$  (3%). Sulfate is the most concentrated anion in 63% of our samples, followed by  $\text{NO}_3^-$  (21%) and  $\text{Cl}^-$  (16%).

The completeness of major ion analysis can be checked by the charge balance (ratio of major cation equivalents to major anion equivalents). A value not significantly different from one indicates an excellent balance between measured cations and anions and suggests all major ions present have been accounted for in the analyses. The median ratio of all samples is 1.17, indicating a cation excess that is present in 63% of the samples. In particular, high dust inputs as evidenced by increased concentrations of  $\text{Ca}^{2+}$  and  $\text{Mg}^{2+}$  are associated with a charge ratio much greater than one. Dust inputs probably include carbonate ions ( $\text{HCO}_3^-$  and  $\text{CO}_3^{2-}$ ) in concentrations large enough to balance the observed cation excesses (Toom-Sauntry and Barrie, 2002). The remaining 37% of the samples have an excess of anions that is presumably balanced by  $\text{H}^+$ , which is generally the most abundant positive ion in water samples.

### **Sea-salt Calculations**

Calculations of sea-salt (ss) and non-sea-salt (nss) fractions indicate that nearly all of the  $\text{Ca}^{2+}$  (99%),  $\text{K}^+$  (86%) and  $\text{Mg}^{2+}$  (83%) at Eclipse are from non-sea-salt sources, presumably crustal dust. Sulfate is also mostly (97%) from non-sea-salt sources, which include oxidation of sulfur dioxide from anthropogenic sources and volcanic emissions, oxidation of dimethylsulfide produced by phytoplankton, and crustal dust and evaporate deposits. Although we assumed all of the  $\text{Na}^+$  present is from sea salt, a portion of the  $\text{Na}^+$  may be crustal in origin, particularly in dust-

laden samples. Hence, the sea-salt and non-sea-salt fractions we calculated represent maximum and minimum estimates, respectively. The  $\text{Cl}^-:\text{Na}^+$  micro-equivalent ratio in snow at Eclipse averages 1.26, a 9% enrichment in  $\text{Cl}^-$  relative to the seawater ratio of 1.16 (Keene *et al.*, 1986). The  $\text{Cl}^-$  enrichment at Eclipse is considerably less than that observed at South Pole (40%) or Summit, Greenland (23%) (Whitlow *et al.*, 1992). Excess chloride in polar snow is derived from reaction of sea-salt particles with acidic aerosols leading to release of gaseous  $\text{HCl}$  (Herron, 1982). Gas phase  $\text{HCl}$  is highly soluble and readily scavenged by snowfall. Hence, chloride enrichment in snow may be interpreted as an indicator of long-range transport of marine aerosol, allowing greater volatilization of sea-salt chloride (Legrand and Delmas, 1988). Therefore, the proximity of Eclipse to sea-salt sources relative to Summit or South Pole may allow for less sea salt acidification and volatilization of  $\text{HCl}$ , resulting in less chloride enrichment at Eclipse and a  $\text{Cl}^-:\text{Na}^+$  ratio closer to that of seawater.

Calculations of sea-salt and non-sea-salt fractions do not change appreciably if an iterative approach is used to find the limiting sea salt species instead of assuming that all of the  $\text{Na}^+$  is from sea-salt. The limiting sea salt species is that species present in the lowest concentration relative to the seawater ratio. Therefore the limiting species provides an estimate of the minimum sea salt contribution, assuming no fractionation during production, transport, and deposition of sea salt aerosol (Keene *et al.*, 1986). Sodium is found to be the limiting species in 99% of the samples. The limiting species in the remaining 1% of the samples is  $\text{K}^+$ ,  $\text{Mg}^{2+}$ , or  $\text{Ca}^{2+}$ , while  $\text{SO}_4^{2-}$  is not found to be limiting in any of the samples. Again, nearly all of the  $\text{Ca}^{2+}$  (99%),  $\text{K}^+$  (88%),  $\text{Mg}^{2+}$  (84%) and  $\text{SO}_4^{2-}$  (95%) are found to be from non-sea-salt species, while nearly all of the  $\text{Na}^+$  (92%) and  $\text{Cl}^-$  (85%) are present in sea-salt ratios. In contrast, up to 100% of the  $\text{Mg}^{2+}$  in Antarctica can be from sea salt (Whitlow *et al.*, 1992). In such situations, determining the limiting sea salt species is a necessary step to determine whether  $\text{Na}^+$  or  $\text{Mg}^{2+}$  provides the better sea-salt indicator for calculations of sea-salt and non-sea-salt fractions.

### **Dependence on accumulation rate**

We used linear regression to investigate the relationship between the annually-averaged concentration ( $\mu\text{eq l}^{-1}$ ) of major ions and snow accumulation rate (m water equivalent  $\text{yr}^{-1}$ ) at Eclipse using the 100-year record provided by the Eclipse 1996 ice core (Yalcin and Wake, 2001). Results were similar using the Eclipse 2002 ice core data. For all species, correlation coefficients are less than 0.15, indicating that snow accumulation rate is not an important control on the concentration of major ions at Eclipse (Figure III.5). Yang *et al.* (1995) reached the same conclusion in their study of the GISP2 and 20D (Greenland) and Mt. Logan (Yukon) ice core datasets.

We also used linear regression to evaluate the dependence of chemical flux ( $\mu\text{g cm}^{-2} \text{yr}^{-1}$ ) on snow accumulation rate (Figure III.6). Positive relationships between chemical flux and snow accumulation are evident, with correlation coefficients ranging from 0.27 for  $\text{K}^+$  to as high as 0.51 for  $\text{NO}_3^-$ . This indicates between 7% and 26% of the variance in the flux data can be explained by a linear relationship with snow accumulation rate. Our results agree with those of Yang *et al.* (1995) who report that the strongest correlation exists between nitrate flux and snow accumulation rate. Furthermore, our best fit linear regression between nitrate flux and snow accumulation rate ( $F = 0.035A - 0.35$ , where  $F$  is nitrate flux in  $\mu\text{g cm}^{-2} \text{yr}^{-1}$  and  $A$  is the snow accumulation rate in m w.e.  $\text{yr}^{-1}$ ) compares favorably to the relationship derived by Yang *et al.* (1995) for Mt. Logan ( $F = 0.054A - 0.19$ ). We also find that 12-25% of the variance in the  $\text{NH}_4^+$ ,  $\text{Mg}^{2+}$ ,  $\text{Ca}^{2+}$ ,  $\text{Cl}^-$ , and  $\text{SO}_4^{2-}$  flux data is explained by a linear relationship with snow accumulation. Although no more than 20% of the flux variance of these species at GISP2 was explained by a linear relationship with snow accumulation rate, 36% of the variance in the Mt. Logan sulfate flux data was explained (Yang *et al.*, 1995). This may indicate a greater importance of wet deposition at high accumulation rate sites such as Eclipse relative to the sites in the interior of ice

sheets such as GISP2 where dry and especially fog deposition can be an important contributor to chemical species flux (Bergin *et al.*, 1995).

### **Seasonal variations**

Comparison of individual species concentration profiles to the  $\delta^{18}\text{O}$  profile and to each other reveals distinct seasonal variations in all of the glaciochemical parameters measured. Similar seasonal glaciochemical variations are also observed in ice cores from Eclipse (Yalcin and Wake, 2001), allowing us to summarize seasonal input timing at Eclipse over the last century (Figure III.7). However, in any given year the relative timing of concentration peaks can differ markedly from the pattern described, especially for species influenced by episodic events, such as volcanic eruptions ( $\text{SO}_4^{2-}$ ) or forest fires ( $\text{NH}_4^+$ ). The most regular seasonal variations at Eclipse are seen in the  $\delta^{18}\text{O}$  record, which exhibits the classic signal of isotopically heavier (more negative) precipitation in winter and isotopically lighter (less negative) precipitation in summer (e.g., Dansgaard *et al.*, 1973). Typical  $\delta^{18}\text{O}$  values for summer snowfall at Eclipse are  $-24\text{‰}$  with winter snowfall typically in the  $-30\text{‰}$  range.

Summer-winter variations are also evident in the major ion records and can broadly be divided between sea-salt species ( $\text{Na}^+$ ,  $\text{Cl}^-$ ) that peak in late fall-winter and dust ( $\text{Ca}^{2+}$ ,  $\text{Mg}^{2+}$ ,  $\text{K}^+$ ) and other species ( $\text{NH}_4^+$ ,  $\text{NO}_3^-$ ,  $\text{SO}_4^{2-}$ ,  $\text{C}_2\text{O}_2^{2-}$ ) that peak in late spring-summer (Figure III.7). Concentrations of  $\text{Na}^+$  and  $\text{Cl}^-$ , derived mostly from sea-salt, peak in late fall or winter either coincident with the  $\delta^{18}\text{O}$  minima or, less commonly, on the descending leg. This is presumably due to greater storminess in the nearby Gulf of Alaska during fall and winter, with higher wind speeds generating more wave action and enhanced entrainment of sea-salt aerosols, as well as more frequent advection of maritime air masses over Eclipse associated with greater inland penetration of stronger synoptic frontal systems (Taylor-Barge, 1969). Sea-salt concentrations are at their annual minima during summer.

Other species peak at Eclipse during spring or summer, with generally lower concentrations during winter. First to peak are those species indicative of dust such as  $\text{Ca}^{2+}$  and  $\text{Mg}^{2+}$  that most often peak on the rising leg of the  $\delta^{18}\text{O}$  curve, although their concentration maxima can extend throughout the summer. The low  $\text{K}^+$  concentrations make it difficult to infer any seasonality in  $\text{K}^+$  deposition at Eclipse. However,  $\text{K}^+$  concentration peaks often coincide with  $\text{Ca}^{2+}$ - $\text{Mg}^{2+}$  peaks suggesting a  $\text{K}^+$  source from crustal dust, or with  $\text{NH}_4^+$  peaks suggesting a biomass-burning source. Slightly lagging the spring peak in crustal dust is the  $\text{NH}_4^+$  maxima which also tends to peak on the rising leg of the  $\delta^{18}\text{O}$  curve. However, episodic biomass burning events can overwhelm the seasonal  $\text{NH}_4^+$  cycle and produce concentration maxima anytime between spring and fall. Peak oxalate ( $\text{C}_2\text{O}_4^{2-}$ ) concentrations tend to coincide with the spring to early summer  $\text{NH}_4^+$  peak.

Sulfate and nitrate concentrations typically peak with the  $\delta^{18}\text{O}$  maxima, and hence slightly lag dust concentration peaks, although there is considerable overlap. Elevated  $\text{SO}_4^{2-}$  and  $\text{NO}_3^-$  concentrations associated with dust inputs suggest uptake of sulfate and nitrate by dust particles during atmospheric transport from continental source areas (Jordan *et al.*, 2003). The summer  $\text{NO}_3^-$  peak could be due to  $\text{NO}_x$  released by thermal decomposition of peroxyacetyl nitrate (PAN) in the presence of higher OH concentrations in summer (Yang *et al.*, 1995). Alternatively, the summer  $\text{NO}_3^-$  peak could indicate a summer peak in  $\text{NO}_3^-$  production by biological activity, biomass burning, or lightning (Legrand and Kirchner, 1990). Holdsworth and Peake (1985) reported similar seasonal variations in nitrate in their analysis of snowpits and shallow firn cores from Eclipse. However, extensive post-depositional alteration of  $\text{NO}_3^-$  in snowpacks by photochemical recycling and an incomplete understanding of the underlying physical mechanisms responsible complicates interpretation of glaciochemical  $\text{NO}_3^-$  records (Dibb *et al.*, 2002).



Although the observed seasonality at Eclipse is similar to that observed at Summit, Greenland (Whitlow *et al.*, 1992), distinct differences exist. Sodium concentrations at Summit tend to lag the  $\delta^{18}\text{O}$  minima and hence frequently overlap the spring dust concentration peak. This is thought to reflect an under-representation of winter snow accumulation in the snowpack at Summit, allowing winter and spring concentration peaks separated in time by three months or more to overlap in the snowpack (Dibb, 1996). In contrast, the even distribution of snow accumulation throughout the year at Eclipse (with the exception of Pit 3) preserves distinct sea-salt maxima in winter and dust maxima in spring. Ammonium concentration peaks at Summit tend to occur in summer, coincident with the  $\delta^{18}\text{O}$  maxima, while at Eclipse they most often peak on the rising (spring) leg of the  $\delta^{18}\text{O}$  curve. Meanwhile,  $\text{SO}_4^{2-}$  concentrations tend to peak later at Eclipse in the vicinity of the  $\delta^{18}\text{O}$  maxima, while at Summit peak  $\text{SO}_4^{2-}$  concentrations are a spring phenomena. Relative input timing for dust species (spring) and  $\text{NO}_3^-$  (summer) are the same at Eclipse and Summit.

### **Spatial variations**

Box plots for each glaciochemical parameter measured in each individual snowpit provide a first order perspective of the spatial variability at Eclipse (Figure III.4). Median values for oxygen isotopes are relatively constant for the four snowpits, although pit 2 displays a much greater range in oxygen isotope values. Oxygen isotope values at Pit 3 are skewed towards less negative values, reflecting the relative lack of winter accumulation at that site. Not surprisingly,  $\text{Na}^+$  and  $\text{Cl}^-$  concentrations are lower at Pit 3, since the time of maximum sea salt concentrations (winter) is under-represented at that site. Median values for dust species ( $\text{Ca}^{2+}$ ,  $\text{Mg}^{2+}$ ) are lower for Pits 3 and 5, while  $\text{NH}_4^+$ ,  $\text{NO}_3^-$ , and  $\text{SO}_4^{2-}$  have similar median values for all snowpits. For all species, the within group variance, as indicated by the size of the box representing the variance of the samples about the median, is greater than the between group variance as represented by the

difference in median values between snowpits. This suggests that temporal or seasonal variability in snow chemistry is greater than the spatial variability.

We used empirical orthogonal function (EOF) analyses to further investigate the spatial variability between snowpits for each of the parameters measured (Table III.2). The data from all four snowpits was pooled and a separate EOF decomposition was run for each of the species measured. Oxalate was excluded from this analysis because 56% of the snowpit samples were below detection limits for this species. The EOF technique splits the temporal variance of a data set into patterns termed empirical eigenvectors that are orthogonal in nature (Peixoto and Oort, 1992). The first eigenvector explains the greatest percentage of variance in the dataset, with each successive eigenvector describing the maximum remaining variance. In this case, the first eigenvector describes the variance common to all four snowpits, since each snowpit has a positive correlation with the first EOF. The variance or signal common to all four snowpits identified by EOF 1 ranges from 49% of the total variance for  $\text{Na}^+$  and  $\text{Cl}^-$  to as high as 80% of the total variance for  $\text{SO}_4^{2-}$ .

Our results indicate that chemical species found in the accumulation mode ( $\text{NH}_4^+$ ,  $\text{SO}_4^{2-}$ ) or gas-phase ( $\text{NO}_3^-$ ) show less glaciochemical variability in snowpits at Eclipse than those species associated with coarse mode dust ( $\text{Ca}^{2+}$ ,  $\text{Mg}^{2+}$ ) or sea salt ( $\text{Na}^+$ ,  $\text{Cl}^-$ ) particles (Table III.2). These results are consistent with studies of spatial variability in Greenland snow chemistry (e.g., Dibb and Jaffrezo, 1997). Sulfate and ammonium, presumably present primarily in the accumulation mode as  $(\text{NH}_4)_2\text{SO}_4$  (Seinfeld and Pandis, 1998), shows the least variability in our snowpits as evidenced by high EOF 1 loadings, with between 55 and 83% of the signal common between snowpits. Nitrate, found mostly in the gas phase, has more variability at Eclipse than accumulation mode species (50- 76% of the signal common between snowpits), though less than coarse mode particles. Uptake of nitrate by dust particles could result in an association of a portion of the snow nitrate with dust particles, increasing the spatial variability in nitrate concentrations. Meanwhile, species associated with sea salt ( $\text{Na}^+$  and  $\text{Cl}^-$ ) and dust ( $\text{Ca}^{2+}$ ,  $\text{K}^+$ ,

Mg<sup>2+</sup>) particles display greater variability in our snowpits as evidenced by lower EOF 1 loadings. The results obtained from the EOF analysis agree well with the box plots of Figure III.4, which showed a greater range in median values for particle associated species (Na<sup>+</sup>, Cl<sup>-</sup>, Ca<sup>2+</sup>, Mg<sup>2+</sup>) than for species with gas phase precursors (NH<sub>4</sub><sup>+</sup>, NO<sub>3</sub><sup>-</sup>, SO<sub>4</sub><sup>2-</sup>).

### **Conclusions**

We have presented a glaciochemical survey of Eclipse Icefield using four 4 m snowpits each representing approximately one years' accumulation that were sampled for major ions and stable isotopes. The anomalously low accumulation since the end of the 2001 melt season at Pit 3 (0.77 m w.e.) is due to an under-representation of winter snowfall at this site as indicated by snowpit stratigraphy and chemical records. This could reflect enhanced wind erosion and removal of low-density winter snow at Pit 3 via a funneling effect of the mountain slope to the east serving to focus wind energy. Calcium and sulfate are the dominant cation and anion in snow at Eclipse, respectively. Charge balance calculations indicate a cation excess during high dust periods that is presumably balanced by carbonate and/or bicarbonate ions. Linear regressions of annual chemical concentration versus snow accumulation rate for the 100 year Eclipse 1996 ice core record demonstrates no relationship between individual species annual mean concentration and snow accumulation rate. However up to 26% of the variance in chemical flux can be explained by a linear dependence on snow accumulation rate. The relationship between flux and accumulation is strongest for NO<sub>3</sub><sup>-</sup>, in agreement with previous studies (e.g., Yang *et al.*, 1995).

Summer-winter variations are evident in the major ion records and can broadly be divided between sea-salt species (Na<sup>+</sup>, Cl<sup>-</sup>) that peak in late fall-winter and dust (Ca<sup>2+</sup>, Mg<sup>2+</sup>, K<sup>+</sup>) and other species (NH<sub>4</sub><sup>+</sup>, NO<sub>3</sub><sup>-</sup>, SO<sub>4</sub><sup>2-</sup>, C<sub>2</sub>O<sub>2</sub><sup>2-</sup>) that peak in late spring-summer. This understanding of seasonal input timing will aid interpretation of accumulation rate records from Eclipse Icefield ice cores by facilitating recognition of anomalously low accumulation years that

are due to a lack of preserved winter snowfall. Analysis of spatial variation in snowpit chemistry suggests that species derived from coarse mode sea-salt and dust particles ( $\text{Na}^+$ ,  $\text{Cl}^-$ ,  $\text{Ca}^{2+}$ ,  $\text{Mg}^{2+}$ ,  $\text{K}^+$ ) display more spatial variability in their glaciochemical concentrations than do species found primarily in the accumulation mode or gas phase ( $\text{NH}_4^+$ ,  $\text{NO}_3^-$ ,  $\text{SO}_4^{2-}$ ) due to the spotty nature of coarse particle deposition, in agreement with the results of other studies (e.g., Dibb and Jaffrezo, 1997). Spatial variability in snow chemistry appears to be linked to the physical state of the species being deposited. The large amount of signal common to all four snowpits is encouraging for the use of ice cores from Eclipse Icefield in paleoclimatic reconstructions. Since sulfate has the highest amount of signal common to all four snowpits (73- 83%), our use of the Eclipse sulfate record in reconstructions of both anthropogenic sulfate deposition and the atmospheric effects of volcanic eruptions in the North Pacific are likely to be particularly robust paleoclimatic reconstructions.

#### **Acknowledgments**

We would like to thank E. Blake, S. Bastien, and A. Mondrick for field assistance, and the Geological Survey of Canada (D. Fisher and C. Zdanowicz) for logistical support. The National Science Foundation Office of Polar Programs funded this research.

**Table III.1.** Summary statistics of snowpit chemical composition.

	Na <sup>+</sup>	NH <sub>4</sub> <sup>+</sup>	K <sup>+</sup>	Mg <sup>2+</sup>	Ca <sup>2+</sup>	Cl <sup>-</sup>	NO <sub>3</sub> <sup>-</sup>	SO <sub>4</sub> <sup>2-</sup>	ΔC <sup>1</sup>
mean	0.39	0.34	0.06	0.52	1.63	0.49	0.67	0.93	0.79
median	0.25	0.21	0.04	0.31	0.81	0.36	0.45	0.64	0.22
std. dev.	0.40	0.33	0.08	0.62	2.47	0.41	0.61	0.92	2.30
maximum	2.93	2.05	0.98	4.72	23.74	3.05	4.38	5.90	21.44
minimum	0.01	0.03	0.00	0.03	0.00	0.05	0.08	0.12	-3.54

<sup>1</sup>Sum of measured cations minus sum of measured anions.

**Table III.2.** Snowpit percent variance explained ( $r^2$ ) by EOF 1. All loadings positive.

	$\delta^{18}\text{O}$	$\text{NH}_4^+$	$\text{SO}_4^{2-}$	$\text{NO}_3^-$	$\text{Na}^+$	$\text{Cl}^-$	$\text{K}^+$	$\text{Ca}^{2+}$	$\text{Mg}^{2+}$
Pit 2	58.3	54.5	73.0	50.1	28.2	30.6	13.5	45.0	51.9
Pit 3	77.2	87.5	78.7	61.8	40.3	42.1	69.5	80.4	60.0
Pit 4	70.2	76.0	83.0	75.8	58.9	54.8	51.3	90.4	83.2
Pit 5	82.4	81.2	83.4	61.8	68.2	68.3	81.6	31.8	61.6
Total	72.0	74.8	79.5	62.4	48.9	49.0	54.0	61.9	64.2

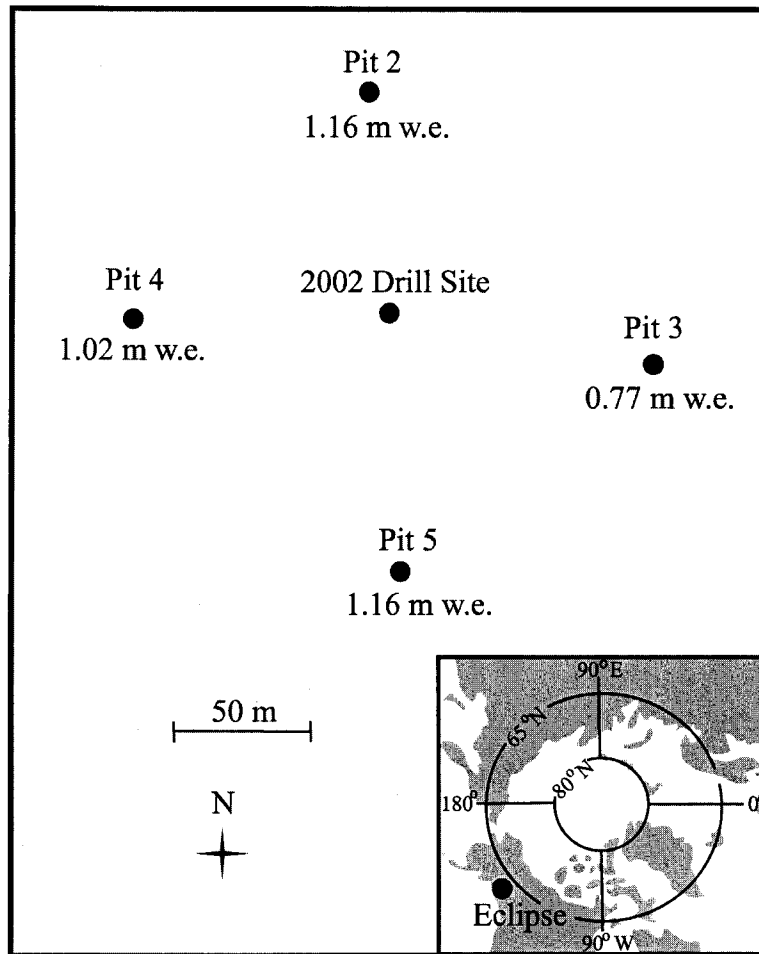


**Figure III.1.** Location map for 2002 Eclipse Icefield snowpits in relation to the 2002 drill site. The accumulation in m water equivalent (w.e.) at each snowpit since the end of the 2001 melt season is indicated.

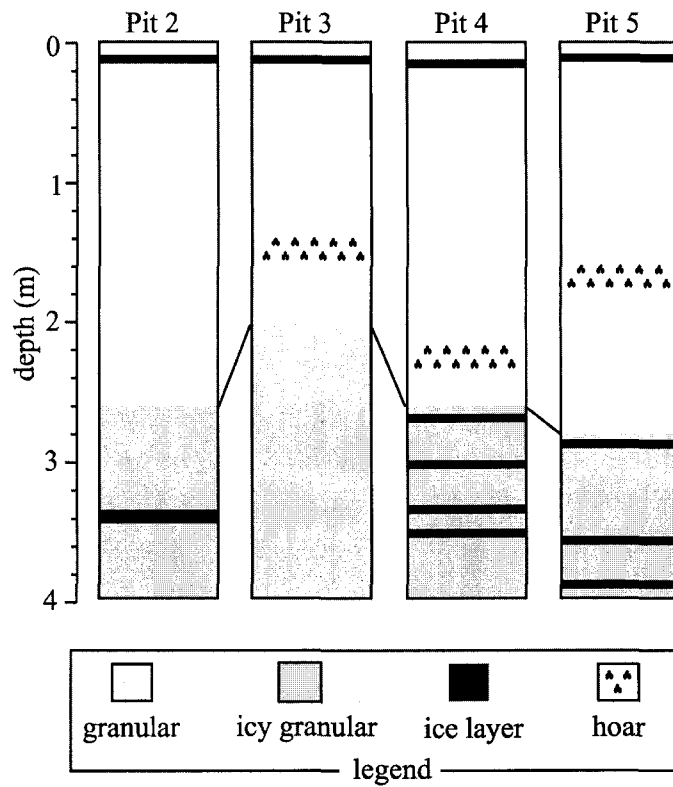


**Figure III.2.** Key stratigraphic features used to date the snowpits. The tie-line marking the end of the 2001 melt season is indicated. Note the lower winter snow accumulation in Pit 3.



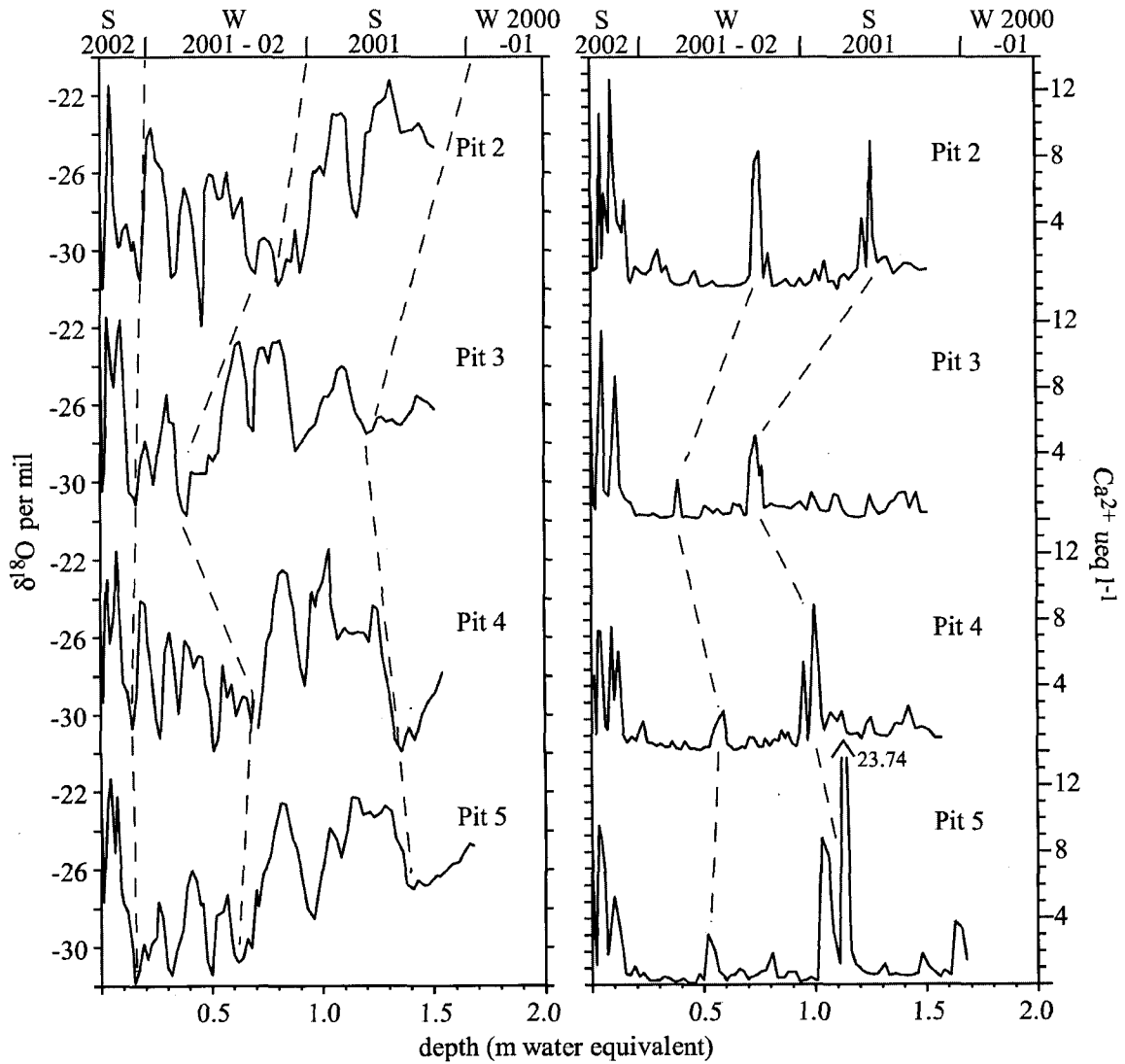


**Figure III.3.** Glaciochemical parameters used to date the snowpits. Left,  $\delta^{18}\text{O}$ . Right,  $\text{Ca}^{2+}$ . Dashed lines indicate tie lines used for dating.

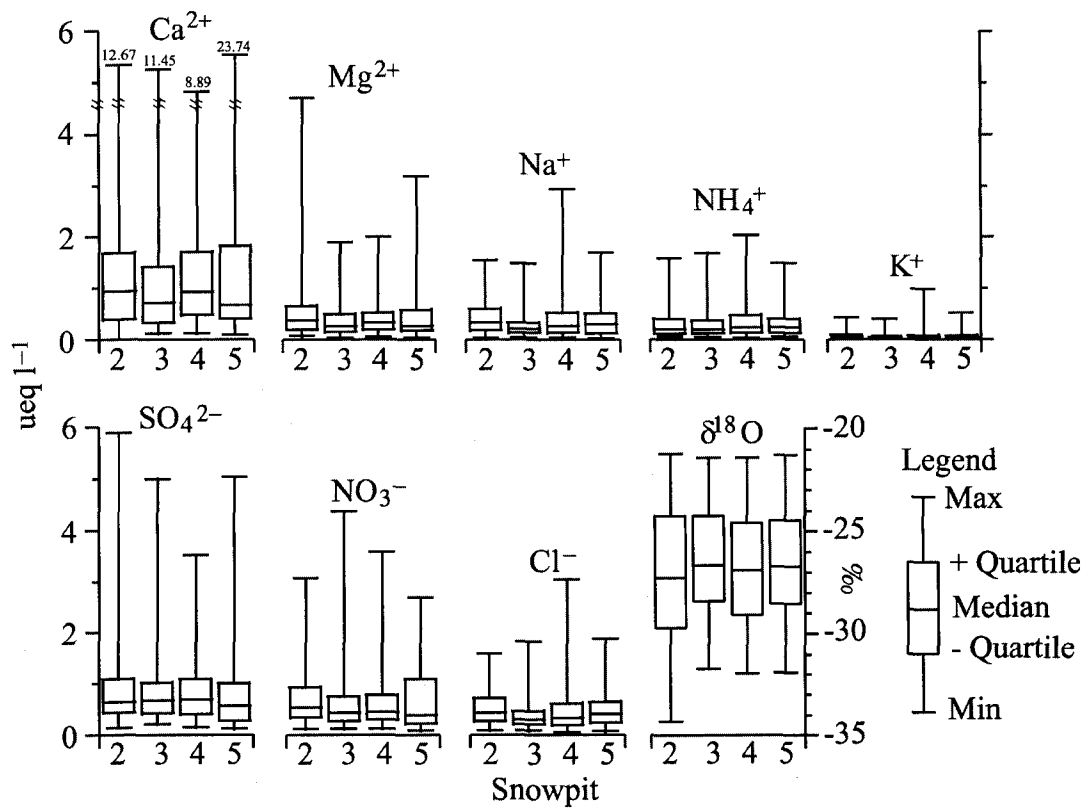
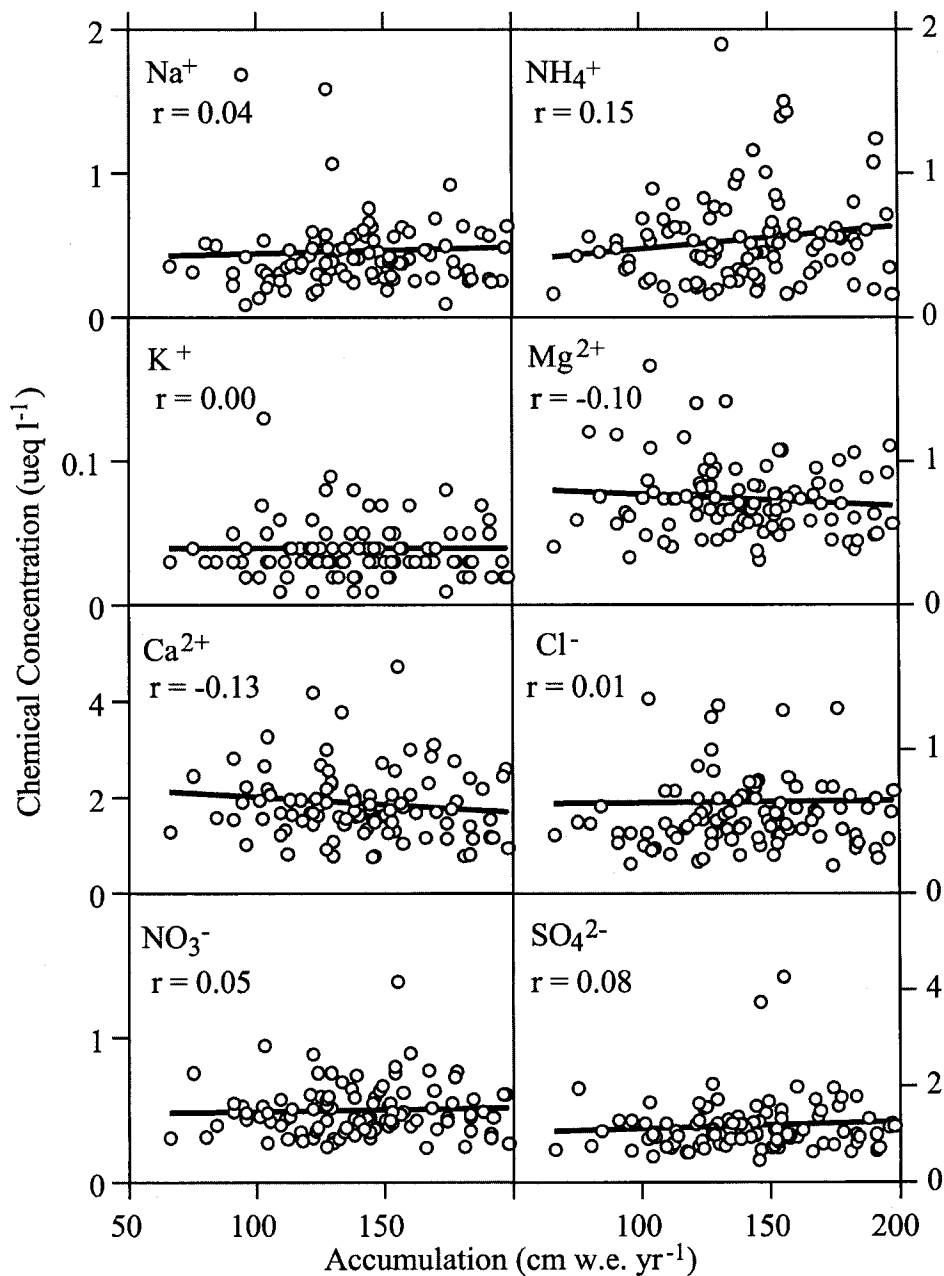
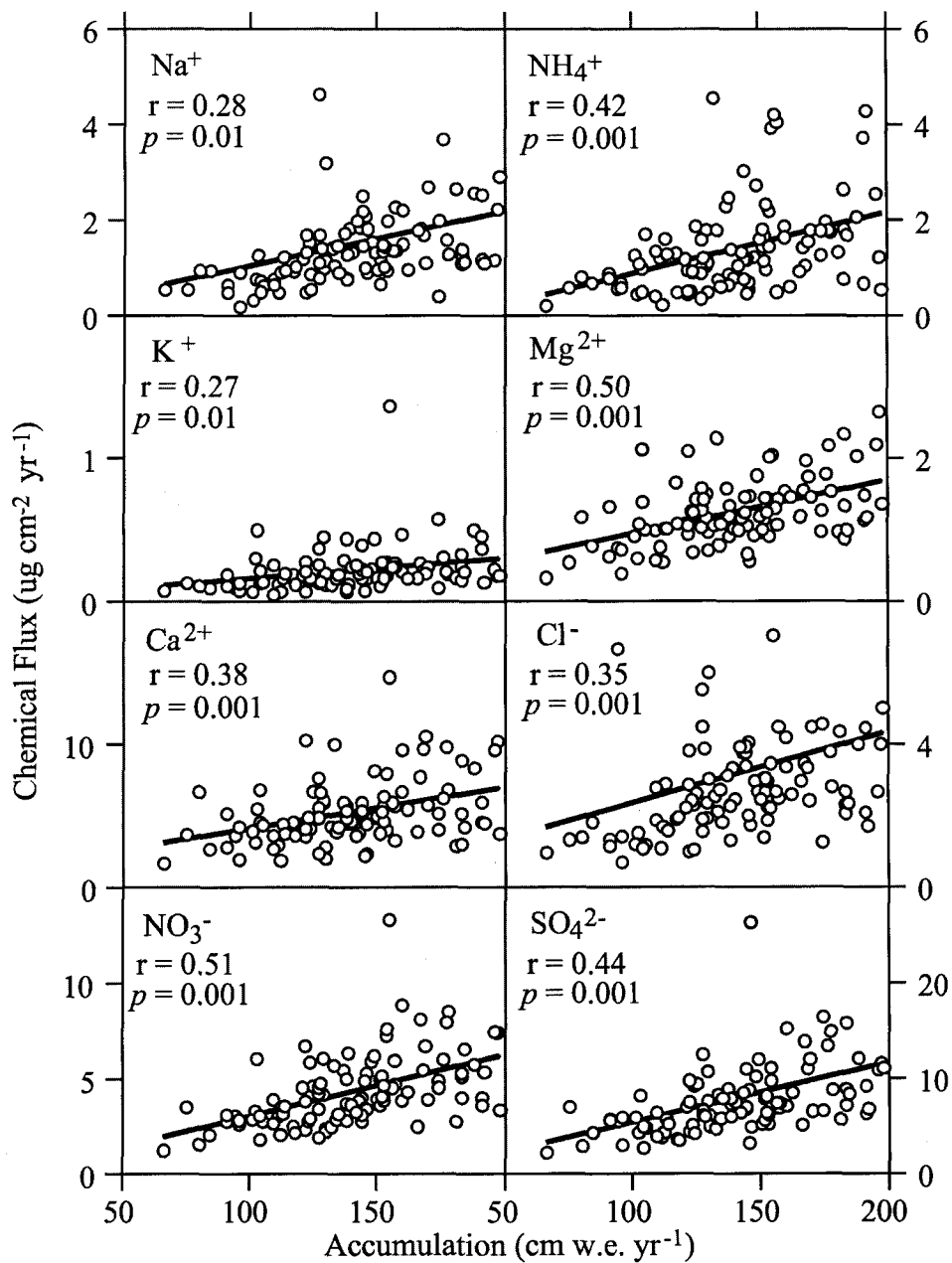


Figure III.4. Box plot summary of snowpit chemical composition.



**Figure III.5.** Annual mean chemical concentration versus snow accumulation for the Eclipse 1996 ice core. The solid line is the least squares fitted regression line for each species, with correlation coefficients ( $r$ ) as indicated. None of these correlations are statistically significant at the 95% confidence level.



**Figure III.6.** Chemical flux versus snow accumulation for the Eclipse 1996 ice core. The solid line is the least squares fitted regression line for each species, with correlation coefficients ( $r$ ) as indicated. Statistical significance levels ( $p$ ) as indicated ( $n = 100$ ).

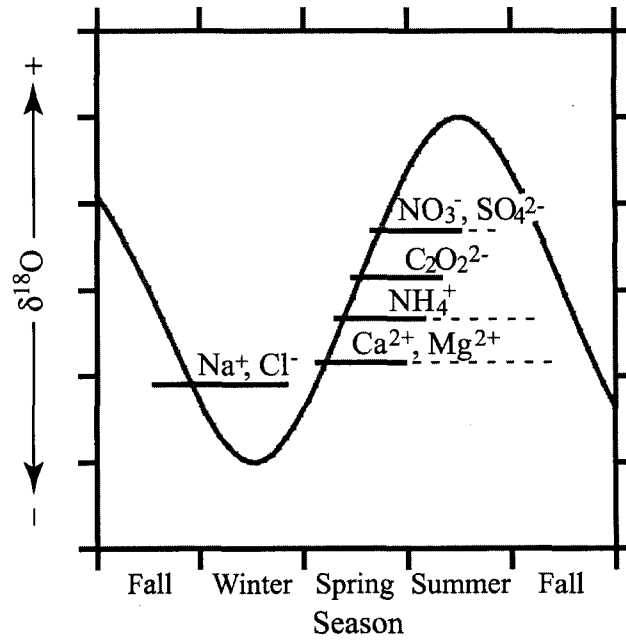


**Figure III.7.** Summary of chemical species input timing at Eclipse with respect to an idealized oxygen isotope curve (after Whitlow *et al.*, 1992). Solid lines indicate times when maximum concentrations frequently occur, while dashed extensions indicate periods where peaks are sometimes noted.

## References

- Bergin, M.H., J.L. Jaffrezo, C.I. Davidson, J.E. Dibb, S.N. Pandis, R. Hillamo, W. Maenhaut, H.D. Kuhns, and T. Makela, The contributions of snow, fog, and dry deposition to the summer flux of anions and cations at Summit, Greenland, *Journal of Geophysical Research*, 100, 16,275-16,288, 1995.
- Dansgaard, W., S.J. Johnsen, H.B. Clausen, and N. Gundestrup, Stable isotope glaciology, *Meddelelser om Gronland Bd*, 197, N2, 1-53, 1973.
- De Bell, L.J., M. Vozella, R.W. Talbot, and J.E. Dibb, Asian dust storm events of spring 2001 and associated pollutants observed in New England by the AIRMAP monitoring network, *Journal of Geophysical Research*, 109, 1304, doi: 10. 1029/2003JD003733, 2004.
- Dibb, J.E., Overview of field data on the deposition of aerosol-associated species to the surface snow of polar glaciers, particularly recent work in Greenland; in *Processes of Chemical Exchange between the Atmosphere and Polar Snow*, NATO ASI Series, vol. 43, edited by E.W. Wolff and R. C. Bales, 249-274, Springer, New York, 1996.
- Dibb, J.E., and J.L. Jaffrezo, Air-snow investigations at Summit, Greenland: An overview; *Journal of Geophysical Research*, 102, 26,795-26,807, 1997.
- Dibb, J. E., M. Arsenault, M.C. Peterson and R.E. Honrath, Fast nitrogen oxide photochemistry in Summit, Greenland snow, *Atmospheric Environment*, 36, 2501- 2511, 2002.
- Fisher, D.A., R.M. Koerner, W.S.B. Paterson, W. Dansgaard, N. Gundestrup, and N. Reeh, Effect of wind scouring on climatic records from ice core oxygen isotope profiles, *Nature*, 301, 205-209, 1983.
- Goto-Azuma, K., R.M. Koerner, M. Nakawo, and A. Kudo, Snow chemistry of Agassiz Ice Cap, Ellesmere Island, Canada, *Journal of Glaciology*, 43, 199-206, 1997.
- Herron, M.M., Impurity sources of F<sup>-</sup>, Cl<sup>-</sup>, NO<sub>3</sub><sup>-</sup>, and SO<sub>4</sub><sup>2-</sup> in Greenland and Antarctic precipitation, *Journal of Geophysical Research*, 87, 3052- 3060, 1982.
- Holdsworth, G. and E. Peake, Acid content of snow at a mid-troposphere sampling site on Mt. Logan, Yukon, Canada, *Annals of Glaciology*, 7, 153- 159, 1985.
- Jordan, C.E., J.E. Dibb, B.E. Anderson, and H.E. Fuelberg, Uptake of nitrate and sulfate on dust aerosols during TRACE-P, *Journal of Geophysical Research*, 108, 8817, doi: 10. 1029/2002JD003101, 2003.
- Keene, W.C., A.P. Pszenny, J.N. Galloway, and M.E. Hawley, Sea-salt corrections and interpretation of constituent ratios in marine precipitation, *Journal of Geophysical Research*, 91, 6647- 6658, 1986.
- Kreutz, K.J, P.A. Mayewski, L.D. Meeker, M.S. Twickler, and S.I Whitlow, The effect of spatial and temporal accumulation rate variability in West Antarctica on soluble ion deposition, *Geophysical Research Letters*, 27, 2517-2520, 2000.

- Kreutz, K.J., P.A. Mayewski, M.S. Twickler, S.I. Whitlow, J.W.C. White, C.A. Shuman, C.F. Raymond, H. Conway, and J.R. McConnell, Seasonal variations of glaciochemical, isotopic, and stratigraphic properties in Siple Dome (Antarctica) surface snow, *Annals of Glaciology*, 29, 38-44, 1999.
- Legrand, M.R., and R.J. Delmas, Formation of HCl in the Antarctic atmosphere, *Journal of Geophysical Research*, 93, 7153-7168, 1988.
- Legrand, M.R., and S. Kirchner, Origins and variations of nitrate in south polar precipitation, *Journal of Geophysical Research*, 95, 3493-3507, 1990.
- Legrand, M., and P.A. Mayewski, Glaciochemistry of polar ice cores: a review, *Reviews of Geophysics*, 35, 219-243, 1997.
- Mayewski, P.A., M.J. Spencer, M.S. Twickler, and S. Whitlow, A glaciochemical survey of the Summit region, Greenland, *Annals of Glaciology*, 14, 186-190, 1990.
- Peixoto, J.P., and A.H. Oort, *Physics of Climate*, American Institute of Physics, New York, 1992.
- Seinfeld, J.H., and S.N. Pandis, *Atmospheric Chemistry and Physics: from Air Pollution to Climate Change*, John Wiley, New York, 1998.
- Taylor-Barge, B, The summer climate of the St. Elias mountain region, *Arctic Institute of North America, Research Paper No. 53*, 1969.
- Toom-Saunty, D., and L.A. Barrie, Chemical composition of snowfall in the high Arctic: 1990-1994, *Atmospheric Environment*, 36, 2683-2693, 2002.
- Wake, C., Yalcin, K. and Gundestrup, N., The climate signal recorded in the oxygen isotope, accumulation, and major ion time-series from the Eclipse ice core, Yukon, *Annals of Glaciology*, 35, 416-422, 2002.
- Wake, C.P., P.A. Mayewski, and S. Kang, Climatic interpretation of the gradient in glaciochemical signals across the crest of the Himalaya, in *Earth Paleoenvironments: Records preserved in Mid- and Low-Latitude Glaciers*, edited by L.D. Cecil, pp. 81-94, Kluwer Academic Publishers, 2004.
- Whitlow, S., P.A. Mayewski, and J.E. Dibb, A comparison of major chemical species seasonal concentration and accumulation at the South Pole and Summit, Greenland, *Atmospheric Environment*, 26A, 2045-2054, 1992.
- Yalcin, K. and C.P. Wake, Anthropogenic signals recorded in an ice core from Eclipse Icefield, Yukon, Canada, *Geophysical Research Letters*, 28, 4487-4490, 2001.
- Yalcin, K., C.P. Wake and M. Germani, A 100-year record of North Pacific volcanism in an ice core from Eclipse Icefield, Yukon, Canada, *Journal of Geophysical Research*, 108, 10.1029/2002JD002449, 2003.
- Yalcin, K., C.P. Wake, K.J. Kreutz, and S.I. Whitlow, Forest fire signals recorded in ice cores from Eclipse Icefield, Yukon, Canada, *Eos Transactions, American Geophysical Union*, 85 (47), Fall Meeting Supplement, Abstract PP23C-06, 2004.

- Yang, Q., P.A. Mayewski, S. Whitlow, M. Twickler, M. Morrison, R. Talbot, J. Dibb, and E. Linder, Global perspective of nitrate flux in ice cores, *Journal of Geophysical Research*, *100*, 5113-5121, 1995.
- Yang, Q, P.A. Mayewski, E. Linder, S. Whitlow, and M. Twickler, Chemical species spatial distribution and relationship to elevation and snow accumulation rate over the Greenland ice sheet, *Journal of Geophysical Research*, *101*, 18,629-18,637, 1996.
- Zdanowicz C., Y. Amelin, I. Girard, G. Hall, J. Percival, J. Vaive, P. Biscaye, and A. Bory, Trans-Pacific Transport of Asian Desert Dust: Characterization of Fallout in the St-Elias Mountains, Yukon, Canada, *Eos Transactions, American Geophysical Union*, *85*(17), Joint Assembly Supplement, Abstract A23C-06, 2004.



## CHAPTER IV

### AEROSOL, SNOW, AND FIRN CORE CHEMISTRY AT KING COL, MT. LOGAN MASSIF, YUKON, CANADA

#### Abstract

Simultaneous samples of aerosol (n=48) and recent snow (n=193) chemistry were collected at King Col (4135 m) in the St. Elias Mountains, Yukon, between May 17 and June 11, 2001. A 15 m snowpit/firn core covering the period May 2001 to winter 1992-1993 was also collected. Major ion concentrations in aerosol samples were quite low with the total ionic burden averaging  $5.52 \text{ neq m}^{-3}$  at standard temperature and pressure (STP). Inter-species aerosol relationships indicate the presence of  $(\text{NH}_4)_2\text{SO}_4$  aerosol at King Col and an aerosol Cl<sup>-</sup> deficiency relative to seawater due to volatilization of HCl by reaction with unneutralized  $\text{SO}_4^{2-}$  that is present in half of the samples. Backwards trajectories for select aerosol concentration peaks document the transport of Asian dust and anthropogenic emissions, the eruption plume from the May 22 eruption of Sheveluch, Kamchatka, and sea salt from the marine boundary layer over the Gulf of Alaska to King Col at discrete times during the sampling period. Fresh snow chemistry generally mimics aerosol chemistry with similar relative abundances and inter-species relationships except for large enrichments in snow Cl<sup>-</sup> and NO<sub>3</sub><sup>-</sup> relative to aerosol due to snow scavenging of gas phase HCl and HNO<sub>3</sub>. Although relatively strong correlations between aerosol and snow concentrations were observed for species associated with accumulation mode aerosols, e.g. NH<sub>4</sub><sup>+</sup> (r = 0.56) and SO<sub>4</sub><sup>2-</sup> (r = 0.43), only weak correlations were observed for dust and sea salt species. These results may be influenced by greater variability in concentrations between replicate snow samples for species associated with coarse mode dust and sea salt particles. Analysis of a 15 m snowpit/firn core indicates the average annual accumulation at King Col

(4135 m) from 1993 to 2000 was 1.04 m water equivalent, compared to 1.42 m water equivalent at nearby Eclipse Icefield (3017 m) over the same period. Comparison of average annual major ion concentrations and fluxes from 1993-2000 at King Col and Eclipse Icefield demonstrates greater inputs of sea salt and dust at Eclipse by factors of two to five, respectively. The average  $\text{Cl}^-/\text{Na}^+$  micro-equivalent ratio in snow at Eclipse (1.37) more closely approaches the seawater ratio than King Col snow (2.56), indicating less snow scavenging of gas phase HCl at Eclipse. The April 2001 Asian dust plume is clearly recorded at King Col, where it contributes between 33 and 94% of the average annual flux for  $\text{Na}^+$ ,  $\text{K}^+$ ,  $\text{Mg}^{2+}$ , and  $\text{Ca}^{2+}$  even though snowfall affected by this event accounts for only 3% of the average annual accumulation. No clear signature from the 2001 Asian dust plume is observed at Eclipse Icefield.

## Introduction

Ice cores retrieved from the polar ice sheets and suitably located mountain glaciers arguably provide the highest resolution and most direct view of Earth's paleo-atmosphere over time scales ranging from decades to hundreds of thousands of years (e.g., Legrand and Mayewski, 1997). In the circum-Arctic region ice core records are available from sites throughout Greenland (e.g., Mayewski *et al.*, 1986; Hammer *et al.*, 1997; Fischer *et al.*, 1998, Mosley-Thompson *et al.*, 2001) as well as the Agassiz, Devon, and Penny Ice Caps in the eastern Canadian Arctic (e.g., Koerner *et al.*, 1999; Murphy, 2000; Grunet *et al.* 2001). In the Eurasian Arctic ice cores have been recovered from Svalbard (Goto-Azuma *et al.*, 1995), Franz Josef Land (Kotlyakov *et al.*, 2004), Akademii Nauk (Fritzsche *et al.*, 2002), and the summit ice cap of Ushkovsky Volcano on the Kamchatka Peninsula (Shiraiwa *et al.*, 1997).

Recently, the St. Elias Mountains in northwest North America have become the focus of an international ice coring effort (Figure IV.1). Early work on ice cores recovered from the Northwest Col (5430 m) of Mt. Logan in 1980 and Eclipse Icefield (3017 m) in 1996 demonstrated that differences in elevation allow the sites to sample different layers of the atmosphere, resulting in complementary and distinct records (Holdsworth *et al.*, 1988; Yalcin and Wake, 2001; Wake *et al.*, 2002; Yalcin *et al.*, 2003). During the 2001 and 2002 field seasons, a suite of new ice cores were recovered from the St. Elias Mountains spanning an elevation range from 3017 to 5340 m. Ice cores were drilled at both Prospector-Russell Col (5340 m) and King Col (4135) on Mt. Logan (Goto-Azuma *et al.*, 2003; Fisher *et al.*, 2004). Additional cores were drilled at the saddle (4400 m) between Mt. Bona and Mt. Churchill (Thompson *et al.*, 2004) and the summit ice cap (4100 m) of Mt. Wrangell (Kanamori *et al.*, 2004), and two new ice cores were collected from Eclipse Icefield (3017 m) (Yalcin *et al.*, 2004). Together, these records offer a unique opportunity to construct a three-dimensional view of the paleo-atmosphere.

However, interpreting the unique chemical records contained in ice cores requires knowledge of the site-specific relationships between snow chemistry and that of the precipitating

air mass that can be obtained by simultaneous collection of aerosol and snow samples (e.g., Dibb and Jaffrezo, 1997). Such investigations are important given the wealth of paleoenvironmental information potentially available from ice cores and the uncertainty in relating glaciochemical to atmospheric concentrations. Programs such as the Dye 3 Gas and Aerosol Sampling Program and the Summit, Greenland atmospheric research program represent international collaborative efforts to better understand the processes influencing chemical species eventually preserved in Greenland ice cores (e.g., Jaffrezo and Davidson, 1993; Dibb and Jaffrezo, 1997). Sampling campaigns have also characterized the aerosol at high elevation sites in Central Asia (Wake *et al.*, 1994; Shrestha *et al.*, 2000) and the European Alps (Henning *et al.*, 2003), and investigated the air-snow relationships at mountain glacier sites (Baltensperger *et al.*, 1992; Shrestha *et al.*, 1997, 2002; Sun *et al.*, 1998).

In support of ice coring efforts on the summit plateau of Mt. Logan, an intermediate elevation climbing camp and research station was established at King Col (60.35° N, 140.36° W, 4135 m elevation) on the Mt. Logan massif during the 2001 field season (Figure IV.1). From May 17 to June 11, twice daily aerosol and three to five replicate fresh or surface snow samples were collected. Samples from a 3 m snowpit and a 12 m firn core were also collected. The resulting database provides the information needed to characterize the late spring-early summer aerosol at King Col, examine the relationships between aerosol and snow chemistry on an event basis, and compare major ion concentrations and fluxes at King Col to those at nearby Eclipse Icefield.

### **Methods**

Twice-daily aerosol samples were collected at King Col from May 17 to June 11 using a 24V high volume pump with inline flow meter powered by a combination of photovoltaic cells and batteries. Aerosol sampling was conducted on the south side of the col, 120 m from camp in a direction perpendicular to the prevailing wind direction to minimize potential local contamination from the camp. Samples were collected on 1 µm pore size; 90 mm diameter Teflon

filters (Fluropore filters, Millipore, Bedford, MA). Filters were changed twice daily at around 8 am and 8 pm and therefore represent approximately daytime and nighttime samples. Sample collection times ranged from eight to fifteen hours and averaged twelve hours. Corrections for ambient temperature and pressure allowed conversion of the measured air volumes to standard cubic meters ( $\text{m}^3$  STP). Sampled volumes ranged from 17.19 to 42.63  $\text{m}^3$  STP and averaged 29.89  $\text{m}^3$  STP. The mean flow rate was 2.4  $\text{m}^3$  STP  $\text{hr}^{-1}$  yielding a velocity at the face of the filter of 10.5  $\text{cm s}^{-1}$ . This velocity is high enough for this kind of filter to have collection efficiency greater than 90% for aerosol particles larger than 0.3  $\mu\text{m}$  (Hinds, 1999). The cutoff for large particles, as given by their sedimentation velocity, is estimated at about 20  $\mu\text{m}$  (Hinds, 1999).

Care was taken to minimize contamination. Each filter was pre-loaded onto a polyethylene cassette in a class 100 clean room at the University of New Hampshire and sealed inside a clean polyethylene bag. Just prior to sample collection, the filter was removed from the sealed bag and mounted face down inside a 0.20 m diameter protective cylindrical Delrin housing 2 m above the snow surface. After sampling, the filters, still in their cassettes, were returned to their original clean polyethylene bags, double sealed in plastic bags, and stored in a snow cave. Ten procedural blanks were collected in the course of the sampling campaign by placing a loaded filter cassette in the housing and immediately removing and re-sealing. Filter blanks were analyzed with the samples to quantify blank levels and check for contamination.

Concurrently with aerosol sample collection, three to five replicate fresh or aged surface snow samples were collected about 20 m away from the aerosol sampling site by scraping the surface snow layer directly into pre-cleaned polypropylene cups. A non-particulating suit, face mask, and polyethylene gloves were worn at all times during aerosol and snow sample collection. A total of 48 aerosol samples and 193 fresh and aged surface snow samples were collected during the sampling period. In addition, a 3 m snowpit was excavated on May 26 and sampled continuously at 5 cm resolution for major ions using clean techniques detailed elsewhere

(Mayewski *et al.*, 1990). A 12 m firn core was taken from the bottom of the pit using a SIPRE hand auger and returned frozen to the University of New Hampshire where it was continuously sampled at 10 cm resolution using clean techniques.

All samples were returned frozen to the Climate Change Research Center at the University of New Hampshire for processing and analysis. The aerosol extraction followed the same procedures used by the Atmospheric Investigation, Regional Modeling, Analysis, and Prediction (AIRMAP) network (Slater and Dibb, 2003). Filters were saturated with 0.5 ml high purity methanol and the soluble components extracted with three successive 5 ml aliquots of deionized Milli-Q water, and preserved with chloroform. Filter extracts as well as fresh and aged surface snow, snowpit, and firn core samples were analyzed by suppressed ion chromatography for eight inorganic ions ( $\text{Na}^+$ ,  $\text{NH}_4^+$ ,  $\text{K}^+$ ,  $\text{Mg}^{2+}$ ,  $\text{Ca}^{2+}$ ,  $\text{Cl}^-$ ,  $\text{NO}_3^-$ ,  $\text{SO}_4^{2-}$ ) and one organic ion ( $\text{C}_2\text{O}_4^{2-}$ ) in a dedicated laboratory at the University of New Hampshire Climate Change Research Center. The cation system used a CS12A column with CSRS-ultra suppressor in auto suppression recycle mode with 20 mM MSA eluent. The anion system used an AS11 column with an ASRS-ultra suppressor in auto suppression recycle mode with 6 mM NaOH eluent. Precision of the results was monitored by running ten percent of the samples in duplicate and found to be 10% for aerosol  $\text{Mg}^{2+}$ , less than 5% for other aerosol cations, and less than 2% for aerosol anions. For snow and firn core samples, precision was 7% for  $\text{K}^+$ , 4% for  $\text{NH}_4^+$ , 3% for  $\text{Ca}^{2+}$ , and less than 2% for other species.

Aerosol detection limits were defined as two standard deviations of the blank values divided by the mean sample volume (Shrestha *et al.*, 2000). The detection limits for aerosol species were (in  $\text{neq m}^{-3}$  STP):  $\text{Na}^+$  (0.281),  $\text{NH}_4^+$  (0.008),  $\text{K}^+$  (0.034),  $\text{Mg}^{2+}$  (0.023),  $\text{Ca}^{2+}$  (0.025),  $\text{Cl}^-$  (0.236),  $\text{NO}_3^-$  (0.004),  $\text{SO}_4^{2-}$  (0.049),  $\text{C}_2\text{O}_4^{2-}$  (0.002). The mean concentration of the ten aerosol procedural blanks were subtracted from the sample concentrations, which resulted in below detection limit (b.d.) values for  $\text{Na}^+$  (6 samples),  $\text{NH}_4^+$  (2 samples),  $\text{K}^+$  (5 samples),  $\text{Mg}^{2+}$  (11 samples),  $\text{Ca}^{2+}$  (6 samples), and  $\text{Cl}^-$  (12 samples). Aliquots of firn core samples were also

analyzed for stable isotopic composition at the University of Maine Stable Isotope Laboratory with a Eurovector Cr pyrolysis unit coupled to a GV Isoprime mass spectrometer for  $\delta D$  (precision  $\pm 0.5\text{‰}$ ). Sea salt (ss) and non-sea-salt (nss) fractions for aerosol and snow samples were estimated by determining the limiting sea salt species in each sample and using that species as the sea salt indicator (Keene *et al.*, 1986).

## **Results and Discussion**

### **Characterization of King Col aerosol**

Summary statistics of King Col aerosol chemical composition measured between May 17 and June 11, 2001 are presented in Table IV.1 and time series of aerosol concentrations for major inorganic ions are presented in Figure IV.2. In general aerosol concentrations are very low, reflecting the remote location of the King Col site relative to source regions. The average total ionic burden (total cations plus total anions) ranged from 1.30 to 13.21 neq m<sup>-3</sup> STP, and averaged 5.52 neq m<sup>-3</sup> STP. Ammonium and sulfate are the dominant ions present, on average accounting for 49% of the total aerosol load. The sum of cations exceeds the sum of anions in all but three samples; with the charge balance (sum of cations minus sum of anions) averaging 0.71 neq m<sup>-3</sup> STP. This cation excess could be balanced by carbonate ions (HCO<sub>3</sub><sup>-</sup>/CO<sub>3</sub><sup>2-</sup>) that were not measured in this study. In fact, if the observed concentrations of Ca<sup>2+</sup> and Mg<sup>2+</sup> are assumed to be accompanied by an equal amount of carbonate ions (Toom-Sauntry and Barrie, 2002), the calculated charge balance is excellent (averaging 0.14 neq m<sup>-3</sup> STP). The remaining cation excess is likely balanced by small amounts of organic acids (e.g., formate, acetate, methylsulfonate) (Toom-Sauntry and Barrie, 2002).

On average, higher concentrations of Na<sup>+</sup> (11%), Cl<sup>-</sup> (7%), and K<sup>+</sup> (13%) are observed in daytime aerosol samples. Meanwhile, higher concentrations of Ca<sup>2+</sup> (9%), Mg<sup>2+</sup> (27%), NH<sub>4</sub><sup>+</sup> (11%), NO<sub>3</sub><sup>-</sup> (9%), SO<sub>4</sub><sup>2-</sup> (11%), and C<sub>2</sub>O<sub>4</sub><sup>2-</sup> (14%) are seen in nighttime samples. However, a Student's T-test indicates that none of these differences are statistically significant. Conversely,

large differences in aerosol concentrations between day and night samples have been observed at high altitude sites in the Alps (Baltensperger *et al.*, 1997; Lugauer *et al.*, 1998) and Himalayas (Shrestha *et al.*, 2002) with generally lower aerosol concentrations present at night. These differences have been attributed to regionally extensive mountain/valley wind systems that transport air with higher aerosol concentrations from lower elevations during the day, and pull cleaner air down from aloft at night (Whiteman, 1990). Although the Alps and Himalayas are affected by lower-elevation regional pollution sources to a much greater extent than the St. Elias Mountains, no diurnal variability in aerosols species from natural sources (e.g., dust) is observed at King Col either. The lack of diurnal fluctuations in aerosol concentrations at King Col suggests that mountain/ valley wind systems, if present, are not sufficiently extensive to advect air with higher aerosol burdens from comparatively distant, non-glacierized regions.

Linear regression on all water soluble species in the aerosol (Table IV.2) showed that the sea salt species  $\text{Na}^+$  and  $\text{Cl}^-$  are highly correlated ( $r = 0.89$ ) and the dust indicators  $\text{Ca}^{2+}$  and  $\text{Mg}^{2+}$  are well correlated ( $r = 0.76$ ). Likewise,  $\text{NH}_4^+$  is highly correlated with  $\text{SO}_4^{2-}$  ( $r = 0.90$ ) and also correlates well with  $\text{NO}_3^-$  ( $r = 0.73$ ), suggesting that these species are present in the same air masses. The higher correlation of  $\text{NH}_4^+$  with  $\text{SO}_4^{2-}$  than with  $\text{NO}_3^-$  reflects the preferential reaction of ammonia with sulfuric rather than nitric acid (Bassett and Seinfeld, 1983). The mean  $\text{NH}_4^+/\text{SO}_4^{2-}$  molar ratio is 2.16, suggesting the principal form of ammonium sulfate particles at King Col is  $(\text{NH}_4)_2\text{SO}_4$  and not  $\text{NH}_4\text{HSO}_4$ . This result differs from those of Barrie and Barrie (1990) and Shrestha *et al.* (1997) who demonstrated that  $\text{NH}_4\text{HSO}_4$  was the principal sulfate aerosol species in the high Arctic and Himalayas, respectively. Because sufficient  $\text{NH}_4^+$  exists in King Col aerosols to fully neutralize  $\text{SO}_4^{2-}$  more than half the time, ammonium nitrate aerosol ( $\text{NH}_4\text{NO}_3$ ) may be present at King Col, as implied by the good correlation between  $\text{NH}_4^+$  and  $\text{NO}_3^-$ . Dust species, for example  $\text{Ca}^{2+}$ , are highly correlated with  $\text{NO}_3^-$  ( $r = 0.91$ ) and well correlated with  $\text{SO}_4^{2-}$  ( $r = 0.75$ ), implying uptake of sulfate and nitrate by dust particles (e.g., Jordan *et al.*, 2003). However, we do not observe a strong relationship between the equivalence



ratios of  $\text{NH}_4^+/\text{SO}_4^{2-}$  and  $\text{Ca}^{2+}/\text{SO}_4^{2-}$  ( $r = 0.20$ ) as has been reported from high elevations sites in central Asia (e.g., Sun *et al.*, 1998). This is probably due to lower dust loadings in the King Col aerosol relative to Central Asian aerosols, making  $(\text{NH}_4)_2\text{SO}_4$  a far more important sulfate bearing aerosol species than  $\text{CaSO}_4$  at King Col. King Col aerosol  $\text{Ca}^{2+}$  averages  $0.52 \text{ neq m}^{-3}$  STP, while at a 5000 m site in the Himalaya they average  $1.24 \text{ neq m}^{-3}$  STP during the monsoon season, when dust loadings are at their annual minimum (Shrestha *et al.*, 1997).

The  $\text{Cl}^-/\text{Na}^+$  equivalent ratio in our samples averages 0.69, considerably less than the seawater ratio of 1.16 (Keene *et al.*, 1986), indicating a  $\text{Cl}^-$  deficiency in the King Col aerosol relative to  $\text{Na}^+$  despite the high correlation between the two. A chloride excess is observed in only one sample, with all other samples chloride deficient. Differences in  $\text{Cl}^-/\text{Na}^+$  ratios relative to seawater are attributed to acidification of sea salt particles by reaction with  $\text{H}_2\text{SO}_4$  (Legrand and Delmas, 1988; Gard *et al.*, 1998). This reaction volatilizes sea salt chloride to produce gas-phase and highly soluble  $\text{HCl}$ , resulting in depletion of aerosol  $\text{Cl}^-$  and enrichment of  $\text{Cl}^-$  in precipitation. Although the mean  $\text{NH}_4^+/\text{SO}_4^{2-}$  molar ratio in the King Col aerosols is 2.16, suggesting  $(\text{NH}_4)_2\text{SO}_4$  is the principal ammonium sulfate species, there is an equivalence excess of  $\text{SO}_4^{2-}$  relative to  $\text{NH}_4^+$  in 49% of the samples. A good correlation between the chloride deficit and unneutralized sulfate (sulfate minus ammonium, in equivalence units) in our samples ( $r=0.57$ ) suggests this mechanism is indeed responsible for the chloride deficiency in the King Col aerosol. Apportionment of the King Col aerosol into sea salt and non- sea salt fractions using  $\text{Na}^+$  and  $\text{Mg}^{2+}$  as the sea salt indicators ( $\text{K}^+$ ,  $\text{Ca}^{2+}$ , and  $\text{SO}_4^{2-}$  were not found to be limiting in any of the samples) suggests that nearly all (>90%) of the aerosol  $\text{Na}^+$  and  $\text{Cl}^-$  at King Col is from sea salt, while nearly all (>90%) of the aerosol  $\text{K}^+$ ,  $\text{Ca}^{2+}$ , and  $\text{SO}_4^{2-}$  is from non-sea salt sources. Only  $\text{Mg}^{2+}$  is found to have significant contributions from both sea salt and non-sea salt sources, with 1/3 of the aerosol  $\text{Mg}^{2+}$  at King Col from sea salt.

### **Temporal variations in aerosol chemical composition**

Multi-day variations in aerosol concentrations at King Col (Figure IV.2) can be related to changes in aerosol source regions and transport and to the timing of precipitation events. To investigate aerosol source regions and transport pathways, backward trajectories using King Col as the end point were calculated for elevations of 3500, 4200 and 5000 m above sea level using the Hybrid Single-Particle Lagrangian Integrated Trajectory (HYSPLIT) model (Draxler and Hess, 1997) with the NCEP global reanalysis data and model vertical velocity (<http://www.arl.noaa.gov/ready/hysplit4.html>). Although the complex terrain of the St. Elias Mountains cannot be captured, the backward trajectories can indicate source regions and large scale circulation patterns affecting the region during the sampling campaign (e.g., Carrico *et al.*, 2003). Although trajectories indicate the movement of air masses rather than the location of atmospheric injection, knowledge of likely aerosol source regions (e.g., arid regions for dust aerosols, urban centers for anthropogenic aerosols) can be used to infer where different aerosols were added to an air mass. Tightly coupled trajectory paths between 3500 and 5000 m elevation provide confidence in the model calculations for trajectory paths reaching King Col, while divergent trajectory paths over this elevation range suggest a degree of uncertainty in the trajectory paths. In particular, we discuss aerosol source regions as deduced using backward trajectories for four aerosol concentration peaks observed during the May 17 to June 11 sampling period, as well as a “clean air” period free of local precipitation (Figure IV.3).

Events 1 and 2 are characterized by high concentrations of  $\text{Ca}^{2+}$ ,  $\text{Mg}^{2+}$ ,  $\text{NO}_3^-$ ,  $\text{NH}_4^+$ , and  $\text{SO}_4^{2-}$  on May 22 and May 26- 27 (Figure IV.2). Dust ( $\text{Ca}^{2+}$  and  $\text{Mg}^{2+}$ ) and  $\text{NO}_3^-$  concentrations are higher for the May 22 event, while  $\text{NH}_4^+$  and  $\text{SO}_4^{2-}$  concentrations are higher for the May 26-27 event. HYSPLIT model back trajectories for Event 1 diverge significantly after only 48 hours. Consequently, we have less confidence in source region identification; although an Asian influence is suggested by the trajectories ending at 4200 and 5000 m. However, trajectory paths for Event 2 are tightly coupled back through time, especially above 3500 m, and indicate an

Asian source region incorporating both crustal dust from Central Asia and anthropogenic pollution from northeast China and Korea (Figure IV.3). Trajectories move around the base of a low pressure trough from central Siberia and across the Gobi desert region, as would be expected during an outbreak of continental polar air concomitant with dust storm generation (Sun *et al.*, 2001). Trajectories continue across industrialized regions of Korea and northeast China where an anthropogenic  $\text{SO}_4^{2-}$  and  $\text{NO}_3^-$  component could have been added to the air mass. The air then moves north around a high pressure ridge over the western Pacific where precipitation scavenging would be minimal before being entrained by the Aleutian Low and advected into the St. Elias Mountains.

Because wet deposition is an important aerosol removal process (Barrie, 1985), precipitation plays an important role in short-term reductions of aerosol concentrations (e.g., Shrestha *et al.*, 2000). This is illustrated by abrupt decreases in aerosol concentrations at King Col that are closely tied to the timing of local snowfall events. For example, the King Col aerosol was cleansed by snowfall events on May 22-23 and May 27, as reflected by abrupt decreases in aerosol concentrations, ending the aerosol concentration peaks associated with Events 1 and 2 (Figure IV.2). Interestingly, Event 1 aerosol concentrations do not immediately respond to the onset of precipitation on May 22. In fact, peak aerosol loading during Event 1 occurs during the first twelve hours of snowfall. In contrast, Event 2 aerosol concentrations immediately drop with the onset of snowfall on May 27. This cleansing by precipitation is also seen in the surface snow following these two events, with discernible increases in all the aforementioned species in the snow that fell during and immediately after the aerosol concentration peaks (Figure IV.2).

Event 3 is a peak in aerosol  $\text{SO}_4^{2-}$  on May 30-31 without concurrent increases in other aerosol species indicative of marine ( $\text{Na}^+$ ,  $\text{Cl}^-$ ) or continental ( $\text{Ca}^{2+}$ ,  $\text{Mg}^{2+}$ ) sources (Figure IV.2), suggesting a volcanic origin of the observed sulfate peak. In fact, three major eruptions from Sheveluch Volcano on the Kamchatka peninsula occurred between May 19 and May 22 (Bulletin of the Global Volcanism Network, 2001). The eruption of May 22 was the largest, producing a

mushroom cloud to 20 km height. Back trajectories suggest the May 22 eruption plume did in fact reach the St. Elias on May 31 within a narrow elevation range centered on King Col. Trajectories arriving at lower (3500 m) or higher (5000 m) elevations between May 30-31 originated south of the Aleutians or near the Bering Strait, respectively. Hence, air masses at elevations below or above King Col may not have carried the signature of the Sheveluch eruption. Consequently, this moderately large eruption (VEI 4) may not be identifiable in glaciochemical records from lower (Eclipse Icefield) or higher (Mt. Logan) sites, illustrating that transport of volcanic plumes at different elevations can result in distinct paleovolcanic records from these three sites.

Event 4 is a three-pronged peak in sea salt species ( $\text{Na}^+$  and  $\text{Cl}^-$ ) with the peak aerosol concentrations occurring on June 3, 5, and 7 (Figure IV.2). The days following the concentration peaks (June 4, 6, and 8) were days with snow, again illustrating the cleansing effect of precipitation on aerosol concentrations. Back trajectories for all three days of high sea salt concentrations were similar, indicating air masses originating in the Gulf of Alaska moved along the southeast Alaska coast and into the St. Elias Mountains (Figure IV.3). Furthermore, the air masses sampled at King Col during this period had been lofted from marine boundary layer within the prior 48 hours. These trajectories provide clear evidence that sea salt aerosols from the marine boundary layer over the North Pacific in general and the Gulf of Alaska in particular are responsible for the sea salt concentration peaks observed at King Col. This marine boundary layer trajectory is similar to trajectories associated with clean air and low concentrations of all aerosol species, such as was observed on June 2 (Figure IV.2). However, the trajectories of June 2 had been cleansed by orographic passage over the Coast Mountains of British Columbia within the 48 hours prior to reaching the St. Elias Mountains (Figure IV.3). Hence, low aerosol concentrations at King Col occur when air masses have recently been scavenged during orographic uplift prior to reaching the St. Elias Mountains, or following local precipitation events.

### Characterization of fresh and surface snow chemistry

Concentrations of water soluble ions in fresh and surface snow at King Col are presented in Table IV.3 and Figure IV.2. The average total ionic burden (total cations plus total anions) ranged from 1.88 to 11.79 ueq l<sup>-1</sup> and averaged 5.07 ueq l<sup>-1</sup>. As was observed in King Col aerosols, NH<sub>4</sub><sup>+</sup> and SO<sub>4</sub><sup>2-</sup> are the dominant ions present, on average accounting for 40% of the total soluble ionic impurities. Both dust (Ca<sup>2+</sup> and Mg<sup>2+</sup>; 23%) and NO<sub>3</sub><sup>-</sup> (20%) represent greater fractions of the total soluble ions in snow relative to the aerosol (11% and 5%, respectively). The charge balance (sum of cations minus sum of anions) of King Col fresh and surface snow averages -0.39 ueq l<sup>-1</sup>, with an anion excess in 62% of the samples that is presumably balanced by the hydrogen ion. Samples with a cation excess are presumably balanced by carbonate ions, in the case of samples with high dust concentrations, and/or organic acids (e.g., formate, acetate, methylsulfonate).

As with aerosol samples, linear regression of species measured in snow samples (Table IV.4) showed that the sea salt species Na<sup>+</sup> and Cl<sup>-</sup> are highly correlated ( $r = 0.90$ ), as are the dust species Ca<sup>2+</sup> and Mg<sup>2+</sup> ( $r=0.89$ ). Calcium and magnesium are also highly correlated with SO<sub>4</sub><sup>2-</sup> ( $r=0.87$  and  $0.83$ , respectively), but not as well correlated with NO<sub>3</sub><sup>-</sup> in snow samples ( $r=0.63$  and  $0.58$ , respectively) compared to aerosol samples ( $r=0.90$  and  $0.80$ , respectively). The equivalence ratios NO<sub>3</sub><sup>-</sup>/NH<sub>4</sub><sup>+</sup> and NO<sub>3</sub><sup>-</sup>/SO<sub>4</sub><sup>2-</sup> suggest enrichment of NO<sub>3</sub><sup>-</sup> in snow (1.36 and 1.09, respectively) relative to the aerosol (0.20 and 0.19, respectively). This could reflect dry deposition or snow scavenging of gas phase HNO<sub>3</sub> (e.g., Baltensperger *et al.*, 1992; Shrestha *et al.*, 1997; Toom-Saunty and Barrie, 2002). Furthermore, NH<sub>4</sub><sup>+</sup> is highly correlated with SO<sub>4</sub><sup>2-</sup> ( $r=0.70$ ) in snow, as with the aerosol, but not as well correlated with NO<sub>3</sub><sup>-</sup> ( $r=0.55$ ), again suggesting snow scavenging of gas phase HNO<sub>3</sub>. Although enrichment of SO<sub>4</sub><sup>2-</sup> relative to NH<sub>4</sub><sup>+</sup> is often observed in precipitation due to heterogeneous SO<sub>2</sub> oxidation in clouds (e.g., Calvert *et al.*, 1985), SO<sub>4</sub><sup>2-</sup>/NH<sub>4</sub><sup>+</sup> ratios at King Col suggest only slight sulfate enrichment in snow (1.06 relative to aerosol (0.93). This result implies that much of the sulfur reaching King Col has

already been oxidized to form  $\text{SO}_4^{2-}$  aerosol. Interestingly, all correlations are positive for the snow data while the aerosol data show negative correlations between sea salt ( $\text{Na}^+$ ,  $\text{Cl}^-$ ) and some non-sea-salt ( $\text{Ca}^{2+}$ ,  $\text{NH}_4^+$ ,  $\text{NO}_3^-$ ) species (Table IV.2). This reflects the greater importance of removal processes (wet and dry deposition, riming) in controlling concentrations in snow, while air mass source region and transport processes are of greater importance in controlling aerosol concentrations.

In addition to snow scavenging of gas phase nitrate, there is also evidence for snow scavenging of gas phase HCl at King Col. While the  $\text{Cl}^-/\text{Na}^+$  ratio in aerosol samples showed a chloride deficit relative to the seawater ratio, snow samples show a chloride excess. The  $\text{Cl}^-/\text{Na}^+$  equivalent ratio in our samples averages 2.12, considerably more than the seawater ratio of 1.16 (Keene *et al.*, 1986) and much larger than the ratio of 0.69 observed in aerosol samples. Excess chloride in snow is attributable to precipitation scavenging of HCl produced by acidification of sea-salt particles (Legrand and Delmas, 1988; Toom-Saunty and Barrie, 2002). However, 25% of snow samples still show a chloride deficit relative to seawater. With respect to the snow data,  $\text{Na}^+$  was the limiting sea salt species in 90% of the samples,  $\text{Mg}^{2+}$  in 8%,  $\text{K}^+$  in 1%, and  $\text{SO}_4^{2-}$  in 1%. As was the case for aerosols, nearly all of the  $\text{Ca}^{2+}$  (99%),  $\text{SO}_4^{2-}$  (96%), and  $\text{K}^+$  (90%) are from non-sea-salt sources while nearly all of the  $\text{Na}^+$  (96%) is from sea salt. Only  $\text{Mg}^{2+}$  has both significant sea salt (35%) and non sea salt (65%) sources.

### **Relationships between aerosol and snow chemistry**

To quantify the relationship between concentrations of soluble ionic impurities in King Col snow and aerosols, scavenging ratios ( $W$ ) were calculated according to:

$$W = p_{\text{air}} C_{\text{snow}} / C_{\text{air}}$$

where  $C_{\text{snow}}$  is the concentration in snow ( $\text{ng g}^{-1}$ );  $C_{\text{air}}$  is the concentration of aerosol ( $\text{ng m}^{-3}$  STP), and  $p_{\text{air}}$  is the density of air ( $1225 \text{ g m}^{-3}$  at standard temperature and pressure) (Davidson *et al.*, 1993). Large values of  $W$  indicate efficient scavenging of that species by precipitation.

Scavenging ratios were calculated from those aerosol samples with concurrent fresh snow samples (21 of 48 aerosol samples) and limited to aerosol measurements above detection limits.

Calculated scavenging ratios (Table IV.5) were consistent with values reported in the literature for sites in Greenland (Davidson *et al.*, 1985, 1993; Silvente *et al.*, 1993) and Central Asia (Sun *et al.*, 1998; Shrestha *et al.*, 2002), except for  $\text{Ca}^{2+}$ , which is found to be a factor of 2 higher at King Col. Scavenging ratios, as seen by their standard deviations, are highly variable for all species. This variability could be due to differences in precipitation formation, particularly the extent of snowflake riming, but may also be influenced by spatial variability in snow chemistry, wind redistribution and mixing of fresh snow with older snow, and differences in aerosol compositions between precipitating air masses. Higher scavenging ratios are observed for species associated with coarse dust particles (e.g.,  $\text{Ca}^{2+}$  and  $\text{Mg}^{2+}$ ) compared to species associated with accumulation mode aerosols (e.g.,  $\text{NH}_4^+$  and  $\text{SO}_4^{2-}$ ), reflecting more efficient precipitation scavenging of coarse dust particles. The highest scavenging ratios are observed for  $\text{NO}_3^-$ , reflecting enrichment of  $\text{NO}_3^-$  in snow relative to aerosol by precipitation scavenging of gas phase  $\text{HNO}_3$  (e.g., Davidson *et al.*, 1985; Shrestha *et al.*, 2002). Likewise, scavenging ratios for  $\text{Cl}^-$  are twice those observed for  $\text{Na}^+$ , indicating snow scavenging of gaseous  $\text{HCl}$ , leading to enrichment of  $\text{Cl}^-$  in snow relative to aerosol and relative to sea water ratios.

As evident from the time series of aerosol and fresh/surface snow chemical concentrations measured at King Col (Figure IV.2), increased concentrations in the aerosol are generally reflected by increased concentrations in the snow, and vice versa. To further investigate the relationship between aerosol concentrations and concentrations in snow, linear regressions were performed between aerosol and fresh snow concentrations for each of the nine species measured. Aerosol samples were paired with concurrent fresh snow samples collected immediately after the aerosol sample was collected. We used the mean concentrations of the three to five replicate snow samples collected. Correlation coefficients (*r* values) are low for species associated with sea salt ( $\text{Na}^+$  and  $\text{Cl}^-$ ) and dust particles ( $\text{Ca}^{2+}$ ,  $\text{Mg}^{2+}$ ,  $\text{K}^+$ ), ranging from

0.12 to 0.26. Correlations between aerosol and snow concentrations are also low for  $\text{NO}_3^-$  ( $r = 0.20$ ). Stronger correlations between aerosol and snow concentrations are observed for species present primarily as accumulation mode aerosols, such as  $\text{NH}_4^+$  ( $r = 0.56$ ) and  $\text{SO}_4^{2-}$  (0.43). Accumulation mode aerosols (0.1 to 1.0 micron diameter) represent coagulation of ultra-fine nuclei mode particles produced by gas-to-particle conversions, such as  $\text{SO}_4^{2-}$  from  $\text{SO}_2$ ,  $\text{NH}_4^+$  from  $\text{NH}_3$  and  $\text{NO}_3^-$  from  $\text{NO}_x$  (Hinds, 1999). The correlation between aerosol and snow concentrations is also high for  $\text{C}_2\text{O}_4^{2-}$  ( $r = 0.63$ ). The high correlation for  $\text{C}_2\text{O}_4^{2-}$  could reflect the consistently low concentrations and lack of variability in both the aerosol and snow data.

A significant contribution from gas phase  $\text{HNO}_3$  to snow  $\text{NO}_3^-$  concentrations has already been demonstrated; hence the weak correlation between aerosol  $\text{NO}_3^-$  and snow  $\text{NO}_3^-$  is expected. Likewise, snow scavenging of gaseous  $\text{HCl}$  could explain the weak correlation between aerosol  $\text{Cl}^-$  and snow  $\text{Cl}^-$ . Furthermore, greater spatial variability in replicate fresh and surface snow samples for species associated with dust and sea salt particles may explain the weaker correlations between aerosol and snow concentrations. The coefficient of variation (standard deviation divided by mean) for replicate snow samples is considerably higher for species present as coarse mode dust ( $\text{Ca}^{2+}$ ,  $\text{Mg}^{2+}$ ) and sea salt ( $\text{Na}^+$ ,  $\text{Cl}^-$ ) particles (0.46 to 0.73) than for species associated with accumulation mode aerosols such as  $\text{NH}_4^+$  (0.23) and  $\text{SO}_4^{2-}$  (0.12). The greater spatial variability in fresh snow concentrations for coarse mode particles significantly weakens the relationship between aerosol and snow concentrations for  $\text{Ca}^{2+}$ ,  $\text{Mg}^{2+}$ ,  $\text{K}^+$ ,  $\text{Na}^+$ , and  $\text{Cl}^-$ . Interestingly, the coefficient of variation is significantly lower for  $\text{Cl}^-$  (0.46) compared to  $\text{Na}^+$  (0.73) since scavenging of gaseous  $\text{HCl}$  is an important contributor to snow chloride concentrations. Likewise, a low coefficient of variation for replicate snow samples was also observed for  $\text{NO}_3^-$  (0.17) since scavenging of gas phase nitrate is an important control on snow  $\text{NO}_3^-$  concentrations. Greater spatial variability for species found on coarse mode particles relative to species found primarily in the accumulation mode or gas phase is a ubiquitous result of snow chemistry surveys (e.g., Dibb and Jaffrezo, 1997; Yalcin *et al.*, in review).



Differences between the observed aerosol and snow concentrations could also be a result of compositional differences between the aerosol sampled at ground level and aerosol concentrations at the heights where snow is forming (e.g., Borys *et al.*, 1992; Dibb and Jaffrezo, 1997), as well as differences in the time integrated by aerosol and snow samples. However, the high elevation of King Col often results in orographic precipitation due to upslope flow, and hence snowflakes are forming at altitudes similar to King Col during such episodes. The degree of snowflake riming could also exert considerable control on snow concentrations and affect the relationship between aerosol and snow concentrations because of different scavenging efficiencies for rimed and unrimed snow and fog (e.g., Davidson *et al.*, 1989; Bergin *et al.*, 1995). This idea is supported by two observations. First, fog was a near daily occurrence at King Col during the sampling period. Second, replicate fresh snow and rime samples collected concurrently from a clean surface on June 4 showed consistently higher concentrations in rime relative to snow samples. Enrichment in rime relative to snow ranged from 21% for  $\text{NH}_4^+$  and 46% for  $\text{SO}_4^{2-}$  to 80% to 95% for dust and sea salt species and 102% for  $\text{NO}_3^-$ . Hence, the extent of riming may affect the relationships between aerosol and snow chemistry to a greater degree for dust, sea salt, and  $\text{NO}_3^-$  relative to  $\text{NH}_4^+$  and  $\text{SO}_4^{2-}$ . However, because rime samples were collected on just a single day, more work is needed to quantify the relative importance of riming for aerosol and snow chemistry at King Col.

#### **King Col snowpit and firn core chemistry**

The combined 3 m snowpit and 12 m firn core chemical record recovered from King Col provides a continuous glaciochemical record covering the period winter 1992-1993 to May 2001. The snowpit and firn core record was dated by annual layer counting of seasonal oscillations in the stable isotope ( $\delta\text{D}$ ) and major ion records. The annual cycle of  $\delta\text{D}$  maxima in summer precipitation and  $\delta\text{D}$  minima in winter precipitation is related at least in part to the temperature at which evaporation and condensation occurs (Dansgaard *et al.*, 1973) and is consistent with the

seasonal cycle observed at Eclipse Icefield (Yalcin and Wake, 2001). The annual cycle of  $\text{Na}^+$  concentration maxima in winter and minima in summer is related to pronounced seasonal changes in the influx of marine aerosols (Whitlow *et al.*, 1992) and is also well-recorded at Eclipse Icefield. Increased storminess and higher wind speeds in the Gulf of Alaska during winter results in enhanced entrainment of sea salt aerosols and more frequent advection of marine air masses into the St. Elias Mountains, producing the observed winter peaks in  $\text{Na}^+$  concentrations. Nitrate concentrations consistently peak in spring at King Col, providing an additional chemical stratigraphic marker, while the seasonal  $\text{NO}_3^-$  cycle is less consistent at Eclipse Icefield.

The average total ionic burden in snowpit and firn core samples (total cations plus total anions) averaged  $4.36 \text{ ueq l}^{-1}$ ; similar to that observed in fresh and surface snow. Ammonium and sulfate the dominant ions present, as in fresh and surface snow samples, on average accounting for 45% of the total soluble ionic impurities. Nitrate (23%), dust (20%), and sea salt (10%) also contribute similarly to the total ionic load in snowpit and firn core samples compared to recent snow chemistry (20, 23, and 15%, respectively). The charge balance of snowpit and firn core samples averaged  $-0.67 \text{ ueq l}^{-1}$ , with an anion excess in 82% of the samples that is presumably balanced by hydrogen ion. This represents a greater anion excess than was observed in snow during the May 17 to June 11 sampling campaign, when the charge balance averaged  $-0.39 \text{ ueq l}^{-1}$  with an anion excess in 62% of the samples. This difference is primarily due to higher  $\text{SO}_4^{2-}$  concentrations in snowpit and firn core samples (averaging  $1.32 \text{ ueq l}^{-1}$ ) compared to recent snow samples (averaging  $0.98 \text{ ueq l}^{-1}$ ). Higher  $\text{SO}_4^{2-}$  concentrations in firn core samples are reflected by a lower  $\text{NH}_4^+/\text{SO}_4^{2-}$  equivalence ratio in the firn core (0.47) relative to recent snow (0.94), while other inter-species relationships are similar for firn core and recent snow samples. This result could be due to anomalous atmospheric circulation during the May 17 to June 11 that produced lower average  $\text{SO}_4^{2-}$  concentrations. However, the lack of significant differences in concentrations for other species suggests circulation patterns were not anomalous during the sampling period compared to the time covered by the firn core.

### **Concentrations and fluxes at King Col compared to Eclipse Icefield**

We compared annual mean concentrations and chemical fluxes at King Col over the period 1993-2000 to those observed at nearby Eclipse Icefield (60.51° N, 139.47° W, 3017 m elevation; Figure IV.1) over the same period, using the top portion of a 130 m firn and ice core recovered in 2002. Although separated by only 45 km, the elevation difference between the two sites allows them to sample different layers of the atmosphere (Table IV.6). Analysis of the Eclipse Icefield ice cores followed the same procedures used in the development of the King Col record, and are detailed by Yalcin and Wake (2001) and Yalcin *et al.* (in press). Annual average concentrations for each of the major ions at both sites were calculated for the years 1993 to 2000, as well as the mean annual concentration for this period. The annual snow accumulation in water equivalent was used to calculate annual fluxes by multiplying the annual average concentration by the accumulation rate for that year.

Mean annual accumulation for the period 1993-2000 at Eclipse (1.42 m water equivalent yr<sup>-1</sup>) was 35% greater than at King Col (1.05 m water equivalent yr<sup>-1</sup>). Major ion concentrations and fluxes at Eclipse and King Col also show distinct differences for most species (Table IV.7). Concentrations of dust species (Mg<sup>2+</sup>, Ca<sup>2+</sup>) are three to five times higher at Eclipse, respectively. The difference is even greater in terms of flux, with four-fold greater Mg<sup>2+</sup> deposition and seven-fold greater Ca<sup>2+</sup> deposition at Eclipse indicating greater inputs of dust at lower elevation sites in the St. Elias Mountains. In addition, Cl<sup>-</sup> and Na<sup>+</sup> concentrations, derived primarily from sea salt, are higher at Eclipse relative to King Col by a factor of two to three respectively. The flux of Cl<sup>-</sup> and Na<sup>+</sup> is even greater at Eclipse relative to King Col, by factors of 2.5 and 4.5, respectively. These observations suggest a greater input of marine-derived aerosols at Eclipse, even though the Eclipse site is 40 km further inland. The horizontal transport of sea salt aerosols appears to be greater than vertical transport. The average Cl<sup>-</sup>/Na<sup>+</sup> equivalence ratio in snow at Eclipse (1.37) more closely approaches the seawater ratio than King Col snow (2.56). This suggests greater acidification of sea salt particles reaching King Col to produce highly soluble HCl.

Meanwhile,  $\text{NO}_3^-$  and  $\text{SO}_4^{2-}$  concentrations are higher at King Col by nearly a factor of two; whereas the difference in fluxes is not as great due to the higher accumulation rate at Eclipse. Given the higher concentrations of sulfate and nitrate at King Col and similar fluxes, it appears likely that King Col is receiving an anthropogenic sulfate and nitrate signal. However, it will take a longer glaciochemical record than the one presented here to establish the existence of an anthropogenic trend at King Col. Higher  $\text{NO}_3^-$  and  $\text{SO}_4^{2-}$  concentrations at King Col may also contribute to greater acidification of sea salt particles, resulting in the observed enhancement of  $\text{Cl}^-$  relative to  $\text{Na}^+$ . Annual average  $\text{K}^+$  concentrations are identical at the two sites, but given the high accumulation rate the flux of  $\text{K}^+$  is greater at Eclipse. The annual average  $\text{NH}_4^+$  concentration is higher at King Col, whereas the average annual  $\text{NH}_4^+$  flux is nearly the same at the two sites. The distinct glaciochemical differences between Eclipse Icefield and King Col illustrate that the 1100 m elevation gradient between the two sites allows them to sample layers of the atmosphere with different air mass sources, resulting in complementary and distinct records (e.g., Holdsworth *et al.*, 1988; Yalcin and Wake, 2001, Wake *et al.*, 2002; Yalcin *et al.*, 2003).

#### **Impact of April 2001 Asian dust plume on St. Elias snow chemistry**

Differences in site elevation are also illustrated by the variable impact of the April 2001 Asian dust storm on St. Elias snow chemistry. In April 2001 several very large dust storms were generated in the Tarim Pendi Basin of Western China and in the Gobi Deserts of southern Mongolia and northern China (DeBell *et al.*, 2004). The resulting dust plumes were observed by the Total Ozone Mapping Spectrometer (TOMS) as they crossed the Pacific to North America. One of these events blanketed large areas of the St. Elias Mountains with a visibly dusty snow layer in mid-April. At sites below ~3000 m, snowpit trace and rare earth element data from 2001 and 2002 demonstrate that dust in these years is primarily derived from regional sources, with a geochemical signature similar to Alaska and Yukon loess (Zdanowicz *et al.*, 2004). Meanwhile, trace and rare earth element data from high elevation sites (King Col and Mt. Logan) sampled in 2001 closely matches Asian dust sources.

The April 2001 Asian dust layer was sampled in a 10 cm thick brown snow layer (3 cm water equivalent) near the top of the May 2001 snowpit at King Col, allowing assessment of the impact of this event on major ion concentrations and fluxes. Concentrations of all major ions except  $\text{NO}_3^-$  are elevated above their annual averages due to fallout of Asian dust (Table IV.8). Although  $\text{SO}_4^{2-}$  and  $\text{Cl}^-$  were present at concentrations 1.5 to 2.5 times their annual average concentration at King Col in the snow layer impacted by the 2001 Asian dust plume, very large enhancements were observed for  $\text{Na}^+$  (ten-fold) and  $\text{K}^+$ ,  $\text{Mg}^{2+}$ , and  $\text{Ca}^{2+}$  (thirty-fold). The flux of  $\text{Na}^+$ ,  $\text{K}^+$ ,  $\text{Mg}^{2+}$ , and  $\text{Ca}^{2+}$  from this event represents between 33 and 94% of the 1993-2000 annual average flux of these species (Table IV.8), although snowfall affected by the event accounts for only 3% of the average annual accumulation at King Col. It is apparent that episodic transport of Asian dust can deliver large amounts of dust related species to the St. Elias Mountains.

Identification of the 2001 Asian dust plume in snow at Eclipse is ambiguous. Although intervals of elevated dust concentrations are observed in the Eclipse ice core during spring 2001, none of these events stands out as unique when compared to adjacent years. At elevations of 3000 m and lower in the St. Elias, snowfall impacted by the Asian dust plume was not quickly buried by subsequent snowfalls. Wind-redistribution of the affected snowfall while it was exposed at the snowpack surface resulted in patchy distribution of the visibly dusty snow as observed at Quintino Sella Glacier (2800 m) in May 2001. This patchy character to the dusty snow layer was also observed while flying over the St. Elias Mountains in May and June 2001. Consequently, it is possible that the 2002 Eclipse ice core may have not sampled this layer due its patchy nature at small scales. It is also possible that the 2001 Asian dust layer was not deposited at Eclipse because no snowfall occurred at Eclipse while the dust passed overhead. The 2001 Asian dust storm provides another example of elevation-dependent differences in glaciochemical records from the St. Elias on event to multi-annual time scales.

## Conclusions

From May 17 to June 11, twice daily aerosol and three to five replicate fresh or surface snow samples were collected in addition to a 15 m snowpit/firn core record covering the period May 2001 to winter 1992-1993. The resulting database provides the information needed to characterize the late spring-early summer aerosol at King Col, examine the relationships between aerosol and snow chemistry on an event basis, and compare major ion concentrations and fluxes at King Col to those at nearby Eclipse Icefield. Major ion concentrations in aerosol samples were quite low with the total ionic burden averaging  $5.52 \text{ neq m}^{-3}$  at standard temperature and pressure (STP). Ammonium and sulfate represent 49% of the ionic component of the aerosol, and are highly correlated ( $r=0.90$ ) with a mean  $\text{NH}_4^+/\text{SO}_4^{2-}$  molar ratio of 2.16 indicating their presence as  $(\text{NH}_4)_2\text{SO}_4$ . However, there is an excess of  $\text{SO}_4^{2-}$  charge equivalents relative to  $\text{NH}_4^+$  in 49% of the samples. Dust species (e.g.,  $\text{Ca}^{2+}$ ) are well correlated with  $\text{SO}_4^{2-}$  ( $r = 0.75$ ) and  $\text{NO}_3^-$  ( $r = 0.91$ ), implying uptake by dust particles. Nitrate is also well correlated with  $\text{NH}_4^+$  ( $r= 0.73$ ), which together with the high  $\text{NH}_4^+/\text{SO}_4^{2-}$  ratio suggests  $\text{NH}_4\text{NO}_3$  aerosol may also be present. King Col aerosol is  $\text{Cl}^-$  deficient relative to seawater due to volatilization of  $\text{HCl}$  by reaction with unneutralized  $\text{SO}_4^{2-}$  present in 49% of the samples.

Backwards trajectories for select aerosol concentration peaks document the transport of Asian dust and anthropogenic emissions, the eruption plume from the May 22 eruption of Sheveluch, Kamchatka, and sea salt from the marine boundary layer over the Gulf of Alaska to King Col at discrete times during the sampling period. Fresh snow chemistry generally mimics aerosol chemistry with similar relative abundances and inter-species relationships except for large enrichments in snow  $\text{Cl}^-$  and  $\text{NO}_3^-$  relative to aerosol due to snow scavenging of gas phase  $\text{HCl}$  and  $\text{HNO}_3$ . Although relatively strong correlations between aerosol and snow concentrations were observed for species associated with accumulation mode aerosols, such as  $\text{NH}_4^+$  ( $r = 0.56$ ) and  $\text{SO}_4^{2-}$  ( $r = 0.43$ ), only weak correlations were observed for dust and sea salt species. These results may be influenced by greater variability in replicate snow samples for species associated

with coarse mode dust and sea salt particles. The extent of snowflake riming may also influence air-snow relationships.

Comparison of average annual major ion concentrations and fluxes from 1993-2000 at King Col (4135 m) to nearby Eclipse Icefield (3017 m) demonstrate greater inputs of sea salt and dust at Eclipse by factors of two to five, respectively. Meanwhile,  $\text{NO}_3^-$  and  $\text{SO}_4^{2-}$  concentrations are higher at King Col by nearly a factor of two; whereas the difference in fluxes is not as great due to the higher accumulation rate at Eclipse. In addition, the average  $\text{Cl}^-/\text{Na}^+$  equivalence ratio in snow at Eclipse (1.37) more closely approaches the seawater ratio than King Col snow (2.56), suggesting a more aged marine aerosol at King Col. The signature of the April 2001 Asian dust plume was clearly recorded at King Col, depositing between 33 and 94% of the 1993-2000 annual average flux of  $\text{Na}^+$ ,  $\text{K}^+$ ,  $\text{Mg}^{2+}$ , and  $\text{Ca}^{2+}$  even though snowfall visibly impacted by the 2001 Asian dust plume accounts for only 3% of the average annual accumulation. There is no clear signal from this event at Eclipse Icefield. The elevation difference between these two sites allows them to sample different layers of the atmosphere with different aerosol source regions and transport histories, resulting in distinct glaciochemical records despite their proximity.

#### **Acknowledgments**

We would like to thank G. Holdsworth (Arctic Institute of North America at the University of Calgary) and C. Zdanowicz (Geological Survey of Canada) for field assistance, and the D. Fisher of the Geological Survey of Canada for logistical support. We would also like to thank D. Introne for stable isotope analyses of the King Col firn core. The National Science Foundation Office of Polar Programs funded this research.

**Table IV.1.** Summary of aerosol composition at King Col ( $\text{neq m}^{-3}$  STP), May 17 to June 11, 2001, where b.d. denotes below detection limit and  $\Delta\text{C}$  is the charge balance (sum of measured cations minus sum of measured anions). A total of 48 aerosol samples were collected.

	$\text{Na}^+$	$\text{NH}_4^+$	$\text{K}^+$	$\text{Mg}^{2+}$	$\text{Ca}^{2+}$	$\text{Cl}^-$	$\text{NO}_3^-$	$\text{SO}_4^{2-}$	$\text{C}_2\text{O}_4^{2-}$	$\Delta\text{C}$
mean	1.26	1.34	0.17	0.15	0.52	0.94	0.24	1.38	0.07	0.71
median	0.86	1.22	0.15	0.10	0.40	0.64	0.18	1.12	0.06	0.73
std. dev.	1.04	0.89	0.11	0.12	0.45	0.83	0.20	0.96	0.05	0.60
max	4.13	4.12	0.47	0.57	2.36	3.29	1.08	4.59	0.19	3.09
min	b.d	b.d	b.d	b.d	b.d	b.d	0.05	0.17	0.01	-1.30

**Table IV.2.** Correlation coefficients between soluble ionic species in aerosol samples ( $n=48$ ) collected at King Col, May 17 to June 11, 2001. Correlations in bold are significant at the 99% confidence level.

	$\text{Na}^+$	$\text{NH}_4^+$	$\text{K}^+$	$\text{Mg}^{2+}$	$\text{Ca}^{2+}$	$\text{Cl}^-$	$\text{NO}_3^-$	$\text{SO}_4^{2-}$
$\text{NH}_4^+$	-0.18							
$\text{K}^+$	<b>0.92</b>	-0.01						
$\text{Mg}^{2+}$	<b>0.38</b>	<b>0.55</b>	<b>0.39</b>					
$\text{Ca}^{2+}$	-0.16	<b>0.68</b>	-0.15	<b>0.76</b>				
$\text{Cl}^-$	<b>0.89</b>	-0.14	<b>0.84</b>	<b>0.39</b>	-0.10			
$\text{NO}_3^-$	-0.05	<b>0.73</b>	0.00	<b>0.80</b>	<b>0.91</b>	-0.01		
$\text{SO}_4^{2-}$	0.03	<b>0.90</b>	0.13	<b>0.71</b>	<b>0.75</b>	0.05	<b>0.83</b>	
$\text{C}_2\text{O}_4^{2-}$	-0.07	<b>0.70</b>	0.11	<b>0.42</b>	<b>0.45</b>	-0.07	<b>0.53</b>	<b>0.71</b>

**Table IV.3.** Summary of fresh and surface snow composition at King Col ( $\text{ueq l}^{-1}$ ), May 17 to June 11, 2001.  $\Delta\text{C}$  is the charge balance (sum of measured cations minus sum of measured anions). A total of 193 fresh and surface snow samples were collected.

	$\text{Na}^+$	$\text{NH}_4^+$	$\text{K}^+$	$\text{Mg}^{2+}$	$\text{Ca}^{2+}$	$\text{Cl}^-$	$\text{NO}_3^-$	$\text{SO}_4^{2-}$	$\text{C}_2\text{O}_4^{2-}$	$\Delta\text{C}$
Mean	0.29	0.79	0.08	0.21	0.97	0.45	1.07	1.18	0.05	-0.39
Median	0.19	0.78	0.05	0.17	0.82	0.36	0.97	1.06	0.04	-0.21
std. dev.	0.34	0.34	0.09	0.15	0.65	0.38	0.78	0.75	0.05	0.90
Max	3.04	1.74	0.80	0.65	3.81	4.02	3.44	3.91	0.30	1.90
Min	0.01	0.13	0.00	0.03	0.09	0.06	0.17	0.13	0.01	-3.16



**Table IV.4.** Correlation coefficients (n = 193) between soluble species in fresh and surface snow collected at King Col, May 17 to June 11, 2001. Bold entries denote correlations significant at the 99% confidence level. Italicized entries are significant at the 90% confidence level.

	Na <sup>+</sup>	NH <sub>4</sub> <sup>+</sup>	K <sup>+</sup>	Mg <sup>2+</sup>	Ca <sup>2+</sup>	Cl <sup>-</sup>	NO <sub>3</sub> <sup>-</sup>	SO <sub>4</sub> <sup>2-</sup>
NH <sub>4</sub> <sup>+</sup>	<b>0.43</b>							
K <sup>+</sup>	<b>0.90</b>	<b>0.57</b>						
Mg <sup>2+</sup>	0.09	<b>0.63</b>	<i>0.23</i>					
Ca <sup>2+</sup>	0.08	<b>0.67</b>	<i>0.23</i>	<b>0.94</b>				
Cl <sup>-</sup>	<b>0.81</b>	<b>0.61</b>	<b>0.90</b>	<i>0.32</i>	<b>0.37</b>			
NO <sub>3</sub> <sup>-</sup>	0.06	<b>0.64</b>	<b>0.37</b>	<b>0.60</b>	<b>0.67</b>	<b>0.55</b>		
SO <sub>4</sub> <sup>2-</sup>	0.16	<b>0.75</b>	<b>0.37</b>	<b>0.87</b>	<b>0.91</b>	<b>0.44</b>	<b>0.71</b>	
C <sub>2</sub> O <sub>4</sub> <sup>2-</sup>	0.16	<b>0.54</b>	<b>0.51</b>	<i>0.33</i>	<i>0.33</i>	<b>0.50</b>	<b>0.72</b>	<b>0.50</b>

**Table IV.5.** Scavenging ratios for water soluble ions calculated from concurrent measurements of aerosol and fresh snow chemistry (n = 21) at King Col, May 17 to June 11, 2001.

	Na <sup>+</sup>	NH <sub>4</sub> <sup>+</sup>	K <sup>+</sup>	Mg <sup>2+</sup>	Ca <sup>2+</sup>	Cl <sup>-</sup>	NO <sub>3</sub> <sup>-</sup>	SO <sub>4</sub> <sup>2-</sup>	C <sub>2</sub> O <sub>4</sub> <sup>2-</sup>
mean	462	1559	700	2697	4540	872	8253	1708	1421
std. dev.	361	1504	479	1893	2972	779	5744	1072	817

**Table IV.6.** Comparison of the Eclipse and King Col sites.

	Lat. (°N)	Log. (°W)	Elev. (m)	Snow Accum. Rate (m w.e.)
<b>Eclipse Icefield</b>	60.85	139.78	3017	1.42
<b>King Col</b>	60.58	140.60	4135	1.05

**Table IV.7.** Annual average concentrations and fluxes at Eclipse Icefield and King Col for the period 1993 to 2000.

	Annual Average Concentration 1993-2000 ( $\mu\text{eq l}^{-1}$ )							
	Na <sup>+</sup>	NH <sub>4</sub> <sup>+</sup>	K <sup>+</sup>	Mg <sup>2+</sup>	Ca <sup>2+</sup>	Cl <sup>-</sup>	NO <sub>3</sub> <sup>-</sup>	SO <sub>4</sub> <sup>2-</sup>
<b>Eclipse</b>	0.39	0.37	0.03	0.62	1.65	0.39	0.53	0.75
(std. dev.)	0.19	0.14	0.01	0.25	0.69	0.19	0.17	0.29
-----								
<b>King Col</b>	0.12	0.51	0.03	0.12	0.57	0.21	0.94	1.30
(std. dev.)	0.03	0.27	0.02	0.04	0.33	0.08	0.16	0.46
	Annual Average Flux 1993-2000 ( $\mu\text{g cm}^{-2} \text{yr}^{-1}$ )							
	Na <sup>+</sup>	NH <sub>4</sub> <sup>+</sup>	K <sup>+</sup>	Mg <sup>2+</sup>	Ca <sup>2+</sup>	Cl <sup>-</sup>	NO <sub>3</sub> <sup>-</sup>	SO <sub>4</sub> <sup>2-</sup>
<b>Eclipse</b>	1.28	0.96	0.19	1.12	4.83	1.95	4.62	5.29
(std. dev.)	0.61	0.45	0.08	0.53	2.15	0.96	1.58	2.17
-----								
<b>King Col</b>	0.28	0.92	0.12	0.15	1.25	0.79	6.04	6.52
(std. dev.)	0.09	0.41	0.06	0.06	0.80	0.37	0.91	2.18

**Table IV.8.** The 2001 Asian dust plume as recorded at King Col.

	Na <sup>+</sup>	NH <sub>4</sub> <sup>+</sup>	K <sup>+</sup>	Mg <sup>2+</sup>	Ca <sup>2+</sup>	Cl <sup>-</sup>	NO <sub>3</sub> <sup>-</sup>	SO <sub>4</sub> <sup>2-</sup>
conc. ( $\mu\text{eq l}^{-1}$ )	1.43	1.16	1.00	3.46	16.56	0.54	0.93	1.94
% annual avg.	1213	228	3297	2993	2907	250	98	149
flux ( $\mu\text{g cm}^{-2}$ )	0.09	0.06	0.11	0.12	0.95	0.05	0.16	0.26
% annual avg.	33	7	94	81	76	7	3	4

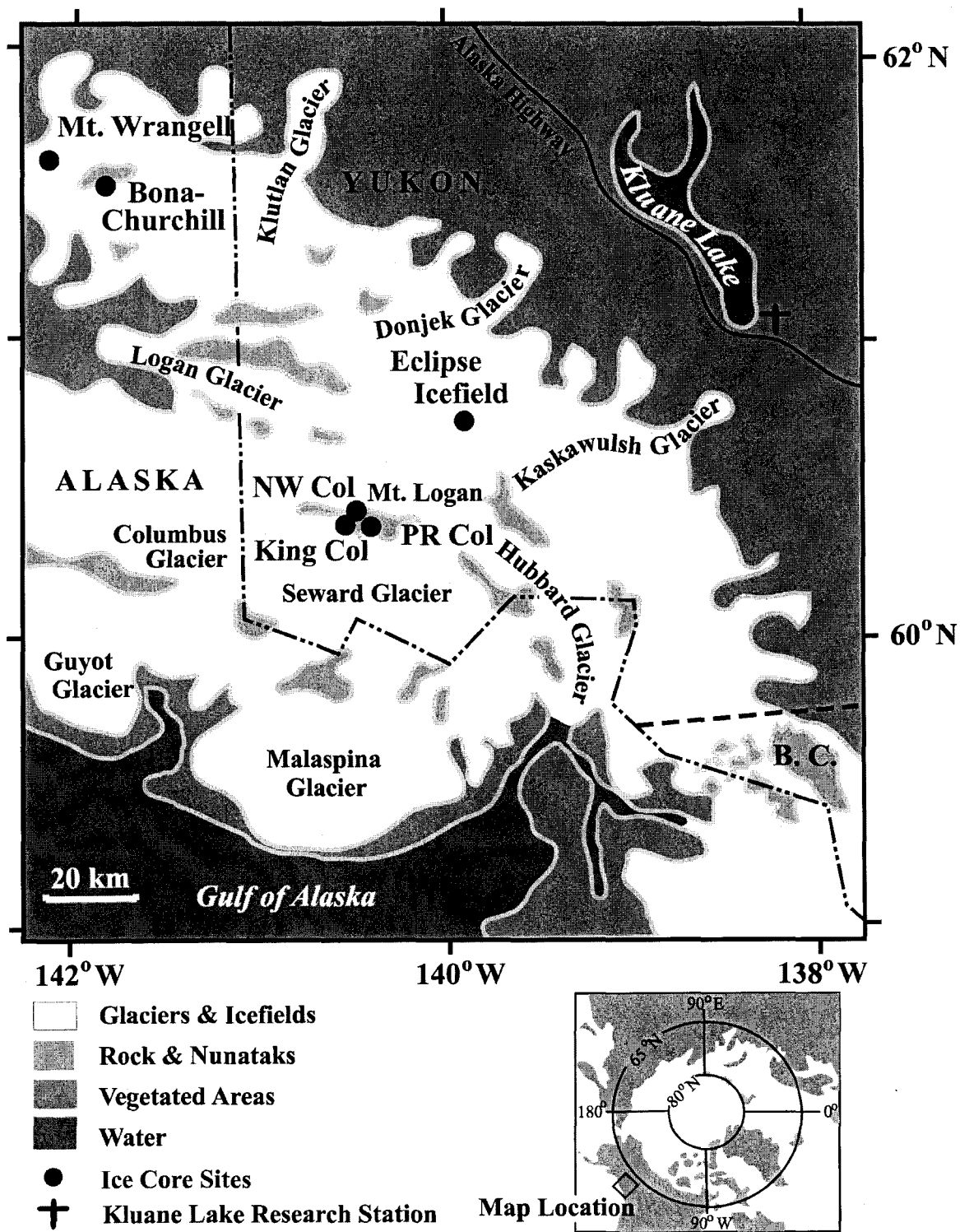


**Figure IV.1.** Map of the St. Elias Mountains, southwest Yukon, showing the location of the ice coring sites at King Col (4135 m) and Eclipse Icefield (3017 m). Additional ice core sites in the St. Elias Mountains include Northwest Col (5340 m) and Prospector-Russell Col (5340 m) on the summit plateau of Mt. Logan, Bona-Churchill (4400 m), and Mt. Wrangell (4100 m).

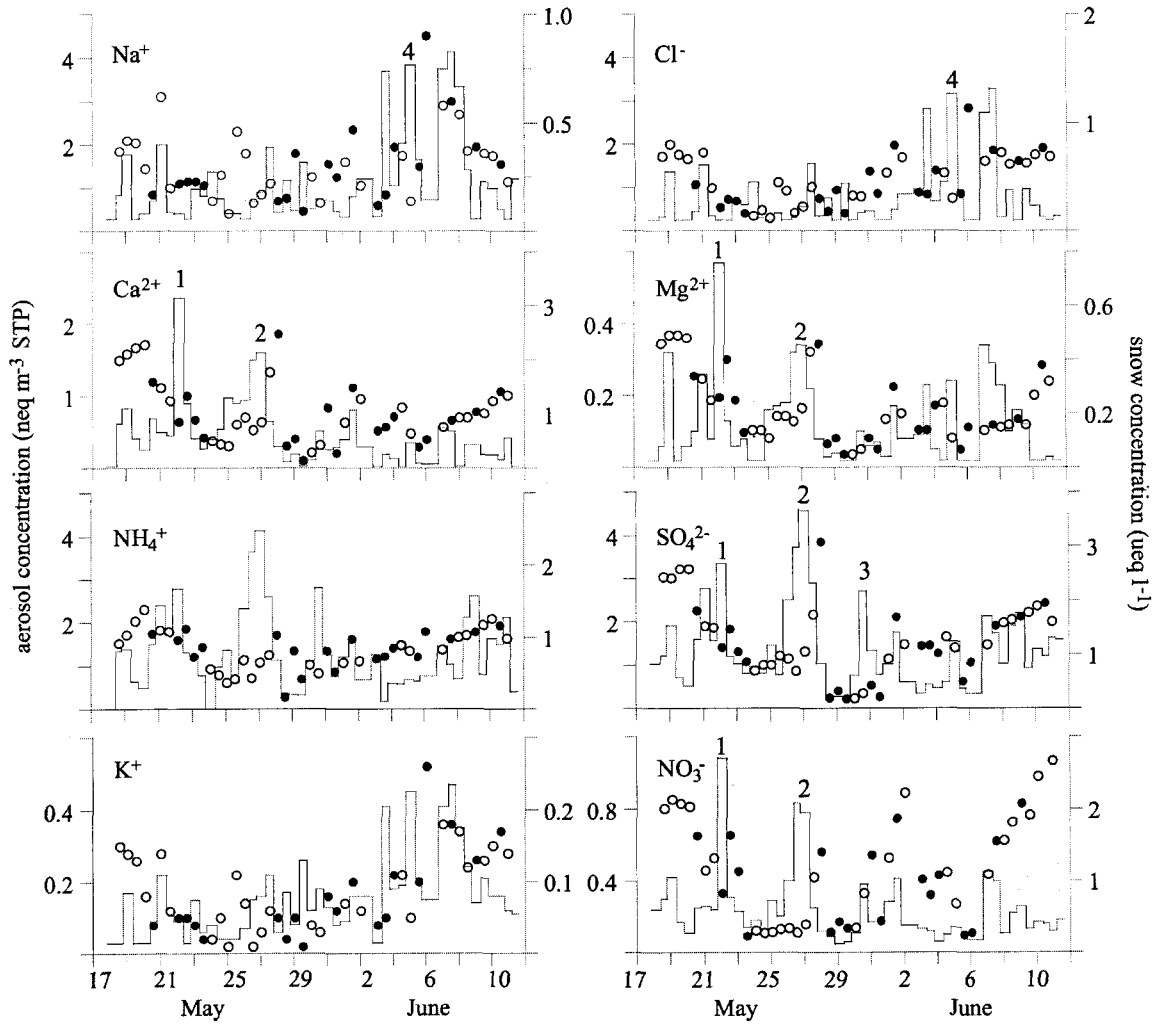


**Figure IV.2.** Concentrations of soluble ionic species in aerosol samples (solid line) and concurrent fresh (solid circles) and aged surface (open circles) snow samples collected at King Col between May 17 and June 11, 2001.

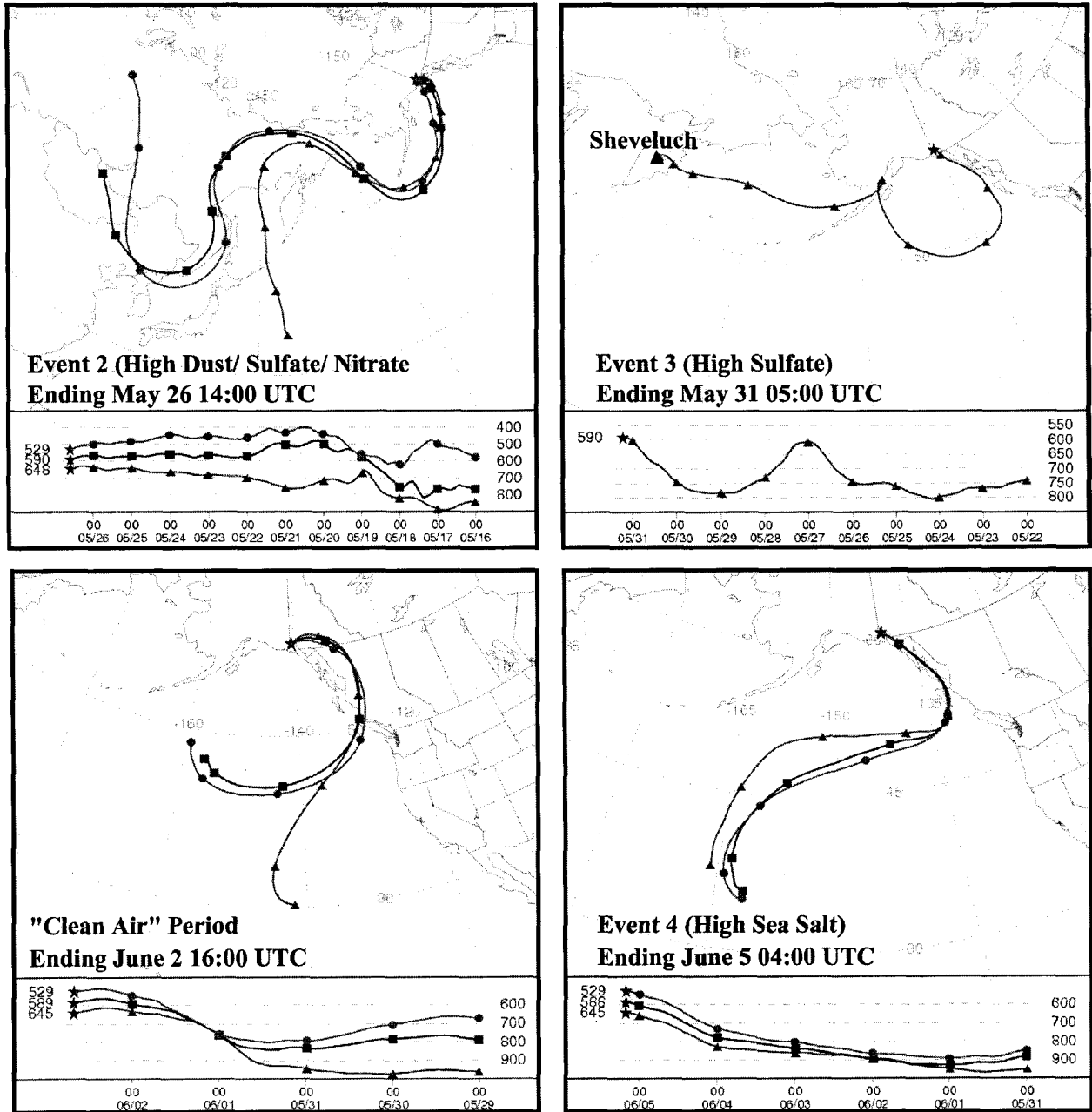


**Figure IV.3.** Air mass back-trajectories generated using the NOAA HYSPLIT model for four aerosol concentration events observed at King Col during the May 17 to June 11 sampling period. Top left: high  $\text{Ca}^{2+}$ - $\text{Mg}^{2+}$ - $\text{NH}_4^+$ - $\text{SO}_4^{2-}$ - $\text{NO}_3^-$  event, May 26-27. Top right: high  $\text{SO}_4^{2-}$  event, May 30-31. Bottom left: "clean air" period, June 2. Bottom right: high  $\text{Na}^+$ - $\text{Cl}^-$  event, June 5.

## References

- Baltensperger, U., M. Schwikowski, H.W. Gaggeler, and D.T. Jost, The scavenging of atmospheric constituents by alpine snow, in *Precipitation Scavenging and Atmosphere-Surface Exchange*, edited by S.E. Schwartz and W.G.N. Slinn, pp. 483-493, Hemisphere, Washington, 1992.
- Baltensperger, U., H.W. Gaggeler, D.T. Jost, M. Lugauer, M. Schwikowski, and E. Weingartner, Aerosol Climatology at the high alpine site Jungfrauoch, Switzerland, *Journal of Geophysical Research*, 102, 19,707-19,715, 1997.
- Barrie, L.A., Atmospheric particles: their physical and chemical characteristics and depositional processes relevant to the chemical composition of glaciers, *Annals of Glaciology*, 7, 100-108, 1985.
- Barrie, L.A., and M.J. Barrie, Chemical components of lower tropospheric aerosol in the high Arctic: six years of observations, *Journal of Atmospheric Chemistry*, 11, 211-226, 1990.
- Bassett, M., and J.H. Seinfeld, Atmospheric equilibrium model of sulfate and nitrate aerosols, *Atmospheric Environment*, 17, 2237-2252, 1983.
- Bergin, M.H., J.L. Jaffrezo, C.I. Davidson, J.E. Dibb, S.N. Pandis, R. Hillamo, W. Maenhaut, H.D. Kuhns, and T. Makela, The contribution of snow, fog, and dry deposition to the summer flux of anions and cations at Summit, Greenland, *Journal of Geophysical Research*, 100, 16,275-16,288, 1995.
- Borys, R.D., D. del Vecchio, J.L. Jaffrezo, J.E. Dibb, and D.L. Mitchell, Field observations, measurements, and preliminary results from a study of wet deposition processes influencing snow and ice chemistry at Summit, Greenland, in *Precipitation Scavenging and Atmosphere-Surface Exchange Processes*, vol. 3, edited by S.E. Schwarz, and W.G.N. Slinn, pp. 1693-1702, Hemisphere, Washington, D.C. , 1992.
- Bulletin of the Global Volcanism Network*, v. 26, n. 4, 2001.
- Calvert, J.K., A. Lazrus, G.L. Kok, B.G. Heikes, J.H. Walega, J. Lind, and C.A. Cantrell, Chemical mechanisms of acid generation in the troposphere, *Nature*, 317, 27-35, 1985.
- Carrico, C.M., M.H. Bergin, A.B. Shrestha, J.E. Dibb, L. Gomes, and J.M. Harris, The importance of carbon and mineral dust to seasonal aerosol properties in the Nepal Himalaya, *Atmospheric Environment*, 37, 2811-2824.
- Dansgaard, W., S.J. Johnsen, H.B. Clausen, and N. Gundestrup, Stable isotope glaciology, *Meddelelser om Gronland Bd*, 197, N2, 1-53, 1973.
- Davidson, C.I., S. Santhanam, R.C. Fortmann, and M.P. Olson, Atmospheric transport and deposition of trace elements onto the Greenland Ice Sheet, *Atmospheric Environment*, 19, 2065-2081, 1985.
- Davidson, C.I., J.R. Harrington, M.J. Stephenson, F.P. Boscoe, and R.E. Gandley, Seasonal variations in sulfate, nitrate, and chloride in the Greenland Ice Sheet: relation to atmospheric concentrations, *Atmospheric Environment*, 23, 2483-2491, 1989.

- Davidson, C.I., J.L. Jaffrezo, B.W. Mosher, J.E. Dibb, R.D. Borys, B.A. Bodhaine, R.A. Rasmussen, C.F. Boutron, F.M. Ducroz, M. Cahier, J. Ducret, J.L. Colin, N. Z. Heidam, K. Kemp, And R. Hillamo, Chemical Constituents in the air and snow at Dye 3, Greenland II. Analysis of episodes in April 1989, *Atmospheric Environment*, 27, 2723-2737, 1993.
- DeBell, L.J., M. Vozella, R.W. Talbot, and J.E. Dibb, Asian dust storm events of spring 2001 and associated pollutants as observed in New England by the Atmospheric Investigation, Regional Modeling, Analysis and Prediction (AIRMAP) network, *Journal of Geophysical Research*, 109, D01304, doi: 10.0129/2003JD003733, 2004.
- Dibb, J. E., and J. L. Jaffrezo, Air-snow investigations at Summit, Greenland: An overview; *Journal of Geophysical Research*, 102, 26,795-26,807, 1997.
- Draxler, R.R., and G.D. Hess, Description of the HYSPLIT-4 modeling system, *NOAA Technical Memo, ERLARL-224*, 24 pp., 1997.
- Fischer, H., D. Wagenbauch, and J. Kipfstuhl, Sulfate and nitrate firn concentrations on the Greenland ice sheet 2. Temporal anthropogenic deposition changes, *Journal of Geophysical Research*, 103, 21935- 21942, 1998.
- Fisher, D.A., J. Bourgeois, M. Demuth, R. Koerner, M. Parnandi, J. Sekerka, C. Zdanowicz, J. Zheng, C. Wake, K. Yalcin, P. Mayewski, K. Kreutz, E. Osterberg, D. Dahl-Jensen, K. Goto-Azuma, G. Holdsworth, E. Steig, S. Rupper, and M. Wasckiewicz, Mount Logan ice cores: The water cycle of the North Pacific in the Holocene, *Eos ,Transactions, American Geophysical Union*, 85 (47), Fall Meeting Supplement, Abstract PP23C- 07, 2004.
- Fritzsche, D., F. Wilhelms, L.M. Savatyugin, J.F. Pinglot, H. Meyer, H.W. Hubberten, and H. Miller, A new deep ice core from Akademii Nauk ice cap, Sernaya Zemlya, Eurasian Arctic: First results, *Annals of Glaciology*, 35, 25-28, 2002.
- Gard, E.E., M.J. Kleemna, D.S. Gross, L.S. Hughes, J.O. Allen, B.D. Morrical, D.P. Fergenson, T. Dienes, M.E. Galli, R.J. Johnson, G.R. Cass, and K. A. Prather, Direct observation of heterogeneous chemistry in the atmosphere, *Science*, 279, 1184-1186, 1998.
- Goto-Azuma, K., S. Kohshima, T. Kameda, S. Takahashi, O. Watanbe, Y. Fujii, and J. O. Hagen, An ice-core chemistry record from Snofjellaafonna, northwestern Spitsbergen, *Annals of Glaciology*, 21, 213- 218, 1995.
- Goto-Azuma, K., T. Shiraiwa, S. Matoba, T. Segawa, S. Kanamori, Y. Fujii, and T. Yamasaki, An overview of the Japanese glaciological studies on Mt. Logan, Yukon, Canada in 2002, *Bulletin of Glaciological Research*, 20, 65-72, 2003.
- Grumet, N., C. P. Wake, P. A. Mayewski, G. A. Zielinski, S. I. Whitlow, R. M. Koerner, D.A. Fisher, and J. M. Woollett, Variability of sea- ice extent in Baffin Bay over the last millennium, *Climatic Change*, 49, 129- 145, 2001.
- Hammer, C. U., P. A. Mayewski, D. Peel, and M. Stuiver, Greenland Summit ice cores; Greenland Ice Sheet Project 2 (GISP2); Greenland Ice Core Program (GRIP), *Journal of Geophysical Research*, 102, 26,315-26,886, 1997.

- Henning, S., E. Weingartner, M. Schwikowski, H.W. Gaggeler, R. Gehrig, K.P. Hinz, A. Trimborn, B. Spengler, and U. Baltensperger, Seasonal variation of water-soluble ions of the aerosol at the high alpine site Jungfraujoch (3580 m asl), *Journal of Geophysical Research*, *108*, 4030, doi:10.1029/2002JD002439, 2003.
- Hind, W.C., *Aerosol Technology*, John Wiley, New York, 1999.
- Holdsworth, G., H. R. Krouse, and E. Peake, Trace acid content of shallow snow and ice cores from mountain sites in western Canada, *Annals of Glaciology*, *13*, 57- 62, 1988.
- Jaffrezo, J.L., and C.I. Davidson, The Dye 3 Gas and Aerosol Sampling Program: an overview, *Atmospheric Environment*, *27A*, 2703-2707, 1993.
- Jordan, C. E., J. E. Dibb, B. E. Anderson, and H. E. Fuelberg, Uptake of nitrate and sulfate on dust aerosols during TRACE-P, *Journal of Geophysical Research*, *108*, 8817, doi: 10.1029/2002JD003101, 2003.
- Kanamori, S., T. Shiraiwa, K. Goto-Azuma, C.S. Benson, and R. Naruse, Seasonal variations in density profiles and densification processes at Mts. Logan and Wrangell, *Eos Transactions, American Geophysical Union*, *85* (47), Fall Meeting Supplement, Abstract PP21A- 1367, 2004.
- Keene, W.C., A.P. Pszenny, J.N. Galloway, and M.E. Hawley, Sea-salt corrections and interpretation of constituent ratios in marine precipitation, *Journal of Geophysical Research*, *91*, 6647- 6658, 1986.
- Koerner, R.M., D.A. Fisher, and K. Goto-Azuma, A 100 year record of ion chemistry from Agassiz Ice Cap, northern Ellesmere Island, NWT, Canada, *Atmospheric Environment*, *33*, 347- 357, 1999.
- Kotlyakov, V.M., S.M. Arkhipov, K.A. Anderson, and O.V. Nagornov, Deep drilling of glaciers in the Eurasian Arctic as a source of paleoclimate records, *Quaternary Science Reviews*, *23*, 1371-1390, 2004.
- Legrand, M.R., and R.J. Delmas, Formation of HCl in the Antarctic atmosphere, *Journal of Geophysical Research*, *93*, 7153-7168, 1988.
- Legrand, M., and P.A. Mayewski, Glaciochemistry of polar ice cores: a review, *Reviews of Geophysics*, *35*, 219- 243, 1997.
- Lugauer, M., U. Baltensperger, M. Furger, H.W. Gaggeler, D.T. Jost, M. Schwikowski, and H. Wanner, Aerosol transport to the high Alpine sites Jungfraujoch (3454 m asl) and Colle Gnifetti (4452 m asl), *Tellus*, *50B*, 76-92, 1998.
- Mayewski, P.A., W.B. Lyons, M.J. Spencer, M. Twickler, W. Dansgaard, B. Koci, C.I. Davidson, and R.E. Honrath, Sulfate and nitrate concentrations from a south Greenland ice core, *Science*, *232*, 975- 977, 1986.
- Mayewski, P.A., M.J. Spencer, M.S. Twickler, and S. Whitlow, A glaciochemical survey of the Summit region, Greenland, *Annals of Glaciology*, *14*, 186-190, 1990.



- Mosley-Thompson, E., J.R. McConnell, R.C. Bales, Z. Li, P.N. Lin, K. Steffen, L.G. Thompson, R. Edwards, and D. Bathke, Local to regional-scale variability of annual net accumulation on the Greenland ice sheet from PARCA cores, *Journal of Geophysical Research*, 106, 33,839-33,851, 2001.
- Murphy, A., *A glaciochemical record from the Devon Ice Cap and late Holocene reconstruction of past sea-ice extent in the North Water Polynya, eastern Canadian Arctic*, M.S. thesis, University of New Hampshire, Durham, 2000.
- Shiraiwa, T., Y.D. Muravyev, and S. Yamaguchi, Stratigraphic features of firn as proxy climate signals at the summit ice cap of Ushkovsky Volcano, Kamchatka, Russia, *Arctic and Alpine Research*, 29, 414-421, 1997.
- Shrestha, A.B., C.P. Wake, and J.E. Dibb, Chemical composition of aerosol and snow in the high Himalaya during the summer monsoon season, *Atmospheric Environment*, 31, 2815-2826, 1997.
- Shrestha, A.B., C.P. Wake, J.E. Dibb, P.A. Mayewski, S.I. Whitlow, G.R. Carmichael, and M. Ferm, Seasonal variations in aerosol concentrations and compositions in the Nepal Himalaya, *Atmospheric Environment*, 34, 3349-3363, 2000.
- Shrestha, A.B., C. P. Wake, J.E. Dibb, and S.I. Whitlow, Aerosol and precipitation chemistry at a remote Himalayan site in Nepal, *Aerosol Science and Technology*, 36, 441-456, 2002.
- Silvente, E., and M. Legrand, Ammonium to sulfate ratio in aerosol and snow of Greenland and Antarctic regions, *Geophysical Research Letters*, 20, 687-690, 1993.
- Slater, J.F., and J.E. Dibb, Relationships between surface and column aerosol radiative properties and air mass transport at a rural New England site, *Journal of Geophysical Research*, 109, D01303, doi: 10.1029/2003JD003406, 2004.
- Sun, J., D. Qin, P.A. Mayewski, J.E. Dibb, S. Whitlow, Z. Li, and Q. Yang, Soluble species in aerosol and snow and their relationship at Glacier 1, Tien Shan, China, *Journal of Geophysical Research*, 103, 28,021- 28,028, 1998.
- Sun, J., M. Zhang, and L. Tungsheng, Spatial and temporal characteristics of dust storms in China and its surrounding regions, 1960-1999: Relations to source area and climate, *Journal of Geophysical Research*, 106, 18-055-18,066, 2001.
- Thompson, L.G., E. Mosley- Thompson, V. Zagorodnov, M.E. Davis, T.A. Mashiotta, and P. Lin, 1500 years of annual climate and environmental variability as recorded in Bona-Churchill (Alaska) ice cores, *Eos, Transactions, American Geophysical Union*, 85 (47), Fall Meeting Supplement, Abstract PP23C-05, 2004.
- Toom-Saunty, D., and L.A. Barrie, Chemical composition of snowfall in the high Arctic: 1990-1994, *Atmospheric Environment*, 36, 2683-2693, 2002.
- Wake, C.P., J.E. Dibb, P.A. Mayewski, L. Zhongquin, and X. Zichu, The chemical composition of aerosols over the eastern Himalayas and Tibetan Plateau during low dust periods, *Atmospheric Environment*, 28, 675-704, 1994.

- Wake, C., Yalcin, K. and Gundestrup, N., The climate signal recorded in the oxygen isotope, accumulation, and major ion time-series from the Eclipse Ice Core, Yukon, *Annals of Glaciology*, 35, 416-422, 2002.
- Whiteman, D.C., Observations of thermally developed winds systems in mountainous terrain, in *Atmospheric Processes Over Complex Terrain*, edited by W. Blumen, Meteorological Monographs, 23, pp. 5-42, American Meteorological Society, Boston, 1990.
- Whitlow, S., P.A. Mayewski, and J. E. Dibb, A comparison of major chemical species seasonal concentration and accumulation at the South Pole and Summit, Greenland, *Atmospheric Environment*, 26A, 2045-2054, 1992.
- Yalcin, K. and C.P. Wake, Anthropogenic signals recorded in an ice core from Eclipse Icefield, Yukon, Canada, *Geophysical Research Letters*, 28, 4487-4490, 2001.
- Yalcin, K., C.P. Wake and M. Germani, A 100-year record of North Pacific volcanism in an ice core from Eclipse Icefield, Yukon, Canada, *Journal of Geophysical Research*, 108, 10.1029/2002JD002449, 2003.
- Yalcin, K., C.P. Wake, K.J. Kreutz, and S.I. Whitlow, Forest fire signals recorded in ice cores from Eclipse Icefield, Yukon, Canada, *Eos, Transactions, American Geophysical Union*, 85 (47), Fall Meeting Supplement, Abstract PP23C-06, 2004.
- Yalcin, K., C. Wake, S. Whitlow, and K. Kreutz, Seasonal and spatial variability in snow chemistry at Eclipse Icefield, Yukon, Canada, *Annals of Glaciology*, in review.
- Yalcin, K., C.P. Wake, S. Whitlow, and K. Kreutz, A 1000-year record of forest fire activity in three ice cores from Eclipse Icefield, Yukon, Canada, *The Holocene*, in press.
- Zdanowicz C., Y. Amelin, I. Girard, G. Hall, J. Percival, J. Vaive, P. Biscaye, and A. Bory, Trans-Pacific transport of Asian desert dust: characterization of fallout in the St. Elias Mountains, Yukon, Canada, *Eos Transactions, American Geophysical Union*, 85(17), Joint Assembly Supplement, Abstract A23C-06, 2004.

## CHAPTER V

### A 1000-YEAR RECORD OF FOREST FIRE ACTIVITY FROM ECLIPSE ICEFIELD, YUKON, CANADA

(Accepted for publication in *The Holocene*)

#### Abstract

A 1000-year record of forest fire activity has been developed using three annually-dated ice cores from Eclipse Icefield, Yukon, Canada. Forest fire signals were identified as  $\text{NH}_4^+$  residuals above a robust spline and corroborated by an EOF analysis which identified a chemical association in the  $\text{NH}_4^+$ ,  $\text{C}_2\text{O}_4^{2-}$ , and  $\text{K}^+$  records similar to that observed in forest fire plumes. These statistical techniques yielded similar records of forest fire activity, although the EOF analysis provides more conservative identification of forest fire signals. Comparison of forest fire signals in the Eclipse ice cores with the record of annual area burned in Alaska and the Yukon demonstrates that 80% of high fire years in Alaska and 79% of high fire years in the Yukon are identifiable as  $\text{NH}_4^+$  concentration residuals in at least one core from Eclipse Icefield, although any individual core records 36-67% of these events. The Eclipse ice cores record high fire activity in the 1760s, 1780s, 1840s, 1860s, 1880s, 1890s, 1920s-1940s, and 1980s. Peak fire activity occurred in the 1890s, possibly reflecting anthropogenic ignition sources associated with the large influx of people to the Yukon during the Klondike Gold Rush. Periods of low fire activity are evident during the 1770s, 1810s-1830s, 1850s, 1950s, and 1960s. Extending our proxy of fire activity to 1000 A.D. using annual  $\text{NH}_4^+$  concentrations from our one core that extends back this far provides evidence of high fire activity from 1240 to 1410 during the waning stages of the Medieval Warm Period.

## Introduction

The occurrence of fire in the boreal forest is highly variable from year to year, responding largely to climatic variations. Strong correlations have been reported between annual area burned by forest fires in Alaska and both temperature and precipitation, with greater areas burned in warmer and drier years (Kasischke *et al.*, 2002). Relationships have also been demonstrated between annual area burned and indices of atmospheric circulation such as the El Niño-Southern Oscillation and Pacific Decadal Oscillation, which exert considerable influence on temperature and precipitation anomalies in Alaska (Heyerdahl *et al.*, 2002). In fact, annual area burned statistics demonstrate that fifteen of the seventeen largest fire years in Alaska since 1940 occurred during or just after El Niño conditions, which in interior Alaska are accompanied by slightly warmer but significantly drier conditions (Hess *et al.*, 2001). Area burned statistics in Canada and Alaska are also well correlated with lightning frequency, relative humidity, and 500 hPa height anomalies (Flannigan and Harrington, 1988; Skinner *et al.*, 1999, 2002; Kasischke *et al.*, 2002). The sensitivity of high northern latitudes to projected climatic changes over the 21<sup>st</sup> century is expected to result in a significant increase in forest fire activity in the boreal forest due to higher summer temperatures and lengthened fire seasons (Wotton and Flannigan, 1993; Stocks *et al.*, 1998). In fact, anthropogenic climate change may be responsible for the increase in annual area burned by wildfire in Canada since 1970 (Gillett *et al.*, 2004). Long-term records of boreal forest fire activity are needed to evaluate the response of boreal fire regimes to climate change.

Since the boreal forest is an important carbon sink, boreal forest fires also have important implications for the global carbon cycle (e.g., Kasischke *et al.*, 2005). In fact, forest fires in the boreal region of Alaska alone can release as much as 36 teragrams (Tg,  $10^{12}$  g) of carbon to the atmosphere, mostly as CO<sub>2</sub>, in a single high fire year such as 1990 (French *et al.*, 2003). Furthermore, forest fires emit large quantities of aerosols, reactive trace gases, and black carbon soot, all of which play important roles in atmospheric chemistry, regional air quality, and climate (Levine, 1991; DeBell *et al.*, 2004). For example, carbon monoxide and methane from forest

fires reduce the oxidative capacity of the atmosphere by reacting with hydroxyl radical (Crutzen and Andreae, 1990). Nitrogen oxides and hydrocarbons from forest fires participate in tropospheric ozone forming reactions, altering the oxidation pathways of sulfur and nitrogen species (Alexander *et al.*, 2004). Particulate organic carbon in forest fire smoke can act as cloud condensation nuclei, affecting cloud microphysical and optical properties and altering the radiation budget and hydrologic cycle (Penner *et al.*, 1992).

Forest fire plumes also contain large enhancements of aerosol  $\text{NH}_4^+$ ,  $\text{NO}_3^-$ , excess fine  $\text{K}^+$ , and various organic acids such as oxalate, acetate, and formate (Lefter *et al.*, 1994). In fact, forest fires may be the dominant source of  $\text{NH}_4^+$  in the Arctic and Subarctic free troposphere during summer (Talbot *et al.*, 1992). Forest fires are estimated to contribute between 10% and 40% of the total  $\text{NH}_4^+$  deposited on the Greenland Ice Sheet during the Holocene (Fuhrer *et al.*, 1996) and 20% to 30% of total oxalate deposition (Legrand and De Angelis, 1996). Increased concentrations of these species in glacial ice reflect passage of a forest fire plume over a site while snowfall occurred, allowing the use of ice core records in reconstructing forest fire activity (Legrand and De Angelis, 1992, 1996; Fuhrer *et al.*, 1996; Fuhrer and Legrand, 1997; Whitlow *et al.*, 1994; Savarino and Legrand, 1998). Abrupt, short-duration decreases in ice core electrical conductivity (ECM) resulting from  $\text{NH}_4^+$  neutralization of acids present in the ice can also be used to detect forest fire signals in ice cores (Taylor *et al.*, 1996). Other archives of paleo-forest fire activity include fire-scarred tree rings (e.g., Larsen, 1997) and charcoal abundance in lake sediments (e.g., Lynch *et al.*, 2004).

For a forest fire signal to be recorded in glacial ice, meteorological conditions must be favorable for transport of the plume from the fire to the ice core site, loss by scavenging during atmospheric transport must be minimal, wet and/or dry depositional processes must transfer the atmospheric signal to the surface snow, and the labeled snow must be preserved in the ice core (Whitlow *et al.*, 1994; Slater *et al.*, 2001). Since biomass-burning plumes are chemically heterogeneous and depositional processes and post-depositional alteration can produce

considerable spatial variability in glaciochemical signals, there is not, nor should one expect, a one-to-one relationship between forest fires in the source region and detectable forest fire signals in ice core  $\text{NH}_4^+$ ,  $\text{K}^+$ , organic acids, and ECM records. Furthermore, it is not possible to accurately determine the magnitude of a given forest fire event from ice core chemical concentrations due to variable transport distances and meteorological conditions. Instead, ice cores provide a more general record of relative fire activity in upwind regions (Whitlow *et al.*, 1994). Although  $\text{NH}_4^+$  in polar snow and ice has other sources such as emissions from vegetation and soil microbial activity (e.g., Meeker *et al.*, 1997), large, short term increases in  $\text{NH}_4^+$  are uniquely associated with forest fires (Taylor *et al.*, 1996). Oxalate is produced only by combustion processes (Lefer *et al.*, 1994); potentially offering corroboration of ice core  $\text{NH}_4^+$  signals thought to represent forest fires. Meanwhile, peaks in non-sea-salt  $\text{K}^+$  can be associated with crustal dust, making  $\text{K}^+$  an ambiguous tracer of forest fires (Legrand and De Angelis, 1996). Attributing  $\text{NO}_3^-$  concentration peaks in snow solely to forest fires is also problematic due to the multitude of nitrate sources and post-depositional alteration of nitrate signals via photochemical recycling (Dibb *et al.*, 2002).

Studies of Greenland ice cores suggest they preserve a record of forest fire activity in North America, particularly eastern Canada (Legrand and De Angelis, 1992, 1996; Whitlow *et al.*, 1994; Taylor *et al.*, 1996). In fact, a forest fire plume greatly enriched in  $\text{NH}_4^+$ ,  $\text{C}_2\text{O}_4^{2-}$ , and  $\text{K}^+$  originating in the Hudson Bay lowlands has been sampled in real-time at Summit, Greenland (Dibb *et al.*, 1996). Greenland ice cores show increased forest fire activity in North America between 1790 and 1810 and again from 1830 to 1910 (Whitlow *et al.*, 1994). The latter period reflects the large scale burning of forests to clear land for agricultural use during the westward expansion of North American settlement referred to as the Pioneer Agricultural Revolution (Holdsworth *et al.*, 1996). The decrease in forest fire activity post 1910 reflects the increasing importance of active fire suppression in eastern North America (Whitlow *et al.*, 1994). An earlier period of enhanced forest fire activity between 1200 and 1350 A.D. possibly reflects warmer and

drier climatic conditions during the Medieval Warm Period (Savarino and Legrand, 1998). The Mt. Logan ice core records forest fires in northwest North America and Siberia, with periods of high fire activity from 1770-1790, 1810-1830, 1850-1870, and 1930-1980 (Whitlow *et al.*, 1994). In fact, plumes from forest fires burning in Alaska and the Yukon have been directly observed over the Mt. Logan region (Holdsworth *et al.*, 1996). Prior to the building of the Trans-Siberia railroad, lightning probably caused most fires in Siberia because of a relative lack of anthropogenic ignition sources (Stocks, 1991); hence ice cores from Mt. Logan may document a forest fire-climate relationship relatively free of anthropogenic influences (Whitlow *et al.*, 1994).

Here we develop a record of forest fire activity spanning the last 100 to 1000 years using three ice cores from Eclipse Icefield (60.51° N, 139.47° W, 3017 m elevation), St. Elias Mountains, Yukon, Canada (Figure V.1). Although only 45 km northeast of the high elevation ice core sites on Mt. Logan, the Eclipse Icefield provides a distinct record due to the difference in elevation between the two sites, which allows the sites to sample different layers of the atmosphere (Yalcin and Wake, 2001; Yalcin *et al.*, 2003; Wake *et al.*, 2002). The availability of three ice cores from Eclipse Icefield allows us to investigate the variability in forest fire signal preservation and improve confidence in our reconstructions of forest fire activity.

### **Ice Core Analysis and Dating**

A 160 m ice core was recovered from Eclipse Icefield in 1996 (Yalcin and Wake, 2001). Two additional cores (345 m and 130 m) drilled one meter apart were recovered in 2002, one hundred meters up the flow line from the 1996 drill site. All three cores were sampled continuously at high resolution for major ions and stable isotopes to establish a detailed chronology for the core. Sample resolution ranged from 6-15 cm for major ions and 2-15 cm for stable isotopes. Stringent core processing techniques were used to ensure samples were contamination free at the ng g<sup>-1</sup> level. Blanks prepared on a frequent basis showed no contamination of samples during processing of the core. Samples were analyzed for major ions

(Na<sup>+</sup>, NH<sub>4</sub><sup>+</sup>, K<sup>+</sup>, Mg<sup>2+</sup>, Ca<sup>2+</sup>, Cl<sup>-</sup>, NO<sub>3</sub><sup>-</sup>, SO<sub>4</sub><sup>2-</sup>, C<sub>2</sub>O<sub>4</sub><sup>2-</sup>) via ion chromatography using a 0.5 ml sample loop in a dedicated laboratory at the University of New Hampshire Climate Change Research Center. The cation system used a CS12A column with CSRS-ultra suppressor in auto suppression recycle mode with 20 mM MSA eluent. The anion system used an AS11 column with an ASRS-ultra suppressor in auto suppression recycle mode with 6 mM NaOH eluent. Oxalate was not quantified in the 1996 core. Stable isotope samples were analyzed at the University of Maine Stable Isotope Laboratory with a Multiprep CO<sub>2</sub> equilibration system coupled to a VG SIRA mass spectrometer for δ<sup>18</sup>O (precision ± 0.05‰) and a Eurovector Cr pyrolysis unit coupled to a GV Isoprime mass spectrometer for δD (precision ± 0.5‰). A section of each core was analyzed for radionuclides (<sup>137</sup>Cs) via gamma spectroscopy.

All three cores show similar radionuclide profiles, with clear identification of the 1963 and 1961 peaks from atmospheric thermonuclear weapons testing that were observed in real-time aerosol samples collected at Whitehorse, Yukon by the Radiation Protection Bureau, Ottawa (Figure V.2). Radioactive fallout from the 1986 Chernobyl nuclear power plant accident was also detected, providing an additional stratigraphic marker. Average annual accumulation from 1963 to 2002 was 1.30 m water equivalent. The presence of discrete ice layers in the Eclipse ice core averaging 5% of the net accumulation by weight demonstrates that a limited amount of surface melting occurs at the Eclipse site during summer. Meltwater percolation does not significantly alter the glaciochemical records available from the Eclipse ice core as evidenced by the preservation of clear seasonal signals in the major ion and oxygen isotope records, allowing dating of the cores via multi-parameter annual layer counting (Figure V.2).

Annual layers were identified by summer-winter variations in oxygen isotope ratios and sodium concentrations. The annual cycle of δ<sup>18</sup>O maxima in summer precipitation and δ<sup>18</sup>O minima in winter precipitation observed at Eclipse is related in part to the temperatures at which evaporation at the source and cloud condensation of the precipitation occurs (Dansgaard *et al.*,



1973). The annual cycle of  $\text{Na}^+$  concentration maxima in winter and minima in summer is related to pronounced seasonal changes in the influx of marine aerosols (Whitlow *et al.*, 1992). Increased storminess and higher wind speeds in the Gulf of Alaska during winter results in enhanced entrainment of sea salt aerosols and more frequent advection of marine air masses into the St. Elias Mountains, producing the observed winter peaks in sodium concentrations. Age control on the chronology established via annual layer counting is provided by the 1986, 1963 and 1961  $^{137}\text{Cs}$  reference horizons as well as volcanic reference horizons (e.g., Katmai 1912; Tambora 1815; Laki 1783, Kuwae 1453) developed through statistical analysis of the high-resolution sulfate record (Yalcin *et al.*, 2003). In some cases, these identifications have been independently verified using tephrochronology (Figure V.2).

### **Identification of Forest Fire Signals**

We used two techniques to identify forest fire signals in our records. First, a robust spline was used to estimate the time-varying background  $\text{NH}_4^+$  concentrations that represent ammonia emissions from soils and plants (Taylor *et al.*, 1996; Meeker *et al.*, 1997). Residuals above the spline greater than one standard deviation above the mean positive residual ( $0.6 \mu\text{eq l}^{-1}$ ) are then taken to represent forest fire signals (Figure V.3). Although  $\text{NH}_4^+$  in polar snow and ice has other sources including emissions from vegetation, and soil microbial activity (Meeker *et al.*, 1997), large, short term increases in ammonium such as those we have identified as residuals above a robust spline are uniquely associated with forest fires (Taylor *et al.*, 1996). Furthermore, the concentration increases, which we have identified as  $\text{NH}_4^+$  residuals, are not due to changes in accumulation rate because there is no significant correlation between  $\text{NH}_4^+$  concentration and snow accumulation (Yalcin *et al.*, in review).

We also used an empirical orthogonal function (EOF) analysis to identify forest fire signals. The EOF analysis splits the temporal variance of a multi-variant data set into patterns termed empirical eigenvectors that are orthogonal in nature (Peixoto and Oort, 1992). The first

eigenvector explains the greatest percentage of variance in the dataset, with each successive eigenvector describing the maximum remaining variance. Since the modes are orthogonal, there is no correlation between any two modes. This allows differentiation of sources and transport characteristics by relationships between individual species as described by each EOF (Mayewski *et al.*, 1994). Therefore, each EOF can provide information on a different environmental parameter controlling the glaciochemistry of an ice core.

Applying EOF analysis to the suite of ions measured in the Eclipse 2002 ice cores reveals that  $\text{NH}_4^+$ ,  $\text{K}^+$ , and  $\text{C}_2\text{O}_4^{2-}$  are loaded on EOF 3 which describes 14 % of the variance in the full dataset and 25% to 28% of the variance in these three species produced by forest fires (Table V.1). The Eclipse 1996 ice core is also loaded with  $\text{NH}_4^+$  and  $\text{K}^+$  on EOF 3, suggesting similar behavior despite the lack of  $\text{C}_2\text{O}_4^{2-}$  analyses for this core. Comparison of the EOF 3 time series with the raw  $\text{NH}_4^+$ ,  $\text{K}^+$ , and  $\text{C}_2\text{O}_4^{2-}$  time series shows that EOF 3 picks up nearly all the  $\text{NH}_4^+$  and  $\text{C}_2\text{O}_4^{2-}$  peaks, as well as those  $\text{K}^+$  peaks associated with peaks in  $\text{NH}_4^+$  and  $\text{C}_2\text{O}_4^{2-}$ . Furthermore, inspection of the EOF 3 time series reveals an episodic character in the species of interest (Figure V.3), as would be expected if EOF 3 represents an episodic forcing such as forest fire events. The similarity between the chemical association identified by EOF 3 and the chemical enhancements observed in forest fire plumes as well as the similarity to the  $\text{NH}_4^+$  residual time series leads us to conclude that EOF 3 provides a record of forest fire activity.

These two approaches for identifying forest fire signals provide similar records of fire activity (Figure V.3). However, some events identified as  $\text{NH}_4^+$  residuals are not identified by the EOF analysis since they are not associated with concurrent enhancements of  $\text{K}^+$  and  $\text{C}_2\text{O}_4^{2-}$ . Furthermore,  $\text{NH}_4^+$  concentrations provided by EOF 3 (mean plus one standard deviation equal to  $0.3 \mu\text{eq l}^{-1}$ ) are about one-half those given by the  $\text{NH}_4^+$  residuals (mean plus one standard deviation equal to  $0.6 \mu\text{eq l}^{-1}$ ). For these reasons we feel that the EOF analysis provides a more conservative identification of forest fire signals, since it identifies only those events with

enhancements in all three species. Since  $\text{C}_2\text{O}_4^{2-}$  was not quantified in the Eclipse 1996 ice core, the EOF 3 time series are not directly comparable between the 1996 and 2002 cores. We therefore limit the remainder of our discussion to events identified as  $\text{NH}_4^+$  residuals in order to incorporate data from all three cores in our analysis. Since most events (70%) are identified as both  $\text{NH}_4^+$  residuals and by EOF analysis, either technique yields a similar proxy for forest fire activity. The chemical association described by EOF 3 provides an additional line of evidence supporting the interpretation of  $\text{NH}_4^+$  peaks in our record as forest fire signals because EOF 3 provides a multi-parameter record of enhancements in  $\text{NH}_4^+$ ,  $\text{K}^+$ , and  $\text{C}_2\text{O}_4^{2-}$ , all species that are produced by forest fires. Studies of forest fire records from Greenland ice cores report that concurrent enhancements in other species such as  $\text{K}^+$  or organic acids are needed to confidently attribute ice core  $\text{NH}_4^+$  spikes to forest fires (Whitlow *et al.*, 1994; Savarino and Legrand, 1998). Since most of the  $\text{NH}_4^+$  spikes in the Eclipse ice cores are also identified by the multi-parameter EOF analysis, forest fires may be the only significant source of  $\text{NH}_4^+$  spikes in our cores. Greenland may be affected by other  $\text{NH}_4^+$  sources necessitating corroboration of suspected forest fire signals using other glaciochemical records such as organic acids.

### **Validation of the Record**

To validate our record as a proxy for forest fire activity, we compared our results to records of annual area burned in potential forest fire source regions affecting Eclipse Icefield. It is important to note that fire activity and annual area burned are not synonymous since a small percentage (3%) of fires account for the vast majority (98%) of acreage burned each year (Stocks *et al.*, 2002). However, periods of increased fire activity can be expected to correspond to larger areas burned. We considered two potential forest fire source regions: Alaska, for which annual area burned statistics are available since 1940 from the Alaska Fire Service, Bureau of Land Management, Fairbanks, Alaska, as discussed in detail by Kasischke *et al.* (2002); and the Yukon, for which annual area burned statistics are available since 1946 (Weber and Stocks,

1998). Since the lifetime of tropospheric  $\text{NH}_4^+$  aerosol is on the order of 1-2 weeks,  $\text{NH}_4^+$  from forest fires in these regions can be transported sufficient distances to reach Eclipse. A third possible source area, British Columbia, does not appear to be an important source region for forest fires affecting Eclipse Icefield, since most forest fires in the province are well downwind of Eclipse to the south and east (Taylor and Thandi, 2002).

We evaluated the preservation of forest fire signals as  $\text{NH}_4^+$  residuals at Eclipse during years of high fire activity in Alaska and the Yukon (Table V.2). High fire years are defined as years in which the area burned was more than 1.5 times the long-term average (Kasischke *et al.*, 2002). For Alaska, a high fire year is one with more than 530,000 hectares burned, while a high fire year in the Yukon burns more than 168,000 hectares because of the smaller area covered by boreal forest in the Yukon relative to Alaska. Although only one in four years can be considered a high fire year based on annual area burned statistics, high fire years account for the majority (60%) of the total area burned in historical records (Kasischke *et al.*, 2002). Therefore, high fire years are those of the most importance in reconstructing past forest fire activity. Our analysis indicates that 80% and 79% of high fire years in Alaska and the Yukon, respectively, are recorded as  $\text{NH}_4^+$  residuals in at least one of the Eclipse ice cores (Table V.3). Furthermore, we found nearly equal sensitivity of our record to high fire years in Alaska and the Yukon, suggesting that Alaska and the Yukon are probably equally important source regions for forest fires impacting Eclipse Icefield. Interestingly, only three years (1950, 1969, and 1977) qualify as high fire years in both Alaska and the Yukon, suggesting considerable regional variability in fire activity.

Given year-to-year variations in meteorological conditions and the remoteness of the Eclipse site at 3017 m elevation from forested regions, it is not surprising that some high fire years in Alaska and the Yukon are not recorded at Eclipse. Nonetheless, this comparison provides evidence that our record provides a reasonable proxy for forest fire activity in these regions, with about four out of every five high fire years identifiable in the record. However,  $\text{NH}_4^+$  concentration spikes frequently occur in years with less than 200,000 hectares burned,

suggesting our record is sensitive to less intense fire activity in nearby areas (southwest Yukon or east-central Alaska) or to meteorological conditions favorable for transport and preservation of forest fire plumes at Eclipse Icefield. It is important to reiterate that quantitative information on the size of a given fire year can not be extracted from ice core data due to year-to-year differences in atmospheric circulation pathways and transport distances between burned areas and an ice core site. For these reasons there is no predictable relationship between size of a fire year and peak  $\text{NH}_4^+$  concentrations in glacial ice.

### **Reconstruction of Fire Activity**

#### **Fire activity over the last 250 years**

We use the proxy for forest fire activity provided by  $\text{NH}_4^+$  residuals in the Eclipse ice cores to reconstruct fire activity in the Yukon region over two time periods: the last 250 and last 1000 years. All ice core data were resampled at constant resolution of eight samples per year for the last 250 years to avoid spurious trends due to changing sample resolution. To identify intervals of high and low fire activity in our record, we counted the number of samples per decade whose  $\text{NH}_4^+$  residual value exceeds the signal threshold of one standard deviation above the mean positive residual (Figure V.4). For time intervals where more than one core is available from Eclipse Icefield, the average number of events recorded is represented by the bar with the number of events recorded in each individual core presented as solid black circles. The average number of fire events recorded per decade at Eclipse Icefield between 1750 and 2000 is six.

The Eclipse ice cores indicate high forest fire activity in the 1760s, 1780s, 1840s, 1860s, 1880s, 1890s, 1920s-1940s, and 1980s. Our record suggests the highest forest fire activity during the last 250 years in this region occurred during the 1890s, coinciding with the discovery of gold in the Yukon and the Klondike Gold Rush. This may represent an anthropogenic influence on fire activity associated with the first large influx of miners and settlers into the Yukon. Our record indicates low fire activity in the 1770s, 1810s-1830s, 1850s, 1950s, and 1960s. Records of forest

fire activity provided by the three Eclipse ice cores are in agreement 70% of the time, with exceptions arising from a higher number of events recorded in one of the three cores during the decades of the 1930s, 1970s, and 1980s. The observed spatial variability in the preservation of glaciochemical signals from forest fires could be a result of reworking of the snow surface by blowing and drifting snow, resulting in an uneven layer thickness for distinct chemical horizons (Dibb and Jaffrezo, 1997). Nonetheless, the fact that three ice cores from Eclipse Icefield indicate similar levels of fire activity 70% of the time provides confidence in our reconstruction of forest fire activity.

Similar  $\text{NH}_4^+$  concentrations between the Eclipse, Mt. Logan (Yukon) and 20D (Greenland) ice cores permits direct comparison of our record of forest fire activity developed from the Eclipse ice cores with the records from the Mt. Logan and 20D ice cores presented by Whitlow *et al.* (1994). For consistency, we also resampled the original Mt. Logan and 20D  $\text{NH}_4^+$  time series at constant resolution of eight samples per year. As for Eclipse, we used a robust spline to estimate background  $\text{NH}_4^+$  concentrations and counted the number of samples per decade whose  $\text{NH}_4^+$  residual consideration above the spline exceeds the signal threshold of one standard deviation above the mean positive residual. Somewhat surprisingly, comparison of the records demonstrates closer agreement between the Eclipse and 20D records than between the Eclipse and Mt. Logan records (Figure V.4). For example, Eclipse and 20D indicate low fire activity during the 1950s and 1960s, while Mt. Logan suggests the 1950s and 1960s were a period of high fire activity. Conversely, Eclipse and 20D indicate high fire activity in the 1880s, 1890s, 1920s and 1940s, while Mt. Logan suggests low or moderate fire activity. The correlation coefficient for decadal fire activity between Eclipse and 20D is 0.28 while it is only 0.08 between Eclipse and Mt. Logan, although these correlations are not statistically significant. A notable exception occurs during the 1830s and 1850s, when both the Eclipse and Logan records indicate low fire activity, while the 20D record indicates high fire activity. This breakdown in the correspondence of high fire activity in eastern and northwest North America could be a result of

the expansion of settlement and agriculture and associated biomass burning in eastern and central North America in the early-to-mid 1800's, a source region for forest fire plumes affecting Greenland. Meanwhile, northwest North America remained relatively free of anthropogenic ignition sources during this time.

### **Fire activity over the last 1000 years**

Prior to 1750, layer thinning limits the temporal resolution available from the Eclipse ice core  $\text{NH}_4^+$  record. However, annual concentration data can be used to extend the Eclipse record to 1000 A.D. Although annual data lacks the temporal resolution to reconstruct fire activity in the same terms used for the period 1750-2000, we can nonetheless analyze the record for fire signals in the same way using a robust spline and consider the residuals above the spline. Our results suggest high forest fire activity during the period 1240 to 1410 (Figure V.5) possibly reflecting climatic conditions during the waning stages of the Medieval Warm Period. The Medieval Warm Period has been variously dated to 900-1200 A.D. (Jones *et al.*, 2001) or 1000-1300 A.D. (Crowley and Lowery, 2000) but is sometimes used to refer to any climatic anomaly between 500 and 1500 A.D. (Bradley *et al.*, 2003). Furthermore, the Medieval Warm Period was not globally synchronous nor was it continuously warm (Hughes and Diaz, 1994; Mann *et al.*, 1999).

The period of high fire activity in the Eclipse ice core between 1240 and 1410 should correspond to warmer and drier conditions in Alaska and the Yukon, as has been demonstrated for years of high fire activity during the twentieth century (Flannigan and Harrington, 1988; Kasischke *et al.*, 2002). Corroborating evidence for climatic conditions favorable to forest fire activity during the waning stages of the Medieval Warm Period is available from regional paleoclimatic reconstructions including glacier fluctuations, tree rings, and lake sediment cores. Although there is a time lag between climatic change and glacier response, the records of alpine glacier fluctuations considered here are sensitive to decadal to centennial scale climate variations (Wiles *et al.*, 1999). The earliest glacier advances in the Wrangell and St. Elias Mountains and in coastal Alaska during the past millennium, as documented by kill dates of trees overrun by ice,

were centered around 1250 A.D. (Wiles *et al.*, 1999, 2002; Calkin *et al.*, 2001). This was followed by a period of general glacier retreat in Alaska and the Yukon in response to warmer and/or drier conditions that prevailed between about 1300 and 1450 (Wiles *et al.*, 2004) but ending by the early 1400's in coastal portions of Alaska (Calkin *et al.*, 2001). Likewise, tree-ring-width indices from western Prince William Sound, Alaska, suggest a multi-decadal warm period centered on 1300 A.D. (Barclay *et al.*, 1999), while tree-ring based reconstructions of summer temperatures in the Canadian Rockies show a warm period circa 1350-1440 (Luckman *et al.*, 1997). A lake-sediment record from the Alaska Range suggests a more prolonged period of relative warmth from 850 to 1450 A.D. (Hu *et al.*, 2001).

The inferred climatic conditions in Alaska and the Yukon favoring glacier retreat and high forest fire activity during the waning stages of the Medieval Warm Period may have been forced by increased solar irradiance in conjunction with a sustained warm phase of the Pacific Decadal Oscillation (Wiles *et al.*, 2004). This interval was followed by renewed Little Ice Age glacial advances throughout Alaska reflecting cooler and/or wetter conditions that culminated between 1650 and 1850 (Wiles *et al.*, 1999, 2002; Calkin *et al.*, 2001). Little Ice Age cooling is also evident in lake sediments from the Alaska Range between 1450 and 1850 (Hu *et al.*, 2001). Tree-ring-width chronologies from coastal Alaska do not indicate a level of warmth comparable to the early 1300's until after 1800 (Barclay *et al.*, 1999). The cooler and/or wetter conditions prevailing during the Little Ice Age are reflected in the Eclipse ice core by a decrease in forest fire activity after 1410.

Higher frequency of ammonium and formate concentration spikes in the Summit, Greenland EUROCORE suggests a similar increase in fire activity between 1200 and 1350 coincident with the warm and dry conditions of the Medieval Warm Period (Savarino and Legrand, 1998). There is also evidence of elevated rates of charcoal accumulation in lake sediment cores from interior Alaska during this same time period (Lynch *et al.*, 2003). Elsewhere, frequent peaks in charcoal abundance are noted in lake sediment records from



southeastern British Columbia between 980 and 1300 (Hallett *et al.*, 2003) and Finland between 1380 and 1470 (Pitkanen and Huttunen, 1999); while higher fire frequency is suggested by fire-scarred tree-rings in giant sequoias of the Sierra Nevada, California, between 1000 and 1300 (Swetnam, 1993). Meanwhile, the ECM record of the GISP2 ice core suggests a more prolonged and somewhat later period of high fire activity from 1250 to 1650 A.D. (Taylor *et al.*, 1996).

Differences in the regional timing of high fire activity associated with the Medieval Warm Period are not unexpected considering that the Medieval Warm Period was neither globally synchronous nor continuously warm (Hughes and Diaz, 1994; Mann *et al.*, 1999). When viewed in climatic context, the Eclipse record and other fire activity proxies indicate the warm and dry conditions of the Medieval Warm Period were more favorable for forest fire activity in the boreal region than at any other time during the last 1000 years. However, in some areas such as the Kenai Peninsula of Alaska, anthropogenic influences over the last 150 years have resulted in even higher fire activity than during the Medieval Warm Period climatic optimum (Lynch *et al.*, 2003). This is not observed in the Eclipse record, which records forest fires in more remote boreal regions of Alaska and the Yukon, although anthropogenic influences on forest fire activity are suggested by high forest fire activity coincident with the Klondike Gold Rush of the 1890's. Nonetheless, the sensitivity of fire regimes to climatic change is illustrated by these records. If the Medieval Warm Period provides a suitable analogy for climatic conditions in the era of anthropogenic greenhouse gas warming, the paleoenvironmental record seems to confirm predictions of increased fire activity in the boreal region during the 21<sup>st</sup> century.

### **Conclusions**

We have presented a proxy of forest fire activity using ice cores from Eclipse Icefield, Yukon, Canada. Forest fire signals were identified by  $\text{NH}_4^+$  residuals above a robust spline and by an EOF analysis that identified a chemical association in the  $\text{NH}_4^+$ ,  $\text{C}_2\text{O}_4^{2-}$ , and  $\text{K}^+$  records similar to that seen in forest fire plumes. Since 70% of the events are identified by both  $\text{NH}_4^+$

residuals and in the EOF analysis, a similar record is obtained using either technique. Comparing our fire activity proxy to records of annual area burned in Alaska and the Yukon since 1940 and 1946, respectively, demonstrates the Eclipse ice cores provide a good proxy for fire activity in these regions since four out of every five high fire years in Alaska and the Yukon are identifiable as  $\text{NH}_4^+$  residuals at Eclipse Icefield. Furthermore, the three cores from Eclipse agree well with respect to decadal fire activity 70% of the time, allowing us to reconstruct fire activity since 1750 with reasonable confidence. The Eclipse ice cores record high fire activity in the 1760s, 1780s, 1840s, 1860s, 1880s, 1890s, 1920s-1940s, and 1980s. Peak fire activity occurred in the 1890s, possibly reflecting anthropogenic ignition sources associated with the first large-scale influx of settlers and miners into the Yukon during the Klondike Gold Rush. Periods of low fire activity are evident during the 1770s, 1810s-1830s, 1850s, 1950s, and 1960s. Extending our proxy of fire activity to 1000 A.D. using annual  $\text{NH}_4^+$  concentrations from a single core provides evidence of high fire activity during the waning stages of the Medieval Warm Period between 1240 and 1410. If the Medieval Warm Period does provide a suitable analogy for future climatic conditions resulting from anthropogenic greenhouse gas emissions, then high fire activity in Alaska and the Yukon seems likely during the 21<sup>st</sup> century.

Our results are compared and contrasted with other ice core proxies of forest fire activity from 20D and Summit, Greenland, and Mt. Logan, Yukon. Somewhat surprisingly, the Eclipse record correlates best with the records from Greenland, with periods of high and low fire activity synchronous in eastern and northwestern North America. This correlation between Eclipse and Greenland breaks down during periods of pioneer land clearing for agriculture in eastern North America that are well recorded in Greenland but for which no evidence is seen in the Eclipse ice core since it is located upwind of the regions affected. Furthermore, both the Eclipse and Summit, Greenland ice cores provide evidence of high fire activity during the later part of the Medieval Warm Period between about 1200 and 1400 A.D. Ice core proxy records of boreal forest fire activity such as the one presented here are useful for evaluating the response of boreal

forest fire regimes to climate change, potentially corroborating model projections of increased fire activity in response to projected climate change in the 21<sup>st</sup> century.

The apparent uniqueness of the Mt. Logan forest fire source region suggests that the Mt. Logan summit plateau records primarily Siberian forest fires, suggesting that the new ice cores from Mt. Logan, as well as the ice core from Belukha Glacier in the Siberian Altai (Olivier *et al.*, 2003), may be suitable for reconstruction of Siberian forest fire activity. Although government compiled fire statistics are available for Russia (Korovin, 1996), comparison of official fire statistics to burned area estimates derived from satellite data (Sukhinin *et al.*, 2004) shows no correlation between the two, indicating the official fire statistics do not provide an unbiased sample of fire activity in Siberia. The Mt. Logan and Belukha Glacier ice cores could be used to develop a record of forest fire activity in Siberia where reliable documentary evidence of fire activity is essentially non-existent prior to the advent of remote sensing technologies (Sukhinin *et al.*, 2004).

#### **Acknowledgements**

We would like to thank E. Blake, S. Bastien, and A. Mondrick for field assistance, and the Geological Survey of Canada (especially D. Fisher and C. Zdanowicz) for logistical support. We would also like to thank D. Introne for stable isotope analyses and C. Girod for helpful discussions. E. Kasischke kindly provided annual area burned statistics for Alaska. We would also like to thank E. Kasischke and an anonymous reviewer for helpful comments that resulted in an improved manuscript. The National Science Foundation Office of Polar Programs funded this research.

**Table V.1** Eclipse 2002 Core 3 EOF Analysis

	Normalized Eigenmodes <sup>1</sup>				Percent Variance Explained <sup>2</sup>			
	EOF 1	EOF 2	EOF 3	EOF 4	EOF 1	EOF 2	EOF 3	EOF 4
Na <sup>+</sup>	0.44	0.78	0.24	-0.18	19.3	60.3	5.5	3.3
NH <sub>4</sub> <sup>+</sup>	0.54	-0.49	0.50	-0.14	29.1	24.3	24.8	1.9
K <sup>+</sup>	0.44	0.25	0.49	0.68	19.3	6.1	24.5	46.3
Mg <sup>2+</sup>	0.73	0.05	-0.46	0.23	52.7	0.2	21.4	5.3
Ca <sup>2+</sup>	0.86	-0.11	-0.37	0.13	74.0	1.1	13.7	1.7
Cl <sup>-</sup>	0.55	0.72	0.14	-0.27	29.8	51.3	1.9	7.3
NO <sub>3</sub> <sup>-</sup>	0.78	-0.33	-0.14	-0.09	60.3	11.0	2.0	0.8
SO <sub>4</sub> <sup>2-</sup>	0.83	-0.05	-0.20	-0.17	68.8	0.3	4.1	2.8
C <sub>2</sub> O <sub>4</sub> <sup>2-</sup>	0.50	-0.44	0.53	-0.15	25.2	19.1	28.0	2.1
	TOTAL				42.0	19.3	14.0	8.0

<sup>1</sup>Correlation coefficient (r-value) between EOF time series and glaciochemical time series

<sup>2</sup>R-squared value between EOF time series and glaciochemical time series

**Table V.2 High Fire Years Recorded in the Eclipse Ice Cores<sup>1</sup>**

Alaska <sup>2</sup>					Yukon <sup>3</sup>				
Year	Hectares	Core 1	Core 2	Core 3	Year	Hectares	Core 1	Core 2	Core 3
2002	883,576	--	Y	Y	1999	194,456	--	Y	
1997	774,696	--		Y	1998	343,672	--	Y	Y
1991	708,766	Y		Y	1995	261,380	Y	Y	Y
1990	1,291,125	Y		Y	1994	421,710	Y		Y
1988	885,841	Y	Y	Y	1989	383,188			Y
1977	960,342	Y			1982	240,111	Y	Y	Y
1969	1,713,287	Y			1977	312,469	Y		
1961	553,318				1971	301,730	Y		
1957	2,044,397	Y		Y	1969	618,109	Y		
1954	562,721				1966	191,648	Y	Y	
1950	1,221,016		Y		1958	889,032		Y	Y
1947	578,905	Y	Y	Y	1953	175,800			
1946	581,618	Y	Y	Y	1951	339,151	Y		
1941	1,476,022		Y	Y	1950	177,024			
1940	1,821,862								

<sup>1</sup>Y denotes NH<sub>4</sub><sup>+</sup> residuals detected in the ice core during that year, blank entries denote no NH<sub>4</sub><sup>+</sup> residuals in the core that year and -- denotes a high fire year that is outside the period of record for that core (Core 1 1894-1996; Core 2 1000-2002; Core 3 1910-2002).

<sup>2</sup>Alaska annual area burned data from the Alaska Fire Service, Bureau of Land Management, Fairbanks, as discussed by Kasischke *et al.*, 2002.

<sup>3</sup>Yukon annual area burned data from Government of Yukon Department of Community Services: <http://www.gov.yk.ca/depts/community/firemanagement/sts46.html>.

**Table V.3** Percentage of high fire years recorded in the Eclipse ice cores.

Percent High Fire Years Recorded (Alaska)					Percent High Fire Years Recorded (Yukon)				
any one core	more than one core	Core 1	Core 2	Core 3	any one core	more than one core	Core 1	Core 2	Core 3
80%	47%	62%	40%	60%	79%	36%	67%	36%	43%
(12/15) <sup>1</sup>	(7/15)	(8/13)	(6/15)	(9/15)	(11/14)	(5/14)	(8/12)	(5/14)	(6/14)

<sup>1</sup>Number of years recorded out of total possible for that core or group of cores.

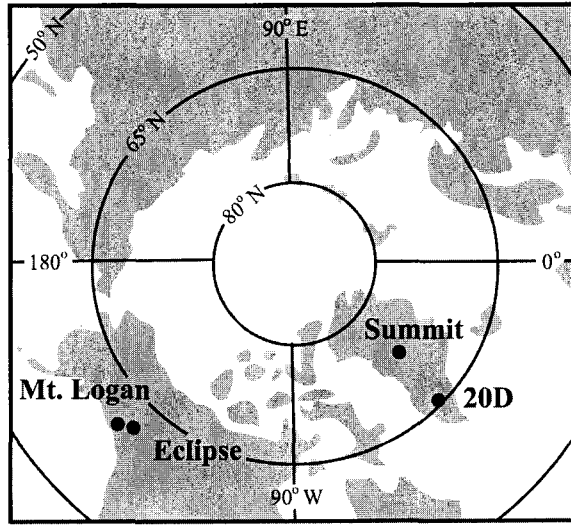


**Figure V.1.** Location of Eclipse Icefield and other ice core sites discussed in this paper.

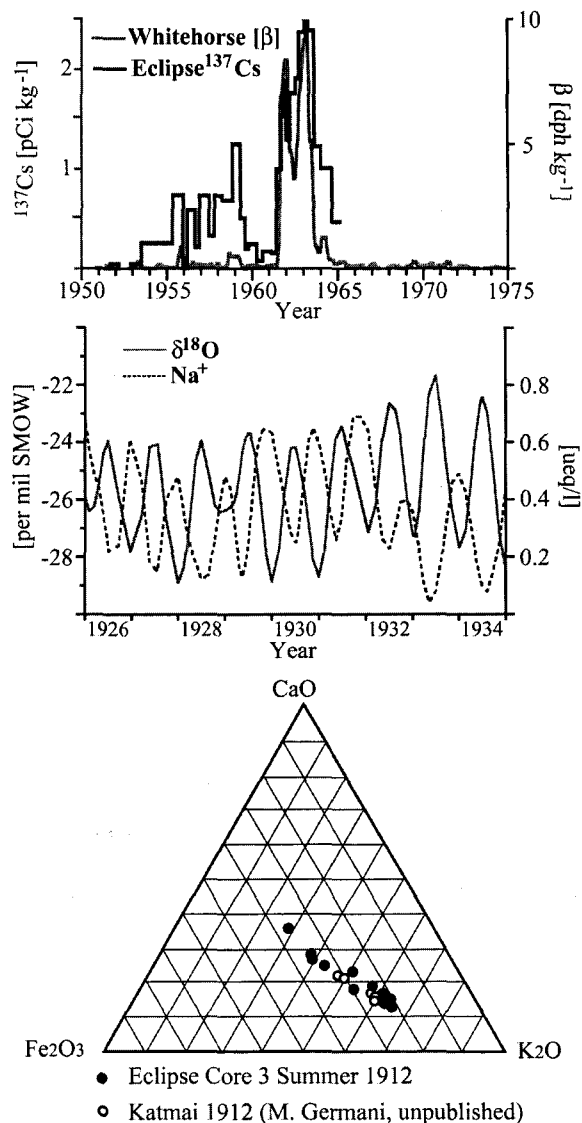


**Figure V.2.** Parameters used in dating of the Eclipse ice cores. Top: Comparison of Eclipse ice core  $^{137}\text{Cs}$  profiles with real-time aerosol samples from Whitehorse, Yukon Territory shows clear identification of the 1963 and 1961 radionuclide peaks from atmospheric nuclear weapons testing. Middle: Seasonal signals in the smoothed  $\delta^{18}\text{O}$  and  $\text{Na}^+$  records used to date the Eclipse ice cores via annual layer counting. Bottom: Major oxide composition of volcanic glass shards found in the summer 1912 layer of all three Eclipse ice cores closely matches the composition of volcanic glass produced by the June 1912 eruption of Katmai, Alaska; providing tephrochronological reference horizons to verify the chronology developed by annual layer counting.



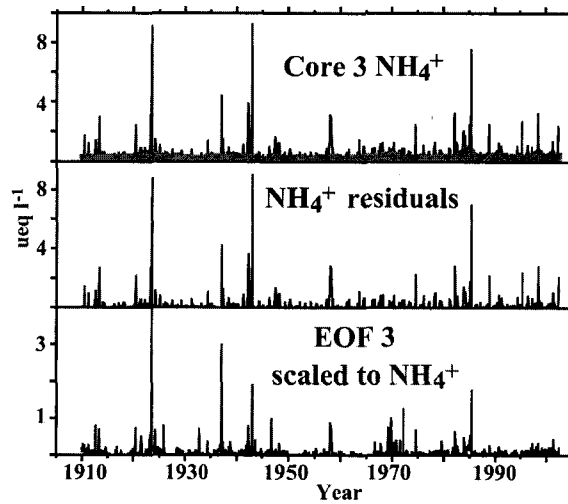


**Figure V.3.** Identification of forest fire signals in the Eclipse 2002 Core 3 ice core. Top: The  $\text{NH}_4^+$  time series is smoothed with a robust spline to estimate background  $\text{NH}_4^+$  concentrations (denoted by solid gray area). Middle: The residuals above the spline are considered to represent forest fire signals. Bottom: The EOF 3 time series, scaled to  $\text{NH}_4^+$  for comparison. Note the different scale of the Y-axis used to plot the EOF 3 time series.

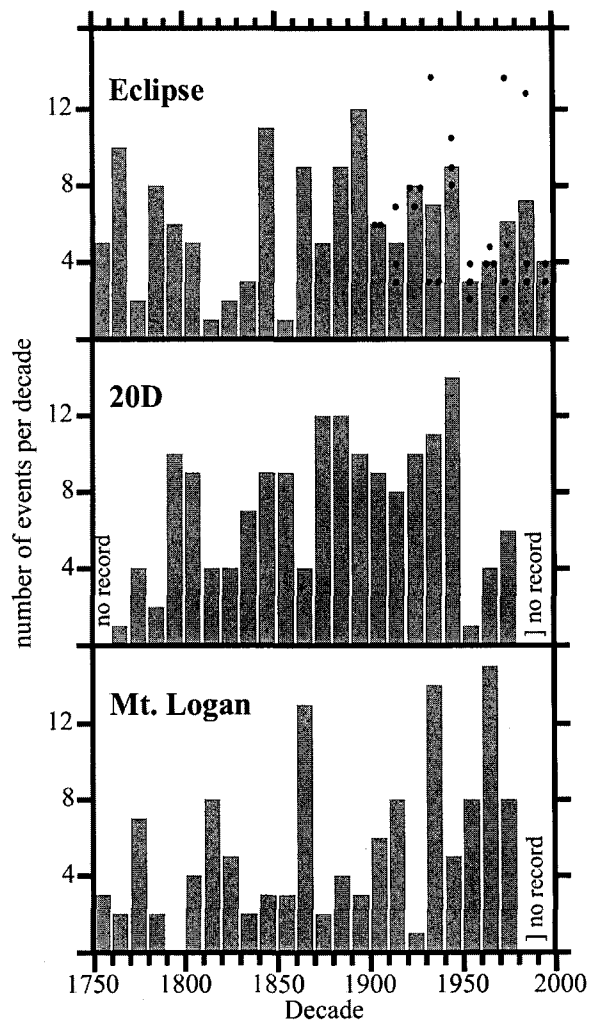


**Figure V.4.** Reconstruction of forest fire activity since 1750 using the Eclipse ice cores (top). Post 1900, the bar represents the average number of forest fire events recorded per decade in the multiple ice cores available, with the number of events recorded in each individual core indicated by solid black circles. From 1910-1990 three cores from Eclipse are available, with two cores available from 1900-1910 and 1990-2000. The Eclipse forest fire record is compared to other ice core proxies of forest fire activity from 20D, South Greenland (middle) and Mt. Logan, Yukon (bottom).

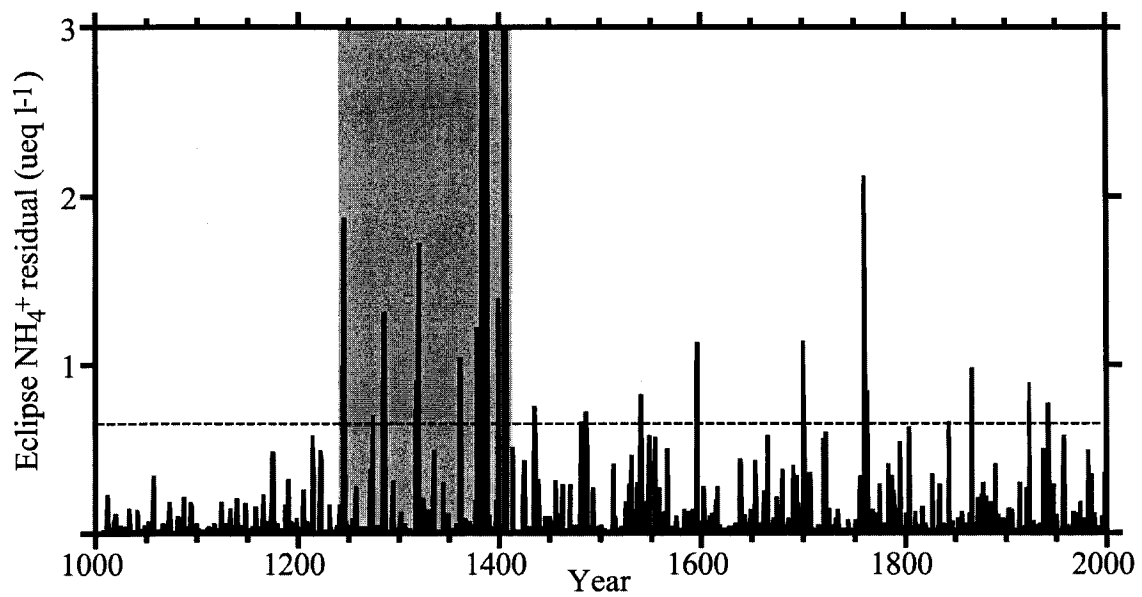


**Figure V.5.** Evaluation of forest fire signals using annual NH<sub>4</sub><sup>+</sup> residuals from Eclipse Icefield suggest the period 1240-1410 (shaded) was the most prolonged period of high fire activity in the Yukon and Alaska in the last one thousand years. Dashed line indicates one standard deviation above the mean positive annual NH<sub>4</sub><sup>+</sup> residual.

## References

- Alexander, B., J. Savarino, K.J. Kreutz, and M.H. Thiemens, Impact of pre-industrial biomass burning emissions on the oxidation pathways of tropospheric sulfur and nitrogen, *Journal of Geophysical Research*, 109, D08303, doi: 10.1029/2003JD004218, 2004.
- Barclay, D.J., G.C. Wiles, and P.E. Calkin, A 1119-year tree-ring-width chronology from western Prince William Sound, southern Alaska, *The Holocene*, 9, 79-84, 1999.
- Bradley, R. S., M.K. Hughes, and H.F. Diaz, Climate in Medieval time, *Science*, 302, 404-405, 2003.
- Calkin, P. E., G.C. Wiles, and D.J. Barclay, Holocene coastal glaciation of Alaska, *Quaternary Science Reviews*, 20, 449-461, 2001.
- Crowley, T.J., and T.S. Lowery, How warm was the Medieval Warm Period? *Ambio*, 29, 51-54, 2000.
- Crutzen, P.J., and M.O. Andreae, Forest fire in the tropics: impact on atmospheric chemistry and biogeochemical cycles, *Science*, 250, 1669-1678, 1990.
- Dansgaard, W., S.J. Johnsen, H.B. Clausen, and N. Gundestrup, Stable isotope glaciology, *Meddelelser om Gronland Bd*, 197, N2, 1-53, 1973.
- DeBell, L.J., R.W. Talbot, J.E. Dibb, J.W. Munger, E.V. Fischer, and S.E. Frohling, A major regional air pollution event in the northeastern United States caused by extensive forest fires in Quebec, Canada, *Journal of Geophysical Research*, 109, 9305, doi: 10.1029/2004JD004840, 2004.
- Dibb, J.E., and J.L. Jaffrezo, Air-snow investigations at Summit, Greenland: An overview; *Journal of Geophysical Research*, 102, 26,795-26,807, 1997.
- Dibb, J.E., R.W. Talbot, S.I. Whitlow, M.C. Shipham, J. Winterle, J. McConnell, and R. Bales, Forest fire signatures in the atmosphere and snow at Summit, Greenland: An event on 5 August, 1994, *Atmospheric Environment*, 30, 553-561, 1996.
- Dibb, J.E., M. Arsenault, M.C. Peterson and R.E. Honrath, Fast nitrogen oxide photochemistry in Summit, Greenland snow, *Atmospheric Environment*, 36, 2501- 2511, 2002.
- Fisher, D.A., J. Bourgeois, M. Demuth, R. Koerner, M. Parnandi, J. Sekerka, C. Zdanowicz, J. Zheng, C. Wake, K. Yalcin, P. Mayewski, K. Kreutz, E. Osterberg, D. Dahl-Jensen, K. Goto-Azuma, G. Holdsworth, E. Steig, S. Rupper, and M. Wasckiewicz, Stable isotope records from Mount Logan and Eclipse ice cores and nearby Jellybean Lake; water cycle of the North Pacific over 2000 years and over 5 vertical kilometers; sudden shifts and tropical connections, *Geographie Physique et Quaternaire*, in press.
- Flannigan, M.D., and J.B. Harrington, A study of the relation of meteorological variables to monthly provincial area burned by wildfire in Canada (1953-1980), *Journal of Applied Meteorology*, 27, 441-452, 1988.

- French, N.H.F., E.S. Kasischke, and D.G. Williams, Variability in the emission of carbon-based trace gases from wildfire in the Alaskan boreal forest, *Journal of Geophysical Research*, *108*, 8151, doi: 10.1029/2001JD000480, 2003.
- Fuhrer, K., A. Neftel, M. Anclin, T. Staffelbach, and M. Legrand, High-resolution ammonium record covering a complete glacial-interglacial cycle, *Journal of Geophysical Research*, *101*, 4147-4164, 1996.
- Fuhrer, K., and M. Legrand, Continental biogenic species in the Greenland Ice Core Project ice core: Tracing back the biomass history of the North American continent, *Journal of Geophysical Research*, *102*, 26,735- 26,745, 1997.
- Gillett, N.P., A.J. Weaver, F.W. Zwiers, and M.D. Flannigan, Detecting the effect of climate change on Canadian forest fires, *Geophysical Research Letters*, *31*, L18211, doi:10.1029/2004GL020876, 2004.
- Hallett, D.J., R.W. Mathewes, and R.C. Walker, A 1000-year record of forest fires, drought, and lake-level change in southeastern British Columbia, Canada, *The Holocene*, *13*, 751-761, 2003.
- Hess, J.C., C.A. Scott, G.L. Hufford, and M.D. Fleming, El Nino and its impact on fire weather conditions in Alaska. *International Journal of Wildland Fire*, *10*, 1-13, 2001.
- Heyerdahl, E.K., L.B. Brubaker, and J.K. Agee, Annual and decadal climate forcing of historical fire regimes in the interior Pacific Northwest, USA, *The Holocene*, *12*, 597-604, 2002.
- Holdsworth, G., K. Higuchi, G.A. Zielinski, P.A. Mayewski, M. Wahlen, B. Deck, P. Chylek, B. Johnson, and P. Damaino, Historical biomass burning: late 19<sup>th</sup> century pioneer agriculture revolution in northern hemisphere ice core data and its atmospheric interpretation, *Journal of Geophysical Research*, *101*, 23,317- 23,334, 1996.
- Hu, F.S., E. Ito, T.A. Brown, B.B. Curry, and D.R. Engstrom, Pronounced climatic variations in Alaska during the last two millennia, *Proceedings of the National Academy of Sciences* *98*, 10,552-10,556, 2001.
- Hughes, M.K., and H.F. Diaz, Was there a 'Medieval Warm Period', and if so, where and when? *Climatic Change*, *26*, 109-142, 1994.
- Jones, P.D., T.J. Osborn, and K.R. Briffa, The evolution of climate over the last millennium, *Science*, *292*, 662-667, 2001.
- Kasischke, E.S., D. Williams, and D. Barry, Analysis of the patterns of large fires in the boreal forest region of Alaska, *International Journal of Wildland Fire*, *11*, 131-144, 2002.
- Kasischke, E.S., E. Hyer, P. Novelli, L.P. Bruhwiler, N.H.F. French, A.I. Sukhinin, J.H. Hewson, and B.J. Stocks, Influences of boreal fire emissions on Northern Hemisphere atmospheric carbon dioxide and carbon monoxide, *Global Biogeochemical Cycles*, *19*, GB1012, doi: 10.1029/2004GB002300, 2005.

- Korovin, G.N., Analysis of the distribution of forest fires in Russia, in *Fire in Ecosystems of Boreal Eurasia*, edited by J.G. Goldammer and V.V. Furyaev, pp. 112-118, Kluwer Academic Publishers, Dordrecht, The Netherlands, 1996.
- Larsen, C.P.S., Spatial and temporal variations in boreal forest fire frequency in northern Alberta, *Journal of Biogeography*, 24, 663-673, 1997.
- Lefer, B.L., R.W. Talbot, R.C. Harriss, J.D. Bradshaw, S.T. Sandholm, J.O. Olson, G.W. Sachse, J. Collins, M.A. Shipman, D.R. Blake, K.I. Klemm, K. Gorzelska, and J. Barrick, Enhancement of acidic gases in biomass-burning impacted air masses over Canada, *Journal of Geophysical Research*, 99, 1721-1737, 1994.
- Legrand, M., and M. De Angelis, Large perturbations of ammonium and organic acids content in the Summit-Greenland ice core: Fingerprint from forest fires? *Geophysical Research Letters*, 19, 473-475, 1992.
- Legrand, M., and M. De Angelis, Light carboxylic acids in Greenland ice: a record of past forest fires and vegetative emissions from the boreal zone, *Journal of Geophysical Research*, 101, 4129-4145, 1996.
- Levine, J.S. (Ed.), *Global Biomass Burning: Atmospheric, Climatic, and Biospheric Implications*, MIT Press, Cambridge, Mass., 1991.
- Luckman, B.H., K.R. Briffa, P.D. Jones, and F.H. Schweingruber, Tree-ring based reconstruction of summer temperatures at the Columbia Icefield, Alberta, Canada, A.D. 1073-1983, *The Holocene*, 7, 375-389, 1997.
- Lynch, J.A., J.S. Clark, N.H. Bigelow, M.E. Edwards, and B.P. Finney, Geographic and temporal variations in fire history in boreal ecosystems of Alaska, *Journal of Geophysical Research*, 107, 8152, doi: 10.1029/2001JD000332, 2003.
- Lynch, J.A., J.L. Hollis, and F.S. Hu, Climatic and landscape controls of the boreal forest fire regime: Holocene records from Alaska, *Journal of Ecology*, 92, 477-489, 2004.
- Mann, M.E., R.S. Bradley, and M.K. Hughes, Northern Hemisphere temperatures during the past millennium: inferences, uncertainties, and limitations, *Geophysical Research Letters*, 26, 759-762, 1999.
- Mayewski, P.A., L.D. Meeker, S. Whitlow, M.S. Twickler, M.C. Morrison, P.M. Grootes, G.C. Bond, R.B. Alley, D.A. Meese, and T. Gow, Changes in atmospheric circulation and ocean ice cover over the North Atlantic region over the last 41,000 years, *Science*, 263, 1747-1751, 1994.
- Meeker, L.D., P.A. Mayewski, M.S. Twickler, S.I. Whitlow, and D.A. Meese, A 110,000 year history of change in continental biogenic emissions and related atmospheric circulation inferred from the Greenland Ice Sheet Project 2 ice core, *Journal of Geophysical Research*, 102, 26489-26505, 1997.
- Olivier, S., M. Schwikowski, S. Brutsch, S. Eyrikh, H.W. Gaggeler, M. Luthi, T. Papina, M. Saurer, U. Schotterer, L. Tobler, and E. Vogel, Glaciochemical investigation of an ice

- core from Belukha Glacier, Siberian Altai, *Geophysical Research Letters*, 30, 2019, doi:10.1029/2003GL018290, 2003.
- Peixoto, J.P., and A.H. Oort, *Physics of Climate*, American Institute of Physics, New York, 1992.
- Penner, J.E., R.E. Dickinson, and C.A. O'Neill, Effects of aerosol from biomass burning on the global radiation budget, *Science*, 256, 1432-1434, 1992.
- Pitkanen, A., and P. Huttunen, A 1300-year forest fire history at a site in eastern Finland based on charcoal and pollen records in laminated lake sediments, *The Holocene*, 9, 311-320, 1999.
- Savarino, J., and M. Legrand, High northern latitude forest fires and vegetation emissions over the last millennium inferred from the chemistry of a central Greenland ice core, *Journal of Geophysical Research*, 103, 8267-8279, 1998.
- Skinner, W.R., B.J. Stocks, D.L. Martell, B. Bonsal, and A. Shabbar, The association between circulation anomalies in the mid-troposphere and area burned by wildfire in Canada, *Theoretical and Applied Climatology*, 63, 89-105, 1999.
- Skinner, W.R., M.D. Flannigan, B.J. Stocks, B.M. Wotton, J.B. Todd, J.A. Mason, K.A. Logan, and E.M. Bosch, A 500 hPa synoptic wildland fire Climatology for large Canadian forest fires, 1959-1996, *Theoretical and Applied Climatology*, 63, 89-105, 2002.
- Slater, J.F., J.E. Dibb, B.D. Keim, and J.D.W. Kahl, Relationships between synoptic-scale transport and interannual variability of inorganic cations in surface snow at Summit, Greenland: 1992-96, *Journal of Geophysical Research*, 106, 20,897-20,912, 2001.
- Stocks, B.J., The extent and impact of forest fires in northern circumpolar countries, in *Global Biomass Burning: Atmospheric, Climatic, and Biospheric Implications*, edited by J.S. Levine, pp. 197-202, MIT Press, Cambridge, Mass., 1991.
- Stocks, B.J., M.A. Fosberg, T.J. Lynham, L. Mearns, B.M. Wotton, Q. Yang, J.Z. Jin, K. Lawrence, G.R. Hartley, J.A. Mason, and D.W. McKenney, Climate change and forest fire potential in Russian and Canadian boreal forests, *Climatic Change*, 38, 1-13, 1998.
- Stocks, B.J., J.A. Mason, J.B. Todd, E.M. Bosch, B.M. Wotton, B.D. Amiro, M.D. Flannigan, K.G. Hirsch, K.A. Logan, D.L. Martell, and W.R. Skinner, Large forest fires in Canada, 1959-1997, *Journal of Geophysical Research*, 107, 8149, doi: 10.1029/2001JD000484, 2002.
- Sukhinin, A.I., N.H.F. French, E.S. Kasischke, J.H. Hewson, A.J. Soja, I.A. Csiszar, E. Hyer, T. Loboda, S.G. Conrad, V.I. Romasko, E.A. Pavlichenko, S.I. Miskiv, and O.A. Slinkin, AVHRR-based mapping of fires in eastern Russia: New products for fire management and carbon cycle studies, *Remote Sensing of the Environment*, 93, 546-564, 2004.
- Swetnam, T.W., Fire history and climate change in giant sequoia groves, *Science*, 262, 885-889, 1993.

- Talbot, R.W., A.S. Vijgen, and R.C. Harris, Soluble species in the Arctic summer troposphere: acidic gases, aerosols, and precipitation, *Journal of Geophysical Research*, 97, 16531-16544, 1992.
- Taylor, K.C., P.A. Mayewski, M.S. Twickler, and S.I. Whitlow, Biomass burning recorded in the GISP2 ice core: a record from eastern Canada? *The Holocene*, 6, 1-6, 1996.
- Taylor, S.W., and G. Thandi, *Development and Analysis of a Provincial Natural Disturbance Database*, FRBC Final Report, Project PAR02003-19, 22 pp., 2002.
- Wake, C.P., K. Yalcin, and N. Gundestrup, The climate signal recorded in the oxygen isotope, accumulation, and major ion time-series from the Eclipse Ice Core, Yukon, *Annals of Glaciology*, 35, 416-422, 2002.
- Weber, M.G., and B.J. Stocks, Forest fires and sustainability in the boreal forests of Canada, *Ambio*, 27, 545-550, 1998.
- Whitlow, S., P.A. Mayewski, and J.E. Dibb, A comparison of major chemical species seasonal concentration and accumulation at the South Pole and Summit, Greenland, *Atmospheric Environment*, 26A, 2045-2054, 1992.
- Whitlow, S., P. Mayewski, J. Dibb, G. Holdsworth, and M. Twickler, An ice-core-based record of forest fire in the Arctic and Subarctic, 1750-1980, *Tellus*, 46B, 234-242, 1994.
- Wiles, G. C., D.J. Barclay, and P.E. Calkin, Tree-ring-dated 'Little Ice Age' histories of maritime glaciers from Western Prince William Sound, Alaska, *The Holocene*, 9, 163-173, 1999.
- Wiles, G.C., G.C. Jacoby, N.K. Davi, and R.P. McAllister, Late Holocene glacier fluctuations in the Wrangell Mountains, Alaska, *Geological Society of America Bulletin*, 114, 896-908, 2002.
- Wiles, G.C., R.D. D'Arrigo, R. Villalba, P.E. Calkin, and D.J. Barclay, Century-scale solar variability and Alaskan temperature change over the past millennium, *Geophysical Research Letters*, 31, doi: 10.1029/2004GL020050, 2004.
- Wotton, B.M., and M.D. Flannigan, Length of the fire season in a changing climate, *Forestry Chronicle*, 69, 187-192, 1993.
- Yalcin, K. and C.P. Wake, Anthropogenic signals recorded in an ice core from Eclipse Icefield, Yukon, Canada, *Geophysical Research Letters*, 28, 4487-4490, 2001.
- Yalcin, K., C.P. Wake and M. Germani, A 100-year record of North Pacific volcanism in an ice core from Eclipse Icefield, Yukon, Canada, *Journal of Geophysical Research*, 108, doi: 10.1029/2002JD002449, 2003.
- Yalcin, K., C.P. Wake, K.J. Kreutz, and S.I. Whitlow, Seasonal and spatial variability in snow chemistry at Eclipse Icefield, Yukon, Canada, *Annals of Glaciology*, in review.



## CHAPTER VI

### ICE CORE PALEOVOLCANIC RECORDS FROM THE ST. ELIAS MOUNTAINS, YUKON, CANADA

#### Abstract

Prior work has demonstrated that a record of regionally significant volcanic eruptions in the North Pacific is available from Eclipse Icefield, Yukon, Canada. The acquisition of two new cores from Eclipse Icefield in 2002, along with previously available cores from Eclipse Icefield (1996) and the nearby Northwest Col of Mount Logan (1980) allow us to extend the record of North Pacific volcanism to 600 years before present using a suite of four ice cores spanning an elevation range of 3 to 5 km. Non-sea-salt sulfate residuals above a robust spline and empirical orthogonal function (EOF) analysis were used to identify volcanic sulfate signatures. Comparisons of volcanic sulfate flux records using linear regression demonstrate a high degree of reproducibility of the results, especially for the largest sulfur producing eruptions such as Katmai 1912. Correlation of volcanic sulfate signals with eruptions documented in the historical record indicates that at least one-third of the eruptions recorded in St. Elias ice cores are from Alaskan and Kamchatkan volcanoes. Although there are several moderately large ( $VEI \geq 4$ ) eruptions recorded in only one of the three available cores from Eclipse Icefield, the use of multiple records provides signals in at least one core from all known  $VEI \geq 4$  eruptions in Alaska and Kamchatka since the 1820's. Tephrochronological evidence from the Eclipse ice core documents eruptions in Alaska (Westdahl, Redoubt, Trident, Katmai), Kamchatka (Avachinsky, Kliuchevskoi, Ksudach), and Iceland (Hekla). Several unidentified tephra-bearing horizons, with available geochemical evidence suggesting Alaskan and Kamchatkan sources, were also found.

## Introduction

Volcanoes are widely recognized as an important component of the climate system (e.g., Robock, 2000; Zielinski, 2000). Explosive volcanic eruptions perturb climate via the radiative properties of sulfate aerosols and the direct blocking of solar radiation by volcanic ash. Although volcanic ash quickly settles out of the atmosphere, limiting its climatic effects (Robock and Mass, 1982; Legrand and Delmas, 1987), sulfate aerosols produced by oxidation of sulfur-rich eruptive gases (SO<sub>2</sub> and H<sub>2</sub>S) can remain aloft for several years in the stratosphere, reflecting solar radiation and cooling surface temperatures (Rampino and Self, 1984; Bluth *et al.*, 1993; Pyle *et al.*, 1996). Volcanic emissions into the free troposphere from moderately explosive eruptions are a major source of relatively long-lived tropospheric sulfate aerosol with important implications for cloud microphysics and radiative climatic forcing (Graf *et al.*, 1997; Robock, 2000). Large, explosive eruptions in the tropical latitudes can perturb climate on a global scale because their aerosols will be dispersed poleward into both hemispheres by the mean meridional stratospheric circulation over a timescale of 1-2 years (Robock, 2000). Meanwhile, mid-to-high latitude eruptions will affect primarily their hemisphere of origin because inter-hemispheric aerosol transport is limited (Zielinski, 2000). However, the lower altitude of the tropopause at higher latitudes allows greater penetration of moderately- explosive eruptions from high latitude volcanoes such those in Alaska, Kamchatka, and Iceland into the stratosphere, potentially resulting in a disproportionately greater climatic influence and societal impact (Jacoby *et al.*, 1999; Zielinski, 2000).

Instrumental temperature records document summer cooling following large eruptions such as Tambora 1815, Cosiguina 1835, Krakatau 1883, Katmai 1912, El Chichon 1982, and Pinatubo 1991 (Self *et al.*, 1981; Rampino and Self, 1984; Angell and Korshover, 1985; Bradley, 1988; Sigurdsson, 1990; Robock and Mao, 1995; Chenoweth, 2001; Robock, 2002a). In contrast, winter warming is observed over North America and northern Eurasia with winter cooling from the Mediterranean to China and over Greenland (Groisman, 1992; Robock and Mao, 1992; 1995;

Kelly *et al.*, 1996; Robock, 2000; Jones *et al.*, 2004). This pattern of Northern Hemisphere winter temperature anomalies is a result of a dynamical winter response to volcanic aerosol forcing through a positive shift in the Arctic Oscillation (Kirchner *et al.*, 1999; Stenchikov *et al.*, 2002, Shindell *et al.*, 2004). Direct radiative cooling dominates during boreal summer, when atmospheric dynamics are less responsive, and throughout the year at lower latitudes (Robock, 2000; Shindell *et al.*, 2004). However, other climatic oscillations such as the El Niño-Southern Oscillation can obscure the volcanic temperature response (Angell, 1988; Mass and Portman, 1989; Robock and Mao, 1995; Portman and Gutzler, 1996). It has also been suggested that ENSO may itself be sensitive to volcanic perturbation, with the El Niño state favored following major tropical eruptions (Adams *et al.*, 2003); although other studies (e.g., Self *et al.*, 1997) report no link between volcanic eruptions and ENSO events.

Dendrochronological records also document volcanic perturbations of climate in the form of frost rings, narrow ring widths, and low maximum latewood density (LaMarche and Hirschboeck, 1984; Jones *et al.*, 1995; Briffa *et al.*, 1998). These characteristics all indicate colder than normal temperatures during the growing season following eruptions such as Kuwae 1453, Huaynaputina 1600, Parker 1641, Laki 1783, Tambora 1815, and Katmai 1912 (Briffa *et al.*, 1992, 1998; Jones *et al.*, 1995; D'Arrigo and Jacoby, 1999). The annually resolved dating of tree rings offers the potential for precise dating of large explosive eruptions; however other climatic influences on tree growth must not be neglected (Jones *et al.*, 1995). Corals may record below average sea-surface temperatures following large eruptions, although the influence of El Niño events on such records must be accounted for (Crowley *et al.*, 1997). Collectively, instrumental and proxy evidence as well as model simulations demonstrate large spatial and temporal variability in temperature changes following volcanic eruptions due to differences in the seasonal timing of eruptions, prevailing atmospheric circulation patterns, and resulting aerosol distributions (Rampino and Self, 1984; Kelley *et al.*, 1996; Briffa *et al.*, 1998; D'Arrigo and Jacoby, 1999; Jones *et al.*, 2004; Shindell *et al.*, 2004).

Understanding the role of volcanic eruptions in regulating past climates is hampered by a poor understanding of the amount of sulfur produced by specific eruptions. Direct measurements of volcanic aerosol loading and dispersion by remote sensing technologies are only available since 1979 for comparison with instrumental temperature records (Bluth *et al.*, 1993; McCormick *et al.*, 1993). Pyrheliometric measurements document optical depth perturbations by volcanic eruptions since Krakatau in 1883 (Sato *et al.*, 1993; Stothers, 1996). Estimates of volcanic aerosol loading for earlier eruptions may be made from volcanological data (Devine *et al.*, 1984; Paliás and Sigurdsson, 1989; Scaillet *et al.*, 2004) or observations of atmospheric phenomena such as lunar eclipses, twilight glows, and dimmed stars (Keen, 1983; Stothers, 1984, 2000). Despite these observations, the historical record of volcanism is incomplete (Simkin and Seibert, 1994); especially in remote areas such as Alaska and Kamchatka where major eruptions may have gone unnoticed as late as 1960 (Newhall and Self, 1982). Although there are Alaskan eruptions documented historically as early as 1760, the record is spotty in nature and many eruptions undoubtedly went unnoticed, even during the past century (Miller *et al.*, 1998). Large eruptions of global influence have gone unnoticed as recently as the 1809 event known only from ice core records (Cole-Dai *et al.*, 1991).

Ice cores represent a valuable archive of paleovolcanic data (Hammer *et al.*, 1980; Moore *et al.*, 1991; Zielinski *et al.*, 1994; Clausen *et al.*, 1997; Cole-Dai *et al.*, 1997; Yalcin *et al.*, 2003). Ice cores preserve both acidic emissions ( $\text{SO}_4^{2-}$ , Cl) and silicate ash particles (tephra) from volcanic eruptions. Since the pioneering work of Hammer (1977), records of past volcanism have been developed from ice cores via detection of volcanic acids as elevated levels of electrical conductivity (Hammer *et al.*, 1980; Clausen and Hammer, 1988) and by direct measurement of volcanic sulfate signals using ion chromatography (Zielinski *et al.*, 1994; 1996). General agreement between glaciochemical signals identified as volcanic with the known record of volcanism (Simkin and Siebert, 1994) validates the use of ice cores in reconstructing past volcanism. Tephrochronological work matching ice core tephra to suspected source volcanoes

provides additional confidence in the attribution of ice core signals to specific eruptions (Palais *et al.*, 1990; Fiacco *et al.*, 1994; Zielinski *et al.*, 1995a; de Silva and Zielinski, 1998; Zdanowicz *et al.*, 1999). Long records of volcanism spanning hundreds to thousands of years have been developed from ice cores collected from both Greenland (Lyons *et al.*, 1990; Zielinski *et al.*, 1996; Clausen *et al.*, 1997) and Antarctica (Moore *et al.*, 1991; Delmas *et al.*, 1992; Cole-Dai *et al.*, 1997), enhancing our understanding of past volcanism by documenting the atmospheric effects of known eruptions as well as previously unrecognized eruptions of global concern, such as the eruptions of 1809 A.D. (Cole-Dai *et al.*, 1991) and 1259 A.D. (Palais *et al.*, 1992, Oppenheimer, 2003). Ice core reconstructions also provide estimates of volcanic aerosol forcing for general circulation models used to investigate past climate variability (Robertson *et al.*, 2001).

As no single ice core can provide a complete record of even the largest volcanic eruptions (Delmas *et al.*, 1985; Clausen and Hammer, 1988; Zielinski *et al.*, 1997), volcanic records should be developed from as many ice cores sampling as many regions as possible. Recently, a number of new ice core volcanic records from Antarctica have become available (Cole-Dai *et al.*, 2000; Palmer *et al.*, 2001; Stenni *et al.*, 2002; Castellano *et al.*, 2004), providing a more complete picture of explosive volcanism in the Southern Hemisphere than was previously possible. Attention has also focused on identifying prominent bipolar volcanic signals seen in both Antarctica and Greenland, improving our understanding of volcanic perturbations of climate on a global scale and providing bipolar index horizons for chronological control (Palais *et al.*, 1992; Langway *et al.*, 1995; Kohno and Fujii, 2002). However, improvement of the spatial network of volcanic ice core records in the Northern Hemisphere has recently lagged behind the development of volcanic records from Antarctica. To more fully understand the frequency and climatic influence of volcanic eruptions, more ice core data is needed, especially from Alaska and other high Arctic sites (Robock, 2002b).

Ice cores also provide the data needed to calculate stratospheric aerosol loading and resulting optical depth (Zielinski, 1995b; Robertson *et al.*, 2001), a parameter critical to

evaluating the climatic response to volcanism (Lacis *et al.*, 1992). However, a potentially large uncertainty exists in such calculations due to spatial variability in ice core chemical concentrations. Clausen and Hammer (1988) calculated the atmospheric sulfate loading from the Laki and Tambora eruptions using a suite of 11 ice cores from the Greenland Ice Sheet, with values ranging from 188 to 389 Mt H<sub>2</sub>SO<sub>4</sub> for Laki and 188 to 263 Mt H<sub>2</sub>SO<sub>4</sub> for Tambora. By comparing ice core volcanic records from different sites worldwide, Robock and Free (1995) found that only the largest sulfur producing eruptions such as Katmai (1912), Tambora (1815), and Laki (1783) are consistently recorded, either globally in the case of tropical eruptions or within their respective hemisphere in the case of high latitude eruptions. More recently, Zielinski *et al.* (1997) evaluated the El Chichon signal in Greenland snowpits and found that, even for a relatively large eruption like El Chichon, there is only a 75% chance that it will be recorded at any one site in central Greenland. Using a suite of snowpits collected from a 400 km<sup>2</sup> area centered around South Pole, Cole-Dai and Mosley-Thompson (1999) reported volcanic sulfate fluxes from the 1991 Pinatubo eruption that varied by a factor of 1.5 and the 1991 Cerro Hudson eruption by a factor of 2.8. These results suggest that volcanic sulfate fluxes calculated from a single ice core will be uncertain due to spatial variability in glaciochemical signals.

We have previously reported a 100-year record of North Pacific volcanism developed from an ice core collected at Eclipse Icefield (60.51° N, 139.47° W, 3107 m elevation), Yukon, Canada (Yalcin *et al.*, 2003). Due to its elevation and location directly downwind and close to vigorous volcanic arcs in the Alaska Peninsula, the Aleutian Islands, and Kamchatka, the Eclipse Icefield is suitably located to preserve signals from eruptions in these regions (Figure VI.1), providing a Northern Hemisphere volcanic record complementary to the record from Greenland, where the effects of Icelandic eruptions predominate (Hammer, 1984). The volcanic arcs of Alaska and Kamchatka are among the world's most vigorous with three major explosive eruptions of volcanic explosivity index (VEI) 5 or greater occurring in the last century: Ksudach (1907), Katmai (1912) and Bezymianny (1956) (Simkin and Siebert, 1994). Smaller but

regionally significant eruptions occur in these regions more frequently. However, the eruptive history of Alaska and Kamchatka is poorly known, with increasingly fewer historically documented eruptions and large dating uncertainties prior to 1900 (Simkin and Seibert, 1994).

A suite of ice cores spanning an elevation range from 3.0 to 5.4 km in the St. Elias Mountains of the Yukon and Alaska offers an unprecedented opportunity to construct a three-dimensional view of climate change, including the atmospheric effects of volcanic eruptions in the North Pacific. The acquisition of two new ice cores from Eclipse Icefield in 2002 allows us to extend our record of North Pacific volcanism to 1400 A.D. and assess the variability in volcanic signal preservation at Eclipse Icefield. We include here a revised version of our original one hundred year volcanic record from Eclipse Icefield for this purpose. We also develop a paleovolcanic record using the ice core record from the Northwest Col of Mount Logan covering the period 1690 to 1980. The Eclipse (3017 m elevation) and Logan (5340 m elevation) records are compared to assess vertical gradients in volcanic sulfate loading between the lower and middle troposphere. Together, these records offer a more complete picture of past volcanic eruptions in the North Pacific than would be possible from any one core.

### **Ice Core Analysis and Dating**

A 160 m ice core (Core 1) was recovered from Eclipse Icefield in 1996 (Yalcin and Wake, 2001; Yalcin *et al.*, 2003). Two additional cores, 345 m (Core 2) and 130 m (Core 3) in length, were recovered in 2002. All three cores were continuously sampled at 10 to 15 cm resolution for major ions and stable isotopes. Thinning of annual layers in the lower 120 m of Core 2 required higher resolution sampling to establish an annually dated chronology. Therefore, Core 2 was resampled at 2 to 6 cm resolution continuously for stable isotopes and around select high sulfate horizons for major ions. Stringent core processing techniques were used to ensure samples were contamination free at the  $\text{ng g}^{-1}$  level. Blanks showed no significant contamination of samples during processing of the core, except in the case of  $\text{NO}_3^-$  in the top portion of Core 2

(1970-2000) processed for trace metals. Samples were analyzed for major ions ( $\text{Na}^+$ ,  $\text{NH}_4^+$ ,  $\text{K}^+$ ,  $\text{Mg}^{2+}$ ,  $\text{Ca}^{2+}$ ,  $\text{Cl}^-$ ,  $\text{NO}_3^-$ ,  $\text{SO}_4^{2-}$ ) at the University of New Hampshire Climate Change Research Center via ion chromatography using a 0.5 ml sample loop. The cation system used a CS12A column with CSRS-ultra suppressor in auto suppression recycle mode with 20 mM MSA eluent. The anion system used an AS11 column with an ASRS-ultra suppressor in auto suppression recycle mode with 6 mM NaOH eluent. An aliquot of each sample was analyzed at the University of Maine Stable Isotope Laboratory with a Multiprep  $\text{CO}_2$  equilibration system coupled to a VG SIRA mass spectrometer for  $\delta^{18}\text{O}$  (precision  $\pm 0.05\%$ ) and a Eurovector Cr pyrolysis unit coupled to a GV Isoprime mass spectrometer for  $\delta\text{D}$  (precision  $\pm 0.5\%$ ).

A section of each core was also analyzed for radionuclides ( $^{137}\text{Cs}$ ) via gamma spectroscopy. Samples for radionuclide analysis were collected from the outside of the core, melted, acidified, and gravity filtered twice through cation exchange filters (MN 616-LSA-50, Macherey-Nagel, Germany). Radionuclide concentrations (including  $^{137}\text{Cs}$ ) were determined by non-destructive gamma spectrometry using a Canberra gamma spectrometer with a germanium well detector and multi-channel analyzer (Dibb, 1989). The radionuclide concentration profiles were dated by comparison to real-time aerosol samples collected at Whitehorse, Yukon by the Radiation Protection Bureau, Ottawa. All three cores show nearly identical radionuclide profiles, with clear identification of the 1963 and 1961 radionuclide peaks from atmospheric nuclear weapons testing (Figure VI.2). Fallout from the 1986 Chernobyl nuclear power plant accident was also detected, providing an additional stratigraphic marker. Average annual accumulation from 2002 to 1963 was 1.30 m water equivalent. This compares favorably to the value of 1.38 m water equivalent for the period 1996 to 1963 determined from the Eclipse 1996 core by identification of the 1963 beta activity peak (Yalcin *et al.*, 2003).

The presence of discrete ice layers in the Eclipse ice core averaging 5% of the net accumulation by weight demonstrates that a limited amount of surface melting occurs at Eclipse



during summer. Meltwater percolation does not significantly alter the glaciochemical records available from the Eclipse ice core as evidenced by the preservation of clear seasonal signals in the major ion and oxygen isotope records. This allows dating of the Eclipse ice cores by counting of annual layers delineated by summer maxima in  $\delta^{18}\text{O}$  and  $\delta\text{D}$  and winter maxima in  $\text{Na}^+$  concentrations (Figure VI.3). The maxima in stable isotope ratios in summer precipitation and minima in winter precipitation observed at Eclipse and other ice core sites is due at least in part to the temperature at which evaporation and condensation occurs (Dansgaard *et al.*, 1973). The  $\text{Na}^+$  concentration maxima in winter and minima in summer are related to pronounced seasonal changes in the influx of marine aerosols. Increased storminess and higher wind speeds in the Gulf of Alaska during winter results in enhanced entrainment of sea salt aerosols and more frequent advection of marine air masses into the St. Elias Mountains, producing the observed winter peaks in  $\text{Na}^+$  concentrations.

Age control on the chronology established via annual layer counting is provided by the 1986, 1963 and 1961  $^{137}\text{Cs}$  reference horizons as well as reference horizons provided by major volcanic eruptions (Katmai, Tambora, Laki, Kuwae). Dating error is estimated based on the number of independently dated reference horizons (radioactivity, volcanic eruptions), and ranges from  $\pm 1$  year between 2002 and 1912 and between 1815 and 1783,  $\pm 2$  years between 1912 and 1815, and up to  $\pm 5$  years (1%) between 1783 and 1450 due to the lack of independently dated horizons between the Laki and Kuwae eruptions. Although Core 2 covers the last 1000 years, the core is not annually dated prior to 1450. Therefore, we limit our discussion of volcanic signals in the core to the period 1400-2002.

### **Identification of Volcanic Signals**

Volcanic eruptions are recorded in ice cores as large  $\text{SO}_4^{2-}$  spikes above background levels independent of continental dust or sea salt deposition, sometimes accompanied by other volcanic acids (such as HCl and HF) and/or tephra (Herron, 1982; Zielinski *et al.*, 1994).

However, the identification of volcanic signals in ice core  $\text{SO}_4^{2-}$  records is not straightforward due to the presence of multiple  $\text{SO}_4^{2-}$  sources including sea salt, continental dust, evaporate deposits, oxidation of biogenic reduced gases, and anthropogenic emissions (Zielinski *et al.*, 1996). This requires the use of robust statistical techniques to estimate the variable non-volcanic  $\text{SO}_4^{2-}$  background and separate it from possible volcanic signals (Cole-Dai *et al.*, 1997; Castellano *et al.*, 2004). Furthermore, the relative magnitude of the  $\text{SO}_4^{2-}$  signal in an ice core will depend on the size of the eruption, the location of the source volcano, atmospheric circulation and depositional processes, and post depositional alteration due to wind scour and melting. In addition, the lag between the time of an eruption and deposition of the resulting aerosols in the polar regions can be as much as two years, depending on latitude of the eruption and time of year (Zielinski *et al.*, 1994).

We used two methods to identify volcanic  $\text{SO}_4^{2-}$  signals in our record (Figure VI.4). First, we used an empirical orthogonal function (EOF) decomposition to describe the variance in the Eclipse glaciochemical data set. The EOF technique splits the temporal variance of a data set into patterns termed empirical eigenvectors that are orthogonal in nature (Peixoto and Oort, 1992). The first eigenvector explains the greatest percentage of variance in the dataset, with each successive eigenvector describing the maximum remaining variance. Since the modes are orthogonal, there is no correlation between any two modes. This allows differentiation of sources and transport characteristics by relationships between individual species as described by each EOF (Mayewski *et al.*, 1994). Therefore, each EOF often provides information on a different environmental parameter controlling ice core glaciochemistry.

Applying EOF analysis to the suite of ions measured in the Eclipse ice cores (excluding  $\text{NH}_4^+$ ) reveals that, for all three cores, EOF 5 is loaded solely with  $\text{SO}_4^{2-}$  and describes 3.8-5.3% of the total variance in the dataset, but 12.9-20.8% of the variance in the sulfate time series (Table VI.1). Volcanic eruptions have been identified as the source of this  $\text{SO}_4^{2-}$  (Yalcin *et al.*, 2003). Previously, we excluded both  $\text{NH}_4^+$  and  $\text{NO}_3^-$  from EOF analysis of Core 1; but now recognize

that by including  $\text{NO}_3^-$  in the EOF analysis,  $\text{SO}_4^{2-}$  from anthropogenic sources is more robustly accounted for and separated from volcanic  $\text{SO}_4^{2-}$ . Note that when  $\text{NO}_3^-$  is included, EOF 4 describes an association between  $\text{NO}_3^-$  and  $\text{SO}_4^{2-}$ ; inspection of the EOF 4 time series demonstrates that peak values are reached from 1970 to 1990, which is consistent with the timing of peak anthropogenic deposition at Eclipse Icefield (Yalcin and Wake, 2001). We considered signals with an EOF 5  $\text{SO}_4^{2-}$  value greater than one standard deviation above the mean positive EOF 5  $\text{SO}_4^{2-}$  value to potentially represent an identifiable volcanic eruption (Table VI.2). Note that although the Eclipse ice cores cover variously one hundred to one thousand years, the use of one standard deviation above the mean positive EOF 5  $\text{SO}_4^{2-}$  value as the selection criteria for volcanic  $\text{SO}_4^{2-}$  signals yields a similar threshold criterion for the three cores (27 to 31  $\text{ng g}^{-1}$ ).

The processing of the top thirty years of Core 2 for trace metals resulted in occasionally high blank values for  $\text{NO}_3^-$ . Although separate lines were used to collect core meltwater into acid washed and deionized water washed bottles for trace metal and major ion analysis, respectively, nitric acid vapors from acid-cleaned bottles were apparently present in sufficient amounts in the laboratory environment to adversely affect  $\text{NO}_3^-$  blank values. One-quarter of blanks had  $\text{NO}_3^-$  concentrations in excess of 12  $\text{ng g}^{-1}$  (one-third of the 20<sup>th</sup> century average  $\text{NO}_3^-$  concentration at Eclipse). Other anions ( $\text{SO}_4^{2-}$ ,  $\text{Cl}^-$ ) were not affected. Therefore, we ran a separate EOF decomposition on the affected core section (1970-2002) excluding both  $\text{NH}_4^+$  and  $\text{NO}_3^-$ . In this analysis, EOF 4 is loaded solely on  $\text{SO}_4^{2-}$  and explains 13.9% of the variance in the  $\text{SO}_4^{2-}$  time series. Although this proportion is similar to the variance explained by EOF 5 when  $\text{NO}_3^-$  is included in the analysis, EOF 4  $\text{SO}_4^{2-}$  values tend to be ~30% higher. For example, the mean plus one standard deviation of the positive EOF 4  $\text{SO}_4^{2-}$  values in the affected section of Core 2 is 39  $\text{ng g}^{-1}$ , compared to 29  $\text{ng g}^{-1}$  for EOF 5  $\text{SO}_4^{2-}$  values in Core 3 over the same time period. We believe this to be the result of anthropogenic  $\text{SO}_4^{2-}$  being included in the EOF 4  $\text{SO}_4^{2-}$  values. When comparing volcanic  $\text{SO}_4^{2-}$  concentrations and fluxes in the three Eclipse cores, the inflation

of EOF 4  $\text{SO}_4^{2-}$  in Core 2 between 1970 and 2000 by anthropogenic  $\text{SO}_4^{2-}$  should be considered. The remainder of our data is unaffected by this problem.

We also evaluated the Northwest Col ice core from Mount Logan for volcanic signatures using EOF analysis. The details of the core analysis and dating are provided elsewhere (Holdsworth *et al.*, 1984; Mayewski *et al.*, 1993). Since there is no detectable anthropogenic  $\text{SO}_4^{2-}$  input in ice cores from the summit plateau of Mount Logan (Mayewski *et al.*, 1993), separation of anthropogenic from volcanic  $\text{SO}_4^{2-}$  by including  $\text{NO}_3^-$  in the EOF analysis is unnecessary. In fact, when  $\text{NO}_3^-$  is included volcanic  $\text{SO}_4^{2-}$  in the Mount Logan ice core is apparently split between EOF 3 and EOF 4 as noted by visual inspection of EOF time series around known volcanic horizons such as Laki and Katmai. Therefore, we excluded both  $\text{NH}_4^+$  and  $\text{NO}_3^-$  from EOF analysis of the Mount Logan ice core. In this case, EOF 3 is loaded solely on  $\text{SO}_4^{2-}$  and explains a large proportion (73%) of the variance in the  $\text{SO}_4^{2-}$  time series (Table VI.3). Because ice cores from the Logan summit plateau are free of anthropogenic sulfate, volcanism is a more important  $\text{SO}_4^{2-}$  source than at Eclipse, where anthropogenic  $\text{SO}_4^{2-}$  is detectable. Since EOF 3 explains a much larger proportion of the variance in the  $\text{SO}_4^{2-}$  time series at Mount Logan than EOF 5 does at Eclipse, the threshold criterion for volcanic  $\text{SO}_4^{2-}$  signals is higher at Mount Logan (Table VI.2).

We also used non-sea salt  $\text{SO}_4^{2-}$  residuals above a robust spline to identify volcanic signals at Eclipse and Mount Logan. First, we estimated the amount of  $\text{SO}_4^{2-}$  from sea salt using the ratios of  $\text{SO}_4^{2-}$  to other ions in seawater (Keene *et al.*, 1986), resulting in an excess or non-sea-salt (nss) fraction. Sea-salt  $\text{SO}_4^{2-}$  is a small fraction of the total  $\text{SO}_4^{2-}$  in the Eclipse ice cores (<5%) with  $\text{Na}^+$  the limiting sea salt species in nearly all of the samples (occasionally, a sample is limited by  $\text{Mg}^{2+}$ ). We then used a low-tension robust spline (tension parameter set to 0.1 resulting in a 98% smooth) to estimate background  $\text{SO}_4^{2-}$  deposition and considered the resulting residuals above the spline (Zielinski *et al.*, 1994; Yalcin *et al.*, 2003). We considered those residuals greater than one standard deviation above the mean positive residual as possible volcanic signals (Table VI.2).

This results in similar threshold criterion for Core 1 (110 ng g<sup>-1</sup>) and Core 3 (108 ng g<sup>-1</sup>), while the threshold criterion for Core 2 is lower (70 ng g<sup>-1</sup>) due to lower temporal sample resolution with increasing rates of layer thinning. For consistency, we use the higher threshold criterion given by Core 1 and Core 3 for the overlapping section of Core 2 (1894 to 2002), while adopting the lower threshold for the older portion of Core 2. Threshold criteria for non-sea-salt SO<sub>4</sub><sup>2-</sup> residuals at Mount Logan (98 ng g<sup>-1</sup>) are comparable to Eclipse due to similar annual mean SO<sub>4</sub><sup>2-</sup> concentrations at the two sites (44 and 49 ng g<sup>-1</sup>, respectively).

We also evaluated the Cl<sup>-</sup> record from each core for possible volcanic signatures because some volcanic eruptions release large amounts of halogen gases, including HCl, HF, and HBr (Herron, 1982). We calculated excess Cl<sup>-</sup> using Na<sup>+</sup> as the sea salt indicator. The Cl<sup>-</sup>/Na<sup>+</sup> equivalence ratio at Eclipse averages 1.23, slightly more than the seawater ratio of 1.16 (Keene *et al.*, 1986); at Mount Logan this ratio averages 2.32, twice the seawater ratio. Around 18.5% of the Cl<sup>-</sup> deposition at Eclipse is in excess of seawater ratios, while at Mount Logan 57% of the Cl<sup>-</sup> is excess. Differences in Cl<sup>-</sup>/Na<sup>+</sup> ratios relative to seawater are attributed to acidification of sea salt particles by reaction with H<sub>2</sub>SO<sub>4</sub> (Legrand and Delmas, 1988; Gard *et al.*, 1998). This reaction volatilizes sea salt Cl<sup>-</sup> to produce gas-phase and highly soluble HCl that is effectively scavenged by precipitation, resulting in enrichment of Cl<sup>-</sup> in snow relative to seawater ratios. A robust spline was used to estimate background levels of excess Cl<sup>-</sup> deposition. The excess Cl<sup>-</sup> residuals greater than one standard deviation above the mean positive residual that were also accompanied by a volcanic SO<sub>4</sub><sup>2-</sup> signal were considered to be volcanic in origin. We found 39 of 122 volcanic SO<sub>4</sub><sup>2-</sup> signals at Eclipse and 15 of 31 volcanic SO<sub>4</sub><sup>2-</sup> signals at Mount Logan were accompanied by a volcanic Cl<sup>-</sup> signal.

We calculated the total volcanic SO<sub>4</sub><sup>2-</sup> flux for each event as the product of the volcanic EOF SO<sub>4</sub><sup>2-</sup> value and the water equivalent length of the sample, summed for all samples containing fallout attributable to a particular event. We made this same calculation using non-sea SO<sub>4</sub><sup>2-</sup> residual concentrations for comparative purposes. Annual layers become progressively thinner

with depth in the Eclipse ice cores, requiring reconstruction of original annual layer thicknesses by correcting for ice creep. We used an empirical approach based on the observed layer thicknesses from annual layer counting of the Eclipse ice cores because no ice flow or strain rate measurements were made on the Eclipse boreholes, and radar soundings of the ice thickness suggested bedrock should have been reached around 320 m but had not been reached when drilling was stopped at 345 m because that was the cable length. Assuming the average accumulation rate from identification of the 1963 radioactivity maximum of 1.38 and 1.30 m water equivalent for the 1996 and 2002 cores, respectively, has not changed significantly and no creep deformation in the firn section of the cores, we calculated a decompression ratio for each annual layer from a smoothed fit to the observed layer thicknesses (Holdsworth *et al.*, 1992). This ratio was then applied to the observed thickness of each annual layer to reconstruct the original thickness. Because the mean annual accumulation rate at the 1996 drill site is 7% higher than at the 2002 drill site, an additional correction factor of 0.93 is applied to the Core 1 fluxes so that they are directly comparable to the volcanic fluxes measured in Core 2 and Core 3. Mount Logan flux calculations use the reconstructed layer thicknesses provided by Holdsworth *et al.* (1992).

Glaciochemical signals identified as volcanic along with the volcanic  $\text{SO}_4^{2-}$  flux for each event are summarized for each core in Tables VI.4 to VI.7. Contemporaneous events observed in more than one of the Eclipse ice cores are assumed to represent the same eruption or eruptions, and are therefore assigned the same event number; hence event numbering is not continuous in any one Eclipse core. We report the start of each signal, the length of fallout in years, peak volcanic EOF  $\text{SO}_4^{2-}$ , nss  $\text{SO}_4^{2-}$  residual, and nss Cl<sup>-</sup> residual concentrations, and total volcanic  $\text{SO}_4^{2-}$  flux for each event. Italicized entries indicate EOF or nss residual concentrations that did not meet our concentration thresholds for one of these parameters, but did for the other.

Comparing the EOF and  $\text{SO}_4^{2-}$  residual analyses (Figure VI.4) shows that nss  $\text{SO}_4^{2-}$  residuals are about three times volcanic EOF  $\text{SO}_4^{2-}$  values at Eclipse, since the EOF analysis more

robustly accounts for  $\text{SO}_4^{2-}$  from non-volcanic sources such as anthropogenic emissions (Yalcin *et al.*, 2003). Meanwhile, Mount Logan volcanic EOF 4  $\text{SO}_4^{2-}$  values and non-sea-salt  $\text{SO}_4^{2-}$  residuals are similar. It appears that EOF analysis provides more conservative identification of  $\text{SO}_4^{2-}$  signals attributable to volcanic eruptions at sites impacted by anthropogenic  $\text{SO}_4^{2-}$ . For sites unaffected by anthropogenic  $\text{SO}_4^{2-}$  such as the Mount Logan summit plateau similar paleovolcanic records can be obtained using either technique.

Volcanic flux calculations suggest several false positive volcanic signals are identified by the non-sea-salt  $\text{SO}_4^{2-}$  residuals because they are accompanied by negligible volcanic EOF  $\text{SO}_4^{2-}$  fluxes. For example, the residuals identify a suspected volcanic event in 1988 in two of the Eclipse ice cores, although flux calculations show a negligible volcanic EOF  $\text{SO}_4^{2-}$  flux from this event. Because this event can not be matched to a documented volcanic eruption and it seems unlikely, though not impossible, that a regionally significant volcanic eruption went unnoticed in 1988, the most plausible explanation is that the non-sea-salt  $\text{SO}_4^{2-}$  residual does not represent a volcanic eruption in this case. This rationale suggests other false positive signals are given by non-sea-salt  $\text{SO}_4^{2-}$  residuals (i.e., 1934). However, there are several examples of non-sea-salt  $\text{SO}_4^{2-}$  residuals with negligible volcanic EOF  $\text{SO}_4^{2-}$  flux that can be linked to known eruptions (i.e., 1996, 1985). Hence, confident attribution of a suspected signal as volcanic is made by confirmation with the historical record.

To evaluate the spatial variability in volcanic signal preservation at Eclipse Icefield, we considered the annual flux of volcanic  $\text{SO}_4^{2-}$  rather than using concentration data (Legrand and Delmas, 1987). Correlation coefficients ( $r$ ) range from 0.77 to 0.81 for the three Eclipse cores (Table VI.8), meaning 60 to 66% of the volcanic  $\text{SO}_4^{2-}$  signal is shared among the three cores. These high correlations are driven by the largest eruptions, as seen by lower correlations (0.42 to 0.50) when the Katmai years (1912 and 1913) are excluded from this analysis. Correlation coefficients between the Eclipse records and the record from Mount Logan range from 0.44 to 0.81. Again, the high correlations are driven by the largest eruptions, with correlations between

the Eclipse records and the Logan record ranging from 0.11 to 0.13 when the Katmai years are excluded. This poor correlation between Eclipse and Logan for smaller events highlights the larger number of smaller eruptions recorded at Eclipse. These results are encouraging because they demonstrate the reproducibility of atmospheric  $\text{SO}_4^{2-}$  loading from volcanic eruptions as reconstructed from ice cores, particularly for the larger eruptions. Furthermore, it is the largest sulfur producing eruptions that are most important in climate-forcing studies.

### **Identification of Source Volcanoes**

#### **Correlation with known eruptions**

In assigning possible sources for each signal we used the Smithsonian Institution's Global Volcanism Program database of Holocene volcanism (Simkin and Seibert, 1994, and updated online: [www.volcano.si.edu](http://www.volcano.si.edu)) to match events identified as volcanic using both the robust spline and EOF techniques with known eruptions. We considered Northern Hemisphere eruptions with a volcanic explosivity index (VEI)  $\geq 4$  as possible sources because one criteria for an eruption to be designated VEI 4 is stratospheric injection (Newhall and Self, 1982), which favors long-range transport of volcanic sulfate aerosols and their deposition in glacial ice (Zielinski *et al.*, 1994). We also considered high northern latitude VEI 3 eruptions in Alaska, Kamchatka, and Iceland as eruptions of this magnitude are capable of "substantial" tropospheric injection (Newhall and Self, 1982). Due to the smaller distances involved, transport entirely within the troposphere is capable of delivering their aerosols to Eclipse. Furthermore, the relatively low altitude of the tropopause at high latitudes increases the likelihood of stratospheric injection and transport of moderate VEI 3 class eruptions. Using the above outlined criteria, we matched 96 of the 116 volcanic signals recorded at Eclipse Icefield over the last six hundred years and 27 of the 31 volcanic signals recorded at Mount Logan over the last three hundred years to a known volcanic eruption within the time constraints established on each signal via annual layer



counting. In some cases, eruptions closely spaced in time make assignment of a signal to a single eruption ambiguous; in these cases we list multiple potential source volcanoes.

The good agreement between the historical record of explosive volcanism and the glaciochemical signals we identified as volcanic makes St. Elias ice cores promising records of regionally significant volcanic activity. However, there are a number of volcanic signals that can not be matched to known eruptions. Some of these signals, such as the 1809 event, are well known from other ice core studies and are attributed to previously undocumented volcanic eruptions (Cole-Dai *et al.*, 1991). Others, such as 1516, have not been recognized previously. In fact, the 1516 event is the largest  $\text{SO}_4^{2-}$  concentration peak in the last 500 years in not only the Eclipse Core 2 ice core but also in the new ice cores from Prospector-Russell Col on Mount Logan and Bona-Churchill, Alaska (Fisher *et al.*, 2004, Mashiotta *et al.*, 2004). The recognition of contemporaneous signals in multiple ice cores increases confidence that these signals represent regionally significant and previously undocumented volcanic eruptions. In addition to the large 1516 signal, unknown eruptions in 1866 and 1910 are recorded as moderate events at both Eclipse and Mount Logan. Likewise, unknown eruptions in 1895, 1908, 1915, 1942, and 1955 are seen in multiple Eclipse cores.

Although not seen in the Mount Logan core, the unknown volcanic eruptions recorded at Eclipse in mid-1891 and early 1893 are corroborated by pyrheometric optical depth measurements showing stratospheric injections by unknown volcanoes erupting in the summer of 1890 and again in early 1893 (Stothers, 1996). The one-year lag between the first appearance of increased optical depths in August 1890 and deposition of volcanic sulfate aerosols at Eclipse implies the unknown 1890 volcano is in the tropical latitudes. The synchronous appearance of increased optical depths and volcanic  $\text{SO}_4^{2-}$  deposition at Eclipse in 1893 suggests that the 1893 volcano is in the high northern latitudes.

In our previous work identifying volcanic signals utilizing a single ice core from Eclipse Icefield, there were several significant North Pacific eruptions not apparent in the record, such as

Sheveluch, Kamchatka, 1964 (VEI 4+); Aniakchak, Alaska, 1931 (VEI 4); and Kliuchevskoi, Kamchatka, 1931 (VEI 4) (Yalcin *et al.*, 2003). Utilizing a suite of four ice core records, there are no Alaskan or Kamchatkan eruptions with a VEI  $\geq 4$  that are not seen in at least one Eclipse core since the 1820s. Clearly, the acquisition of multiple ice cores allows a more complete picture of past volcanic eruptions than is possible from any one core. In fact, there are many VEI  $\geq 4$  eruptions in Alaska and Kamchatka that are recorded in only one core, such as Spurr 1992, Augustine 1976, Tolbachik 1975, and Bezymianny 1956. Missing signals from VEI  $\geq 4$  eruptions in Japan occur more frequently, such as Iriomote-Jima 1924, Bandai 1888, and Komaga-Take 1856, reflecting the greater precipitation scavenging of volcanic sulfate aerosols during the longer transport distances involved.

Eruptions from Alaskan or Kamchatkan volcanoes account for one-third of volcanic signals in ice cores from the St. Elias Mountains (Table VI.9). This proportion represents a minimum because the number of known eruptions in Alaska and Kamchatka decreases markedly prior to the 20<sup>th</sup> century. For example, the Smithsonian Volcanism Database contains 126 eruptions in Alaska and Kamchatka of VEI  $\geq 3$  since 1900, but only 58 in the preceding 500 years. Hence, a large proportion of the unidentified signals in the ice cores records, especially prior to 1900, are undoubtedly from undocumented eruptions in Alaska and Kamchatka. Eruptions elsewhere in the Northern Hemisphere extra-tropics, specifically Iceland, Japan and the Kurile Islands, are more important sources of volcanic SO<sub>4</sub><sup>2-</sup> signals at 5340 m on Mount Logan (39% of signals) than at 3017 m on Eclipse Icefield (15% of signals), even though the ice core sites are separated by only 45 km. We speculate that in order for volcanic plumes to survive the long transport distances from Japan and Iceland to the St. Elias Mountains, they must be transported primarily in the upper troposphere to minimize precipitation scavenging. Mount Logan, at 5 km elevation, is suitably located to sample the upper troposphere but misses plumes confined to the lower troposphere, and hence records a greater proportion of signals from eruption clouds traveling at higher altitudes. Meanwhile, Eclipse Icefield at 3 km elevation, is suitably located to

sample the lower troposphere, and hence records a greater proportion of signals from moderate eruptions carried in the lower troposphere.

Discerning the relative importance of tropical versus high northern latitude eruptions in these records is more problematic. Recent large tropical eruptions such as Agung 1963, El Chichon 1982 and Pinatubo 1991, were all concurrent with moderate eruptions in Alaska and Kamchatka. Hence, it is difficult to attribute what proportion, if any, of the resulting ice core signal originated from the tropical volcano. Preferring to attribute these signals to tropospheric transport of nearby eruptions rather than stratospheric fallout from distant eruptions, our study of the record of 20<sup>th</sup> century volcanism provided by Core 1 concluded that the Eclipse site does not provide a good record of major tropical eruptions (Yalcin *et al.*, 2003). However, clear signals from older tropical eruptions such as Cosiguina 1835, Babuyan 1832, Galunggung 1822, Tambora 1815, and the unknown 1809 volcano, generally presumed to be in the tropics (e.g., Cole Dai *et al.*, 1991; but see also Yalcin *et al.*, in review), are all seen in the Eclipse ice core. Likewise, there are strong  $\text{SO}_4^{2-}$  signals centered on 1884 and 1641 that match well with the eruptions of Krakatau in 1883 and Parker in 1641, but the extra-tropical eruptions of Augustine, Alaska 1883 and Komaga-Take, Japan, 1640 could be partially responsible for these signals.

It is apparent that changes in atmospheric circulation between the Little Ice Age and modern regimes have affected the connectivity of the St. Elias ice cores to the tropics (Moore *et al.*, 2001, Fisher *et al.*, 2004). Hence, changes in atmospheric circulation may have more readily allowed older tropical eruptions to leave distinct sulfate signals at Eclipse than recent tropical eruptions. However, studies of the accumulation and stable isotopic records from Mount Logan demonstrate that the Little Ice Age (prior to 1843) was characterized by stronger zonal vapor flow in the North Pacific and weaker tropical connections, whereas the modern regime (after 1843) has been characterized by enhanced meridional vapor flow from the tropics. It is unknown if these regime shifts have affected the stratospheric circulation, the primary mode of transport for aerosols from tropical eruptions to the high latitudes.

In the Mount Logan Northwest Col ice core, the tropical eruptions of Cosiguina and Tambora eruptions left strong  $\text{SO}_4^{2-}$  signals, and we assign the moderate volcanic signal in 1862 to the December 1861 eruption of Makian in Indonesia. However there are no distinct  $\text{SO}_4^{2-}$  signals attributable to Babuyan, Galunggung, or the unknown 1809 volcano in this core. While the Krakatau eruption left a strong  $\text{SO}_4^{2-}$  signal at Eclipse, the relatively weak 1884 signal in the Mount Logan Northwest Col ice core could be wholly attributable to Augustine, Alaska. Given the limited number of large tropical eruptions during the 1690 to 1980 period covered by the Northwest Col ice core, it would be highly tenuous, and quite probably incorrect, to conclude that Mount Logan offers a poor record of tropical eruptions, as it was to make that conclusion from the 100 year record provided by Core 1 from Eclipse Icefield. Separating the effects of regionally significant eruptions in the North Pacific from tropical eruptions of global concern is critical, however to the interpretation of paleovolcanic records from the St. Elias, given their close proximity to, and the high frequency of eruptions in, Alaska and Kamchatka.

### **Tephrochronological evidence**

By locating and analyzing volcanic glass in an ice core, the source eruption responsible for a volcanic  $\text{SO}_4^{2-}$  signal can be identified by matching the chemical composition of ice core tephra to glass from the suspected eruption (DeAngelis *et al.*, 1985; Palais *et al.*, 1990; Fiacco *et al.*, 1994; Basile *et al.*, 2001; Dunbar *et al.*, 2003; Yalcin *et al.*, 2003). The use of tephrochronological techniques provides independent verification of the source volcano responsible for an ice core  $\text{SO}_4^{2-}$  signal, with the added benefit of providing additional ice core chronological control. However, this approach has several limitations. First, since silicate particles settle out of the atmosphere much faster than the secondary aerosol products of an eruption (Zielinski, 2000), only a limited number of ice core volcanic  $\text{SO}_4^{2-}$  signals will be associated with tephra. For example, between 30 and 40 Icelandic volcanoes have been active during historical time (after 870 A.D., Thorarinsson and Saedmundsson 1979), but tephra from

only three historical Icelandic eruptions has been recovered from Greenland ice: Laki 1783 (Fiacco *et al.*, 1994), Oraefajokull 1362 (Palais *et al.*, 1991), and the Settlement Ash ~870 A.D. (Gronvold *et al.*, 1995), and possibly a fourth, the A.D. 930s Eldgja eruption (Zielinski *et al.*, 1995a). In special cases tephra may travel hundreds to thousands of kilometers from the source, as shown by identification of glass shards from very large tropical eruptions in Antarctic ice cores (Palais *et al.*, 1990). The distribution of tephra from a particular eruption depends on many factors, including particle size and extent of aggregation, plume height, wind speed and wind direction (e.g., Fisher and Schminke, 1984). Furthermore, tephra within a given ice core layer may be highly variable in composition, different volcanoes can produce tephra with similar major oxide distributions, and the composition of tephra produced by a given volcano can change between eruptions or even within the course of a single eruption if the magma chamber is compositionally zoned (Basile *et al.*, 2001). Geochemical differences can also result from the use of different analytical techniques or instrumentation (e.g., Hunt and Hill, 1993). Analysis of individual, micro-meter sized tephra grains in ice core sections can also result in more variability (scatter) of the results compared to polished sections from geologic deposits near the source volcano (Zielinski *et al.*, 1997).

To independently verify our identifications of source volcanoes responsible for the volcanic signatures in the Eclipse ice core, we collected tephra from the Eclipse ice cores for analysis and comparison to products from suspected source volcanoes. Tephra was collected by filtering of core melt water from high-sulfate horizons through 0.2-micron pore-diameter polycarbonate membrane filters (Whatmann). Visual examination of filters under a microscope suggested a significant number of volcanic glass particles on ~10% of the filters. These samples were analyzed at Micromaterials Research for particles greater than 1 micron in diameter using an electron microprobe (JEOL JXA-8600) following established procedures (Germani and Buseck, 1991). An energy-dispersive x-ray spectrum was acquired for 15 seconds from each particle and analyzed for 27 regions of interest including Si, Ti, Al, Fe, Mg, Ca, Na, and K. Size, shape, and

location were also determined for each particle with 400-500 particles analyzed from each sample. Cluster analysis was performed using relative intensity data to identify volcanic glass particles, which ranged in number from less than 10 to several hundred shards per sample.

Individual glass shards were reanalyzed for major oxide composition ( $\text{SiO}_2$ ,  $\text{TiO}_2$ ,  $\text{Al}_2\text{O}_3$ ,  $\text{FeO}$ ,  $\text{MgO}$ ,  $\text{CaO}$ ,  $\text{Na}_2\text{O}$ ,  $\text{K}_2\text{O}$ ) using a Hitachi S-570 automated scanning electron microscope (SEM) with an energy-dispersive x-ray (EDX) micro-analyzer. Analysis of individual glass shards via SEM provides a grain-specific method of geochemically characterizing and correlating distal tephra. Several representative, microlite-free volcanic glass particles greater than 4 microns with glass shard morphology were selected from each filter because analyzing larger particles minimizes the effect of particle size and shape on quantitative x-ray microanalysis. Only glass shards were selected for analysis because their composition reflects the composition of the magma at the time of eruption. Reported major oxide compositions are normalized to 100% by weight on an anhydrous basis, with total Fe as FeO. Oxides not determined in this study ( $\text{MnO}$ ,  $\text{P}_2\text{O}_5$ ) typically account for less than 1% of volcanic glass compositions by weight (e.g., Dunbar *et al.*, 2003).

The composition of volcanic glass particles found in the Eclipse ice cores are summarized in Table VI.10 for 20<sup>th</sup> century eruptions in Core 1 and Core 3 and Table VI.11 for older eruptions in Core 2, along with pertinent compositional information from suspected sources. Chemical classification of tephra found in the Eclipse cores follows the nomenclature of LeBas *et al.* (1986) according to  $\text{SiO}_2$  and total alkali ( $\text{Na}_2\text{O} + \text{K}_2\text{O}$ ) content (Figure VI.6 and Figure VI.7). Differentiation between tholeiitic and calc-alkaline magma series using plots of  $\text{FeO}/\text{MgO}$  (Miyashiro, 1974) can also provide insight into potential source volcanoes. For example, calc-alkaline magmas predominate in the eastern, continental margin portion of the Aleutian arc with average silica contents of 60-61 %, while the western, oceanic island portion of the Aleutian arc shows a more even distribution of tholeiitic and cal-alkaline signatures and more mafic rocks averaging 54-55% silica (Miller *et al.*, 1998). Possible sources for the tephra found in the Eclipse

ice core were identified by comparing the major oxide composition of ice core tephra to published analyses from suspected source volcanoes. In the following paragraphs we discuss the glass compositions found in the Eclipse ice core and possible source volcanoes for each glass-bearing layer.

A single glass particle of trachyandesite composition was found in the summer 1994 sample from Core 3 (Figure VI.6). This shard could be from the short-lived May 25, 1994 eruption of Cleveland Volcano in the Aleutian Islands that sent an ash plume to an altitude of 10.5 km (Miller *et al.*, 1998). Although the mafic composition and tholeiitic affinity of this particle is consistent with magmas erupted from the oceanic-island portion of the Aleutian Arc (all centers west of 165°W, including Cleveland Volcano), no compositional information is available for Cleveland Volcano. Furthermore, we recognize that interpretation of glass composition based on a single shard is tenuous at best.

Three distinct glass compositions were found in the Fall 1991 layer sampled in Core 3 (Figure VI.6). The dominant glass present (nine of the particles sampled) is trachyandesite and spans the spectrum from andesite to trachyte. The most likely source of this glass is the fissure eruption of Westdahl volcano in the Aleutians. The eruption began on November 30, 1991 with fountaining and phreatic activity that produced ash plumes to 7 km altitude, with vigorous activity continuing to mid-December (Miller *et al.*, 1998). The composition of the Eclipse shards matches well with the composition of tephra from the 1978 Westdahl eruption (Table VII.11). The minor differences could be the result of compositional differences between the 1978 and 1991 Westdahl magmas. Single particles were also observed with tephriphonolite and rhyolitic compositions in the Fall 1991 sample. The 1991 eruption of Pinatubo volcano in the Philippines is a possible source of the rhyolitic glass (Table VI.10; Luhr and Melson, 1995). However, it is also possible that the rhyolitic particle could represent aeolian remobilization of one of the older, voluminous rhyolitic tephtras present in the region, such as the White River Ash (Richter *et al.*,

1995); making attribution of the Eclipse shard to Pinatubo ambiguous. The tephriphonolitic particle is presumably from an oceanic island arc volcano in the Aleutians.

A large population of glass was recovered from the 1989 layer in both Core 1 and Core 3 (we did not sample the 1989 layer in Core 2 for volcanic glass). The analyzed shards are dominantly rhyolitic, with a single trachyte shard present (Figure VI.6). These compositions closely match glass produced by the December 1989 to April 1990 eruption sequence of Redoubt Volcano (Table VI.10; Swanson *et al.*, 1994). Compositionally homogenous rhyolitic glass was produced throughout the 1989-1990 Redoubt eruption sequence. The December 14 and 15, 1989 and January 2 eruptions also produced a minor amount of dacitic (trachyte) glass (Swanson *et al.*, 1994); one such shard was recovered from the Eclipse ice core. In all, twenty-three major explosive events occurred at Redoubt Volcano between December 1989 and April 1990 which intermittently produced ash-rich plumes exceeding 10 km in altitude (Miller *et al.*, 1998). Since the December 14-15 and January 2 eruptions were the only eruptions during the cycle to produce dacitic (trachyte) glass, the presence of such a shard in the Eclipse sample, in conjunction with the observed timing of particle fallout in the Eclipse core corresponding to winter 1989-1990, suggests that the explosive eruptions of December 14-15 and January 2 are those responsible for the glass shards at Eclipse.

Two distinct glass compositions are present in the 1953 layer: a rhyolitic glass (73.3% SiO<sub>2</sub>, three particles), and a basaltic trachyandesite glass (51.7% silica, one particle) (Figure VI.6). There were two VEI<sub>≥</sub>3 eruptions in Alaska during this time: the Crater Peak vent of Mount Spurr (VEI 4, July 1953, Juhle and Coulter, 1955); and the southwest cone of Trident Volcano (VEI 3, February 1953, Muller *et al.*, 1954). The rhyolitic shards are similar to glasses erupted from Southwest Trident (Table VI.10; Coombs *et al.*, 2000), whose 1953 eruptions reached altitudes of more than 9 km. Although Crater Peak is the only Cook Inlet volcano known to produce widely-dispersed mafic tephtras (Riehle, 1985), the basaltic trachyandesite shard is too low in silica to be from Crater Peak, which during its well-studied 1992 eruptions produced



dominantly andesitic glass (61-62 SiO<sub>2</sub>) with minor amounts of dacitic (63-69% SiO<sub>2</sub>) and rhyolitic (74-77% SiO<sub>2</sub>) glasses (Swanson *et al.*, 1995). Prehistoric eruptions of Crater Peak produced only slightly more mafic glasses (58-59% SiO<sub>2</sub>; Beget *et al.*, 1994). Another possible source is the October 1953 eruption of Shishaldin volcano in the Aleutians (VEI 2). Although no chemical analyses are available from this eruption, glass from the 1999 Shishaldin eruption (Stelling *et al.*, 2002) is chemically similar to the shard found in the Eclipse core. For example, both are distinctly elevated in TiO<sub>2</sub>.

Two distinct glass compositions are observed in the 1947 sample from Core 1: a trachytic glass (seven particles) and a rhyolitic glass (two particles) (Figure VI.6). We previously attributed this tephra to the March 1947 eruption of Hekla in Iceland (VEI 4). The Plinian nature of the eruption along with documented fallout of Hekla 1947 tephra in mainland Scandinavia illustrated the potential for long range transport of tephra from this eruption in the high northern latitudes (Larsen *et al.*, 1999). Recently, new analyses of volcanic glass shards from historical age silicic tephra in Iceland have become available which strengthen this interpretation (Larsen *et al.*, 1999). Most glass shards from the 1947 Hekla eruption are dacite to trachyte in composition, and match well with the dominant glass composition in the Eclipse ice core (Table VI.10). Furthermore, the Hekla magma chamber is compositionally zoned, and glass compositions change during the course of the eruption (Larsen *et al.*, 1999). Small volumes of highly silicic magma are ejected during the opening stages of most, if not all, Hekla eruptions. Proximal 1947 tephra deposits contain minor quantities of rhyolitic glass shards with a composition closely matching the rhyolitic glass shards present in the Eclipse ice core, strengthening the interpretation that the ice core glass is from Hekla.

Basaltic trachyandesite to trachyandesite glass shards (five particles) were recovered from the 1945 annual layer in Core 1 (Figure VI.6). There were major (VEI 4) eruptions at both Kliuchevskoi (January 1) and Avachinsky (February 25) volcanoes in Kamchatka in 1945. Comparison of the Eclipse glass to available analyses from Kliuchevskoi (1972 eruption; Ivanov

*et al.*, 1981) and Avachinsky (1991 eruption, Turner *et al.*, 1998) demonstrates the Eclipse glass is similar, but not an exact match (Table VI.10). Furthermore, the similar chemical compositions reported from Kliuchevskoi and Avachinsky precludes attributing the Eclipse shards to one or the other of these volcanoes. A more robust identification may be possible using trace and rare element data that was not obtained in this study (e.g., Basile *et al.*, 2001).

A visible tephra layer in the form of a brown colored, cloudy band in the ice several centimeters thick and dated to 1912 was observed in all three Eclipse ice cores. Glass shards were analyzed from both Core 1 and Core 3 and demonstrate that the source of this tephra layer is the Plinian June 6-8, 1912 eruption of Novarupta (Katmai) Volcano (VEI 6). The 1912 Katmai eruption was the largest volcanic eruption of the 20<sup>th</sup> century in terms of cumulative volume with 13 km<sup>3</sup> of magma erupted in less than 60 hours to produce 17 km<sup>3</sup> of tephra fall deposits and 11 ± 3 km<sup>3</sup> of ignimbrite (Fierstein and Hildreth, 1992). Though widely referred to as Katmai, the nearby Novarupta vent is the source of nearly all of the eruption products and the only Plinian vent active in 1912 (Fierstein and Hildreth, 1992), while compensatory caldera collapse occurred 10 km east of Novarupta at Mt. Katmai volcano (Hildreth, 1987). The volume of eruptive products implies a minimum volumetric eruptive rate of 3 x 10<sup>4</sup> m<sup>3</sup> s<sup>-1</sup> and a column height of 22-30 km (Fierstein and Hildreth, 1986) that easily penetrated the tropopause. Some 120,000 km<sup>2</sup> were covered with an ash layer at least one cm thick (Fierstein and Hildreth, 1992), with contemporary reports of ash fall from the eruption from as far away as the Puget Sound region, some 3000 km distant (Griggs, 1922). Pyrheliometric optical depth perturbations demonstrate that the Katmai aerosol veil was confined poleward of 30°N, with a maximum optical depth of 0.23 between 45°N and 60°N (Stothers, 1996). From petrologic evidence, Palais and Sigurdsson (1989) estimate that 7.9 x 10<sup>9</sup> kg of H<sub>2</sub>SO<sub>4</sub> and 3.2 x 10<sup>9</sup> kg HCl was released by the eruption. An average temperature decrease of 0.2 °C has been estimated for the Northern Hemisphere in the years immediately following the eruption (Self *et al.*, 1981).

The extraordinary compositional range of the 1912 ejecta (50.4% to 77.4% SiO<sub>2</sub>) includes andesite (1 km<sup>3</sup>), dacite (4.5 km<sup>3</sup>), and rhyolite (7.5 km<sup>3</sup>), with a 68- 76% silica gap unprecedented among documented zoned eruptions worldwide (Hildreth and Fierstein, 2000). Regardless of bulk rock composition, glass shards are all rhyolitic (Fierstein and Hildreth, 1992), and closely match the composition of glass shards found in the Eclipse ice cores (Table VI.10). We also analyzed proximal tephra samples from the Katmai eruption for comparison to the shards found in the Eclipse cores to eliminate spurious geochemical differences arising from the use of different instrumentation, and found good agreement between the Eclipse glass, our analyses of Katmai tephra, and analyses of Katmai glass by Fierstein and Hildreth (1992). Our identification of Katmai tephra permits the use of several glaciochemical parameters to characterize the atmospheric effects of this eruption. Furthermore, all four ice cores used in this study record the Katmai fallout, and hence we are able to offer a robust assessment of the atmospheric effects of this eruption.

A Katmai signal has been reported from many circum-Arctic ice cores, including the Crete, Dye 3, 20D, GISP2, and GRIP, Greenland ice cores (Hammer, 1977; Neftel *et al.*, 1985; Lyons *et al.*, 1990; Zielinski *et al.*, 1994; Clausen *et al.*, 1997) as well as ice cores from the Agassiz Ice Cap, eastern Canadian Arctic (Barrie *et al.*, 1985) and Mt. Logan, Yukon (Holdsworth and Peake, 1985). The beginning of volcanic SO<sub>4</sub><sup>2-</sup> deposition from the Katmai eruption is synchronous with the tephra layer in the Eclipse cores implying rapid tropospheric transport of sulfate aerosols to the St. Elias Mountains. A maximum in volcanic SO<sub>4</sub><sup>2-</sup> concentrations is quickly reached, followed by a gradual decline to a local minimum during the winter of 1912-1913. Total volcanic SO<sub>4</sub><sup>2-</sup> fallout during the first year following the eruption ranges from 10.51 to 11.10 ug cm<sup>-2</sup> at Eclipse (three cores) and 9.53 ug cm<sup>-2</sup> at Mount Logan (one core). A subsidiary SO<sub>4</sub><sup>2-</sup> peak is seen through the 1913 annual layer we interpret to represent stratospheric fallout of SO<sub>4</sub><sup>2-</sup> aerosols from the eruption followed by a return to background levels by the end of 1914. Volcanic SO<sub>4</sub><sup>2-</sup> fallout in the second year following the eruption ranges from

2.05 to 3.94  $\mu\text{g cm}^{-2}$  at Eclipse and 0.61  $\mu\text{g cm}^{-2}$  at Mount Logan. However, by mid-1915 there is detectable volcanic  $\text{SO}_4^{2-}$  deposition once again in all three Eclipse cores. Because pyrroliometric optical depth measurements show that atmospheric turbidity following the eruption had decayed to a negligible level by October 1914 (Volz, 1975; Stothers, 1996), we have not included  $\text{SO}_4^{2-}$  deposition in 1915 and 1916 in calculations of the Katmai volcanic flux.

The initial Katmai sulfate peak is associated with a large non-sea-salt (nss)  $\text{Cl}^-$  residual an order of magnitude larger than any other  $\text{Cl}^-$  event observed in this suite of ice cores. Adjacent samples in Core 1 have nss  $\text{Cl}^-$  residual concentrations of 1478 and 1662  $\text{ng g}^{-1}$ , respectively, while Core 2 contains one sample with a nss  $\text{Cl}^-$  residual concentration of 3166  $\text{ng}^{-1}$ . Given the observed concentrations, it appears that the  $\text{Cl}^-$  rich horizon is split between two adjacent samples in Core 1. High volcanic  $\text{Cl}^-$  concentrations are also observed in Core 3 (113  $\text{ng g}^{-1}$ ) and the Mount Logan core (158  $\text{ng g}^{-1}$ ), ranking as the second and fifth largest  $\text{Cl}^-$  events in their respective cores. A  $\text{Cl}^-$  signal attributed to Katmai is also reported in Greenland ice cores (Lyons *et al.*, 1990; Clausen *et al.*, 1997). In contrast to the long period (2+ years) of  $\text{SO}_4^{2-}$  deposition,  $\text{Cl}^-$  levels rapidly fall to normal levels, implying a much shorter atmospheric residence time for volcanic  $\text{Cl}^-$  aerosols. A study of the effects of the 1989-90 Redoubt, Alaska eruptions on snow chemistry also suggested rapid deposition of volcanic  $\text{Cl}^-$  aerosols (Jaffe *et al.*, 1994). Given the short duration of the  $\text{Cl}^-$  fallout, possibly occurring in a single snowfall event, irregularities in the snow surface could be responsible for the much lower Katmai  $\text{Cl}^-$  concentrations observed in Core 3. The lack of  $\text{Cl}^-$  concentrations of comparable magnitude in the Mount Logan ice core to those seen in Core 1 and Core 2 suggest the  $\text{Cl}^-$  component of the volcanic plume was primarily in the lower troposphere.

Our data suggests that the Katmai eruption plume ( $\text{SO}_4^{2-}$  and  $\text{Cl}^-$  aerosols and silicate microparticles) consisted of two components. A lower tropospheric component consisting of sulfate and chloride aerosols and silicate microparticles was rapidly transported to the St. Elias in the summer of 1912 as evidenced by peaks in  $\text{SO}_4^{2-}$  and  $\text{Cl}^-$  synchronous with Katmai tephra.

Residence time of these products in the lower troposphere was on the order of days to weeks (Jaenicke, 1984) and was readily scavenged by snowfall at the ice core sites. Second, a portion of the eruptive products, mostly sulfur gases but perhaps including silicate microparticles, was injected into the upper troposphere and lower stratosphere. Sulfur oxidation rates are much slower in the stratosphere, and so the sulfur gases from the eruption could have remained aloft for as much as three years after the eruption (Legrand and Delmas, 1987). At high northern latitudes, the cold dark winter months further limit sulfur oxidation rates in the stratosphere (Laj *et al.*, 1990), and so a local minima in volcanic  $\text{SO}_4^{2-}$  fallout from the eruption is observed in the Eclipse ice cores during the winter of 1912-1913. Periodically, sulfur gases transported within the upper troposphere and lower stratosphere were reintroduced to the lower troposphere, where the sulfur gases were rapidly oxidized to  $\text{SO}_4^{2-}$  and deposited in snow at Eclipse producing the subsidiary sulfate peak in the 1913 annual layer. A possible mechanism for reintroduction of the sulfur gases to the lower troposphere could have involved several tropopause folding events in the spring of 1913, as was observed with El Chichon  $\text{SO}_4^{2-}$  aerosols over Greenland (Shapiro *et al.*, 1984).

The Mt. Logan record also shows a  $\text{NO}_3^-$  peak coincident with the Katmai  $\text{SO}_4^{2-}$  and Cl peak. This was interpreted as a sudden injection of  $\text{NO}_3^-$  followed by a slow decay, suggesting fallout of stratospheric aerosols (Holdsworth and Peake, 1985). We see no comparable  $\text{NO}_3^-$  peak at Eclipse associated with this eruption or any other in our records, in agreement with the work of Herron (1982) who found no volcanic effect on ice core  $\text{NO}_3^-$  in Greenland. This may suggest that the Katmai signal at Mt. Logan is more influenced by the stratospheric component of the eruption plume, whereas the tropospheric component is the dominant signal at Eclipse. However, the larger amount of  $\text{SO}_4^{2-}$  fallout at Eclipse relative to Mount Logan during the second year following the eruption, when all fallout must be stratospheric, argues against this interpretation.

A single basanite glass particle recovered from the 1908 layer in Core 1 can not be related to any known eruption. The composition of this particle suggests it may be from an undocumented sub-Plinian basaltic eruption in the Aleutian Arc, similar in style, magnitude (VEI

3), and composition to the 1999 Shishaldin eruption (Stelling *et al.*, 2002). Although basaltic sub-Plinian eruptions are rare, comparison of the 1999 Shishaldin ejecta to pre-historic deposits around the volcano suggests this style of eruption is relatively common at Shishaldin, with at least 11 such eruptions as voluminous as the 1999 eruption during the Holocene (Stelling *et al.*, 2002). This eruption style and composition may also be relatively common elsewhere in the Aleutians.

The 1907 sample contains glass spanning the compositional range from basaltic andesite to basaltic trachyandesite and trachyandesite (Figure VI.6). The ice core glass closely matches the composition of tephra from the 1907 Ksudach eruption (Table VI.10; Melekestsev *et al.*, 1996). The Ksudach massif is one of Kamchatka's most explosive volcanic centers, consisting of five nested calderas formed in successive collapse events since the late Pleistocene with the latest occurring around AD 240 (Braitseva *et al.*, 1996). Since that time all voluminous eruptions have originated from Shtyubel stratovolcano within the caldera, with the March 28, 1907 eruption (VEI 5) the most recent and largest explosive eruption from Shtyubel to date, totaling 2.4 km<sup>3</sup> dense rock equivalent (Volynets *et al.*, 1999). The eruption developed a Plinian column to a height of 22 km with the main axis of visible fallout dispersed north- northeast and consisting of basaltic andesite and andesite products (Bursik *et al.*, 1993) similar to those observed in the Eclipse ice core.

Identifying source volcanoes for glass-bearing layers in the Eclipse ice core that predate the 20<sup>th</sup> century becomes increasingly difficult due to the incomplete nature of the historical volcanism record, the lack of chemical analyses for comparison, and the limited compositional range of the tephra observed in the ice core (Figure VI.7). The 1809, 1804, and 1630 samples are similar in composition, plotting in the trachyte field with considerable overlap. The 1809 volcanic SO<sub>4</sub><sup>2-</sup> horizon is well-documented in ice cores from both polar regions (Cole-Dai *et al.*, 1991) and by glass shards of andesitic composition recovered from the South Pole and Dome C ice cores, Antarctica (Palais *et al.*, 1990). The presence of glass shards in the Eclipse tephra with a chemical composition distinctly different from 1809 glass found in Antarctica demonstrates

there was a second volcanic eruption in the Northern Hemisphere in 1809 (Yalcin *et al.*, in review). The only documented volcanic eruption in 1804 is a VEI 3 eruption of Maly-Semiachik, Kamchatka (Simkin and Seibert, 1994). The only chemical data from this volcano we are aware of is a whole-rock analysis of basaltic lava of Holocene age (Turner *et al.*, 2000) and therefore unsuitable for comparison to the Eclipse 1804 glass shard chemistry.

A VEI 5 eruption of Mount Vesuvius in December 1631 is within the dating uncertainty of the 1630 glass sample, however glass from this eruption is phonolitic in composition (Rolandi *et al.*, 1993) and clearly unrelated to the Eclipse 1630 glass. Products of the September 1630 eruption of Furnas Volcano on San Miguel Island in the Azores are a better match for the glass shards in the Eclipse core (Table VI.11). This eruption (VEI 5) produced 0.65 km<sup>3</sup> (dense rock equivalent) of explosive products with ash fall reported up to 550 km away (Cole *et al.*, 1995). Two analyses of pumice from this eruption are available, both are trachytic in composition. While there is a good match between Furnas pumice and glass compositions found in the Eclipse ice core for some elements (e.g., SiO<sub>2</sub>, Al<sub>2</sub>O<sub>3</sub>), the match is poor for other elements (e.g., CaO, K<sub>2</sub>O). Given the relatively modest column heights of 8-14 km inferred for this eruption (Cole *et al.*, 1995), the large distance between Furnas (38°N) and Eclipse, and chemical differences seen for some elements, linking the shards found in the Eclipse ice core to Furnas is tenuous.

The 1516 glass-bearing horizon is one of only two events in the last 1000 years to leave a visible tephra layer in the Eclipse ice cores, sharing this distinction with the 1912 Katmai eruption. Furthermore, SO<sub>4</sub><sup>2-</sup> concentrations associated with the 1516 eruption are the highest observed in the entire Eclipse ice core. Likewise, the highest SO<sub>4</sub><sup>2-</sup> concentration in the last 1000 years of the Bona-Churchill ice core (Mashiotta *et al.*, 2004) and the highest ECM value in the Prospector-Russell ice core from Mount Logan (Fisher *et al.*, 2004) are observed in the early 1500s. These three ice core signals are synchronous within their respective dating uncertainties; hence it is likely they represent the same eruption. Despite the high SO<sub>4</sub><sup>2-</sup> concentration associated with the 1516 eruption, sulfate deposition lasts for only 0.5 year, compared to 2+ years

in the case of the Katmai eruption. The combination of a visible tephra layer and brief and concentrated interval of  $\text{SO}_4^{2-}$  deposition implies a nearby volcano, possibly one in the Wrangell Volcanic Field of southeast Alaska and southwestern Yukon (Richter *et al.*, 1990). At least two Wrangell volcanoes have been active in the late Holocene: Mount Churchill, which produced the voluminous White River Ash in two eruptions radiocarbon dated to ~800 and ~300 A.D (Richter *et al.*, 1995), and Mount Wrangell, the only Wrangell volcano active in the 20<sup>th</sup> century (Miller *et al.*, 1998). In fact, radar imaging and glacier-flow modeling of glaciocvolcanic stratigraphy within the Mount Wrangell ice-filled caldera suggests at least five eruptions of Mount Wrangell in the last three hundred years (Clarke *et al.*, 1989). The average composition of Wrangell volcanic rocks (Richter *et al.*, 1990) is very similar to the trachyandesite to andesite 1516 glass in the Eclipse ice core for most elements, although differences exist in the case of MgO and Na<sub>2</sub>O (Table VI.11). Nonetheless, the available chemical data supports the possibility that an eruption in the Wrangell Volcanic Field is responsible for the 1516 tephra layer in the Eclipse ice core, consistent with the nature of the ice core signal suggesting a nearby source.

Two distinct glass compositions are found in the 1460 layer: a basaltic trachyandesite to trachyandesite glass (nine particles) and a trachyte glass (one particle). The basaltic trachyandesite to trachyandesite glass clearly represents a different volcanic center than other tephra bearing layers in Core 2, as it well separated from other glasses in a total alkali-silica diagram (Figure VI.7). The composition of this glass is similar to glasses found in Core 1 and dated to 1907 and 1945 (Table VI.11), which are known to be from Kamchatkan volcanoes (Ksudach, Avachinsky, Kliuchevskoi). Hence, we believe that the 1460 layer records a previously undocumented Kamchatka eruption, as there are no eruptions from Kamchatka in the Smithsonian database thought to have occurred around this time. The trachyte glass is similar to other glasses found in Core 2, and presumably was erupted from an Alaskan Volcano. There was an eruption of Augustine Volcano around this time, but glass from Augustine is rhyolitic in composition (Beget *et al.*, 1994).



A trachytic glass spanning a silica range of 63 to 67% is dated to 1456. This layer is within the dating uncertainty of the cataclysmic eruption which formed the Kuwae Caldera in Vanuatu (Monzier *et al.*, 1994). The large volume of magma erupted (~35 km<sup>3</sup> dense rock equivalent) places Kuwae among the largest known Holocene eruptions, including Santorini (30 km<sup>3</sup>), Tambora (50 km<sup>3</sup>), and Mazama-Crater Lake (55 km<sup>3</sup>). Since the caldera-forming phase of Kuwae eruption produced dacitic glass (Robin *et al.*, 1994) similar in composition to that found in the Eclipse 1456 layer (Table VI.11), it is tempting to assign the ice core glass to the Kuwae eruption. However, several lines of evidence argue against this interpretation. First, the first phase of the Kuwae caldera event produced glass spanning a range of 65 to 69% silica, with second phase slightly wider, 64 to 72%. Although there is some overlap between the ice core and Kuwae glasses, some of the Eclipse glasses clearly fall outside of the range of Kuwae caldera products. Other geochemical differences exist as well, notably for TiO<sub>2</sub>, Al<sub>2</sub>O<sub>3</sub>, and FeO. Second, the 1456 glass is not associated with a particularly large SO<sub>4</sub><sup>2-</sup> spike. The 1456 signal does not exceed our threshold concentration criteria for either EOF SO<sub>4</sub><sup>2-</sup> values or non-sea-salt SO<sub>4</sub><sup>2-</sup> residuals, and the volcanic SO<sub>4</sub><sup>2-</sup> flux from this event is only 0.27 ug cm<sup>-2</sup>. In contrast, Antarctic ice core studies report volcanic fallout from the Kuwae eruption was as much as 92% that from Tambora (Cole-Dai *et al.*, 1997). Finally, the 1456 glass is compositionally similar to most other tephtras found in the Eclipse core, tephtras that originate mostly from Alaskan and Kamchatkan volcanoes (Figure VI.7). Hence, we interpret the 1456 glass as originating from a moderate eruption in the North Pacific.

A much larger volcanic signal in the Eclipse ice core at 1453, one-half the magnitude of the Tambora signal, is assigned to Kuwae. This is consistent with the 1452 date for the eruption as deduced from historical and dendrochronological evidence (Pang, 1993; Briffa *et al.*, 1998) and sulfate deposition in Antarctic ice cores (Delmas *et al.*, 1992; Cole-Dai *et al.*, 1997, 2000; Stenni *et al.*, 2002). However, the GISP2 (Greenland) and Law Dome (Antarctica) ice cores ascribe a signal in 1459/1460 to Kuwae (Zielinski *et al.*, 1994; Palmer *et al.*, 2001). If these

signals are from Kuwae, the dating uncertainty reported for the GISP2 ( $\pm 5$  years) and Law Dome ( $\pm 1$  year) chronologies should be larger. Unfortunately no tephra has been recovered to date to definitively link the ice core signals to Kuwae and resolve the timing of the eruption. Ice core studies suggest asymmetric distribution of the Kuwae aerosols between the Northern and Southern Hemispheres, with volcanic sulfate fluxes in Arctic ice cores attributed to Kuwae one-half (Eclipse Core 2, Table VI.5) to two-thirds (GISP2; Zielinski, 1995) that of Tambora. Meanwhile, the Kuwae fallout in Antarctica is 92% that of Tambora (Cole Dai *et al.*, 1997). This result is not surprising given the 17°S latitude of the volcano.

Two distinct glass compositions are present in the ~1370 horizon: a trachyte glass (seven particles) and a rhyolitic glass (one particle) (Figure VI.7). These compositions are similar to intermediate silica eruptions of Hekla, such as the 1510 eruption (Table VI.11; Larsen *et al.*, 1999). There were also eruptions of Hekla in 1341 (VEI 3) and 1389 (VEI 3), although the lack of glass chemistry for these eruptions, their moderate size, and the large dating uncertainty for this horizon makes it difficult to attribute the Eclipse glass to either of these eruptions from Hekla with any confidence. Other Icelandic eruptions around this time such as Oraefajokull 1362 (VEI 5) and Katla 1357  $\pm$  3 years (VEI 4) can be ruled out on the basis of the glasses produced (rhyolitic and basaltic, respectively; Larsen *et al.*, 1999). Eruptions of Kikhpinych, Kamchatka (VEI 4), Parker, Philippines (Plinian), and Inyo Craters, California (VEI 4) also occurred around this time (Simkin and Seibert, 1994). However, the most plausible source for the 1370 glass in the Eclipse ice core, due to its calc-alkaline affinity, is an undocumented eruption in the continental margin portion of the Alaskan-Aleutian arc.

### **Climatic Implications**

The climatic effect of major eruptions (VEI $\geq$ 5) recorded at Eclipse is assessed using the Eclipse stable isotope ( $\delta^{18}\text{O}$  and  $\delta\text{D}$ ) record and instrumental temperature records from the Gulf of Alaska region. The Eclipse  $\delta^{18}\text{O}$  record provides an indicator of climatic conditions at the

Eclipse site. Comparison of the Eclipse  $\delta^{18}\text{O}$  record with regional temperature records reveals significant positive correlations with summertime temperature records along the Gulf of Alaska coastline and with stations in interior Alaska north of the Alaska Range (Wake *et al.*, 2002), allowing the Eclipse  $\delta^{18}\text{O}$  record to be used as a proxy for regional summertime temperature. For the twentieth century eruptions we discuss here, instrumental records can also be used to directly infer climatic conditions following the eruption. A regional instrumental temperature record for the Gulf of Alaska region was constructed by stacking standardized monthly mean temperature anomalies for all available stations (Table VI.12) to identify the common signal in these records. Station data was obtained from the Global Historical Climatological Network (GHCN). Since high frequency climate variability associated with the El Niño-Southern Oscillation (ENSO) could obscure the climatic response to volcanism, we first removed the ENSO influence on these records by means of a regression line with the Southern Oscillation index following techniques described by Angell (1990) (Figure VI.8). We then evaluated the statistical significance of summer negative temperature anomalies and winter positive temperature anomalies following the eruptions by comparing the means of 6-month summer and winter periods after the to the means of 3, 5, and 10 year periods before the eruption using a Student's t- test. Since there is significant autocorrelation in these records, confidence intervals were derived from Monte Carlo simulations of randomly generated red noise series.

Three major explosive eruptions of volcanic explosivity index (VEI) 5 or greater occurred in the North Pacific during the last century: Ksudach (1907), Katmai (1912) and Bezymianny (1956). Since the 1956 Bezymianny eruption was a laterally-directed blast similar to Mt. St. Helens in 1980 (Belousov 1996), it produced only a modest sulfur release and is not consistently recorded in St. Elias ice cores. Therefore, we focus our discussion of climatically effective volcanism in the North Pacific region during the instrumental period on the Ksudach and Katmai eruptions. Our analysis of instrumental temperature records from the Gulf of Alaska

region does not identify a statistically significant negative temperature anomaly following the Ksudach eruption (Figure VI.9). Bradley (1988) reported a statistically significant drop in temperature over northern hemisphere continental land areas in the summer (June, July, August) of 1907. While we find no evidence of such a drop in temperature records from the Gulf of Alaska region following the eruption, a pronounced negative temperature anomaly immediately precedes this eruption. Therefore, cooler than normal temperatures in late 1906 and early 1907, at least in the Gulf of Alaska region, are not attributable to the March 1907 Ksudach eruption. However, the summer 1908  $\delta^{18}\text{O}$  peak at Eclipse is very subdued, suggesting cool conditions prevailed though the summer of 1908 at the Eclipse site (Figure VI.9). This is not likely to be a result of the 1907 Ksudach eruption, given the lack of a similar response in the summer of 1907 immediately following the eruption and the lack of evidence for volcanic sulfate deposition continuing beyond a few months after the eruption.

The climatic impact of the much larger Katmai 1912 eruption can also be studied in detail using the glaciochemical parameters we measured in our ice core and available instrumental records from the region spanning the time of the eruption. Our analysis of regional temperature records shows a 28-month period of generally cooler than normal conditions, nearly one degree Celsius below the 100 year mean, following the eruption (Figure VI.9). This anomaly is significant at the 90% confidence interval as determined from a student's t-test comparing the means of one and two year periods after the eruption with the mean of the three year period before the eruption. Using a longer base period before the eruption incorporates a very cold period in late 1906 and early 1907 that lowers the mean of the pre-eruption period so that its mean is no longer statistically different from the mean of the post-eruption years. Evidence for summer cooling following the Katmai eruption is more robust in the instrumental record than is the evidence for winter warming. However, the Eclipse  $\delta^{18}\text{O}$  record suggests warmer than normal temperatures during the winter of 1912-1913, as evidenced by the lack of a distinct

minima in  $\delta^{18}\text{O}$  during the winter of 1912–1913 (Figure VI.10). This could represent corroborating evidence for warmer than normal winters (Robock and Mao, 1992) associated with volcanic eruptions. Evidence for summer cooling in the Eclipse  $\delta^{18}\text{O}$  record is inconclusive.

The instrumental temperature record from the Gulf of Alaska region is not sufficiently long to robustly investigate possible volcanic climate effects as the number of large eruptions during the past 100 years is limited. Therefore, we must look into the past using proxy data such as that available from the Eclipse ice cores. This allows us to investigate the climatic response in the Gulf of Alaska region following large eruptions such as Tambora, Laki, and Kuwae. The 1815 eruption of Tambora is among the very largest volcanic eruptions during the Holocene, and was followed by very cold temperatures during the summer of 1816, often referred to as the year without a summer in New England (e.g., Harrington, 1992). The Eclipse  $\delta\text{D}$  record suggests that the summer of 1816 was unusually cold in the Gulf of Alaska region as well (Figure VI.10). Peak summer  $\delta\text{D}$  averages  $-180\text{‰}$  at Eclipse between 1812 and 1820, but is only  $-195\text{‰}$  in 1816. The winter of 1815–1816 appears to be anomalously warm at Eclipse, reaching a minimum of  $-205\text{‰}$  compared to the local average (1812–1820) of  $-220\text{‰}$ . The unknown 1809 volcanic eruption also appears to fall within the class of volcanic eruptions large enough to affect climate. However, the 1809 eruption occurred during one of the coldest periods of the Little Ice Age, so any climatic response to the eruption is difficult to separate from cooling already underway. The summers of 1810 and 1811 appear to be among the coldest at Eclipse in the last few centuries, with peak summer  $\delta\text{D}$  values of only  $-200\text{‰}$  and  $-205\text{‰}$ , respectively. Because the unusually cold years of 1810 and 1811 represent the culmination of a decade-long cooling trend which began around 1800, any climatic response to the 1809 eruption is superimposed on a climatic oscillation already underway.

The 1783 eruption of Laki, Iceland appears to have caused an exceptionally cold summer in 1784 throughout northwest North America that in the indigenous oral tradition is known as the

year summer did not come (Jacoby *et al.*, 1999). Tree-ring records indicate that the summer of 1784 was the coldest in the region in at least the last 400 years. The year 1784 is also unique in the Eclipse  $\delta D$  record because it lacks a well-defined winter 1783-1784 minimum and summer 1784 maximum (Figure VI.10). Instead,  $\delta D$  values fall monotonically, with the exception of a 20 ‰ oscillation in spring 1784, from fall 1783 to fall 1784. In contrast, the average seasonal  $\delta D$  amplitude at Eclipse is about -80 ‰. The Laki eruption appears to have resulted in an exceptionally warm winter (1783-1784; -185‰) and exceptionally cold summer (1784; -200‰) at Eclipse compared to the average values of -240‰ and -160‰, respectively. Meanwhile, the unidentified 1516 eruption, thought to be a local eruption, is responsible for the highest sulfate concentration observed in the 550+ years covered by the Eclipse ice cores. However, no anomalous signal is observed in the stable isotope record that could be interpreted as a volcanic temperature effect. Because this eruption is not observed in ice cores from Greenland or the eastern Canadian Arctic, it apparently affected only the local troposphere and therefore it had little to no climatic effect. From these examples it is apparent that the climatic response to volcanism is highly variable and dependant on the location of the volcanic, the style and magnitude of the eruption, and the state of the climate system at the time of the eruption.

### **Conclusions**

We have presented records of regionally significant volcanic eruptions using a suite of three ice cores from Eclipse Icefield and one ice core from Mount Logan in the St. Elias Mountains, Yukon, Canada. These cores cover variously 90, 100, 290 and 1000 years. Volcanic horizons were identified by statistical analysis of the ice core  $SO_4^{2-}$  and Cl<sup>-</sup> records. Comparison of results from an EOF analysis and from using non-sea-salt residuals above a robust spline demonstrates that the EOF analysis provides a more conservative estimation of volcanic  $SO_4^{2-}$ . Furthermore, use of non-sea-salt residuals occasionally results in false positive signals, as

suggested by negligible volcanic  $\text{SO}_4^{2-}$  flux from such events. However, ice core sites with no or negligible  $\text{SO}_4^{2-}$  deposition from anthropogenic sources will yield comparable results using either technique. Comparisons of volcanic  $\text{SO}_4^{2-}$  flux records using linear regression demonstrate a high degree of reproducibility of the results, especially for the largest sulfur producing eruptions such as Katmai 1912, which are also the eruptions of greatest interest in climate forcing studies.

Correlation of volcanic  $\text{SO}_4^{2-}$  signals with eruptions documented in the historical record indicates that one-third of the eruptions recorded in St. Elias ice cores are from Alaskan and Kamchatkan volcanoes. This is a minimum proportion, because many of the unidentified signals in these records are undoubtedly also from eruptions in Alaska and Kamchatka, regions where the number of historically documented eruptions decreases markedly prior to the 20<sup>th</sup> century. Although there are several moderately large ( $\text{VEI} \geq 4$ ) eruptions recorded in only one of the three available cores from Eclipse Icefield, the use of multiple records provides signals from all known  $\text{VEI} \geq 4$  eruptions in Alaska and Kamchatka since the 1820's in at least one core. Clearly, multiple cores can provide a more complete picture of regionally significant volcanic events than is possible from any one core. The large number of eruptions in Alaska and Kamchatka recorded in the St. Elias cores provides a Northern Hemisphere volcanic aerosol record complementary to the records already available from Greenland where Icelandic eruptions predominate.

The St. Elias ice cores record a large volcanic  $\text{SO}_4^{2-}$  signal in the early 1500's that is not prominent in the eastern Arctic. Analysis of volcanic glass shards from this eruption in the Eclipse ice core suggest it could be from an undocumented eruption in the Wrangell Volcanic Field of southeast Alaska. Tephrochronological evidence from the Eclipse ice core also documents eruptions in Alaska (Redoubt, Trident, Katmai), Kamchatka (Avachinsky, Kliuchevskoi, Ksudach), and Iceland (Hekla). Several unidentified tephra-bearing horizons, with available geochemical evidence suggesting Alaskan and Kamchatkan sources, are also found in the Eclipse ice core. Trace and rare earth element analysis of glass shards via ICP-MS could provide more robust identifications of source volcanoes, with the potential for identifying

previously unrecognized volcanic eruptions, as many of the tephtras older than 1900 can not be correlated to any known eruption. Investigation of the climatic influence of the largest eruptions record at Eclipse using instrumental temperature records where available and the proxy temperature recorded provide by the Eclipse stable isotope record highlights the variable response of the climate system to volcanism. The Laki eruption of 1783 appears to have produced the largest temperature response in the form of summer cooling and winter warming following a volcanic eruption in this region. These results are encouraging for the development of longer paleovolcanic records of these poorly-known and active volcanic regions using ice cores from the St. Elias Mountains, incorporating both glaciochemical and tephrochronological evidence.

#### **Acknowledgements**

We thank E. Blake, S. Williams, A. Mondrick, and S. Bastien for field assistance and drilling the core, S. Whitlow for major ion analysis, D. Fisher for oxygen isotope analysis of Eclipse Core 1, and G. Holdsworth for use of the Mt. Logan ice core data. We also thank J. Fournelle for sharing analyses of Westdahl glass. The National Science Foundation Office of Polar Programs supported this research.



**Table VI.1.** EOF analysis of the variance in the data set of seven of the eight species measured in the three ice cores from Eclipse Icefield ( $\text{NH}_4^+$  was excluded). For all three cores, EOF 5 is loaded solely on  $\text{SO}_4^{2-}$  and explains a large proportion of the variance in the  $\text{SO}_4^{2-}$  time series.

Eclipse Core 1 EOF Analysis (1894-1996)												
	Eigenvector Components						Percent Variance Explained					
	EOF	EOF	EOF	EOF	EOF	EOF	EOF	EOF	EOF	EOF	EOF	EOF
	1	2	3	4	5	6	1	2	3	4	5	6
$\text{Na}^+$	0.58	0.76	0.09	-0.03	0.06	0.27	33.4	58.1	0.8	0.1	0.3	7.3
$\text{K}^+$	0.62	0.38	-0.39	0.56	-0.06	-0.10	38.4	14.2	15.0	31.0	0.4	0.9
$\text{Mg}^{2+}$	0.70	-0.35	0.55	0.21	0.01	0.00	49.6	12.0	30.0	4.3	0.0	0.0
$\text{Ca}^{2+}$	0.81	-0.45	0.23	0.09	0.00	0.01	66.1	20.5	5.2	0.7	0.0	0.0
$\text{Cl}^-$	0.57	0.67	0.24	-0.33	-0.13	-0.21	32.5	45.0	5.6	10.7	1.8	4.4
$\text{NO}_3^-$	0.71	-0.43	-0.37	-0.24	-0.34	0.08	49.6	18.1	13.5	6.0	11.7	0.7
$\text{SO}_4^{2-}$	0.81	-0.18	-0.32	-0.23	<b>0.40</b>	-0.05	64.9	3.3	10.3	5.2	<b>15.8</b>	0.3
Total Variance Explained							47.8	24.5	11.5	8.3	4.3	1.9

Eclipse Core 2 EOF Analysis (1000-1970)												
	Eigenvector Components						Percent Variance Explained					
	EOF	EOF	EOF	EOF	EOF	EOF	EOF	EOF	EOF	EOF	EOF	EOF
	1	2	3	4	5	6	1	2	3	4	5	6
$\text{Na}^+$	0.51	0.80	-0.15	-0.08	-0.10	0.21	25.7	63.4	2.2	0.7	1.0	4.5
$\text{K}^+$	0.41	0.28	0.84	0.22	0.04	-0.02	16.9	7.9	70.2	4.9	0.1	0.0
$\text{Mg}^{2+}$	0.80	-0.17	-0.28	0.45	-0.05	-0.17	63.7	3.0	7.6	20.6	0.2	2.9
$\text{Ca}^{2+}$	0.86	-0.33	-0.10	0.23	-0.02	0.21	74.4	10.9	1.0	5.1	0.0	4.5
$\text{Cl}^-$	0.57	0.75	-0.15	-0.16	-0.01	-0.20	32.0	56.1	2.3	2.4	0.0	3.8
$\text{NO}_3^-$	0.66	-0.47	0.17	-0.40	-0.39	-0.05	43.8	21.9	3.0	15.6	15.4	0.2
$\text{SO}_4^{2-}$	0.78	-0.27	0.01	-0.33	<b>0.45</b>	-0.01	61.1	7.3	0.0	10.8	<b>20.3</b>	0.0
Total Variance Explained							45.4	24.3	12.3	8.6	5.3	2.3

Eclipse Core 3 EOF Analysis (1910-2002)												
	Eigenvector Components						Percent Variance Explained					
	EOF	EOF	EOF	EOF	EOF	EOF	EOF	EOF	EOF	EOF	EOF	EOF
	1	2	3	4	5	6	1	2	3	4	5	6
$\text{Na}^+$	0.52	0.77	-0.20	0.02	-0.18	-0.26	27.0	58.5	4.0	0.0	3.4	6.9
$\text{K}^+$	0.43	0.39	0.81	0.09	0.05	0.02	18.1	14.9	65.9	0.8	0.2	0.0
$\text{Mg}^{2+}$	0.78	-0.24	-0.13	0.54	-0.02	0.09	60.1	5.6	1.7	28.6	0.0	0.9
$\text{Ca}^{2+}$	0.87	-0.34	-0.03	0.22	0.01	-0.09	76.0	11.7	0.1	4.6	0.0	0.8
$\text{Cl}^-$	0.63	0.66	-0.25	-0.14	0.08	0.29	39.5	43.0	6.1	1.9	0.6	8.5
$\text{NO}_3^-$	0.73	-0.43	0.12	-0.39	-0.34	0.08	53.0	18.1	1.4	14.9	11.4	0.6
$\text{SO}_4^{2-}$	0.83	-0.22	-0.05	-0.34	<b>0.34</b>	-0.12	69.4	4.7	0.3	11.8	<b>11.9</b>	1.5
Total Variance Explained							49.0	22.4	11.4	9.0	3.9	2.7

**Table VI.2.** Threshold criterion for detection of volcanic SO<sub>4</sub><sup>2-</sup> signals (ng g<sup>-1</sup>).

	Core 1		Core 2		Core 3		Mt. Logan NW Col	
	1894-1996		1000-2002		1910-2002		1690-1980	
	EOF 5	nss res	EOF 5 <sup>1</sup>	nss res	EOF 5	nss res	EOF 3	nss res
Mean	12	45	11	28	11	43	37	35
std. dev.	19	66	16	42	18	65	63	63
mean+1σ	31	110	27	70	29	108	99	98
n <sup>2</sup>	37	34	80	72	28	22	20	31

<sup>1</sup>Period ~1000 to 1970 only. See text for explanation.

<sup>2</sup>Number of signals recovered.

**Table VI.3.** EOF analysis of the variance in the data set of six of the eight species measured in the Mount Logan Northwest Col ice core (NH<sub>4</sub><sup>+</sup> and NO<sub>3</sub><sup>-</sup> was excluded). Note that EOF 3 is loaded solely on SO<sub>4</sub><sup>2-</sup> and explains a large proportion of the variance in the SO<sub>4</sub><sup>2-</sup> time series.

	Mt. Logan Northwest Col Volcanic EOF Analysis (1690-1980)											
	Eigenvector Components						Percent Variance Explained					
	EOF 1	EOF 2	EOF 3	EOF 4	EOF 5	EOF 6	EOF 1	EOF 2	EOF 3	EOF 4	EOF 5	EOF 6
Na <sup>+</sup>	0.85	-0.45	-0.11	-0.14	-0.09	0.20	72.1	20.0	1.2	2.0	0.7	4.0
K <sup>+</sup>	0.81	-0.37	-0.13	0.42	0.05	-0.05	65.9	13.8	1.8	18.0	0.2	0.2
Mg <sup>2+</sup>	0.57	0.76	-0.19	-0.06	0.24	0.05	32.2	57.6	3.6	0.4	6.0	0.3
Ca <sup>2+</sup>	0.47	0.80	-0.28	0.03	-0.24	-0.05	22.1	64.0	8.0	0.1	5.6	0.2
Cl <sup>-</sup>	0.89	-0.28	0.18	-0.27	0.02	-0.18	78.4	8.0	3.1	7.4	0.0	3.1
SO <sub>4</sub> <sup>2-</sup>	0.34	0.37	<b>0.86</b>	0.10	-0.03	0.05	11.2	14.0	<b>73.4</b>	1.0	0.1	0.3
	Total Variance Explained						47.0	29.6	15.2	4.8	2.1	1.3

**Table VI.4.** Volcanic signals in the Eclipse Core 1 ice core, with start of signal, length of signal, peak concentrations, and total volcanic  $\text{SO}_4^{2-}$  flux for each event. Events recorded in more than one core from Eclipse Icefield are assigned the same event number in each core; hence event numbering is not continuous in any one core. Volcanic eruptions are from the chronology of Simkin and Siebert (1994) and online update.

Eclipse Core 1 Volcanic Events (1894-1996)									
#	Start Date	Length (years)	Peak Conc. ( $\text{ng g}^{-1}$ )			$\text{SO}_4^{2-}$ Flux		Possible Source(s) with Date	VEI
			$\text{SO}_4^{2-}$		Cl	EOF	nss		
			EOF	nss	nss	5	res		
			5	res	res	( $\mu\text{g cm}^{-2}$ )			
3	1996.1	0.4	20	284	--	0.09	1.91	Karymsky (Kamchatka) 1/1996	3
								Akademia Nauk (Kamchatka) 1/1996	3
6	1993.4	0.7	33	145	--	0.73	5.72	Bezymianny (Kamchatka) 10/1993	3
7	1992.4	0.5	41	301	--	0.44	4.69	Spurr (Alaska) 6/1992	4
								Bogoslof (Aleutian Is.) 7/1992	3
8	1991.5	0.6	37	59	35	0.57	1.61	Westdahl (Alaska) 11/1991	3
								Pinatubo (Philippines) 6/1991	5+
9	1989.8	1.0	146	360	34	1.01	2.39	Redoubt (Alaska) 12/1989	3
								Kliuchevskoi (Kamchatka) 1/1990	4
10	1988.3	0.5	4	163	21	0.04	3.04	???	
12	1986.2	0.9	30	134	--	0.59	3.71	Augustine (Alaska) 3/1986	4?
								Sheveluch (Kamchatka) 3/1986	3
								Pavlof (Alaska) 4/1986	3
								Kliuchevskoi (Kamchatka) 11/1986	3
								Bezymianny (Kamchatka) 12/1986	3
13	1985.4	0.3	14	210	--	0.16	2.94	Bezymianny (Kamchatka) 6/1985	3
15	1982.3	0.9	25	155	497	0.37	1.96	Gareloi (Aleutian Is.) 1/1982	3
								El Chichon (Mexico) 4/1982	5
								Galunggung (Indonesia) 5/1982	4
16	1980.9	0.7	65	189	--	0.76	3.01	Pavlof (Alaska) 11/1980	3
								Okmok (Aleutian Is.) 3/1981	3?
								Alaid (Kurile Is.) 4/1981	4
17	1979.2	1.0	50	353	32	0.59	5.03	Bezymianny (Kamchatka) 2/1979	3
								Westdahl (Alaska) 2/1979	3?
18	1978.3	0.3	27	42	--	0.51	1.01	Westdahl (Alaska) 2/1978	3
19	1977.0	0.5	23	133	24	0.39	2.27	Bezymianny (Kamchatka) 3/1977	3
								Ukinkrek Maars (Alaska) 3/1977	3
20	1975.5	0.6	186	544	--	4.65	22.51	Tolbachik (Kamchatka) 7/1975	4+
								Augustine (Alaska) 1/1976	4
21	1973.3	0.4	134	355	66	3.17	8.68	Tiatia (Kurile Is.) 7/1973	4
22	1972.3	0.4	19	112	--	0.40	2.07	Alaid (Kurile Is.) 6/1972	3
23	1971.2	0.6	13	111	--	0.30	1.97	Bezymianny (Kamchatka) 3/1971	3
24	1970.1	0.5	42	345	--	0.37	3.80	Kolokol (Kurile Is.) 2/1970	3
25	1969.1	0.5	25	120	--	0.37	1.40	Trident (Alaska) 11/1968	3
27	1966.1	0.5	19	117	--	0.12	2.32	Awu (Indonesia) 8/1966	4
								Kelut (Indonesia) 4/1966	4
28	1965.4	0.4	39	213	--	0.59	3.84	Kliuchevskoi (Kamchatka) 8/1965	3
								Taal (Philippines) 9/1965	4

Table VI.4. (Continued)

#	Start Date	Length (years)	Eclipse Core 1 Volcanic Events (Continued)					Possible Source(s) with Date	VEI
			Peak Conc. (ng g <sup>-1</sup> )			SO <sub>4</sub> <sup>2-</sup> Flux			
			SO <sub>4</sub> <sup>2-</sup>		Cl <sup>-</sup>	EOF	nss		
			5	nss	nss	5	res		
		5	res	res		(ug cm <sup>-2</sup> )			
30	1963.1	1.5	99	233	--	2.55	6.44	Amukta (Aleutian Is.) 2/1963	3
								Agung (Indonesia) 3/1963	5
								Trident (Alaska) 4/1963	3
31	1960.1	1.2	59	260	--	2.02	5.27	Karymysky (Kamchatka) 4/1960	3
								Sarychev (Kurile Is.) 8/1960	3
								Okmok (Aleutian Is.) 10/1960	3
								Kliuchevoskoi (Kamchatka) 12/1960	3
33	1958.8	0.7	65	130	--	2.79	5.16	Okmok (Aleutian Is.) 8/1958	3
34	1957.6	0.7	28	96	23	0.84	2.90	Zavaritzki (Kurile Is.) 11/1957	3
36	1955.2	0.5	29	90	--	0.72	1.49	???	
37	1953.2	0.7	40	78	46	1.09	1.33	Trident (Alaska) 2/1953	3
								Spurr (Alaska) 7/1953	4
38	1951.5	1.5	102	261	--	3.07	7.17	Ambyrm (Vanuatu) 1951	4+
								Kelut (Indonesia) 8/1951	4
								Bagana (Bougainville Island) 2/1952	4
39	1949.2	1.0	35	140	--	0.57	1.02	???	
40	1946.5	1.2	27	65	34	0.54	2.52	Sarychev (Kurile Is.) 11/1946	4
								Hekla (Iceland) 3/1947	4
41	1945.0	0.9	76	303	--	1.43	5.29	Kliuchevoskoi (Kamchatka) 1/1945	4?
								Avachinsky (Kamchatka) 2/1945	4
43	1942.4	0.8	29	53	--	0.76	2.46	???	
45	1939.2	0.6	40	89	32	1.23	3.69	Veniaminof (Alaska) 5/1939	3
47	1935.1	0.7	41	261	--	1.31	8.32	Augustine (Alaska) 3/1935	3
								Kliuchevoskoi (Kamchatka) 4/1935	3
48	1934.5	0.3	10	119	--	0.14	1.55	???	
51	1929.8	1.1	76	207	--	1.52	2.75	Komaga-Take (Japan) 6/1929	4
								Gorely (Kamchatka) 9/1929	3
								Sarychev (Kurile Is.) 2/1930	3
52	1926.3	0.6	31	151	--	0.65	2.40	Avachinsky (Kamchatka) 4/1926	4
55	1921.1	0.5	32	133	--	0.34	4.63	???	
56	1919.4	0.6	27	57	--	0.80	1.46	Kelut (Indonesia) 5/1919	4
57	1918.5	0.6	56	121	--	1.83	2.17	Katla (Iceland) 10/1918	4
58	1917.3	1.2	84	160	98	2.55	5.80	Agrigan (Mariana Is.) 4/1917	4
								Mutnovsky (Kamchatka) 7/1917	3?
59	1915.5	1.5	30	65	--	1.95	2.30	???	
60	1912.4	2.3	183	351	1662	15.78	25.21	Katmai (Alaska) 6/1912	6
61	1910.1	0.7	24	123	--	0.70	2.27	???	
62	1908.3	0.5	40	83	--	0.96	1.54	???	
63	1907.2	0.6	82	165	--	2.33	3.91	Ksudach (Kamchatka) 3/1907	5
64	1903.6	1.0	26	214	63	1.37	3.20	Grimsvotn (Iceland) 5/1903	4
67	1897.5	0.4	44	80	--	0.90	2.00	Mayon (Philippines) 5/1897	4
68	1895.2	0.6	17	168	--	0.44	2.61	???	

**Table VI.5.** Volcanic signals in the Eclipse Core 2 ice core, with start of signal, length of signal, peak concentrations, and total volcanic SO<sub>4</sub><sup>2-</sup> flux for each event. Events recorded in more than one core from Eclipse Icefield are assigned the same event number in each core; hence event numbering is not continuous in any one core. Volcanic eruptions are from the chronology of Simkin and Siebert (1994) and online update.

Eclipse Core 2 Volcanic Events (1400-2002)									
#	Start Date	Length (years)	Peak Conc. (ng g <sup>-1</sup> )			SO <sub>4</sub> <sup>2-</sup> Flux		Possible Source(s) with Date	VEI
			SO <sub>4</sub> <sup>2-</sup>		Cl	EOF	nss		
			5	res	nss	5	res		
						(ug cm <sup>-2</sup> )			
2	1997.4	0.6	12	153	--	0.27	4.15	Bezymianny (Kamchatka) 5/1997	3
3	1996.1	0.5	3	164	--	0.03	2.79	Karymysky (Kamchatka) 1/1996	3
								Akademia Nauk (Kamchatka) 1/1996	3
4	1995.5	0.4	50	124	--	0.96	2.03	Bezymianny (Kamchatka) 9/1995	3
5	1994.4	0.3	39	79	--	0.89	2.07	Cleveland (Aleutians) 5/1994	3
6	1993.3	0.4	31	79	--	0.77	1.53	Bezymianny (Kamchatka) 10/1993	3
7	1992.3	0.6	20	137	--	0.48	4.69	Sheveluch (Kamchatka) 4/1992	3
								Spurr (Alaska) 6/1992	4
								Bogoslof (Aleutian Is.) 7/1992	3
8	1991.6	0.7	28	52	--	1.01	0.93	Pinatubo (Philippines) 6/1991	5+
								Westdahl (Alaska) 11/1991	3
9	1989.8	0.9	137	208	177	4.59	3.47	Redoubt (Alaska) 12/1989	3
10	1988.3	0.5	38	55	--	1.29	1.18	Kliuchevoskoi (Kamchatka) 1/1990	4
11	1987.4	0.4	35	63	--	1.14	0.97	Cleveland (Aleutian Is.) 6/1987	3
12	1986.2	0.9	36	106	--	1.82	3.89	Augustine (Alaska) 3/1986	4?
								Sheveluch (Kamchatka) 3/1986	3
								Pavlof (Alaska) 4/1986	3
								Kliuchevoskoi (Kamchatka) 11/1986	3
								Bezymianny (Kamchatka) 12/1986	3
14	1984.2	1.0	39	57	--	1.13	1.71	Bezymianny (Kamchatka) 2/1984	3
								Kliuchevoskoi (Kamchatka) 3/1984	3
16	1981.0	0.9	31	152	--	1.05	3.42	Pavlof (Alaska) 11/1980	3
								Okmok (Aleutian Is.) 3/1981	3?
								Alaid (Kurile Is.) 4/1981	4
18	1978.1	0.7	26	40	--	0.95	1.10	Westdahl (Alaska) 2/1978	3
20	1975.8	1.1	28	61	--	1.24	1.98	Tolbachik (Kamchatka) 7/1975	4+
								Augustine (Alaska) 1/1976	4
21	1973.1	0.7	234	444	85	5.31	9.72	Tiatia (Kurile Is.) 7/1973	4
								Vestmannaeyjar (Iceland) 1/1973	3
22	1972.2	0.8	39	45	--	1.83	1.37	Alaid (Kurile Is.) 6/1972	3
25	1969.2	0.3	27	82	--	0.40	1.34	Trident (Alaska) 11/1968	3
26	1967.6	0.4	12	131	--	0.19	3.09	Trident (Alaska) 9/1967	3
								Redoubt (Alaska) 12/1967	3
29	1964.6	1.6	29	34	--	0.75	0.66	Sheveluch (Kamchatka) 11/1964	4+
30	1962.9	1.6	42	132	--	2.68	6.59	Amukta (Aleutian Is.) 2/1963	3
								Agung (Indonesia) 3/1963	5
								Trident (Alaska) 4/1963	3

Table VI.5. (Continued)

#	Start Date	Length (years)	Eclipse Core 2 Volcanic Events (Continued)					Possible Source(s) with Date	VEI
			Peak Conc. (ng g <sup>-1</sup> )			SO <sub>4</sub> <sup>2-</sup> Flux			
			SO <sub>4</sub> <sup>2-</sup>		Cl <sup>-</sup>	EOF	nss		
			5	res	nss	5	res		
						(ug cm <sup>-2</sup> )			
31	1960.1	1.1	34	54	--	3.03	4.23	Karymsky (Kamchatka) 4/1960	3
								Sarychev (Kurile Is.) 8/1960	3
								Okmok (Aleutian Is.) 10/1960	3
								Kliuchevoskoi (Kamchatka) 12/1960	3
33	1958.3	0.7	60	107	--	1.44	1.91	Okmok (Aleutian Is.) 8/1958	3
34	1957.8	0.4	98	196	48	3.19	6.12	Zavaritzki (Kurile Is.) 11/1957	3
35	1956.1	1.2	38	240	--	1.87	8.60	Bezymianny (Kamchatka) 3/1956	5
								Veniaminof (Alaska) 3/1956	3
								Koryaksky (Kamchatka) 12/1956	3
36	1955.4	0.5	28	87	--	0.64	1.47	???	
37	1953.7	0.4	27	53	--	0.82	0.87	Trident (Alaska) 2/1953	3
								Spurr (Alaska) 7/1953	4
38	1952.3	1.3	60	98	--	2.47	3.04	Ambyrm (Vanuatu) 1951	4+
								Kelut (Indonesia) 8/1951	4
								Bagana (Bougainville Island) 2/1952	4
42	1943.6	0.3	29	103	--	0.66	1.76	Michoacan (Mexico) 2/1943	4
45	1939.1	0.7	59	140	69	1.80	4.09	Veniaminof (Alaska) 5/1939	3
47	1935.5	0.6	33	85	--	1.05	2.11	Augustine (Alaska) 3/1935	3
								Kliuchevoskoi (Kamchatka) 4/1935	3
49	1933.0	1.0	11	136	26	0.50	3.34	Kharimkotan (Kurile Is.) 1/1933	5
								Kuchinoerabu (Japan) 12/1933	4?
50	1931.4	0.4	13	267	--	0.44	5.68	Kliuchevoskoi (Kamchatka) 3/1931	4
								Aniakchak (Alaska) 5/1931	4
51	1929.9	1.1	42	121	--	1.76	4.11	Komaga-Take (Japan) 6/1929	4
								Gorely (Kamchatka) 9/1929	3
								Sarychev (Kurile Is.) 2/1930	3
57	1918.7	0.5	38	51	--	1.20	1.44	Katla (Iceland) 10/1918	4
58	1917.0	1.7	49	71	74	2.95	3.24	Agrigan (Mariana Is.) 4/1917	4
								Mutnovsky (Kamchatka) 7/1917	3
59	1915.6	1.2	28	41	--	2.01	2.17	???	
60	1912.4	2.1	126	330	3166	12.93	31.67	Katmai (Alaska) 6/1912	6
62	1908.1	0.5	48	100	--	1.28	3.78	???	
63	1907.3	0.8	33	88	--	1.81	4.40	Ksudach (Kamchatka) 3/1907	5
64	1903.7	0.9	40	120	41	2.06	4.50	Grimsvotn (Iceland) 5/1903	4
65	1902.3	0.5	9	69	--	0.16	1.73	Redoubt (Alaska) 1/1902	3
								Seguam (Aleutian Is.) 1902	3
66	1899.5	0.6	2	189	--	0.04	3.94	Okmok (Aleutian Is.) 1899	
67	1897.5	1.7	12	231	--	0.36	6.72	Mayon (Philippines) 5/1897	4
68	1895.0	0.7	17	77	23	0.54	1.36	???	
69	1893.0	0.4	20	97	--	0.58	2.33	???	
70	1891.3	0.6	30	53	--	0.69	1.09	???	
71	1886.2	1.2	14	71	54	0.86	3.44	Tungurahua (Ecuador) 1/1886	4

Table VI.5. (Continued)

Eclipse Core 2 Volcanic Events (Continued)									
#	Start Date	Length (years)	Peak Conc. (ng g <sup>-1</sup> )			SO <sub>4</sub> <sup>2-</sup> Flux		Possible Source(s) with Date	VEI
			SO <sub>4</sub> <sup>2-</sup>		Cl	EOF	nss		
			5	res	nss	5	res		
						(ug cm <sup>-2</sup> )			
72	1884.3	1.8	42	187	25	2.92	6.31	Krakatau (Indonesia) 8/1883	6
73	1883.4	0.8	26	54	49	1.44	2.24	Bogoslof (Aleutian Is.) 9/1883	3
								Augustine (Alaska) 10/1883	4
								Kharimkotan (Kurile Is.) 1883	3
74	1873.8	0.9	37	28	--	1.20	0.94	Grimsvotn (Iceland) 1/1873	4
75	1872.3	1.0	28	65	--	1.20	2.65	Sinarka (Kurile Is.) 1872	4
								Merapi (Indonesia) 4/1872	4
76	1866.5	0.6	--	83	--	--	3.13	???	
77	1864.2	0.6	6	82	47	0.25	2.39	???	
78	1861.3	1.3	72	151	--	5.03	9.69	Makian (Indonesia) 12/1861	4?
79	1858.0	2.0	70	201	107	4.12	8.65	Fuego (Guatemala) 1/1857	4?
80	1842.9	0.4	9	75	--	0.20	1.89	Goriashaia (Kurile Is.) 6/1842	3?
81	1835.5	2.2	33	116	36	4.63	7.64	Cosiguina (Nicaragua) 1/1835	5
82	1832.0	1.5	53	104	--	4.66	10.85	Babuyan (Philippines) 1831	4?
83	1823.3	1.7	20	133	49	1.24	11.23	Galunggung (Indonesia) 10/1822	5
84	1820.0	0.7	29	98	41	1.89	5.76	???	
85	1815.2	2.5	65	168	--	7.08	14.87	Tambora (Indonesia) 4/1815	7
86	1811.5	1.2	10	114	--	0.60	3.67	Atka (Aleutian Is.) 1812	3?
								Augustine (Alaska) 1812	3?
87	1808.5	2.2	36	86	--	3.69	6.89	Unknown Source 1809	?
88	1804.3	0.7	26	102	--	1.75	6.04	Maly-Semiachik (Kamchatka) 1804	3
89	1801.5	0.8	85	42	--	2.97	2.32	St. Helens (Washington) 1/1800	5
90	1798.2	0.8	41	96	--	2.56	6.01	???	
91	1796.5	1.5	58	163	24	2.85	6.29	Westdahl (Alaska) 1795	4
								Bogoslof (Aleutian Is.) 5/1796	3?
92	1791.0	0.8	--	95	--	--	3.58	Kilauea (Hawaii) 11/1790	4
93	1783.9	0.9	223	520	49	4.58	12.13	Laki (Iceland) 6/1783	4+
94	1783.2	0.7	38	95	--	1.38	3.86	Asama (Japan) 8/1783	4
95	1771.3	0.5	32	94	25	1.27	3.47	???	
96	1766.4	1.5	18	89	--	1.29	4.80	Hekla (Iceland) 4/1766	4
97	1748.2	1.3	19	76	20	1.10	6.50	Ksudach (Kamchatka) 1750?	4
98	1736.4	2.2	26	49	20	4.01	7.08	Avachinsky (Kamchatka) 8/1737	3
								Fuego (Guatemala) 8/1737	4?
99	1727.3	2.2	33	87	--	3.81	11.05	Oraefajokull (Iceland) 8/1727	4
100	1685.8	1.8	37	97	--	5.40	9.72	Chikurachki (Kurile Is.) 1690+/-10 yrs	4
101	1679.1	1.9	31	98	38	4.83	14.72	Tongkoko (Indonesia) 1680	5?
102	1657.6	2.6	36	119	30	4.70	15.57	Long Island (New Guinea) 1660 +/- 20 years	6
103	1647.6	1.4	49	116	--	3.84	10.44	Makian (Indonesia) 7/1646	4?
104	1640.7	2.1	39	74	--	3.48	6.37	Komaga-Take (Japan) 7/1640	5
								Parker (Philippines) 1/1641	5?
105	1629.4	3.4	31	74	--	10.69	18.53	Furnas (Azores) 9/1630	5
								Vesuvius (Italy) 12/1631	5?

Table VI.5. (Continued)

Eclipse Core 2 Volcanic Events (Continued)									
#	Start Date	Length (years)	Peak Conc. (ng g <sup>-1</sup> )			SO <sub>4</sub> <sup>2-</sup> Flux		Possible Source(s) with Date	VEI
			SO <sub>4</sub> <sup>2-</sup>		Cl <sup>-</sup>	EOF	nss		
			5	res	nss	5	res		
						(ug cm <sup>-2</sup> )			
106	1588.2	1.4	31	68	--	6.08	12.78	Kelut (Indonesia) 1586 Billy Mitchell (Bougainville Is.) 1580 +/- 20yrs	5? 6
107	1555.5	1.1	36	88	--	3.51	8.93	Aniakchak (Alaska) 1560?	4+
108	1516.2	0.5	191	527	--	5.87	15.00	Unknown (Wrangell Volcanic Field?)	
109	1506.9	0.7	24	70	24	4.44	11.55	Augustine (Alaska) 1540 +/- 100 yrs	4?
110	1462.7	2.5	66	234	--	12.01	30.74	Pinatubo (Philippines) 1450 +/- 50 years	5?
111	1459.5	2.0	39	85	74	3.46	15.53	Unknown (Kamchatka?)	6
112	1453.0	2.0	54	135	--	3.61	9.99	Kuwae (Vanuatu) 1452 +/- 10 years	6
113	1443 <sup>1</sup>	0.6	43	119	--	2.09	5.37	Oshima (Japan) 8/1442	4
114	1422	3.1	27	30	--	4.84	5.19	Katla (Iceland) 1416	4?
115	1408	1.4	--	85	--	0.00	11.65	???	
116	1400	0.8	29	105	--	2.36	10.41	Soufrière Guadeloupe 1400?	P

<sup>1</sup>Core chronology is not annually resolved prior to 1450. Consequently, dating uncertainty increases.



**Table VI.6.** Volcanic signals in the Eclipse Core 3 ice core, with start of signal, length of signal, peak concentrations, and total volcanic SO<sub>4</sub><sup>2-</sup> flux for each event. Events recorded in more than one core from Eclipse Icefield are assigned the same event number in each core; hence event numbering is not continuous in any one core. Volcanic eruptions are from the chronology of Simkin and Siebert (1994) and online update.

Eclipse Core 3 Volcanic Events (2002-1910)									
#	Start Date	Length (years)	Peak Conc. (ng g <sup>-1</sup> )			SO <sub>4</sub> <sup>2-</sup> Flux		Possible Source(s) with Date	VEI
			SO <sub>4</sub> <sup>2-</sup>		Cl	EOF	nss		
			5	res	nss	5	res		
						(ug cm <sup>-2</sup> )			
1	1998.2	0.4	5	208	--	0.04	3.05	Sheveluch (Kamchatka) 5/1998	3
								Atka (Aleutian Is) 6/1998	3
2	1997.3	0.6	7	189	--	0.18	1.74	Bezymianny (Kamchatka) 5/1997	3
4	1995.4	0.4	12	128	--	0.08	1.61	Bezymianny (Kamchatka) 9/1995	3
5	1994.4	0.4	57	168	21	0.65	2.31	Cleveland (Aleutians) 5/1994	3
8	1991.5	0.6	47	103	--	0.71	1.33	Pinatubo (Philippines) 6/1991	5+
								Westdahl (Alaska) 11/1991	3
9	1989.9	1.0	60	187	308	1.32	5.22	Redoubt (Alaska) 12/1989	3
								Kliuchevskoi (Kamchatka) 1/1990	4
10	1988.3	0.7	--	109	--	--	2.47	???	
13	1985.4	0.2	--	176	29	--	2.56	Bezymianny (Kamchatka) 6/1985	3
								Kliuchevskoi (Kamchatka) 8/1985	3
15	1982.1	1.3	31	129	--	0.56	4.13	Gareloi (Aleutian Is.) 1/1982	3
								El Chichon (Mexico) 4/1982	5
								Galunggung (Indonesia) 5/1982	4
16	1981.1	0.5	1	180	--	0.01	2.65	Pavlof (Alaska) 11/1980	3
								Okmok (Aleutian Is.) 3/1981	3?
								Alaid (Kurile Is.) 4/1981	4
17	1979.1	1.1	23	131	--	0.44	1.60	Bezymianny (Kamchatka) 2/1979	3
								Westdahl (Alaska) 2/1979	3
18	1978.2	0.6	20	351	22	0.74	4.51	Westdahl (Alaska) 2/1978	3
19	1977.4	0.5	41	48	--	0.60	0.55	Bezymianny (Kamchatka) 3/1977	3
								Ukinkrek Maars (Alaska) 3/1977	3
								Kliuchevskoi (Kamchatka) 8/1977	3
21	1973.3	0.4	145	396	51	3.96	15.14	Tiatia (Kurile Is.) 7/1973	4
22	1972.2	0.6	29	163	--	0.86	3.06	Alaid (Kurile Is.) 6/1972	3
29	1964.5	0.5	191	682	48	2.59	17.93	Sheveluch (Kamchatka) 11/1964	4+
30	1963.0	1.3	57	141	--	2.47	5.39	Amukta (Aleutian Is.) 2/1963	3
								Agung (Indonesia) 3/1963	5
								Trident (Alaska) 4/1963	3
31	1960.4	1.5	20	163	--	1.11	7.10	Karymsky (Kamchatka) 4/1960	3
								Sarychev (Kurile Is.) 8/1960	3
								Okmok (Aleutian Is.) 10/1960	3
								Kliuchevskoi (Kamchatka) 12/1960	3
32	1959.3	0.5	32	81	--	1.39	3.03	???	
33	1958.5	0.5	68	143	--	1.38	2.57	Okmok (Aleutian Is.) 8/1958	3
34	1957.4	0.5	43	88	--	1.21	2.47	Zavaritzki (Kurile Is.) 11/1957	3
35	1956.3	0.5	60	69	--	1.61	1.81	Bezymianny (Kamchatka) 3/1956	5

Table VI.6. (Continued)

Eclipse Core 3 Volcanic Events (Continued)									
#	Start Date	Length (years)	Peak Conc. (ng g <sup>-1</sup> )			SO <sub>4</sub> <sup>2-</sup> Flux		Possible Source(s) with Date	VEI
			SO <sub>4</sub> <sup>2-</sup>		Cl <sup>-</sup>	EOF	nss		
			5	nss res	nss res	5	nss res		
					(ug cm <sup>-2</sup> )				
37	1953.4	0.8	51	93	--	1.58	2.79	Trident (Alaska) 2/1953	3
								Spurr (Alaska) 7/1953	4
40	1946.6	1.4	39	88	--	1.59	3.74	Sarychev (Kurile Is.) 11/1946	4
								Hekla (Iceland) 3/1947	4
43	1942.2	0.8	35	126	--	0.93	3.76	???	
44	1941.1	0.3	32	70	--	0.41	0.77	Tolbachik (Kamchatka) 11/1940	3
46	1937.1	0.6	32	186	--	0.53	4.79	Kliuchevskoi (Kamchatka) 4/1937	3
47	1935.0	0.5	32	89	--	1.09	5.11	Augustine (Alaska) 3/1935	3
								Kliuchevskoi (Kamchatka) 4/1935	3
51	1929.9	1.0	42	105	36	1.32	2.40	Komaga-Take (Japan) 6/1929	4
								Gorely (Kamchatka) 9/1929	3
								Sarychev (Kurile Is.) 2/1930	3
53	1923.4	0.5	53	285	--	2.46	9.21	Zheltovsky (Kamchatka) 2/1923	3
								Raikoke (Kurile Is.) 2/1924	4
54	1922.3	1.2	44	156	40	1.70	4.10	Gareloi (Aleutian Is.) 1922	3
55	1920.9	0.5	28	76	--	0.63	2.00	???	
56	1919.2	0.4	29	50	--	0.83	1.39	Kelut (Indonesia) 5/1919	4
57	1918.3	0.7	35	43	--	1.58	1.52	Katla (Iceland) 10/1918	4
58	1917.2	1.0	57	88	--	2.40	3.25	Agrigan (Mariana Is.) 4/1917	4
								Mutnovsky (Kamchatka) 7/1917	3
59	1915.6	1.3	29	63	--	1.85	1.26	???	
60	1912.3	2.2	141	288	158	13.18	21.15	Katmai (Alaska) 6/1912	6

**Table VI.7.** Volcanic signals in the Mount Logan Northwest Col ice core, with start of signal, length of signal, peak concentrations, and total volcanic SO<sub>4</sub><sup>2-</sup> flux for each event. Volcanic eruptions are from the chronology of Simkin and Siebert (1994) and online update.

Mount Logan Northwest Col Volcanic Events (1690-1980)									
#	Start Date	Length (years)	Peak Conc. (ng g <sup>-1</sup> )			SO <sub>4</sub> <sup>2-</sup> Flux		Possible Source(s) with Date	VEI
			SO <sub>4</sub> <sup>2-</sup> EOF 3	nss res	Cl <sup>-</sup> nss res	EOF 3	nss res		
						(ug cm <sup>-2</sup> )			
1	1976.3	0.5	160	162	52	1.83	1.90	Augustine (Alaska) 1/1976	4
2	1966.8	1.6	15	127	--	0.22	2.05	Redoubt (Alaska) 10/1966 & 12/1967 Trident (Alaska) 9/1967	3 3
3	1964.9	0.7	43	107	--	0.41	0.63	Sheveluch (Kamchatka) 11/1964 Bezymianny (Kamchatka) 3/1965 Karymsky (Kamchatka) 4/65	4+ 3 3
4	1934.7	0.5	151	327	124	1.16	2.21	Augustine (Alaska) 3/1935 Kliuchevskoi (Kamchatka) 4/1935	3 3
5	1926.4	1.0	128	152	--	1.44	2.71	Avachinsky (Kamchatka) 4/1926	4
6	1924.2	0.6	88	105	--	0.36	0.58	Raikoke (Kurile Is.) 2/1924	4
7	1912.1	1.9	518	608	113	10.14	10.59	Katmai (Alaska) 6/1912	6
8	1910.1	0.8	90	98	--	0.77	0.93	???	
9	1908.1	0.9	87	125	86	1.25	1.71	Ksudach (Kamchatka) 3/1907	5
10	1884.0	1.7	66	151	--	0.30	0.57	Krakatau (Indonesia) 8/1883 Augustine (Alaska) 10/1883	6 4
11	1875.1	0.6	110	130	--	0.97	1.13	Askja (Iceland) 3/1875	5
12	1872.9	0.4	86	103	--	0.49	0.50	Grimsvotn (Iceland) 1/1873	4
13	1872.2	0.5	270	300	66	1.84	2.07	Sinarka (Kurile Is.) 1872	4
14	1866.4	0.5	237	264	110	0.29	0.38	???	
15	1862.3	0.9	102	257	55	0.88	1.52	Makian (Indonesia) 12/1861	4?
16	1860.0	0.9	463	565	--	6.80	8.23	Ebeko (Kurile Is.) 9/1859 Katla (Iceland) 5/1860 Alaid (Kurile Is.) 7/1860	3 3 3
17	1853.8	1.0	254	286	50	3.20	3.58	Chikurachki (Kurile Is.) 12/1853 Sheveluch (Kamchatka) 2/1854	5? 5
18	1840.9	0.8	63	171	--	0.38	1.33	???	
19	1836.2	1.1	332	416	36	3.57	4.52	Cosiguina (Nicaragua) 1/1835	5
20	1824.3	0.5	36	126	--	0.13	0.46	Shishaldin (Alaska) 1824 Yunaska (Aleutian Is.) 1824	3 3
21	1816.2	0.7	227	317	--	3.08	4.25	Tambora (Indonesia) 4/1815	7
22	1792.2	2.1	105	142	67	1.72	1.61	Alaid (Kurile Is.) 2/1793	4
23	1783.9	1.5	346	408	153	4.43	4.66	Laki (Iceland) 6/1783	4+
24	1783.2	0.5	125	131	46	1.07	0.91	Asama (Japan) 8/1783	4
25	1755.7	0.8	--	129	--	--	1.91	Katla (Iceland) 10/1755	4+
26	1746.8	2.3	249	262	77	6.02	5.86	Ksudach (Kamchatka) 1750?	4
27	1740.5	1.0	281	354	--	3.92	5.00	Oshima (Japan) 8/1741	4
28	1721.2	1.8	181	193	49	5.60	5.00	Katla (Iceland) 5/1721	4+
29	1712.8	1.7	158	166	--	3.95	0.42	Chirpoi (Kurile Is.) 12/1712±1 yr	4
30	1694.3	1.3	79	126	--	2.40	3.92	Komaga-Take (Japan) 7/1694 Chikurachki (Kurile Is.) 1690±10 yr	4? 4

**Table VI.8.** Correlation coefficients between annual volcanic SO<sub>4</sub><sup>2-</sup> flux records. Correlations in bold are significant at the 99.9% confidence level. Correlations in italics are significant at the 95% confidence level.

	All Years			Excluding Katmai Years		
	Core 1	Core 2	Core 3	Core 1	Core 2	Core 3
Core 2	<b>0.77</b>			Core 2	<b>0.48</b>	
Core 3	<b>0.81</b>	<b>0.77</b>		Core 3	<b>0.42</b>	<b>0.50</b>
Logan	<b>0.81</b>	<b>0.44</b>	<b>0.75</b>	Logan	0.11	<i>0.13</i>

**Table VI.9.** Sources of volcanic signals in St. Elias ice cores used in this study.

	Eclipse Icefield		Mt. Logan NW Col	
	#	%	#	%
Alaska/Kamchatka	43	35%	9	29%
Iceland	7	6%	5	16%
Mid Northern Lat.	11	9%	7	23%
Mixed NH	6	5%	2	6%
Tropical	22	18%	3	10%
Mixed Tropical/NH	7	6%	1	3%
Unknown	20	16%	4	13%
Total	116		27	
Period of Record	1400-2002		1690-1980	

**Table VI.10.** Twentieth century tephra-bearing layers in the Eclipse ice cores and their possible sources. The major oxide composition of tephra (as weight %, recalculated to a sum of 100%) found in the ice cores is presented as the mean for the specified number of samples, with the standard deviation in parentheses, where n is the number of particles analyzed per sample. Tephra found in the Eclipse ice core is compared to previously published analyses from suspected source volcanoes where available. n.d. denotes element below detection limits. Total iron as FeO.

Sample	SiO <sub>2</sub>	TiO <sub>2</sub>	Al <sub>2</sub> O <sub>3</sub>	FeO	MgO	CaO	Na <sub>2</sub> O	K <sub>2</sub> O	n	Source
Core 3 S 1994	59.3	1.8	15.0	8.6	1.7	4.5	7.9	1.1	1	Cleveland 1994
Core 3 F 1991	50.9	1.4	13.4	12.8	3.2	5.6	11.1	1.6	1	Akutan 1991
Core 3 F 1991	58.3 (1.1)	1.4 (0.7)	17.4 (3.9)	6.2 (2.7)	2.5 (1.4)	6.3 (1.6)	6.9 (2.3)	1.1 (0.5)	9	Westdahl 1991
Westdahl (1978)	59.8	1.6	15.5	9.2	2.3	5.5	4.4	1.9	9	J. Fournelle, unpublished
Core 3 F 1991	75.7	0.6	11.5	2.6	0.9	3.5	4.6	0.5	1	
White River	74.1	0.2	14.6	1.5	0.4	1.9	4.2	3.1	15	Beget <i>et al.</i> , 1992
Pinatubo 1991	78.4	0.1	12.8	0.7	0.1	1.2	3.6	3.1	16	Luhr and Melson, 1996
Core 1 W 1989-90	74.5 (2.0)	0.4 (0.2)	13.0 (0.6)	1.9 (0.8)	0.4 (0.6)	1.3 (0.6)	5.3 (0.7)	3.2 (0.4)	12	Redoubt 1989
Core 3 W 1989-90	70.9 (1.8)	0.3 (0.1)	15.4 (1.4)	1.5 (0.8)	n.d.	1.6 (0.6)	6.9 (1.1)	3.4 (0.5)	11	Redoubt 1989
Redoubt 1989	75.0 (0.6)	0.4 (0.0)	13.3 (0.3)	1.9 (0.3)	0.4 (0.2)	1.7 (0.2)	4.0 (0.2)	3.3 (0.1)	231	Swanson <i>et al.</i> , 1994
Core 1 S 1953	52.5	3.1	14.1	12.7	4.2	6.8	5.6	1.0	1	Shishaldin 1953
Shishaldin (1999)	51.1 (2.0)	4.0 (0.6)	11.1 (2.8)	16.6 (3.2)	4.9 (1.1)	8.5 (0.5)	2.6 (0.6)	1.3 (0.3)	3	Stelling <i>et al.</i> , 2002
Core 1 S 1953	73.5 (1.3)	0.5 (0.3)	12.7 (0.6)	2.8 (0.9)	0.1 (0.2)	0.9 (0.4)	6.3 (0.3)	3.2 (0.6)		Trident 1953
Trident 1953	76.5 (0.6)	0.4 (0.1)	11.8 (0.4)	2.1 (0.3)	0.3 (0.2)	1.2 (0.3)	4.2 (0.2)	3.5 (0.5)	14	Coombs <i>et al.</i> , 2000

Table VI.10. (Continued)

Sample	SiO <sub>2</sub>	TiO <sub>2</sub>	Al <sub>2</sub> O <sub>3</sub>	FeO	MgO	CaO	Na <sub>2</sub> O	K <sub>2</sub> O	N	Source
Core 1 Sp 1947	63.6 (1.7)	0.8 (0.2)	16.8 (1.4)	5.2 (1.8)	1.0 (0.7)	4.2 (0.6)	6.7 (0.6)	1.7 (0.2)	7	Hekla 1947
Hekla 1947	63.2 (1.1)	1.0 (0.1)	15.5 (0.2)	8.2 (0.5)	1.4 (0.2)	4.6 (0.3)	4.3 (0.5)	1.7 (0.1)	10	Larsen <i>et al.</i> , 1999
Core 1 Sp 1947	69.9 70.4	1.1 0.5	12.2 14.7	8.1 4.2	1.2 0.2	2.4 1.6	4.0 4.3	1.0 4.0	1 1	Hekla 1947 (initial)
Hekla 1947 (initial)	71.1 70.8	0.4 0.4	13.7 13.7	4.8 4.7	0.2 0.1	1.2 1.1	5.3 5.6	3.4 3.5	1 1	Larsen <i>et al.</i> , 1999
Core 1 F 1945	53.2 (0.7)	2.9 (0.3)	13.8 (1.1)	12.1 (0.6)	3.3 (1.1)	7.7 (0.8)	6.0 (2.0)	0.9 (0.3)	5	
Avachinsky (1991)	56.5	0.9	18.2	7.5	4.2	8.7	3.3	0.7	1	Turner <i>et al.</i> , 1998
Kliuchevskoi (1972)	53.4	1.2	17.2	9.0	5.3	8.9	3.7	1.3	1	Ivanov <i>et al.</i> , 1981
Core 1 S 1912	76.0 (1.1)	0.2 (0.2)	12.5 (0.6)	1.5 (0.4)	n.d.	0.9 (0.4)	5.6 (0.9)	3.3 (0.4)	10	Katmai 1912
Core 3 S 1912	71.1 (2.0)	0.4 (0.2)	15.0 (0.7)	1.7 (0.6)	0.3 (0.1)	1.4 (0.7)	7.1 (1.1)	3.2 (0.4)	12	Katmai 1912
Katmai 1912	77.0 (2.3)	0.5 (0.1)	12.7 (1.3)	1.7 (0.2)	0.3 (0.1)	1.6 (0.2)	2.8 (1.2)	3.4 (1.2)		M. Germani, unpublished
Katmai 1912	77.0 (0.6)	0.3 (0.0)	12.8 (0.7)	1.6 (0.1)	0.2 (0.0)	1.3 (0.1)	3.9 (0.2)	2.9 (0.1)	20	Fierstein and Hildreth, 1992
Core 1 S 1908	46.6	4.2	15.3	10.1	4.9	11.1	5.9	1.9	1	???
Core 1 Sp 1997	56.0 (1.9)	1.8 (0.5)	14.1 (2.2)	10.4 (2.4)	3.0 (0.8)	8.0 (2.7)	5.2 (0.9)	1.4 (0.4)	8	Ksudach 1907
Ksudach 1907	55.8 57.2	1.0 1.0	17.2 15.9	10.2 9.7	4.2 4.0	7.6 8.0	3.3 3.4	0.7 0.8	1 1	Melekestsev <i>et al.</i> , 1996

**Table VI.11.** Tephrochronology of the Eclipse 2002 Core 2 ice core (2002 to ~1000 A.D.). The major oxide composition of tephra (as weight %, recalculated to a sum of 100%) found in the Eclipse ice core is presented as the mean for the specified number of samples, with the standard deviation in parentheses, where n is the number of particles analyzed per sample. Tephra found in the Eclipse ice core is compared to previously published analyses from suspected source volcanoes where available. Total iron as FeO.

Sample	SiO <sub>2</sub>	TiO <sub>2</sub>	Al <sub>2</sub> O <sub>3</sub>	FeO	MgO	CaO	Na <sub>2</sub> O	K <sub>2</sub> O	n	Source
Core 2 W 1809-10	64.9 (1.1)	1.1 (0.2)	16.1 (0.7)	3.8 (0.7)	1.1 (0.5)	3.6 (0.7)	6.6 (0.8)	2.7 (0.3)	10	Unknown
Core 2 Sp 1804	65.3 (1.4)	1.0 (0.1)	16.5 (1.5)	3.4 (0.6)	0.8 (0.5)	3.5 (1.0)	6.7 (0.7)	2.8 (0.4)	10	Maly-Semiachik 1804 (?)
Core 2 1630	63.8 (1.3)	1.1 (0.2)	16.5 (0.9)	4.1 (1.3)	1.3 (0.3)	4.2 (0.8)	6.7 (0.9)	2.2 (0.4)	10	Furnas 1630 (?)
Furnas 1630	63.9 64.1	0.7 0.3	15.8 17.4	5.4 4.5	0.2 0.2	1.7 1.4	5.9 6.1	6.5 6.0	1 1	Cole <i>et al.</i> , 1995
Core 2 Sp 1516	61.5 (1.8)	1.1 (0.3)	16.0 (0.7)	5.9 (1.4)	1.8 (0.5)	5.1 (0.9)	6.8 (1.1)	1.8 (0.2)	10	unknown WVF
WVF <sup>1</sup> (average)	62.0	0.9	16.8	5.5	3.3	5.6	4.0	1.8	201	Richter <i>et al.</i> , 1990
Core 2 1460	56.4 (0.9)	1.3 (0.2)	17.0 (2.5)	7.7 (1.1)	3.7 (1.1)	7.5 (0.9)	5.6 (0.5)	0.9 (0.1)	9	Kamchatkan?
Core 2 1460	64.4	1.0	17.7	2.9	0.9	3.2	7.4	2.5	1	Alaskan?
Core 2 1456	65.0 (1.3)	1.1 (0.4)	16.5 (1.9)	3.5 (1.2)	0.9 (0.6)	3.4 (0.7)	7.0 (1.2)	2.6 (0.5)	12	Alaskan?
Kuwa <sup>2</sup>	66.8 (2.1)	0.7 (0.2)	14.8 (0.1)	5.7 (1.5)	1.2 (0.2)	3.6 (0.4)	4.9 (1.1)	2.2 (1.1)	39	Robin <i>et al.</i> , 1994
Core 2 1375	63.0 (1.5)	0.9 (0.5)	17.5 (3.1)	4.8 (1.7)	1.1 (0.4)	4.1 (1.0)	6.9 (0.7)	1.7 (1.0)	7	Hekla?
Hekla (1510)	63.5 (0.3)	1.0 (0.1)	15.4 (0.2)	7.9 (0.2)	1.3 (0.1)	4.6 (0.2)	4.5 (0.2)	1.8 (0.0)	10	Larsen <i>et al.</i> , 1999
Core 2 1375	70.1	0.4	16.8	1.4	0.2	1.9	5.5	3.6	1	Hekla?

<sup>1</sup>Wrangell Volcanic Field, southeast Alaska. Includes Mount Wrangell and Bona-Churchill, both active in the late Holocene.

<sup>2</sup>Glasses from the caldera-forming phase of the eruption.

**Table VII.12.** Monthly temperature records from meteorological stations surrounding the St. Elias Mountains whose data was used in our analysis. “Begin” is the first year of record, “End” the last year of record, and “% Missing” the percentage of data missing (data available online at <http://www.ncdc.noaa.gov/ghcn/ghcn.SELECT.html>).

<b>Station</b>	<b>Lat. (N)</b>	<b>Long. (W)</b>	<b>Begin</b>	<b>End</b>	<b>% missing</b>
Kenai, AK	60.52	151.25	1899	1996	37.8
Seward, AK	60.12	149.45	1908	1990	7.1
Cordova, AK	60.50	145.50	1909	1996	7.3
Sitka, AK	57.07	135.35	1899	1989	2.4
Ketchikan, AK	55.37	131.72	1910	1990	5.3
Tanana, AK	65.20	152.10	1905	1990	8.3
Fairbanks Univ. AK	64.85	147.87	1904	1990	2.1
Gulkana, AK	62.15	145.45	1910	1996	34.5
Eagle, AK	64.79	141.20	1899	1990	28.4
Dawson, YT	64.05	139.13	1897	1979	5.8
Ft. McPherson, NWT	67.40	134.90	1892	1977	30.6
Atlin, BC	59.57	133.70	1899	1947	29.7



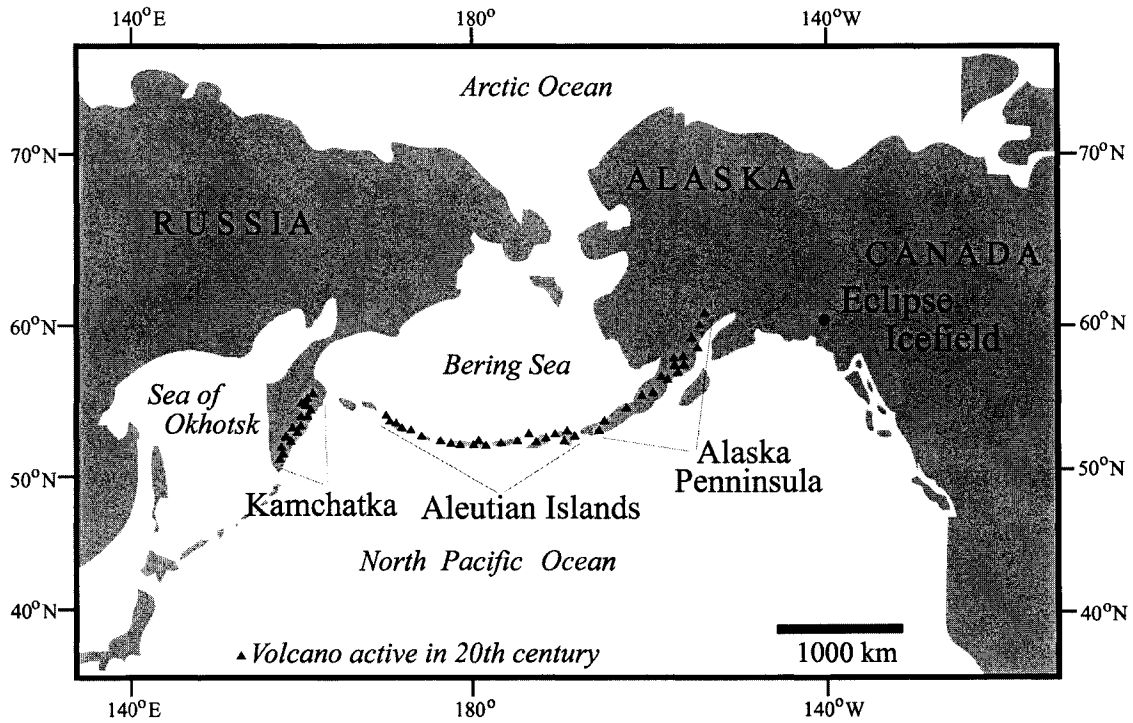


**Figure VI.1.** Eclipse Icefield is located at  $60.51^{\circ}$  N,  $139.47^{\circ}$  W, 3017 m elevation in the St. Elias Mountains, Yukon, Canada. The Eclipse site is directly downwind of vigorous volcanic arcs in the Alaska Peninsula, Aleutian Islands, and Kamchatka, making the Eclipse site suitably located to record volcanic eruptions in these regions.

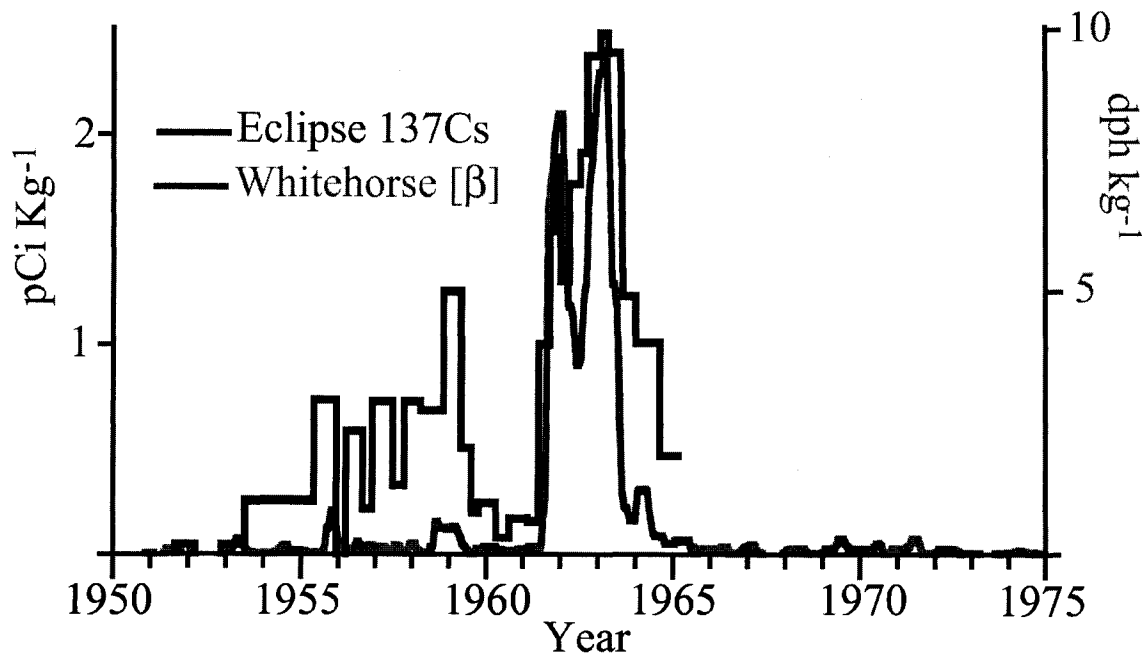


**Figure VI.2.** Comparison of Eclipse ice core <sup>137</sup>Cs profiles with real-time aerosol samples from Whitehorse, Yukon, shows clear identification of the 1963 and 1961 radionuclide peaks from atmospheric nuclear weapons testing.

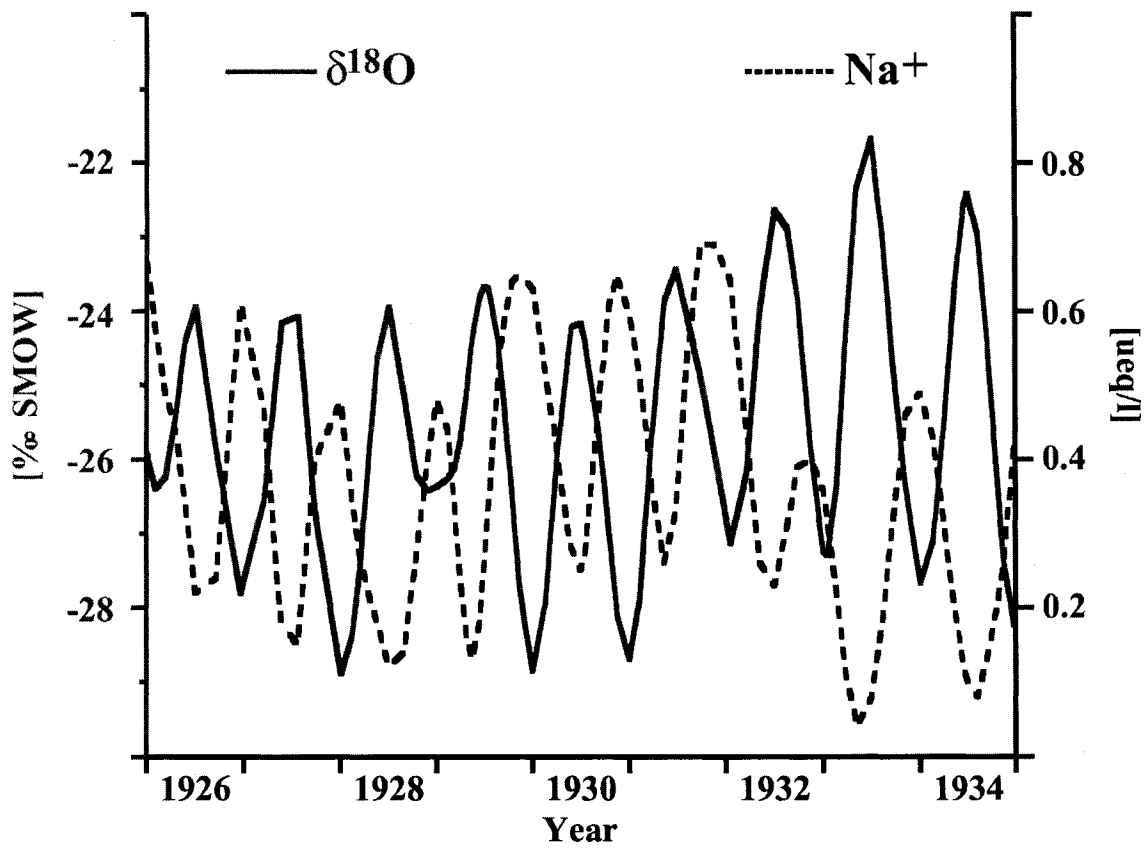


**Figure VI.3.** Seasonal signals in the Eclipse 2002 Core 3  $\delta^{18}\text{O}$  and  $\text{Na}^+$  records used to date the core via annual layer counting. The records shown are smoothed with a robust spline to highlight their seasonal variability.

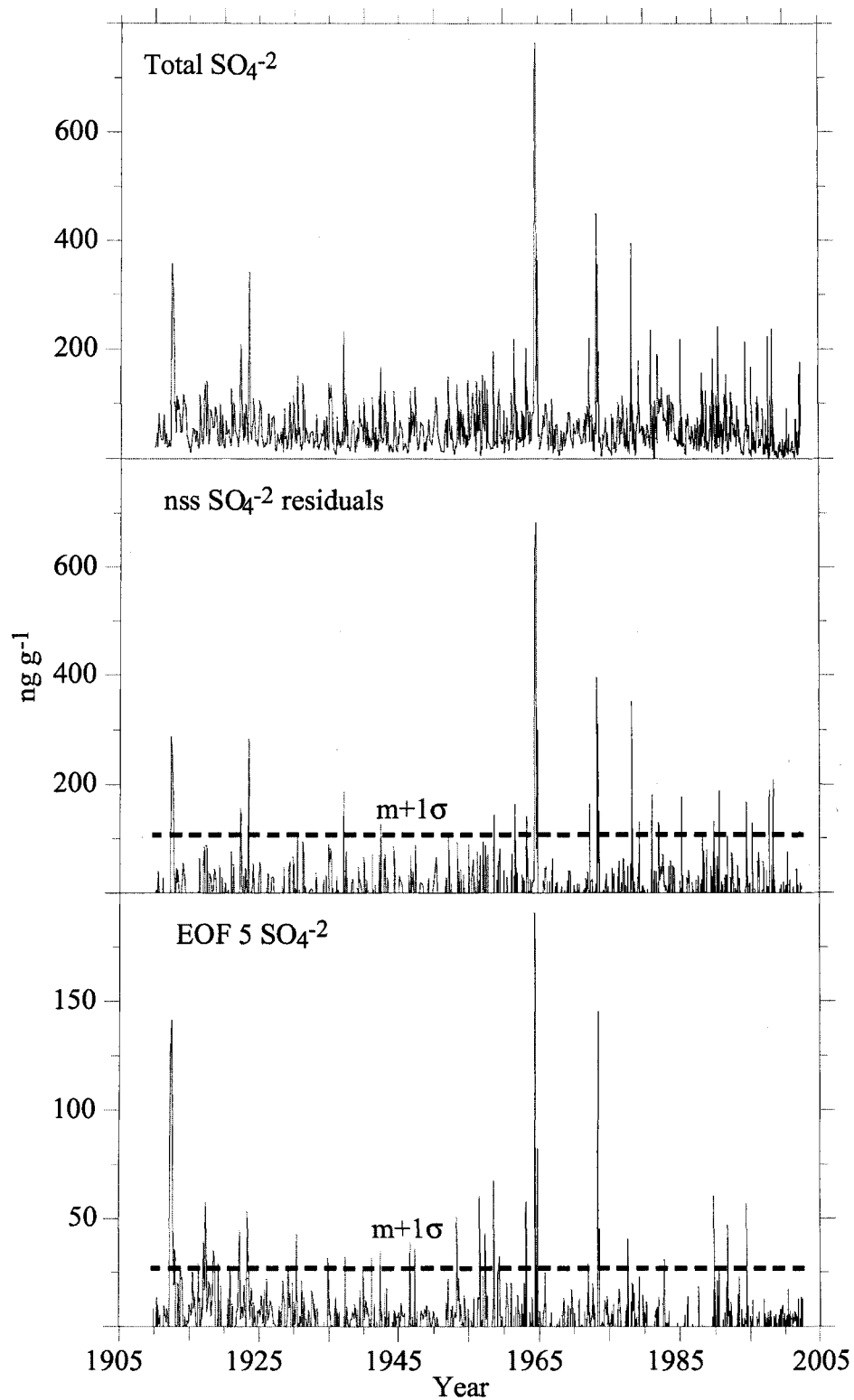


**Figure VI.4.** Identification of volcanic  $\text{SO}_4^{2-}$  signals in the Eclipse Core 3 ice core: top, raw  $\text{SO}_4^{2-}$  time series; middle, nss  $\text{SO}_4^{2-}$  residuals; bottom, EOF 5  $\text{SO}_4^{2-}$  values ( $\text{ng g}^{-1}$ ). One standard deviation above the mean positive value is indicated.

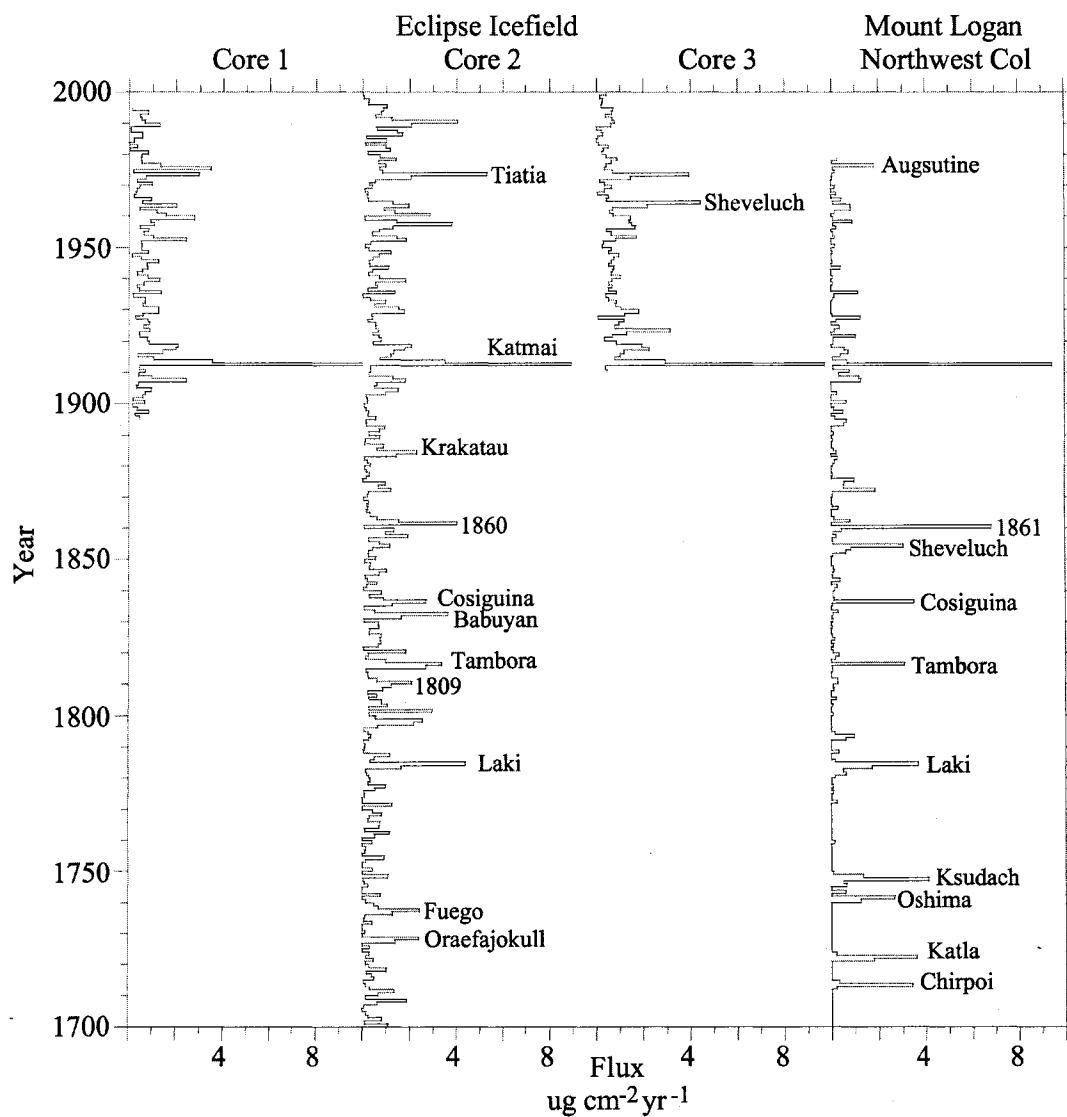


**Figure VI.5.** Comparison of annual volcanic  $\text{SO}_4^{2-}$  flux records from Eclipse Icefield and Mount Logan. Prominent eruptions are indicated.

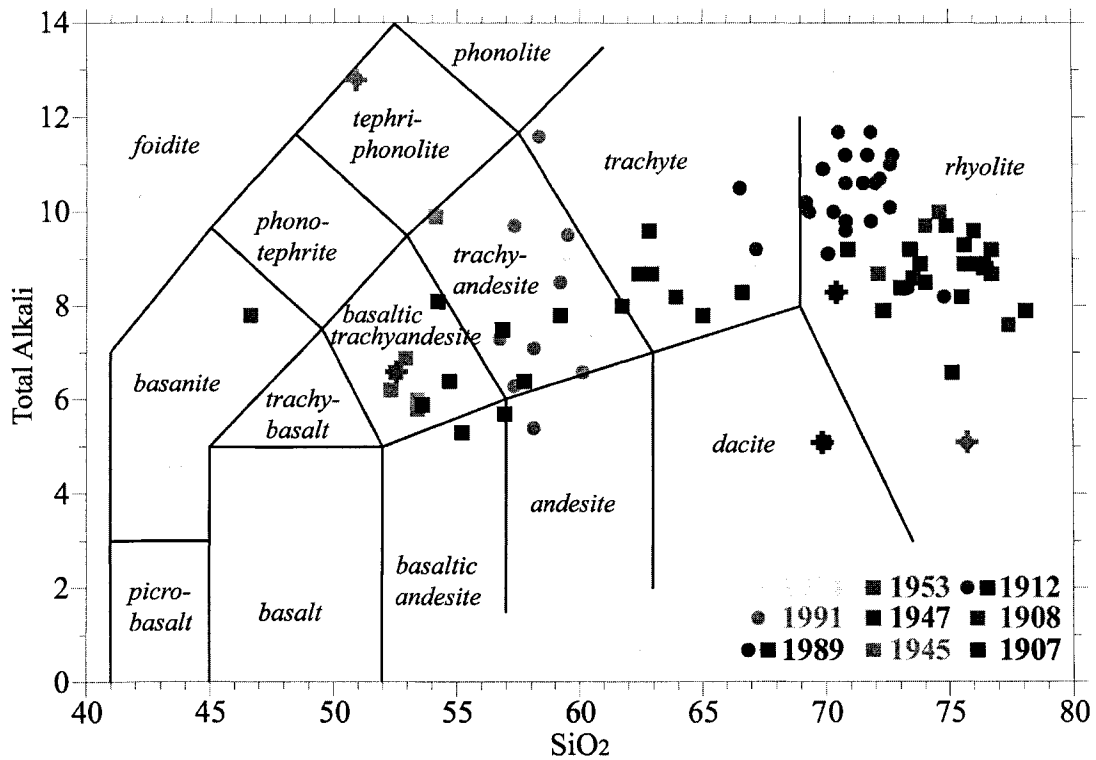


**Figure VI.6.** Total alkali ( $\text{Na}_2\text{O}+\text{K}_2\text{O}$ ) versus silica variation diagram of individual glass shards found in the Eclipse Core 1 and Core 3 ice cores, 1900 to 2000. Chemical classification follows the nomenclature of LeBas *et al.* (1986). Glass shards from Core 1 are represented by squares; shards from Core 3 are represented by circles. Individual shards with a composition distinct from the dominant glass composition in that layer have a cross through them.

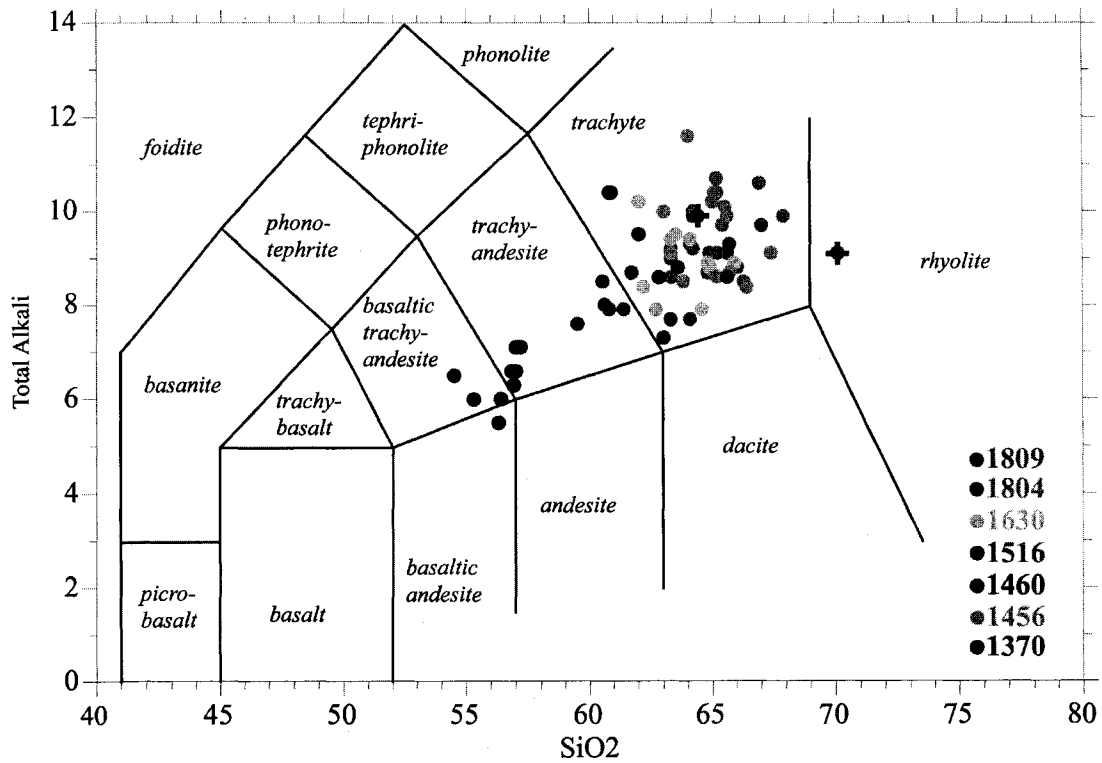


**Figure VI.7.** Total alkali ( $\text{Na}_2\text{O}+\text{K}_2\text{O}$ ) versus silica variation diagram of individual glass shards found in the Eclipse Core 2 ice core, ~1000 to 1900. Chemical classification follows the nomenclature of LeBas *et al.* (1986). Individual shards with a composition distinct from the dominant glass composition in that layer have a cross through them.

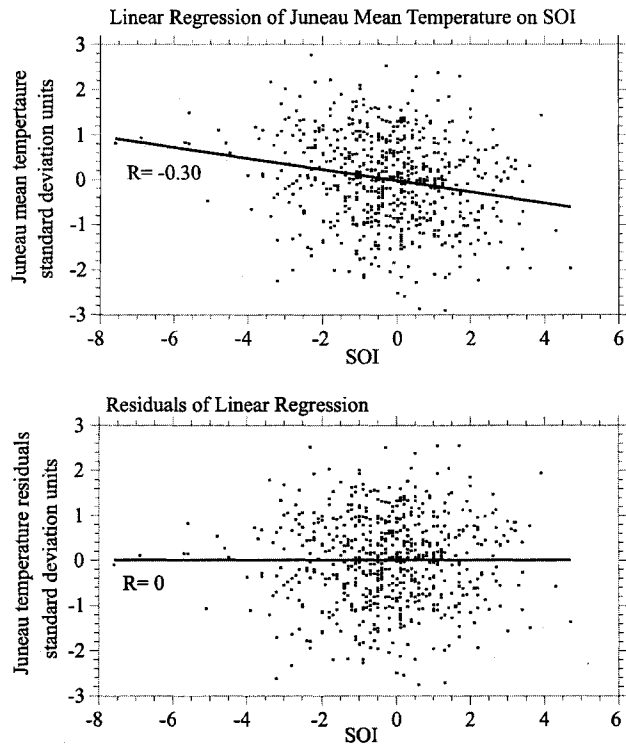


**Figure VII.8.** Example of the removal of the ENSO influence on temperature in the instrumental temperature record from Juneau, Alaska using a regression line. First, a scatterplot of standardized mean monthly temperature versus the standardized Southern Oscillation Index is made. A line is then fitted through the data (top) and the trend of that line subtracted from the original data. The resulting temperature residuals (bottom) have no correlation with the Southern Oscillation Index.



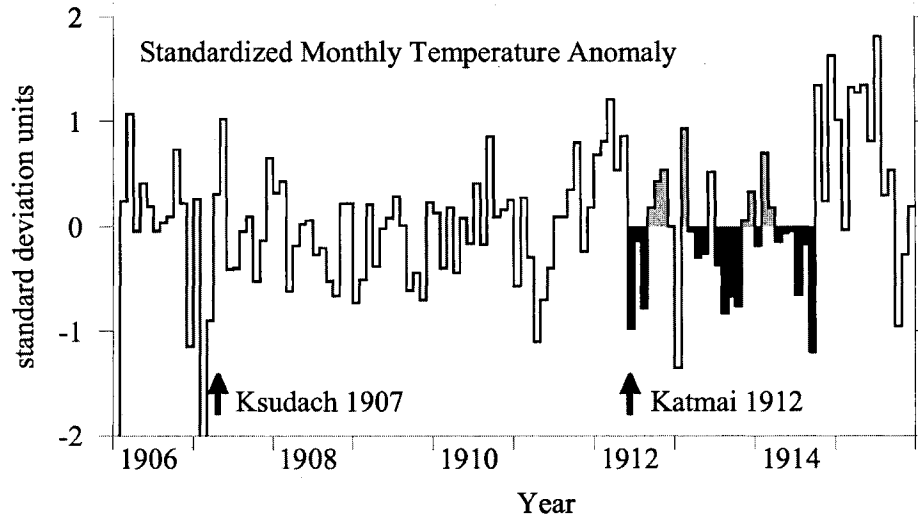


**Figure VI.9.** Standardized monthly temperature anomaly produced by stacking all available instrumental temperature records from the Gulf of Alaska region covering the period 1906-1915. Timing of major ( $VEI \geq 5$ ) eruptions in the North Pacific during this time as indicated.

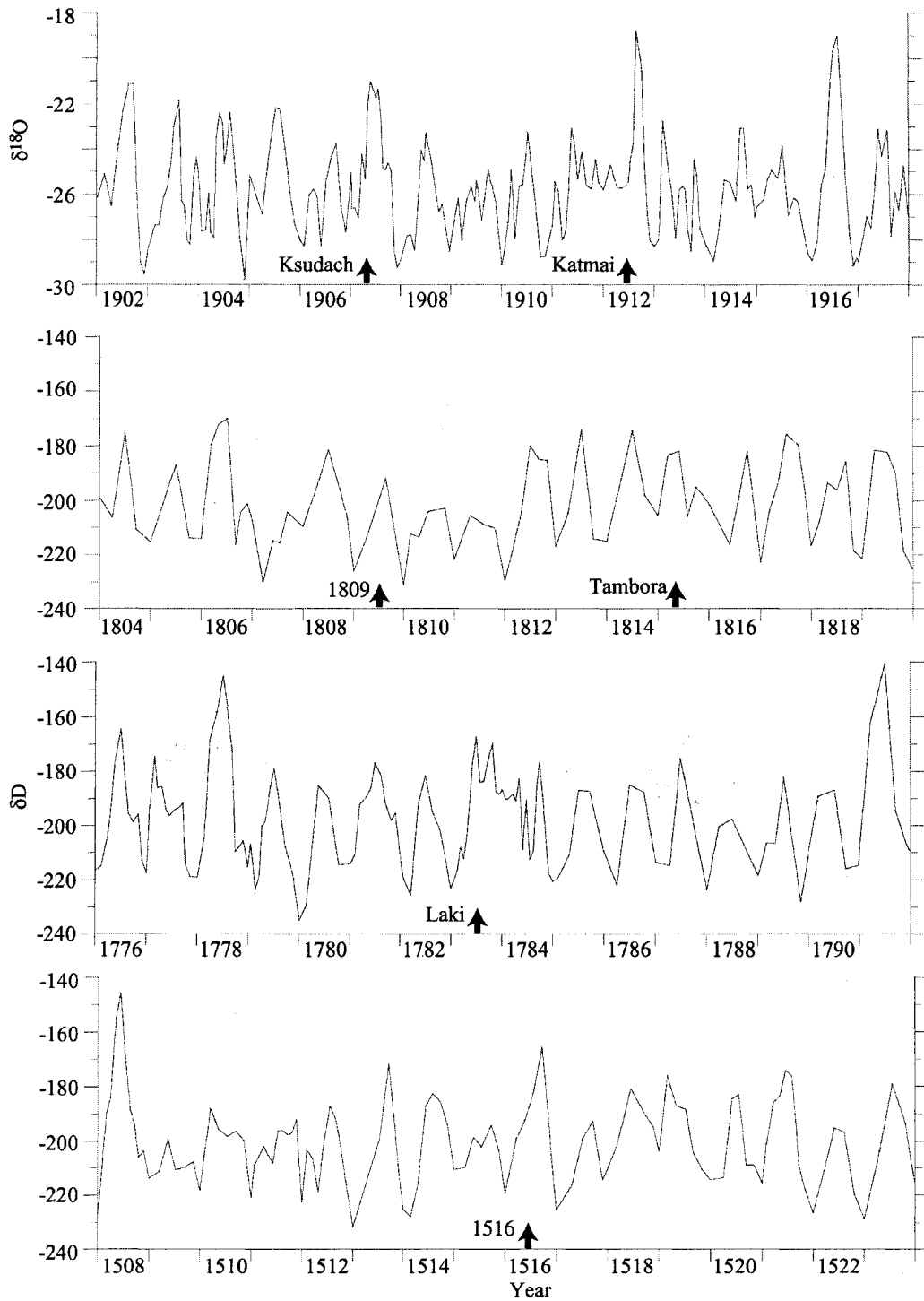


**Figure VI.10.** Stable isotope records from the Eclipse ice cores around prominent volcanic eruptions illustrate the variable climatic response to volcanism. Timing of prominent eruptions as indicated by arrows.

## References

- Adams, J.B., M.E. Mann, and C.M. Ammann, Proxy evidence for an El Nino-like response to volcanic forcing, *Nature*, 426, 274-278, 2003.
- Angell, J.K., and J. Korshover, Surface temperature changes following the six major volcanic episodes between 1780 and 1980, *Journal of Climate and Applied Meteorology*, 24, 937-951, 1985.
- Angell, J.K., Impact of El Nino on the delineation of tropospheric cooling due to volcanic eruptions, *Journal of Geophysical Research*, 93, 3697-3704, 1988.
- Barrie, L.A., D.A. Fisher, and R.M. Koerner, Twentieth century trends in Arctic air pollution revealed by conductivity and acidity observations in snow and ice in the Canadian high Arctic, *Atmospheric Environment*, 19, 2055- 2063, 1985.
- Basile, I., J.R. Petit, S. Touron, F.E. Grousset, and N. Barkov, Volcanic layers in Antarctic (Vostok) ice cores: Source identification and atmospheric implications, *Journal of Geophysical Research*, 106, 31,915-31,931, 2001.
- Beget, J.E., S.D. Stihler, D.B. Stone, A 500 year long record of tephra falls from Redoubt Volcano and other volcanoes in upper Cook Inlet, Alaska, *Journal of Volcanology and Geothermal Research*, 62, 55- 67, 1994.
- Belousov, A., Deposits of the 30 March 1956 directed blast at Bezymianny volcano, Kamchatka, Russia, *Bulletin of Volcanology*, 57, 649-662, 1996.
- Bluth, G.J.S., C.C. Schnetzler, D.A. Krueger, and L.S. Walter, The contribution of explosive volcanism to global sulfur dioxide concentrations, *Nature*, 366, 327- 330, 1993.
- Bradley, R.S., The explosive volcanic eruption record in northern hemisphere and continental temperature records, *Climatic Change*, 12, 221- 243, 1988.
- Braitseva, O.A., I.V. Melekestev, V.V. Ponomareva, V. Kirianov, The caldera-forming eruption of Ksudach volcano about cal. A. D. 240: the greatest explosive event of our era in Kamchatka, Russia, *Journal of Volcanology and Geothermal Research*, 70, 49- 65, 1996.
- Briffa, K.R., P.D. Jones, and F.H. Schweingruber, Tree-ring reconstructions of summer temperature patterns across western North America since 1600, *Journal of Climate*, 5, 735- 754, 1992.
- Briffa, K.R., P.D. Jones, F.H. Schweingruber, and T.J. Osborn, Influence of volcanic eruptions on Northern Hemisphere temperature over the past 600 years, *Nature*, 393, 450-454, 1998.
- Bursik, M., I. Melekestev and O. Braitseva, Most recent fall deposits of Ksudach volcano, Kamchatka, Russia, *Geophysical Research Letters*, 20, 1815- 1818, 1993.
- Castellano, E., S. Becagli, J. Jouzel,, A. Migliori, M. Severi, J.P. Steffensen, R. Traversi, and R. Udisti, Volcanic eruption frequency over the last 45 ky as recorded in the EPICA-Dome C ice core (East Antarctica) and its relationship with climatic changes, *Global and Planetary Change*, 42, 195-205, 2004.

- Chenoweth, M., Two major volcanic cooling episodes derived from global marine air temperature, AD 1807-1827, *Geophysical Research Letters*, 28, 2963-2966, 2001.
- Clarke, G.C., G.M. Cross, and C.S. Benson, Radar imaging of glaciovolcanic stratigraphy at Mount Wrangell Caldera, Alaska: Interpretation model and results, *Journal of Geophysical Research*, 94, 7237-7249, 1989.
- Clausen, H.B., and C.U. Hammer, The Laki and Tambora eruptions as revealed in Greenland ice cores from 11 locations, *Annals of Glaciology*, 10, 16-22, 1988.
- Clausen, H.B., C.U. Hammer, C.S. Hvidberg, D. Dahl-Jensen, J.P. Steffensen, J. Kipfstuhl, and M. Legrand, A comparison of the volcanic records over the past 4000 years from the Greenland Ice Core Project and Dye 3 Greenland ice cores, *Journal of Geophysical Research*, 102, 26, 707-26, 723, 1997.
- Cole, P.D., G. Queiroz, N. Wallenstein, J.L. Gaspar, A.M. Duncan, and J.E. Guest, An historic subplinian/phreatomagmatic eruption: the 1630 AD eruption of Furnas volcano, Sao Miguel, Azores, *Journal of Volcanology and Geothermal Research*, 69, 117-135, 1995.
- Cole-Dai, J., E. Mosley-Thompson, and L. Thompson, Ice core evidence for an explosive tropical eruption 6 years preceding Tambora, *Journal of Geophysical Research*, 96, 17,361-17,366, 1991.
- Cole-Dai, J., E. Mosley-Thompson, and L. Thompson, Annually resolved southern hemisphere volcanic history from two Antarctic ice cores, *Journal of Geophysical Research*, 102, 16,761-16,771, 1997.
- Cole-Dai, J., and E. Mosley-Thompson, The Pinatubo eruption in South Pole snow and its potential value to ice core paleovolcanic records, *Annals of Glaciology*, 29, 99-105, 1999.
- Cole-Dai, J., E. Mosley-Thompson, S. Wight, and L. Thompson, A 4100-year record of explosive volcanism from an East Antarctic ice core, *Journal of Geophysical Research*, 105, 24,341-24,441, 2000.
- Coombs, M.L., J.C. Eichelberger, and M.J. Rutherford, Magma storage and mixing conditions for the 1953-1974 eruptions of Southwest Trident volcano, Katmai National Park, Alaska, *Contributions to Mineralogy and Petrology*, 140, 99-118, 2000.
- Crowley, T.J., T.R. Quinn, F.W. Taylor, C. Henin, and P. Joannot, Evidence for a volcanic cooling signal in a 335-year coral record from New Caledonia, *Paleoceanography*, 12, 633-639, 1997.
- D'Arrigo, R.D., and G.C. Jacoby, Northern North American tree-ring evidence for regional temperature changes after major volcanic events, *Climatic Change*, 41, 1-15, 1999.
- Dansgaard, W., S.J. Johnsen, H.B. Clausen, and N. Gundestrup, Stable isotope glaciology, *Meddelelser om Gronland Bd*, 197, N2, 1-53, 1973.
- De Angelis, M., L. Fehrenbach, C. Jehanno, and M. Maurette, Micrometer-sized volcanic glasses in polar ice and snows, *Nature*, 317, 52-54, 1985.

- De Silva, S.L., and G.A. Zielinski, Global influence of the AD 1600 eruption of Huaynaputina, Peru, *Nature*, 393, 455-458, 1998.
- Delmas, R.J., M. Legrand, A. Aristarian, and F. Zanolini, Volcanic deposits in Antarctic snow and ice, *Journal of Geophysical Research*, 90, 12, 920, 1985.
- Delmas, R.J., S. Kirchner, J.M. Palais, and J.R. Petit, 1000 years of explosive volcanism recorded at the South Pole, *Tellus*, 44, 335- 350, 1992.
- Devine, J.D., H. Sigurdsson, and A.N. Davis, Estimates of sulfur and chlorine yield to the atmosphere from volcanic eruptions and potential climatic effects, *Journal of Geophysical Research*, 89, 6309-6325, 1984.
- Dibb, J.E., The Chernobyl reference horizon (?) in the Greenland Ice Sheet, *Geophysical Research Letters*, 16, 987- 990, 1989.
- Dunbar, N.W., G.A. Zielinski, and D.T. Voisins, Tephra layers in the Siple Dome and Taylor Dome ice cores, Antarctica: Sources and correlations, *Journal of Geophysical Research*, 108, 2374, doi:10.1029/2002JD0020256, 2003.
- Fiacco, R.J., T. Thordarsson, M.S. Germani, S. Self, J.M. Palias, S. Whitlow, and P.M. Grootes, Atmospheric aerosol loading and transport due to the 1783-84 Laki eruption in Iceland as interpreted from ash particles and acidity in the GISP2 ice core, *Quaternary Research*, 42, 231- 240, 1994.
- Fierstein, J., and W. Hildreth, Ejecta dispersal and dynamics of the 1912 eruption at Novarupta, Katmai National Park, Alaska, *Eos, Transactions, American Geophysical Union*, 67, 1246, 1986.
- Fierstein, J., and W. Hildreth, The Plinian eruptions of 1912 at Novarupta, Katmai National Park, Alaska, *Bulletin of Volcanology*, 54, 646- 684, 1992.
- Fisher, R.V., and H.U. Schminke, *Pyroclastic Rocks*, Springer-Verlag, Berlin, 1984.
- Fisher, D.A., J. Bourgeois, M. Demuth, R. Koerner, M. Parnandi, J. Sekerka, C. Zdanowicz, J. Zheng, C. Wake, K. Yalcin, P. Mayewski, K. Kreutz, E. Osterberg, D. Dahl-Jensen, K. Goto-Azuma, G. Holdsworth, E. Steig, S. Rupper, and M. Wasckiewicz, Mount Logan ice cores: The water cycle of the North Pacific in the Holocene, *Eos, Transactions, American Geophysical Union*, 8, (47), Fall Meeting Supplement, Abstract PP23C- 07, 2004.
- Gard, E.E., M.J. Kleemna, D.S. Gross, L.S. Hughes, J.O. Allen, B.D. Morrical, D.P. Fergenson, T. Dienes, M.E. Galli, R.J. Johnson, G.R. Cass, and K. A. Prather, Direct observation of heterogeneous chemistry in the atmosphere, *Science*, 279, 1184-1186, 1998.
- Germani, M.S. and P.R. Buseck, Evaluation of automated scanning electron microscopy for atmospheric particle analysis, *Analytical Chemistry*, 63, 2232-2237, 1991.

- Graf, H.F., J. Feichter, and B. Langmann, Volcanic sulfur emissions: Estimates of source strength and its contribution to the global sulfate distribution, *Journal of Geophysical Research*, 102, 10,727-10,738, 1997.
- Griggs, R.F., *The Valley of Ten Thousand Smokes (Alaska)*, National Geographic Society, Washington, D.C., 340 pp, 1922.
- Groisman, P.Y., Possible regional climate consequences of the Pinatubo eruption, *Geophysical Research Letters*, 19, 1603-1606, 1992.
- Gronvold, K., N. Oskarsson, S. Johnsen, H.B. Clausen, C.U. Hammer, G. Bond, and E. Bard, Ashy layers from Iceland in the Greenland GRIP ice core correlated with oceanic and land sediments, *Earth and Planetary Science Letters*, 135, 149-155, 1995.
- Hammer, C.U., Past volcanism revealed by Greenland ice sheet impurities, *Nature*, 270, 482-486, 1977.
- Hammer, C.U., H.B. Clausen, and W. Dansgaard, Greenland ice sheet evidence of postglacial volcanism and its climatic impact, *Nature*, 288, 230-235, 1980.
- Hammer, C.U., Traces of Icelandic eruptions in the Greenland ice sheet, *Jokull*, 34, 51-65, 1984.
- Herron, M.M., Impurity sources of F<sup>-</sup>, Cl<sup>-</sup>, NO<sub>3</sub><sup>-</sup>, and SO<sub>4</sub><sup>2-</sup> in Greenland and Antarctic precipitation, *Journal of Geophysical Research*, 87, 3052-3060, 1982.
- Hildreth, W., New perspectives on the eruption of 1912 at Valley of Ten Thousand Smokes, Katmai National Park, Alaska, *Bulletin of Volcanology*, 49, 680-693, 1987.
- Hildreth, W., and J. Fierstein, Katmai volcanic cluster and the great eruption of 1912, *Geological Society of America Bulletin*, 112, 1594-1620, 2000.
- Hildreth, W., J. Fierstein, M. Lanphere, and D.F. Siems, Trident Volcano: Four contiguous stratocones adjacent to Katmai Pass, Alaska Peninsula, U.S. *Geological Survey Professional Paper*, 1678, 2003.
- Holdsworth, G., M. Pourchet, F.A. Prantl, and D.P. Meyerhof, Radioactivity levels in a firn core from the Yukon, Canada, *Atmospheric Environment*, 18, 461-466, 1984.
- Holdsworth, G. and E. Peake, Acid content of snow at a mid-troposphere sampling site on Mt. Logan, Yukon, Canada, *Ann. Glaciol.*, 7, 153-159, 1985.
- Holdsworth, G., H.R. Krouse, and M. Nosal, Ice core climate signals from Mount Logan, Yukon AD 1700-1987, in *Climate Since AD 1500*, edited by R.S. Bradley and P.D. Jones, pp. 483-504, Routledge, New York, 1992.
- Hunt, J.B., and P.G. Hill, Tephra geochemistry: a discussion of some persistent analytical problems, *The Holocene*, 3, 271-278, 1993.
- Ivanov, B.V., V.I. Gorelchik, V.N. Andreev, A.M. Maksimov, V.V. Stepanov, and A.M. Chrikov, The 1972-1974 eruption of Kliuchevskoi Volcano, Kamchatka, *Bulletin of Volcanology*, 44, 1-10, 1981.

- Jacoby, G.C., K.W. Workman, and R.D. D'Arrigo, Laki eruption of 1783, tree rings, and disaster for northwest Alaska Inuit, *Quaternary Science Reviews*, 18, 1365-1371, 1999.
- Jaenicke, R., Physical aspects of the atmospheric aerosol, in *Aerosols and their climatic effects*, edited by H.E. Gerber and A. Deepack, pp. 7- 34, Deepack, Hampton, 1984.
- Jaffe, D.A., B. Cerundolo, and J. Kelley, The influence of Redoubt Volcano emissions on snow chemistry, *Journal of Volcanology and Geothermal Research*, 62, 359- 367, 1994.
- Jones, P.D., K.R. Briffa, and F.H. Schweingruber, Tree-ring evidence of the widespread effects of explosive volcanic eruptions, *Geophysical Research Letters*, 22, 1333-13336, 1995.
- Jones, P.D., A. Morberg, T.J. Osborn, and K.R. Briffa, Surface climate response to explosive volcanic eruptions seen in long European temperature records and mid-to-high latitude tree-ring density around the Northern Hemisphere, in *Volcanism and the Earth's Atmosphere, Geophysical Monograph Series, 139*, edited by A. Robock, and C. Oppenheimer, pp. 239-254, American Geophysical Union, Washington, D.C., 2004.
- Juhle, W., and H.W. Coulter, The Mount Spurr eruption, July 9, 1953, *Eos, Transactions, American Geophysical Union*, 36, 199-202, 1955.
- Keen, R.A., Volcanic aerosols and lunar eclipses, *Science*, 222, 1011-1013, 1983.
- Keene, W.C., A.P. Pszenny, J.N. Galloway, and M.E. Hawley, Sea-salt corrections and interpretation of constituent ratios in marine precipitation, *Journal of Geophysical Research*, 91, 6647- 6658, 1986.
- Kelly, P.M., P.D. Jones, and J. Pengqun, The spatial response of the climate system to explosive volcanic eruptions, *International Journal of Climatology*, 16, 537-550, 1996.
- Kirchner, I., G.L. Stenchikov, H.F. Graf, A. Robock, and J.C. Antuna, Climate model simulation of winter warming and summer cooling following the 1991 Mount Pinatubo volcanic eruption, *Journal of Geophysical Research*, 104, 19,039-19,055, 1999.
- Kohno, M., and Y. Fujii, Past 220-year bipolar volcanic signals: remarks on common features of their source eruptions, *Annals of Glaciology*, 35, 217-223, 2002.
- Krueger, A.J., C.C. Schnetzler, and L.S. Walter, The December 1981 eruption of Nyamuragira Volcano (Zaire), and the origin of the "mystery cloud" of early 1982, *Journal of Geophysical Research*, 101, 15,191-15,196, 1996.
- Lacis, A., J. Hansen, and M. Sato, Climate forcing by stratospheric aerosols, *Geophysical Research Letters*, 19, 1607-1610, 1992.
- Laj, P., S. Drummey, M. Spencer, J.M. Palais, and H. Sigurdsson, Depletion of H<sub>2</sub>O<sub>2</sub> in a Greenland ice core: implications for oxidation of volcanic SO<sub>2</sub>, *Nature*, 346, 45-48, 1990.
- LaMarche, V.C., and K.K. Hirschboeck, Frost rings in trees as records of major volcanic eruptions, *Nature*, 307, 121-126, 1984.

- Langway, C.C., K. Osada, H.B. Clausen, C.U. Hammer, and H. Shoji, A 10-century comparison of prominent bipolar volcanic events in ice cores, *Journal of Geophysical Research*, 100, 16,241- 16,247, 1995.
- Larsen, G., A. Dugmore, and A. Newton, Geochemistry of historical age silicic tephras in Iceland, *The Holocene*, 9, 463-471, 1999.
- LeBas, M.J., R.W. Maitre, A. Strickeisen, and B. Zanettin, A chemical classification of volcanic rocks based on the total alkali-silica diagram, *Journal of Petrology*, 27, 745-750, 1986.
- Legrand, M., and R. J. Delmas, A 220 year continuous record of volcanic H<sub>2</sub>SO<sub>4</sub> in the Antarctic ice sheet, *Nature*, 327, 671- 676, 1987.
- Legrand, M.R., and R.J. Delmas, Formation of HCl in the Antarctic atmosphere, *Journal of Geophysical Research*, 93, 7153-7168, 1988.
- Luhr, J.E., and W.G. Melson, Mineral and glass compositions in June 15, 1991, pumices: Evidence for dynamic disequilibria in the dacite of Mount Pinatubo, in *Fire and Mud: Eruptions and Lahars of Mount Pinatubo, Philippines*, edited by C.G. Newhall and R.S. Punongbayan, pp. 733-750, U.S. Geological Survey, Seattle, 1996.
- Lyons, W.B., P.A. Mayewski, M.J. Spencer, and M.S. Twickler, A northern hemisphere volcanic chemistry record (1869- 1984) and climatic implications using a south Greenland ice core, *Annals of Glaciology*, 14, 176- 182, 1990.
- Mashiotta, T.A., L.G. Thompson, and M.E. Davis, The White River Ash: New evidence from the Bona-Churchill ice core record, *Eos, Transactions, American Geophysical Union*, 85 (47), Fall Meeting Supplement, Abstract PP21A-1369, 2004.
- Mass, C.F., and D.A. Portman, Major volcanic eruptions and climate: A critical evaluation, *Journal of Climate*, 2, 566-593, 1989.
- Mayewski, P.A., G. Holdsworth, M.J. Spencer, S. Whitlow, M. Twickler, M.C. Morrison, K.K. Ferland, and L.D. Meeker, Ice-core sulfate from three northern hemisphere sites: origin and temperature forcing implications, *Atmospheric Environment*, 27A, 2915- 2919, 1993.
- Mayewski, P.A., L.D. Meeker, S. Whitlow, M.S. Twickler, M.C. Morrison, P.M. Grootes, G.C. Bond, R.B. Alley, D.A. Meese, and T. Gow, Changes in atmospheric circulation and ocean ice cover over the North Atlantic region over the last 41,000 years, *Science*, 263, 1747- 1751, 1994.
- McCormick, P.M., P.H. Wang, and L.R. Poole, Stratospheric aerosols and clouds, in *Aerosol-Cloud- Climate Interactions*, edited by P. V. Hobbs, pp. 205- 220, Academic, San Diego, Calif., 1993.
- Melekestsev, I.V., O.A. Braitseva, V.V. Ponomareva, and L.D. Sulerzhitskiy, Holocene catastrophic caldera-forming eruptions of Ksudach Volcano, Kamchatka, *Volcanology and Seismology*, 17, 395-422, 1996.



- Miller, T.P., R.G. McGimsey, D.H. Richter, J.R. Riehle, C.J. Nye, M.E. Yount, and J.A. Dumoulin, *Catalog of the Historically Active Volcanoes of Alaska*, U.S. Geological Survey Open- File Report 98-582, 104 pp, 1998.
- Miyashiro, A., Volcanic rock series in island arcs and active continental margins, *American Journal of Science*, 274, 321-355, 1974.
- Monzier, M., C. Robin, and J. Eissen, Kuwae: the forgotten caldera, *Journal of Volcanology and Geothermal Research*, 59, 207-218, 1994.
- Moore, J.C., H. Narita, and N. Maeno, A continuous 770-year record of volcanic activity from East Antarctica, *Journal of Geophysical Research*, 98, 17353- 17359, 1991.
- Moore, G., G. Holdsworth, and K. Alverson, Extra- tropical response to ENSO 1736- 1985 as expressed in an ice core from the St. Elias mountain range in northwestern North America, *Geophysical Research Letters*, 28, 3457-3460, 2001.
- Muller, E.H., W. Juhle, and H.W. Coulter, Current volcanic activity in Katmai National Monument, *Science*, 119, 319-321, 1954.
- Neftel, A., J. Beer, H. Oeschger, F. Zurcher, and R.C. Finkel, Sulphate and nitrate concentrations in snow from South Greenland 1895- 1978, *Nature*, 314, 611- 613, 1985.
- Newhall, C.G., and S. Self, The volcanic explosivity index (VEI): an estimate of explosive magnitude for historical volcanism, *Journal of Geophysical Research*, 87, 1231- 1238, 1982.
- Oppenheimer, C., Ice core and paleoclimate evidence for the timing and nature of the great mid-thirteenth century volcanic eruption, *International Journal of Climatology*, 23, 417-426, 2003.
- Palais, J. and H. Sigurdsson, Petrologic evidence of volatile emissions from major historic and prehistoric volcanic eruptions, *Understanding Climate Change, American Geophysical Union, Geophysical Monograph*, 52, edited by A. Berger, pp. 31- 53, 1989.
- Palais, J.M., S. Kirchner, and R.J. Delmas, Identification of some global volcanic horizons by major element analysis of fine ash in Antarctic ice, *Annals of Glaciology*, 14, 216-220, 1990.
- Palais, J.M. K. Taylor, P.A. Mayewski, and P.M. Grootes, Volcanic ash from the 1362 A.D. Oraefajokull eruption (Iceland) in the Greenland ice sheet, *Geophysical Research Letters*, 18, 1241-1244, 1991.
- Palais, J.M., M.S. Germani, and G.A. Zielinski, Inter-hemispheric transport of volcanic ash from a 1259 A.D. volcanic eruption to the Greenland and Antarctic ice sheets, *Geophysical Research Letters*, 19, 801-804, 1992.
- Palmer, A.S., T.D.S. van Ommen, M.A.J. Curran, V. Morgan, J.M. Souney, and P.A. Mayewski, High precision dating of volcanic events (A.D. 1301-1995) using ice cores from Law Dome, Antarctica, *Journal of Geophysical Research*, 106, 28,089- 28,095, 2001.

- Pang, K.D., Climatic impact of the mid-fifteenth century Kuwae Caldera formation, as reconstructed from historical and proxy data, *EOS, Transactions, American Geophysical Union*, 74, 106, 1993.
- Peixoto, J.P., and A.H. Oort, *Physics of Climate*, American Institute of Physics, New York, 1992.
- Portman, D.A., and D.S. Gutzler, Explosive volcanic eruptions, the El Nino-Southern Oscillation, and U.S. climate variability, *Journal of Climate*, 9, 17-33, 1996.
- Pyle, D.M., P.D. Beattie, and G.J.S. Bluth, Sulfur emissions to the stratosphere from explosive volcanic eruptions, *Bulletin of Volcanology*, 57, 663-671, 1996.
- Rampino, M.R., and S. Self, Sulfur rich volcanic eruptions and stratospheric aerosols, *Nature*, 310, 677- 679, 1984.
- Richter, D.H., J.G. Smith, M.A. Lanphere, G.B. Dalrymple, B.L. Reed, and N. Shew, Age and progression of volcanism, Wrangell Volcanic Field, Alaska, *Bulletin of Volcanology*, 53, 29-44, 1990.
- Richter, D.H., S.J. Preece, R.G. McGimsey, and J.A. Westgate, Mount Churchill, Alaska, source of the late Holocene White River Ash, *Canadian Journal of Earth Sciences*, 32, 741-748, 1995.
- Riehle, J.R., A reconnaissance of the major Holocene tephra deposits in the upper Cook Inlet region, Alaska, *Journal of Volcanology and Geothermal Research*, 26, 37-74, 1985.
- Robertson, A., J. Overpeck, D. Rind, E. Mosley-Thompson, G.A. Zielinski, J. Lean, D. Koch, J., Penner, I. Tegen, and R. Healy, Hypothesized climate forcing time series for the last 500 years, *Journal of Geophysical Research*, 106, 14,783-14,803, 20901.
- Robin, C., M. Monzier, and J.P. Eissen, Formation of the mid-fifteenth century Kuwae caldera (Vanuatu) by an initial hydroclastic and subsequent ignimbritic eruption, *Bulletin of Volcanology*, 56, 170-183, 1994.
- Robock, A., and C. Mass, The Mount St. Helens volcanic eruption of May 18 1980: Large short term surface temperature effects, *Science*, 216, 628-630, 1982.
- Robock, A., and J. Mao, Winter warming from large volcanic eruptions, *Geophysical Research Letters*, 12, 2405- 2408, 1992.
- Robock, A., And J. Mao, The volcanic signal in surface temperature observations, *Journal of Climate*, 8, 1086-1103, 1995.
- Robock, A., and M. P. Free, Ice cores as an index of global volcanism from 1850 to the present, *Journal of Geophysical Research*, 100, 11,549- 11,567, 1995.
- Robock, A., Volcanic eruptions and climate, *Reviews of Geophysics*, 38, 191-219, 2000.
- Robock, A., Blowin' in the wind: Research priorities for climate effects of volcanic eruptions, *EOS, Transactions, American Geophysical Union*, 83, 472, 2002.

- Robock, A., The climatic aftermath, *Science*, 295, 1242-1244, 2002.
- Rolandi, G., A.M. Barrella, and A. Borrelli, The 1631 eruption of Vesuvius, *Journal of Volcanology and Geothermal Research*, 58, 183-201, 1993.
- Sato, M., J.E. Hansen, M.P. McCormick, and J.B. Pollack, Stratospheric aerosol optical depths, 1850- 1990, *Journal of Geophysical Research*, 98, 22, 987- 22,994, 1993.
- Scaillet, B., J. Luhr, and M. R. Carroll, Petrological and volcanological constraints on volcanic sulfur emissions to the atmosphere, in *Volcanism and the Earth's Atmosphere, Geophysical Monograph Series, vol. 139*, edited by A. Robock, and C. Oppenheimer, pp. 11-40, American Geophysical Union, Washington, D.C., 2003.
- Self, S., M.R. Rampino, and J.J. Barbera, The possible effects of large 19<sup>th</sup> and 20<sup>th</sup> century volcanic eruptions on zonal and hemispheric surface temperatures, *Journal of Volcanology and Geothermal Research*, 11, 41- 60, 1981.
- Self, S., M.R. Rampino, J. Zhao, and M.G. Katz, Volcanic aerosol perturbations and strong El Nino events: No general correlation, *Geophysical Research Letters*, 24, 1247-1250, 1997.
- Shapiro, M.A., R.C. Schnell, F.P. Parungo, S.J. Oltmans, and B.A. Bodhaine, El Chichon volcanic debris in an Arctic tropopause fold, *Geophysical Research Letters*, 11, 412- 424, 1984.
- Shindell, D.T., G.A. Schmidt, M.E. Mann, and G. Faluvegi, Dynamic winter climate response to large tropical volcanic eruptions since 1600, *Journal of Geophysical Research*, 109, D05104, doi:10.1029/2003JD004151, 2004.
- Sigurdsson, H., Evidence of volcanic loading of the atmosphere and climate response, *Paleo*, 89, 277- 289, 1990.
- Simkin, T., and L. Siebert, *Volcanoes of the World*, 2<sup>nd</sup> ed., 349 pp., Geoscience, Tucson, AZ, 1994.
- Stelling, P., J. Beget, C. Nye, J. Gardner, J.D. Devine, and R.M. George, Geology and petrology of ejecta from the 1999 eruption of Shishaldin Volcano, Alaska, *Bulletin of Volcanology*, 64, 548-561, 2002.
- Stenchikov, G., A. Robock, V. Ramaswamy, M.D. Schwarzkopf, K. Hamilton, and S. Ramachandran, Arctic Oscillation response to the 1991 Mount Pinatubo eruption: Effects of volcanic aerosols and ozone depletion, *Journal of Geophysical Research*, 107, 4803, doi: 10.1029/2002JD002090, 2002.
- Stenni, B., M. Proposito, R. Gragnani, O. Flora, J. Jouzel, S. Falourd, and M. Frezzotti, Eight centuries of volcanic signal and climate change at Talos Dome, East Antarctica, *Journal of Geophysical Research*, 107, 10.1029/2000JD000317, 2002.
- Stothers, R.B., The mystery cloud of AD 536, *Nature*, 307,344-345, 1984.

- Stothers, R.B., Major optical depth perturbations to the stratosphere from volcanic eruptions: Pyrheliometric period, 1881-1960, *Journal of Geophysical Research*, 101, 3901-3920, 1996.
- Stothers, R.B., Climatic and demographic consequences of the massive volcanic eruption of 1258, *Climatic Change*, 45, 361-374, 2000.
- Swanson, S.E., C.J. Nye, T.P. Miller, and V.F. Avery, Geochemistry of the 1989-1990 eruption of Redoubt Volcano: Part II. Evidence from mineral and glass chemistry, *Journal of Volcanology and Geothermal Research*, 62, 453-468, 1994.
- Swanson, S.E., M.L. Harbin, and J.R. Riehle, Use of volcanic glass from ash as a monitoring tool: An example from the 1992 eruptions of Crater Peak vent, Mount Spurr volcano, Alaska, in *The 1992 eruptions of Crater Peak vent, Mount Spurr volcano, Alaska*, edited by T. Keith, U.S. Geological Survey Bulletin, 2139, pp. 129-137, 1995.
- Thorarinsson, S., and L. Saedmundsson, Volcanic activity in historical time, *Jokull*, 29, 29-32, 1979.
- Turner, S., F. McDermott, C. Hawkesworth, P. Kepezhinskas, A U-Series study of lavas from Kamchatka and the Aleutians: Constraints on source composition and melting processes, *Contributions to Mineralogy and Petrology*, 133, 217-234, 1998.
- Volz, F.E., Distribution of turbidity after the 1912 Katmai eruption in Alaska, *Journal of Geophysical Research*, 80, 2643-2648, 1975.
- Volynets, O.N., V.V. Ponomareva, O.A. Braitseva, I.V. Melekestsev, C.H. Chen, Holocene eruptive history of Ksudach volcanic massif, South Kamchatka: evolution of a large magmatic chamber, *Journal of Volcanology and Geothermal Research*, 91, 23-42, 1999.
- Whitlow, S., P.A. Mayewski, J.E. Dibb, A comparison of major chemical species seasonal concentration and accumulation at the South Pole and Summit, Greenland, *Atmospheric Environment*, 26A, 2045-2054, 1992.
- Yalcin, K., and C. Wake, Anthropogenic signals recorded in an ice core from Eclipse Icefield, Yukon, Canada, *Geophysical Research Letters*, 28, 4487-4490, 2001.
- Yalcin, K., C. P. Wake, and M. Germani, A 100-year record of North Pacific volcanism in an ice core from Eclipse Icefield, Yukon, Canada, *Journal of Geophysical Research*, 108, doi: 10.1029/2002JD002449, 2003.
- Yalcin, K., C.P. Wake, K.J. Kreutz, M.S. Germani, and S.I. Whitlow, Ice core evidence for a second volcanic eruption around 1809 in the Northern Hemisphere, in preparation.
- Zdanowicz, C.M., G.A. Zielinski, and M.S. Germani, Mount Mazama eruption: Calendrical age verified and atmospheric impact assessed, *Geology*, 27, 621-624, 1999.
- Zielinski, G.A., P.A. Mayewski, L.D. Meeker, S. Whitlow, M.S. Twickler, M. Morrison, D. Meese, R.B. Alley, and A.J. Gow, Record of volcanism since 7000 B.C. from the GISP2 Greenland ice core and implications for the volcano-climate system, *Science*, 264, 948-952, 1994.

- Zielinski, G.A., M.S. Germani, G. Larsen, M. Baille, S. Whitlow, M.S. Twickler, and K. Taylor, Evidence of the Eldgja (Iceland) eruption in the GISP2 Greenland ice core: relationship to eruption processes and climatic conditions in the tenth century, *The Holocene*, 5, 129-140, 1995a.
- Zielinski, G.A., Stratospheric loading and optical depth estimates of explosive volcanism over the last 2100 years derived from the GISP2 Greenland ice core, *Journal of Geophysical Research*, 100, 20,937- 20,955, 1995b.
- Zielinski, G.A., P.A. Mayewski, L.D. Meeker, S. Whitlow, and M. Twickler, A 110,000 year record of explosive volcanism from the GISP2 (Greenland) ice core, *Quaternary Research*, 45, 109- 118, 1996.
- Zielinski, G.A., J.E. Dibb, Q. Yang, P.A. Mayewski, S. Whitlow, M.S. Twickler, and M.S. Germani, Assessment of the record of the 1982 El Chichon eruption as preserved in Greenland snow, *Journal of Geophysical Research*, 102, 30,031- 30,045, 1997.
- Zielinski, G., Use of paleo-records in determining variability within the volcano- climate system, *Quaternary Science Reviews*, 19, 417-438, 2000.

## CHAPTER VII

### ICE CORE EVIDENCE FOR A SECOND VOLCANIC ERUPTION AROUND 1809 IN THE NORTHERN HEMISPHERE

(to be submitted to *Geochemistry, Geophysics, Geosystems*)

#### Abstract

A volcanic sulfate signal observed in ice cores from both polar regions six years prior to the 1815 Tambora eruption is attributed to an unknown tropical eruption in 1809. Recovery of dacitic tephra from the 1809 horizon in an ice core from Eclipse Icefield, Yukon, Canada with a chemical composition distinct from andesitic 1809 tephra found in Antarctic ice cores indicates a second eruption in the Northern Hemisphere at this time. Sulfate flux calculations suggest this eruption contributed little additional sulfate to circum-Arctic ice cores, and therefore had negligible climatic significance. The 1809 tephra found in Antarctica is statistically indistinguishable from 1835 eruption products of Cosiguina Volcano, Nicaragua. Although a refined estimate of sulfur production incorporating exsolved sulfur gases demonstrates Cosiguina eruptions can release sulfur in sufficient quantities to perturb climate, the March 1809 eruption date for Cosiguina is now regarded as spurious due to a lack of geologic evidence. The source volcano responsible for the bipolar 1809 volcanic signal remains unknown. Tephrochronological evidence supports coincidental eruptions in both hemispheres, rather than a single tropical eruption, as the source of the 1809 volcanic signals. The similar magnitude and timing of the 1809 volcanic signal in both polar regions and widespread evidence of short term cooling, including in the tropics, suggests a large tropical eruption as the source of the sulfate and Antarctic tephra and a minor Northern Hemisphere eruption as the source of the Eclipse tephra.

## Introduction

Large, explosive volcanic eruptions in the tropical latitudes can perturb climate on a global scale. However, an incomplete record of volcanism complicates investigations of the influence of such eruptions on past climates. Large eruptions of global influence have gone unnoticed as recently as the 1809 eruption identified only in ice core records from Greenland (Cole-Dai *et al.*, 1991; Zielinski *et al.*, 1994; Langway *et al.*, 1995; Clausen *et al.*, 1997; Kohno and Fujii, 2002; Mosley-Thompson *et al.*, 2003) and Antarctica (Legrand and Delmas, 1987; Cole-Dai *et al.*, 1991, 1997, 2000; Moore *et al.*, 1991; Delmas *et al.*, 1992; Langway *et al.*, 1995; Stenni *et al.*, 1999; 2002; Palmer *et al.*, 2001). Using the GISP2 ice core data, Zielinski (1995) calculated a stratospheric H<sub>2</sub>SO<sub>4</sub> loading of 34 to 68 x 10<sup>12</sup> g and an optical depth of 0.11 to 0.28 for this eruption, making it among the largest of the last few centuries.

This eruption may have contributed to a very cold period beginning in 1809 that was compounded by the 1815 Tambora eruption to produce the “year without a summer” in 1816 (Harrington, 1992). A network of tree-ring maximum latewood density for Alaska, the Yukon, the McKenzie Valley, Quebec and Labrador indicates 1810 was the coldest summer in northern North America since 1760 (Briffa *et al.*, 1994). Overall, tree ring densities for the year 1810 were the 15<sup>th</sup> lowest for the Northern Hemisphere over the last 600 years (Briffa *et al.*, 1998). Ship based observations of marine air temperature in the tropics show maximum cooling in 1809 of 0.84± 0.20 °C, four times greater than that observed following Pinatubo (Chenoweth, 2001).

Given its widespread climatic effects, identifying the source of the 1809 eruption is important for improving our understanding of the history of global climate-forcing eruptions. A study of bipolar volcanic signals over the last 220 years led Kohno and Fujii (2002) to conclude that a latitude between 20°N and 10° S and an eruption column height of at least 25 km (Volcanic Explosivity Index (VEI) 5 or greater) are requirements for a volcanic signal to be seen in both Greenland and Antarctica, providing constraints on the location and magnitude of the unknown

1809 eruption. However, no eruption with a VEI greater than 3 is reported in the historical volcanism record between 1801 and 1812 (Simkin and Siebert, 1994).

Analysis of tephra associated with volcanic  $\text{SO}_4^{2-}$  peaks in ice cores can provide information on the source volcano responsible for an eruption. Andesitic tephra associated with the 1809  $\text{SO}_4^{2-}$  peak has been found in ice cores from South Pole (Palais *et al.*, 1990) and Dome C, Antarctica (De Angelis *et al.*, 1985) (Figure VI.1). In the Dome C ice core, the layer containing tephra was initially dated to 1815 and attributed to Tambora but due to a poor match between the composition of glass shards in the ice core and Tambora glass, this layer was later re-interpreted to be from the unknown 1809 eruption (Legrand and Delmas, 1987). Palais *et al.* (1990) suggested the source of the volcanic glass shards found in the South Pole and Dome C ice cores was Cosiguina, Nicaragua, based on the similar chemical compositions of the Antarctic 1809 tephra and Cosiguina 1835 eruption products and a March 1809 eruption date for Cosiguina (VEI 2) in the Simkin and Siebert (1994) chronology of volcanic eruptions.

In this paper we present evidence for a second eruption in the Northern Hemisphere in 1809 using volcanic glass found in a new ice core from Eclipse Icefield, Yukon, Canada. The  $\text{SO}_4^{2-}$  contribution from this eruption to the 1809 volcanic signal in circum-Arctic ice cores is examined to assess the significance of this eruption. We also evaluate the chemical similarity of the 1809 ice core tephra and Cosiguina tephra using a t-test (Keenan, 2003). The potential for Cosiguina eruptions to impact global climate is reassessed in light of recent improvements in the calculation of sulfur release from explosive volcanic eruptions (Scaillet *et al.*, 2004). We conclude with an evaluation of potential sources of the 1809 volcanic signal.

#### **Evidence from Eclipse Icefield for a second 1809 eruption**

The strongest evidence for a tropical source of the unknown 1809 eruption would be provided by identification of volcanic glass shards of similar composition associated with the 1809 horizon in both Arctic and Antarctic ice cores. For example, glass shards of similar



composition associated with the 1259 volcanic signal in ice cores from South Pole and Summit, Greenland, confirmed a common source in the tropical latitudes (Palais *et al.*, 1992). To this end, we collected tephra associated with the 1809 volcanic signal in a 345 m ice core from Eclipse Icefield. This core was analyzed as described for the 1996 Eclipse ice core (Yalcin *et al.*, 2003) and the 1809 horizon dated by annual layer counting of the stable isotope record with age control provided by identification of the Laki 1783 and Tambora 1815 volcanic sulfate reference horizons (Figure VI.2). Tephra was collected by filtering of melt water through a 0.2-micron polycarbonate membrane and individual particles greater than four micrometers with glass shard morphology were analyzed for major oxide composition using a Hitachi S-570 scanning electron microscope (Germani and Buseck, 1991).

Tephra from the 1809 horizon in the Eclipse ice core has a chemical composition that is distinctly different from 1809 tephra found in ice cores from South Pole and Dome C, Antarctica (Table VI.1). Following the total alkali ( $\text{Na}_2\text{O} + \text{K}_2\text{O}$ ) classification scheme, tephra from the South Pole and Dome C ice cores is an andesite to trachyandesite, while the Eclipse tephra has a trachytic composition (Figure VI.3). Note also the considerable overlap between the South Pole and Dome C tephtras, and their separation from the Eclipse tephra. A Student's t-test can be used to evaluate the significance of the differences in chemical composition between the Eclipse, South Pole, and Dome C tephtras (Keenan, 2003). The t-test can only be applied for those constituents whose mean divided by standard deviation is greater than 2.5 in both data sets to be compared so that the assumption of a normal distribution is satisfied. For most constituents satisfying this assumption, the difference between the Eclipse/South Pole tephtras and Eclipse/Dome C tephtras is significant at the 99.9% confidence level (Table VI.2). The only exceptions are  $\text{TiO}_2$ , significant at the 99% confidence level for the Eclipse/South Pole tephtras; and  $\text{Al}_2\text{O}_3$ , difference not significant for the Eclipse/South Pole and Eclipse/Dome C comparisons. Conversely, the t-test detects no significant difference between the South Pole and Dome C tephtras, except for  $\text{TiO}_2$  at the 90% confidence level. These results suggest that the

South Pole and Dome C tephra are from the same volcano while the Eclipse tephra is from a different volcano, implicating a second eruption around 1809 as the source of the Eclipse tephra.

All identified tephra from the Eclipse ice cores are from high northern latitude volcanoes (Alaska, Kamchatka, Iceland; Yalcin *et al.*, in preparation). It therefore follows that unidentified tephra in the Eclipse ice cores, including the 1809 tephra, are most likely also from volcanoes in these regions. Numerous volcanoes in the North Pacific Rim have erupted dacitic products, and hence can be considered possible sources of the Eclipse 1809 tephra. The only volcano in the region known to have been active around this time is Bogoslof Volcano in the Aleutian arc, but its products range from basaltic to andesitic in composition (Miller *et al.*, 1998). Many other Alaskan volcanoes have produced dacitic products, of these Aniakchak, Shishaldin, and Okmok have produced high alkali dacites similar to the Eclipse tephra (Miller *et al.*, 1998). Some Kamchatkan volcanoes also produce dacitic products. Identification of tephra from the eruption of Hekla in 1947 in an ice core from Eclipse (Yalcin *et al.*, 2003) demonstrates that that an Icelandic eruption could also be the source of the 1809 tephra found at Eclipse. However, no Icelandic eruptions are reported between 1797 and 1816. The number of reported eruptions in Iceland is fairly constant over the last several hundred years, with 12 VEI  $\geq$  3 eruptions since 1900, 8 between 1800 and 1900, and 8 between 1700 and 1800 (Simkin and Seibert, 1994). This suggests that the historically documented record of volcanic eruptions in Iceland is reasonably complete over this time interval. Meanwhile there is a dramatic drop in the number of reported VEI $\geq$ 3 eruptions between the 20<sup>th</sup> and 19<sup>th</sup> centuries from both Alaska (57 versus 19) and Kamchatka (69 versus 19). This suggests a large percentage, perhaps two-thirds, of eruptions during the 1800's in Alaska and Kamchatka are not historically documented as it is highly unlikely that the frequency of volcanic eruptions in this region changed by a factor of three between the 19<sup>th</sup> and 20<sup>th</sup> centuries. Clearly, there were many more unreported eruptions in Alaska and Kamchatka during the 19<sup>th</sup> century than in Iceland, making an Alaska or Kamchatka volcano a more likely source of the Eclipse 1809 tephra.

Such an eruption, depending on its magnitude, may or may not be a significant contributor to the 1809 volcanic  $\text{SO}_4^{2-}$  signal in Arctic ice cores. We investigated this possibility by calculating the  $\text{SO}_4^{2-}$  flux for the 1809 eruption at Eclipse relative to the Tambora eruption and compared our results to those calculated for other ice cores from Greenland and Antarctica to assess the possible contribution of the second 1809 eruption to the  $\text{SO}_4^{2-}$  flux at Eclipse. To separate volcanic  $\text{SO}_4^{2-}$  from other  $\text{SO}_4^{2-}$  sources, we used an empirical orthogonal function (EOF) decomposition to describe the variance in the Eclipse glaciochemical data set. Applying EOF analysis to the suite of ions measured in the Eclipse ice core (excluding  $\text{NH}_4^+$ ) reveals that EOF 5 is loaded solely with  $\text{SO}_4^{2-}$  and describes 5.3 % of the total variance in the dataset, but 20.3% of the variance in the  $\text{SO}_4^{2-}$  time series. Volcanic eruptions have been identified as the source of this  $\text{SO}_4^{2-}$  (Yalcin *et al.*, 2003). Total  $\text{SO}_4^{2-}$  deposition, or flux, for both the Tambora and 1809 events was calculated as the product of the volcanic  $\text{SO}_4^{2-}$  concentration and the water equivalent length of the sample (corrected for layer thinning), summed for the samples containing fallout attributable to each event. For comparison with other ice core sites where different mass transfer mechanisms (wet and dry deposition, riming) may vary in importance, we calculated the volcanic  $\text{SO}_4^{2-}$  flux ratio of the 1809 eruption relative to Tambora (Cole-Dai *et al.*, 1997).

We calculated the total volcanic  $\text{SO}_4^{2-}$  flux from the unknown 1809 and Tambora eruptions at Eclipse to be 3.69 and 7.08  $\mu\text{g cm}^{-2}$ , respectively. The total time integration for fallout between the two events is similar, 2.2 years for the 1809 event and 2.5 years for the Tambora event. The volcanic flux from the 1809 event at Eclipse, 54% of Tambora, is in good agreement with results from both Greenland (60-78%) and Antarctica (37-60%) (Table VI.3). This result suggests little additional  $\text{SO}_4^{2-}$  deposition at Eclipse from the coincidental 1809 eruption whose tephra we recovered. The smaller magnitude of the 1809 signal at Eclipse relative to Greenland, even though Eclipse is likely to be closer to the unidentified Northern Hemisphere volcano, is further evidence that this eruption was not a large  $\text{SO}_4^{2-}$  contributor to Arctic ice cores. If it were, the 1809 signal at Eclipse should be enhanced relative to Greenland,

unless the unidentified northern hemisphere eruption was in Iceland. As mentioned earlier, the frequency of reported eruptions over the last 200 years suggests there were many more undocumented eruptions in the North Pacific than in Iceland during the 19<sup>th</sup> century. From these results, we infer that the second 1809 eruption is of negligible climatic significance and most of the SO<sub>4</sub><sup>2-</sup> from the 1809 eruptions in Arctic ice cores is from the global event in the tropics.

We note that the 1809 signal at Summit, Greenland (GRIP and GISP2) appears to be enhanced relative to other sites worldwide, giving a relative magnitude for the 1809 event as 71 and 78% of Tambora, respectively, whereas the 1809 signal elsewhere is less than 60% of Tambora. By comparison with Site T, also in central Greenland, it can be seen that this is due to anomalously low fluxes for the Tambora eruption in the Summit ice cores (Table VI.3). This may be due to incomplete integration of the Tambora fallout by not including volcanic SO<sub>4</sub><sup>2-</sup> deposition in 1817. For example, Plate 4 of Clausen *et al.* (1997) shows SO<sub>4</sub><sup>2-</sup> for the 1817 annual layer was not measured via ion chromatography, and hence not included in their calculation of the total Tambora fallout.

The existence of a second eruption in the Northern Hemisphere around 1809 raises the possibility that the bipolar 1809 volcanic signal was the result of coincidental eruptions in the high latitudes of both hemispheres, rather than a tropical eruption that was dispersed to both hemispheres. There are three lines of evidence that suggest a tropical eruption affecting both hemispheres in 1809. First, Table VII.3 shows that the 1809 signal had a similar magnitude in both hemispheres, as previously shown by other studies (e.g., Cole-Dai *et al.*, 1991). Second, there is a close match in the timing of the 1809 event in both Greenland and Antarctic cores (Cole-Dai *et al.*, 1997). Third, there is both instrumental (Chenoweth, 2001) and proxy (Crowley *et al.*, 1997) evidence of short-term cooling in the tropics in 1809-1810. The coldest tropical marine air temperatures anomalies as recorded by ships of opportunity between 1807 and 1827 were in 1809 ( $-0.84 \pm 0.20$  °C relative to a 14 year non-volcanic base period; Chenoweth, 2001). Instrumental temperature records from Malaysia show abrupt cooling beginning in July 1808 that

persisted until January 1810 (Chenoweth, 2001). A coral record of tropical sea-surface temperatures from New Caledonia also indicate cooling between 1808 and 1810 (Crowley *et al.*, 1997). Although El Nino events also produce cooling of sea-surface temperatures in New Caledonia, there was no El Nino event at this time (Quinn, 1992). Because aerosols from even the largest high latitude eruptions do not reach the tropics, the observed temperature anomalies, if they are indeed volcanic, suggest a tropical eruption in 1808. For example, the aerosol from the large Katmai, Alaska eruption in 1912 (VEI 6) was confined poleward of 30°N (Stothers, 1996). Analysis of instrumental temperature records following the three VEI<sub>≥</sub>5 eruptions in the high northern latitudes during the last century (Ksudach 1907, Katmai 1912, Bezymianny 1956) showed that the tropical temperature response was indistinguishable from noise (Bradley, 1988).

#### **Could Cosiguina be the source of the 1809 ice core tephras?**

To evaluate the hypothesis of Palais *et al.* (1990) that Cosiguina is the source of the 1809 eruption, we use a t-test to compare the chemical composition of the 1809 ice core tephras with tephra from the 1835 Cosiguina eruption (Table VI.2). As noted in the previous section, South Pole and Dome C tephras are statistically indistinguishable and hence likely to be from the same source, while the composition of Eclipse tephra indicates a different source volcano. The t-test detects no significant difference between the South Pole or Dome C tephras and Cosiguina 1835 tephra, except for TiO<sub>2</sub> where the difference is significant at the 95% and 99.9% confidence levels, respectively. A significant difference at the 99% confidence level is also detected for FeO in the case of Dome C. Although the t-test provides statistical backing to claim the Antarctic and Cosiguina tephras are chemically similar with respect to all major chemical constituents except TiO<sub>2</sub>, the t-test results do not prove that the source of the Antarctic ice core tephra is Cosiguina. Meanwhile, the t-test demonstrates significant differences between the Eclipse and Cosiguina tephras, at the 99.9% confidence level for most constituents, clearly ruling out Cosiguina as a possible source of the 1809 tephra seen at Eclipse.

### Could eruptions of Cosiguina affect global climate?

Cosiguina (13.0° N, 87.6° W, 872 m elevation) is a composite andesitic volcano forming a peninsula in the Gulf of Fonseca on the west coast of Nicaragua (Figure VI.1). Given its tropical location, an eruption from Cosiguina, provided its column height is sufficient to reach the tropical stratosphere, could be dispersed to both hemispheres (Robock, 2000). However, Self *et al.* (1989) has demonstrated the magnitude of its 1835 eruption was overestimated, with a total volume of 5.6 km<sup>3</sup> corresponding to 1.8-2.8 km<sup>3</sup> dense rock equivalent (DRE), compared to an earlier estimate of 150 km<sup>3</sup> (Lamb, 1970). Nonetheless, the inferred eruptive column height of 25-28 km was sufficient to reach the tropical stratosphere (Self *et al.*, 1989). In fact, the Cosiguina 1835 eruption is recognized as a prominent bipolar volcanic signal seen in both Arctic (Zielinski, 1995; Langway *et al.*, 1995; Kohno and Fujii, 2002; Yalcin *et al.*, in preparation) and Antarctic ice cores (Legrand and Delmas, 1987; Moore *et al.*, 1991; Delmas *et al.*, 1992; Cole-Dai *et al.*, 1997; 2000; Stenni *et al.*, 1999; 2002; Palmer *et al.*, 2001). Furthermore, tree ring density records indicate that Northern Hemisphere summer temperatures in 1836 and 1837 were the 21st and 15th coldest of the last 600 years, respectively (Briffa *et al.*, 1998).

A critical issue in assessing the climatic effectiveness of Cosiguina eruptions is the volcano's sulfur production. A petrologic method comparing the sulfur content of phenocrysts to matrix glass can be used to estimate sulfur release. Assuming the sulfur content of the inclusions represents the original sulfur content of the magma, the difference between the inclusions and the matrix represents the amount of sulfur degassed to the atmosphere during the eruption (Palais and Sigurdsson, 1989). Combined with estimates of the volume of ejecta this technique yields an estimate of atmospheric mass loading of SO<sub>2</sub>. Citing the similar sulfur content in both melt inclusions (355 ± 63 ppm) and matrix (357 ± 81 ppm) of the 1835 Cosiguina eruption products, Palais and Sigurdsson (1989) suggest a negligible sulfur release from this eruption.

However, petrologic estimates of volatile emissions are considered minimum estimates since the method does not account for exsolved sulfur gas in the accumulated vapor phase of the

magma tapped by an eruption (Wallace, 2001). This excess sulfur source is characteristic of explosive eruptions in subduction zone settings where more than 90% of the sulfur production of an eruption may be via release of the gas phase produced by pre-eruptive exsolution (Scaillet *et al.*, 2003). In fact, petrologic estimates of sulfur production from eruptions like El Chichon (1982), Pinatubo (1991), and Redoubt (1989-90) are as little as 4% of estimates derived from satellite data (Gerlach *et al.*, 1994). Therefore, petrologic estimates can significantly underestimate the sulfur production of an eruption, especially for subduction volcanoes.

Scaillet *et al.* (2003) refined the petrologic technique for estimating sulfur production to include sulfur from the pre-eruption gas phase. Four parameters must be known: the mass of erupted magma, the gas content of the magma, the sulfur content of melt inclusions, and the gas-melt partitioning coefficient for sulfur. From volcanological evidence, andesitic magma is assumed to contain 5% gas by weight prior to eruption with a gas-melt partitioning coefficient for sulfur of 100 (Wallace, 2001). In estimating sulfur release from the 1835 Cosiguina eruption, Scaillet *et al.* (2003) used Williams' (1952) order of magnitude estimate of  $10 \text{ km}^3$  dense rock equivalent (DRE) for the eruptive volume. Using a density of  $2500 \text{ kg m}^{-3}$  for andesite and assuming the magma contains 5% gas by weight, this equates to  $2.5 \times 10^{16} \text{ g}$  of magma erupted and  $1.25 \times 10^{15} \text{ g}$  of total gas released which included water,  $\text{CO}_2$ , halogen, and sulfur gases. Since melt inclusions in Cosiguina 1835 glass contain 355 ppm S (Palais and Sigurdsson, 1989) with a gas-melt partitioning coefficient for S of 100, the S content of the gas is estimated to have been 35,500 ppm, or 3.55% by weight. Therefore, Scaillet *et al.* (2003) estimate a sulfur release of  $44 \times 10^{12} \text{ g}$  sulfur from the accumulated vapor phase in the magma during the 1835 eruption. Using a more precise volume estimate for the 1835 eruption of  $2.3 \pm 0.5 \text{ km}^3$  DRE provided by Self *et al.* (1989), we calculate a sulfur release of  $10 \pm 2 \times 10^{12} \text{ g S}$  from the 1835 Cosiguina eruption. This value is similar to the sulfur release of  $9 \pm 1 \times 10^{12} \text{ g S}$  from the 1991 Pinatubo eruption (Krueger *et al.*, 1995), an eruption of known climatic significance, suggesting that the Cosiguina 1835 eruption released sulfur in sufficient quantities to perturb climate.

### Was Cosiguina the source of the bipolar 1809 volcanic signal?

Although 1835 Cosiguina tephra is chemically similar to Antarctic 1809 tephra and Cosiguina eruptions are capable of releasing sulfur in sufficient quantities to produce the bipolar 1809 volcanic signal, a positive identification of the 1809 volcano requires identification of a geologic deposit that can be reliably dated to 1809. However, recent work on Cosiguina has not uncovered any geologic evidence for an eruption around 1809 (W. Scott, pers. comm.). Furthermore, contemporary accounts of the 1835 eruption describe the volcano as having never been previously active within the memory of persons living at that time (Galindo, 1835; Feldman, 1993). In fact, the 1809 eruption date in the Simkin and Seibert chronology may be spurious and arisen from a misprint (S. Self and L. Seibert, pers. comm.). However, at least one historical account (Caldcleugh, 1836) mentions an eruption of Cosiguina in 1809. Furthermore, Caldcleugh states that the 1835 eruption occurred “after twenty-years of repose,” demonstrating that any possible error in reported Cosiguina eruption dates did not originate in the Simkin and Seibert chronology. Unfortunately, Caldcleugh does not provide his source for Cosiguina eruption dates prior to 1835, making it impossible to verify their accuracy. Nonetheless, given the lack of geologic evidence and the inconsistency of historical accounts concerning activity at Cosiguina prior to 1835, it appears unlikely there was an eruption of Cosiguina around 1809 of sufficient magnitude to produce the bipolar 1809 volcanic signal.

A search of the Global Volcanism Database identifies twenty volcanoes known or thought to have been active in the period 1808-1810 (Table VI.4). Eleven of these can be ruled out as possible sources of the bipolar 1809 volcanic signal for one or both of the following reasons: the volcano is basaltic or dacitic rather than andesitic in composition; or the volcano is located at extra-tropical latitudes where an eruption plume will remain in the hemisphere of origin and not reach both polar regions. Andesitic subduction volcanoes at tropical latitudes are found in Central America, the northern Andes, the West Indies, Indonesia (Sunda and Sangihe arcs), the Philippines, and the tropical Pacific (e.g., New Guinea, New Hebrides). In the following



paragraphs we consider all geologic, geochemical, and historical evidence that we are aware of to ascertain whether any of the volcanoes in these regions thought to have been active around 1809 could be the source of the bipolar 1809 volcanic signal. Of course, it is possible the 1809 source volcano is one whose activity during this time remains unsuspected.

Of the several hundred andesitic volcanoes in the Andean Cordillera, only 47 have recorded historical eruptions (Casertano, 1962). However, there are probably many others with recent eruptions for which no records exist (Thorpe and Francis, 1979). A major eruption at Volcán Putana, northern Chile, was reported in the early 19th century (Rudolph, 1955), while González-Ferrán (1995) reports there were no historical eruptions. However, historical records are especially scarce in the minimally populated Atacama Desert region of northern Chile, and apparently no detailed geologic studies of Volcán Putana have been carried out. Since nearby volcanoes in the Central Andes Volcanic Zone produce more silicic products; the Antarctic 1809 tephra appears to be too basic to have come from Putana (J.E. Guest, pers. comm.). Volcán de Colima, Mexico, was in a state of sporadic activity through 1809 following major activity in 1806 (Gonzalez *et al.*, 2002; Luhr, 2002). Given the relatively minor nature of the activity at Volcán de Colima in 1809 and compositional differences between recent products and the 1809 ice core tephra significant at the 90% confidence level or higher for all constituents, we conclude that Volcán de Colima is not the unknown 1809 volcano. Soufrière Guadeloupe, a dacitic to andesitic volcano in the West Indies, underwent a period of phreatic activity (steam explosions) from 1809 to 1810 but the last magmatic eruption was in the sixteenth century (Feuillard *et al.*, 1983; Ingrin and Poirier, 1986), making Soufrière Guadeloupe an unlikely source of the bipolar 1809 volcanic signal.

Taal Volcano in southwestern Luzon, Philippines, was active during the first half of 1808. All historic activity at Taal has originated from Volcano Island within the Taal caldera lake. Silica contents of Volcano Island lavas generally fall within a narrow compositional range of 50 to 51%, with only a few samples having silica contents approaching 58% (Miklius *et al.*,

1991), making Taal products probably too basic to be the source of the Antarctic 1809 tephra. There were at least five Indonesian volcanoes active between 1808 and 1810. Given the large number of volcanoes in the Sunda-Sangihe arcs spanning a distance of over 6000 km and the relative isolation of parts of the Indonesian archipelago, Indonesia is the most likely location of the 1809 volcano. In fact, 18 eruptions of  $VEI \geq 4$  were reported in Indonesia between 1812 and 2002 (Simkin and Seibert, 1994), an average of one per decade. However, between 1693 and 1812 only one  $VEI \geq 4$  eruption was reported (Makian in 1760). Interestingly, the number of reported eruptions in Indonesia approaches the modern average between 1586 and 1693 with 9  $VEI \geq 4$  eruptions reported. It seems likely that the number of volcanic eruptions in Indonesia was under-reported between 1693 and 1812.

Guntur Volcano in west Java was active in 1809, but its products are too silica-poor (51-57%; de Hoog *et al.*, 2001) to be the source of the Antarctic tephra. Merapi, central Java, probably the most intensively studied volcano in Indonesia, began a period of lava dome growth in 1810 (Voight *et al.*, 2000). Since this activity was minor in nature and Merapi products range from basalts to basaltic andesites, Merapi can also be ruled out as a possible source of the bipolar 1809 volcanic signal. Activity beginning in December 1808 at Lamongan in east Java consisted of Strombolian type eruptions and effusive lava flows with silica contents ranging from 43 to 56 wt. % (Carn, 2000). Such basaltic to basaltic-andesite products are too low in silica (Carn and Pyle, 2001) to be the source of the Antarctic 1809 tephra. There was also an explosive eruption in 1808 at Ruang Volcano in the Sangihe Arc, eastern Indonesia, not to be confused with the better-known Raung Volcano on Java (Neumann van Padang, 1959). However, since Ruang products range from 53 to 57% silica by weight (Morrice *et al.*, 1983), this volcano is also too basic to be the source of the Antarctic 1809 tephra.

There is almost no written record describing historical activity at Agung Volcano, Bali, prior to its well studied 1963 eruption (Zen and Hadikusumo, 1964; Self and King, 1996). Historical accounts of the 1815 Tambora eruption from Banyuwangi, eastern Java report “similar

effects in lesser degree” from an eruption of Carang Assum volcano (Agung) on Bali seven years prior to Tambora (Raffles, 1817). However, Matthews (1965) writes in a narrative of events during the 1963 eruptions in the Balinese village of Iseh that, according to village lore, the last eruption of Agung occurred in A.D. 196. Apparently, no record of Agung eruptions exists in the chronicles of Portuguese or Dutch colonialists (B. de Jung-Boers, pers. comm.), although the volcanic nature of Agung was well known (Matthews, 1965). We used a t-test to compare andesitic glasses from the Agung 1963 eruption (Self and King, 1996) to the Antarctic 1809 tephra. While the  $\text{SiO}_2$ ,  $\text{Al}_2\text{O}_3$ ,  $\text{FeO}$ , and  $\text{MgO}$  contents of the Agung 1963 and South Pole 1809 glasses are statistically indistinguishable, we found differences significant at the 95% level for  $\text{K}_2\text{O}$ , at the 99% level for  $\text{TiO}_2$  and  $\text{CaO}$ , and at the 99.9% level for  $\text{Na}_2\text{O}$ . Compositional differences are more salient when the Agung 1963 and Dome C 1809 glasses are compared, with differences significant at the 90% level for  $\text{MgO}$  and  $\text{K}_2\text{O}$ , and at the 99.9% level for  $\text{TiO}_2$ ,  $\text{FeO}$ ,  $\text{CaO}$ , and  $\text{Na}_2\text{O}$ . Since there have been no geochemical studies of Agung products from earlier eruptions, an assessment of the geochemical variability between eruptions can not be made. Because tephra geochemistry of a given volcano can vary over time, the differences between ice core 1809 and Agung 1963 tephra do not rule out Agung as a possible source of the 1809 signal.

However, the uncertainty surrounding historical accounts of Agung eruptions prior to 1963 and compositional differences between its 1963 glasses and the Antarctic 1809 tephra argue against Agung as the 1809 volcano. Because Agung magma is exceptionally sulfur-rich, a relatively small eruption ( $0.5$  to  $2 \text{ km}^3$ ) from Agung could produce an atmospheric sulfate perturbation as great as much larger eruptions ( $10 \text{ km}^3$  or more) of more silicic, sulfur poor magmas (Rampino and Self, 1982). A volumetrically small, sulfur-rich eruption could be difficult to distinguish in the geologic record, especially in tropical regions where unconsolidated deposits erode quickly. Since the eruptive history of Agung is poorly understood, a detailed geologic investigation to establish a chronology of activity could elucidate when past eruptions of magnitude similar to the climate forcing 1963 eruption have taken place. Such a study could

help expand our knowledge of climate-forcing volcanic eruptions from sulfur-rich andesitic volcanoes, establish the nature of any activity at Agung around 1809, and define any geochemical variations in Agung andesites through time, potentially providing a definitive answer to whether Agung was the 1809 volcano. Determination of the trace and rare earth element composition of volcanic glass shards via ICP-MS, which is very sensitive to petrogenic process of magma generation, provides clearer discrimination of source volcanoes than major oxide data alone (e.g., Basile *et al.*, 2001). In fact, if such analyses are performed on the Antarctic tephra provided by the bipolar 1809 volcanic eruption, it may be possible to pinpoint the volcanic arc responsible for this eruption of global concern, and potentially even the source volcano.

### **Conclusions**

Tephra dated to 1809 in the Eclipse ice core is chemically distinct from 1809 tephra found in Antarctica, pointing to a second eruption in the Northern Hemisphere around this time. This eruption appears to be of negligible significance because little additional  $\text{SO}_4^{2-}$  was contributed by this eruption to the 1809 volcanic signal seen at Eclipse. We have shown that glass shards associated with the unknown 1809 volcanic horizon in ice cores from South Pole and Dome C, Antarctica closely match the composition of eruption products of Cosiguina Volcano. We calculated that the 1835 eruption of Cosiguina may have produced an atmospheric  $\text{SO}_4^{2-}$  perturbation similar to Pinatubo, suggesting that Cosiguina eruptions can release sufficient sulfur to produce the bipolar 1809 volcanic signal and result in global climate perturbations. However, the lack of geologic evidence and the inconsistency of historical accounts concerning activity at Cosiguina prior to 1835 make it unlikely that an eruption of sufficient magnitude occurred around 1809. A survey of andesitic eruptions thought to have taken place from tropical volcanoes between 1808 and 1810 has not elucidated a strong candidate for the 1809 volcano, although several volcanoes can be confidently ruled out. As a result, the source volcano responsible for the bipolar 1809 volcanic signal remains unknown.

### **Acknowledgements**

We thank E. Blake, S. Bastien, and A. Mondrick for field assistance and the Geological Survey of Canada (D. Fisher and C. Zdanowicz) for logistical assistance in recovering the 2002 Eclipse ice core. We also thank J. Palais and J. Johnson for helpful discussions that greatly improved the manuscript, W. Scott and S. Self for insights concerning eruptive activity at Cosiguina prior to 1835, B. de Jung-Boers for searching the Dutch East Indies records for reports of volcanic eruptions in Indonesia, and M. Twickler for assistance with the base map used in Figure VII.1. The National Science Foundation Office of Polar Programs funded this research.

**Table VII.1.** Major oxide composition of 1809 ice core tephra and Cosiguina tephra (1835 eruption). Compositions given as weight %, recalculated to a sum of 100%, where n is the number of samples analyzed. Values are means for the specified number of samples, with the standard deviation in parentheses.

Sample	SiO <sub>2</sub>	TiO <sub>2</sub>	Al <sub>2</sub> O <sub>3</sub>	FeO	MgO	CaO	Na <sub>2</sub> O	K <sub>2</sub> O	n	Reference
1809 Eclipse	64.86 (1.10)	1.15 (0.20)	16.13 (0.66)	3.84 (0.71)	1.12 (0.49)	3.56 (0.73)	6.64 (0.77)	2.70 (0.26)	10	This work
1809 South Pole	60.28 (1.41)	0.84 (0.16)	15.80 (1.77)	7.91 (1.86)	2.35 (0.93)	5.45 (0.92)	4.26 (0.75)	3.11 (1.38)	8	Palais <i>et al.</i> , 1990
1809 Dome C	59.44 (1.63)	0.67 (0.24)	16.43 (0.51)	9.00 (0.72)	2.83 (0.73)	5.44 (0.82)	4.14 (0.52)	2.05 (0.40)	13	De Angelis <i>et al.</i> , 1985
Cosiguina (1835 eruption)	60.47 (2.12)	0.98 (0.08)	16.39 (0.53)	8.14 (1.10)	2.60 (0.74)	5.08 (0.97)	4.20 (0.34)	2.13 (0.19)	21	J. Palais, unpublished data

**Table VII.2.** Calculated t statistics and significance levels for comparisons of 1809 ice core tephra and 1835 Cosiguina tephra, where df indicates the degrees of freedom for the t-test. The assumption of normal distribution required by the t-test is not met for constituents whose mean divided by the standard deviation is less than 2.5 in one or both data sets to be compared. This situation is denoted by n.a. (not applicable). Probability levels are the chance the sample sets would have observed values so different if they were from the same population.

Sample Sets	df	SiO <sub>2</sub>	TiO <sub>2</sub>	Al <sub>2</sub> O <sub>3</sub>	FeO	MgO	CaO	Na <sub>2</sub> O	K <sub>2</sub> O
Eclipse 1809 - SP1809 Probability <	16	<b>7.51</b> 0.001	<b>3.64</b> 0.01	0.50	<b>5.87</b> 0.001	n.a.	<b>4.74</b> 0.001	<b>6.62</b> 0.001	n.a.
Eclipse 1809 - Dome C 1809 Probability <	21	<b>9.48</b> 0.001	<b>5.21</b> 0.001	1.17	<b>17.18</b> 0.001	n.a.	<b>5.80</b> 0.001	<b>8.80</b> 0.001	4.74 0.001
SP 1809 - Dome C 1809 Probability <	19	1.24	<b>1.91</b> 0.1	0.98	1.59	1.24	0.02	0.39	n.a.
SP1809 - Cosiguina 1835 Probability <	27	0.28	<b>2.46</b> 0.05	0.93	0.32	0.68	0.94	0.22	n.a.
Dome C 1809 - Cosiguina 1835 Probability <	32	1.59	<b>4.57</b> 0.001	0.19	<b>2.75</b> 0.01	0.88	1.15	0.37	0.67
Eclipse 1809 - Cosiguina 1835 Probability <	29	<b>7.57</b> 0.001	<b>2.48</b> 0.05	1.09	<b>13.05</b> 0.001	n.a.	<b>4.85</b> 0.001	<b>9.54</b> 0.001	<b>6.24</b> 0.001

**Table VII.3.** Ice core volcanic sulfate fluxes from the 1809 eruption relative to Tambora, where  $f/f_T$  is the flux ratio of the 1809 eruption to the Tambora eruption in the same core. For Siple and South Pole, multiple cores are available.

Location	Site	Sulfate ( $\mu\text{g cm}^{-2}$ )		$f/f_T$	Reference
		1809	Tambora		
Yukon	Eclipse	3.7	7.1	0.52	This work
Greenland	Site T	2.8	4.7	0.60	Cole-Dai <i>et al.</i> , 1991
	GRIP	2.5	3.5	0.71	Clausen <i>et al.</i> , 1997
	GISP2	2.8	3.6	0.78	Zielinski, 1995
Antarctica	Siple (1)	5.3	12.9	0.41	Cole-Dai <i>et al.</i> , 1991
	Siple (2)	5.4	13.3	0.40	Cole-Dai <i>et al.</i> , 1997
	Dyer	5.4	9.0	0.60	Cole-Dai <i>et al.</i> , 1997
	Plateau Remote	0.8	2.2	0.37	Cole-Dai <i>et al.</i> , 2000
	South Pole (1)	3.0	7.2	0.41	Delmas <i>et al.</i> , 1992
	South Pole (2)	3.2	6.8	0.47	Delmas <i>et al.</i> , 1992
	Hercules Neve	0.7	1.7	0.45	Stenni <i>et al.</i> , 1999
	Law Dome	4.5	8.0	0.56	Palmer <i>et al.</i> , 2002



**Table VII.4.** Volcanic activity between 1808 and 1810 as reported by the Global Volcanism Program (www.volcano.si.edu).

Volcano	Location	Lat.	Eruption Date	VEI	Type	Reference
<b>Tropical andesitic volcanoes active between 1808 and 1810:</b>						
Putana	Chile	22° S	1810 ± 10 yrs	?	andesite-dacite	de Silva and Francis, 1991
Merapi	Indonesia	7° S	1810	1	basalt-andesite	Voight <i>et al.</i> , 2000
Soufrière	West Indies	16° N	June 1809	1	andesite-dacite	Ingrin and Poirier, 1986
Guadeloupe	West Indies	16° N	June 1809	1	basaltic andesite	de Hoog <i>et al.</i> , 2001
Guntur	Indonesia	7° S	May 9 1809	2	andesite	
Colima	México	19° N	1809	2?	andesite	Luhr, 2002
Lamongan	Indonesia	8° S	Dec 8 1808	2	basalt-b. andesite	Carn and Pyle, 2001
Taal	Philippines	14° N	Feb 1808	2	basalt-andesite	Miklius <i>et al.</i> , 1991
Ruang	Indonesia	2° N	1808	2	andesite	Morrice <i>et al.</i> , 1983
Agung	Indonesia	8° S	1808	2	andesite	Self and King, 1996
<hr style="border-top: 1px dashed black;"/>						
<b>Other volcanoes active between 1808 and 1810:</b>						
Jabal Yar	Saudi Arabia	17° N	1810 ± 10 yrs	2	basalt	
Piton de la Fournaise	Indian Ocean	21° S	Jul 17 1809	2	basalt	Staudacher <i>et al.</i> , 1998
Zao	Japan	38° N	Jun 12 1809	2	andesite	
Etna	Italy	37° N	Mar 27 1809	2	basalt	Bonaccorso <i>et al.</i> , 2004
San Jorge	Azores	38° N	May 1 1808	1	dacite	
Bandai	Japan	37° N	1808?	2	dacite	
Akan	Japan	43° N	1808?	?	dacite	
Karthala	Indian Ocean	11° S	1808	?	basalt	
Bogoslof	Alaska	54° N	1806-1823	2	basaltic-andesite	Miller <i>et al.</i> , 1998
Shikotsu	Japan	42° N	1804-1817	3	andesite	
Vesuvius	Italy	41° N	1796-1822	3	basalt	Belkin <i>et al.</i> , 1993

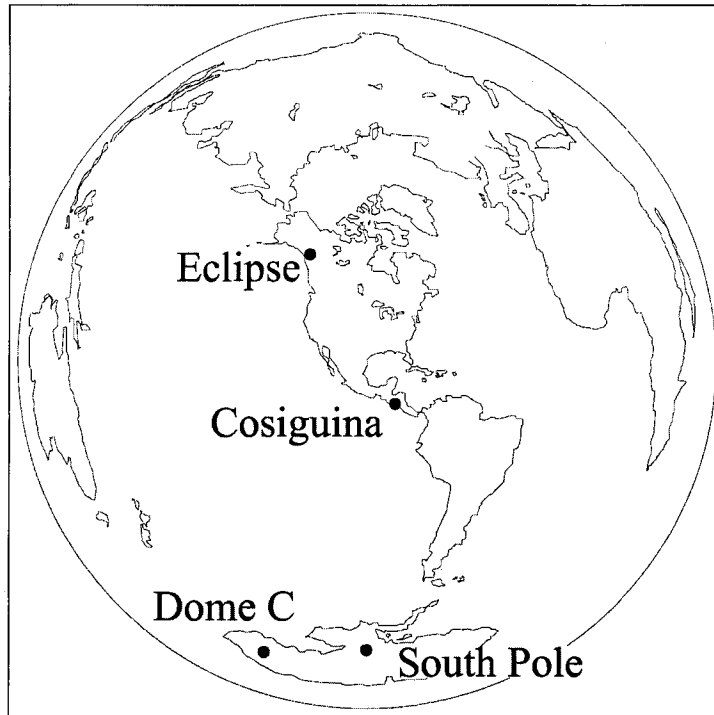


**Figure VII.1.** Location of the Eclipse, Dome C, and South Pole ice cores and Cosiguina Volcano.

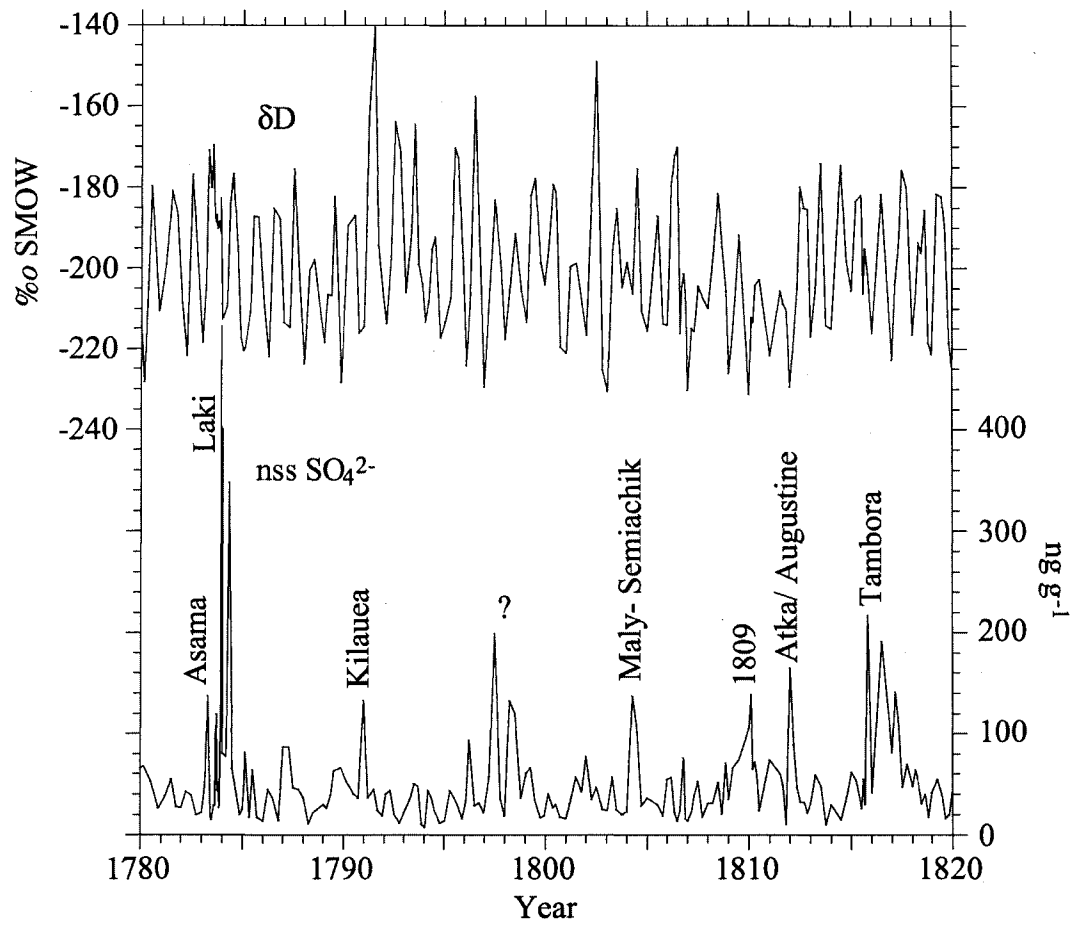


**Figure VII.2.** The  $\delta D$  (top) and non-sea-salt  $SO_4^{2-}$  (bottom) records from the Eclipse ice core for the period 1780 to 1820. Identifications of volcanic  $SO_4^{2-}$  signals are indicated.

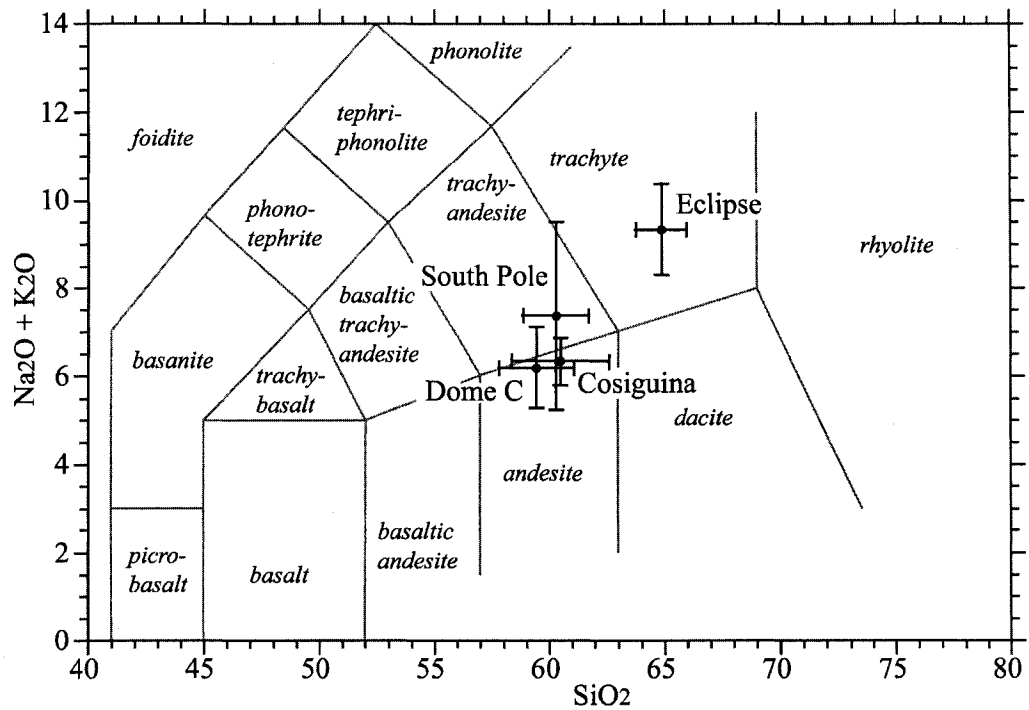


**Figure VII.3.** Chemical classification of 1809 ice core tephras using a total alkali ( $\text{Na}_2\text{O}+\text{K}_2\text{O}$ ) versus silica variation diagram and the nomenclature of LeBas *et al.* (1986). Error bars represent the standard deviation of tephra sets. Also plotted is the composition of tephra from the 1835 eruption of Cosiguina. Note the considerable overlap between the Antarctic tephras, their similarity to Cosiguina tephra, and separation from the Eclipse tephra.

## References

- Basile, I., J.R. Petit, S. Touron, F.E. Grousset, and N. Barkov, Volcanic layers in Antarctic (Vostok) ice cores: Source identification and atmospheric implications, *Journal of Geophysical Research*, 106, 31,915-31,931, 2001.
- Belkin, H.E., C.R. J. Kilburn, and B. de Vito, Sampling and major element chemistry of the recent (A.D. 1631-1944) Vesuvius activity, *Journal of Volcanology and Geothermal Research*, 568, 273-290, 1993.
- Bonaccorso, A., S. Calvari, M. Coltelli, C. Del Negro, and S. Falsaperla, Mt. Etna: Volcanic Laboratory, *Geophysical Monograph Series*, vol. 143, 369 pp., American Geophysical Union, Washington, D.C., 2004.
- Bradley, R.S., The explosive volcanic eruption record in northern hemisphere and continental temperature records, *Climatic Change*, 12, 221-243, 1988.
- Briffa, K.R., P.D. Jones, and F.H. Schweingruber, Summer temperatures across northern North America: regional reconstructions from 1760 using tree-ring densities, *Journal of Geophysical Research*, 99, 25,835-25,844, 1994.
- Briffa, K.R., P.D. Jones, F.H. Schweingruber, and T.J. Osborn, Influence of volcanic eruptions on Northern Hemisphere temperature over the past 600 years, *Nature*, 393, 450-454, 1998.
- Caldcleugh, A. Some account of the volcanic eruption of Coseguina in the Bay of Fonseca, commonly called the Bay of Conchagua, on the western coast of Central America, *Philosophical Transactions of the Royal Society of London*, 126, 27-30, 1836.
- Carn, S.A., The Lamongan volcanic field, East Java, Indonesia: physical volcanology, historic activity and hazards, *Journal of Volcanology and Geothermal Research*, 95, 81-108, 2000.
- Carn, S.A., and D.M. Pyle, Petrology and geochemistry of the Lamongan Volcanic Field, East Java, Indonesia: Primitive arc magmas in an extensional tectonic setting? *Journal of Petrology*, 42, 1643-1683, 2001.
- Casertano, L., General characteristics of active Andean Volcanoes and a summary of their activities during recent centuries, *Bulletin of the Seismological Society of America*, 53, 1415-1433, 1962.
- Chenoweth, M., Two major volcanic cooling episodes derived from global marine air temperature, AD 1807-1827, *Geophysical Research Letters*, 28, 2963-2966, 2001.
- Clausen, H.B., C.U. Hammer, C.S. Hvidberg, D. Dahl-Jensen, J.P. Steffensen, J. Kipfstuhl, and M. Legrand, A comparison of the volcanic records over the past 4000 years from the Greenland Ice Core Project and Dye 3 Greenland ice cores, *Journal of Geophysical Research*, 102, 26707-26723, 1997.
- Cole-Dai, J., E. Mosley-Thompson, and L. Thompson, Ice core evidence for an explosive tropical eruption 6 years preceding Tambora, *Journal of Geophysical Research*, 96, 17,361-17,366, 1991.

- Cole-Dai, J., E. Mosley-Thompson, and L. Thompson, Annually resolved southern hemisphere volcanic history from two Antarctic ice cores, *Journal of Geophysical Research*, 102, 16,761-16,771, 1997.
- Cole-Dai, J., E. Mosley-Thompson, S. Wight, and L. Thompson, A 4100-year record of explosive volcanism from an East Antarctic ice core, *Journal of Geophysical Research*, 105, 24,341-24,441, 2000.
- Crowley, T.J., T.R. Quinn, F.W. Taylor, C. Henin, and P. Joannot, Evidence for a volcanic cooling signal in a 335-year coral record from New Caledonia, *Paleoceanography*, 12, 633-639, 1997.
- De Angelis, M., L. Fehrenbach, C. Jehanno, and M. Maurette, Micrometer-sized volcanic glasses in polar ice and snows, *Nature*, 317, 52-54, 1985.
- de Hoog, J.C.M., B.E. Taylor, and M.J. van Bergen, Sulfur isotope systematics of basaltic lavas from Indonesia: implications for the sulfur cycle in subduction zones, *Earth and Planetary Science Letters*, 189, 237-252, 2001.
- de Silva, S.L., and P.W. Francis, *Volcanoes of the Central Andes*, Springer-Verlag, Berlin, 1991.
- Delmas, R.J., S. Kirchner, J.M. Palais, and J.R. Petit, 1000 years of explosive volcanism recorded at the South Pole, *Tellus*, 44, 335-350, 1992.
- Feldman, L.H., *Mountains of Fire, Lands that Shake: Earthquakes and Volcanic Eruptions in the Historic Past of Central America (1505-1899)*, 295 pp., Labyrinthos, Culven City, California, 1993.
- Feuillard, M., C.J. Allegre, G. Brandeis, R. Gaulon, J.L. Le Mouel, J.C. Mercier, J.P. Pozzi, and M. P. Semet, The 1975-1977 crisis of La Soufrière de Guadeloupe: A still-born magmatic eruption, *Journal of Volcanology and Geothermal Research*, 16, 317-334, 1983.
- Galindo, D.J., On the eruption of the volcano of Cosiguina, in Nicaragua, 17<sup>th</sup> January, 1835, *Journal of the Royal Geographic Society of London*, 5, 387-392, 1835.
- Gerlach, T.M., H.R. Westrich, T.J. Casadevall, and D.L. Finnegan, Vapor saturation and accumulation in magmas of the 1989-1990 eruption of Redoubt Volcano, Alaska, *Journal of Volcanology and Geothermal Research*, 62, 317-337, 1994.
- Germani, M.S. and P.R. Buseck, Evaluation of automated scanning electron microscopy for atmospheric particle analysis, *Analytical Chemistry*, 63, 2232-2237, 1991.
- Gonzalez-Ferran, O., *Volcanes de Chile*, Instituto Geografica Militar, Santiago, Chile, 1995.
- Gonzalez, M.B., J.R. Ramirez, and C. Navarro, Summary of the historical eruptive activity of Volcán de Colima, Mexico, 1519-2000, *Journal of Volcanology and Geothermal Research*, 117, 21-26, 2002.
- Harrington, C.R. (Ed.), *The Year Without a Summer? World Climate in 1816*, Canadian Museum of Nature, Ottawa, 1992.

- Ingrin, J., and J.P. Poirier, Transmission electron microscopy of ejects from the XVth century eruption of the Soufrière, Guadeloupe; microscopic evidence for magma mixing, *Journal of Volcanology and Geothermal Research*, 28, 161-174, 1986.
- Keenan, D.J., Volcanic ash retrieved from the GRIP ice core is not from Thera, *Geochemistry Geophysics Geosystems*, 4, 1097, doi: 10.1029/2003GC000608, 2003.
- Kohno, M., and Y. Fujii, Past 220-year bipolar volcanic signals: remarks on common features of their source eruptions, *Annals of Glaciology*, 35, 217-223, 2002.
- Krueger, A.J., L.S. Walter, P.K. Bhartia, C.C. Schnetzler, N.A. Krotkov, I. Sprod, and G.J.S. Bluth, Volcanic sulfur dioxide measurements from the total ozone mapping spectrometer, *Journal of Geophysical Research*, 100, 14057-17076, 1995.
- Lamb, H., Volcanic dust in the atmosphere with a chronology and assessment of its meteorological significance, *Philosophical Transactions of the Royal Society of London*, 266, 425- 533, 1970.
- Langway, C.C., K. Osada, H.B. Clausen, C.U. Hammer, and H. Shoji, A 10-century comparison of prominent bipolar volcanic events in ice cores, *Journal of Geophysical Research*, 100, 16,241- 16,247, 1995.
- Legrand, M., and R.J. Delmas, A 220 year continuous record of volcanic H<sub>2</sub>SO<sub>4</sub> in the Antarctic ice sheet, *Nature*, 327, 671- 676, 1987.
- Luhr, J.F. Petrology and geochemistry of the 1991 and 1998-1999 lava flows from Volcán de Colima, Mexico: implications for the end of the current eruptive cycle, *Journal of Volcanology and Geothermal Research*, 117, 169-194, 2002.
- Matthews, A., *The Night of Purnama*, 200 pp., Jonathan Cape, London, 1965.
- Miklius, A., M.J.F. Flower, J.P.P. Huijsmans, S.M. Mukasa, and P. Castillo, Geochemistry of lavas from Taal Volcano, Southwestern Luzon, Philippines: evidence for multiple magma supply systems and mantle source heterogeneity, *Journal of Petrology*, 32, 593-627, 1991.
- Miller, T.P., R.G. McGimsey, D.H. Richter, J.R. Riehle, C.J. Nye, M.E. Yount, and J.A. Dumoulin, *Catalog of the Historically Active Volcanoes of Alaska*, U.S. Geological Survey Open-File Report 98-582, 104 pp, 1998.
- Moore, J.C., H. Narita, and N. Maeno, A continuous 770-year record of volcanic activity from East Antarctica, *Journal of Geophysical Research*, 98, 17,353- 17,359, 1991.
- Morrice, M.G., P.A. Jezek, J.B. Gill, D.J. Whitford, and M. Monoarfa, An introduction to the Sangihe Arc: Volcanism accompanying arc-arc collision in the Molucca Sea, Indonesia, *Journal of Volcanology and Geothermal Research*, 19, 135-165, 1983.
- Mosley-Thompson, E., T.A. Mashiotta, and L. Thompson, High-resolution ice core records of late Holocene volcanism: current and future contributions from the Greenland PARCA cores, in *Volcanism and the Earth's Atmosphere*, *Geophysical Monograph Series*, vol.

- 139, edited by A. Robock, and C. Oppenheimer, pp. 153-164, American Geophysical Union, Washington, D.C., 2003.
- Neumann van Padang, M., Changes in the top of Mount Ruang (Indonesia), *Geologie en Mijnbouw*, 21, 113-118, 1959.
- Palais, J. and H. Sigurdsson, Petrologic evidence of volatile emissions from major historic and prehistoric volcanic eruptions, in *Understanding Climate Change, Geophysical Monograph Series, vol. 52*, edited by A. Berger, pp. 31-53, American Geophysical Union, Washington, D.C., 1989.
- Palais, J.M., S. Kirchner, and R.J. Delmas, Identification of some global volcanic horizons by major element analysis of fine ash in Antarctic ice, *Annals of Glaciology*, 14, 216-220, 1990.
- Palais, J.M., M.S. Germani, and G.A. Zielinski, Inter-hemispheric transport of volcanic ash from a 1259 A.D. volcanic eruption to the Greenland and Antarctic ice sheets, *Geophysical Research Letters*, 19, 801-804, 1992.
- Palmer, A.S., T.D.S. van Ommen, M.A.J. Curran, V. Morgan, J.M. Souney, and P.A. Mayewski, High precision dating of volcanic events (A.D. 1301-1995) using ice cores from Law Dome, Antarctica, *Journal of Geophysical Research*, 106, 28,089- 28,095, 2001.
- Palmer, A.S., V.I. Morgan, M.A.J. Curran, T.D. Van Ommen, and P.A. Mayewski, Antarctic volcanic flux ratios from Law Dome ice cores, *Annals of Glaciology*, 35, 329-332, 2002.
- Quinn, W.H., A study of Southern Oscillation-related climatic activity for A.D. 622-1990 incorporating Nile River flood data, in *El Nino: Historical and Paleoclimatic Aspects of the Southern Oscillation*, edited by H.F. Diaz and V. Markgraf, pp. 119-149, Cambridge University Press, New York, 1992.
- Raffles, T.S., *The History of Java*, Black, Parbury, and Allen, London, 1817.
- Rampino, M.R., and S. Self, Historic eruptions of Tambora (1815), Krakatau (1883) and Agung (1963), their stratospheric aerosols and climatic impact, *Quaternary Research*, 18, 127-143, 1982.
- Robock, A., Volcanic eruptions and climate, *Reviews of Geophysics*, 38, 191- 219, 2000.
- Rudolph, W.E., Licancabur: mountain of the Atacamenos, *Geography Review*, 45, 151-171, 1955.
- Scaillet, B., J. Luhr, and M.R. Carroll, Petrological and volcanological constraints on volcanic sulfur emissions to the atmosphere, in *Volcanism and the Earth's Atmosphere, Geophysical Monograph Series, vol. 139*, edited by A. Robock and C. Oppenheimer, pp. 11-40, American Geophysical Union, Washington, D.C., 2003.
- Self, S., M.R. Rampino, and M.J. Carr, A reappraisal of the 1835 eruption of Cosiguina and its atmospheric impact, *Bulletin of Volcanology*, 52, 57- 65, 1989.
- Self, S., and A.J. King, Petrology and sulfur and chlorine emissions of the 1963 eruption of Gunung Agung, Bali, Indonesia, *Bulletin of Volcanology*, 58, 263-285, 1996.



- Simkin, T., and L. Siebert, *Volcanoes of the World*, Geoscience Press, Tucson, Arizona, 1994.
- Staudacher, T., P. Bachelery, M.P. Semet, and J.L. Cheminee, Piton de la Fournaise, *Bulletin of the Global Volcanism Network*, 23, 2-4, 1998.
- Stenni, B., R. Caprioli, L. Cimmino, C. Cremisini, O. Flora, R. Gragnani, A. Longinelli, V. Maggi, and S. Torcini, 200 years of isotope and chemical records in a firn core from Hercules Neve, northern Victoria Land, Antarctica, *Annals of Glaciology*, 29, 106-112, 1999.
- Stenni, B., M. Proposito, R. Gragnani, O. Flora, J. Jouzel, S. Falourd, and M. Frezzotti, Eight centuries of volcanic signal and climate change at Talos Dome, East Antarctica, *Journal of Geophysical Research*, 107, doi:10.1029/2000JD000317, 2002.
- Thorpe, R.S., and P.W. Francis, Variations in Andean andesite compositions and their petrogenic significance, *Tectonophysics*, 57, 53-70, 1979.
- Voight, B., E.K. Constantine, S. Siswoidjyo, and R. Torely, Historical eruptions of Merapi Volcano, Central Java, Indonesia, 1768-1998, *Journal of Volcanology and Geothermal Research*, 100, 69-138, 2000.
- Wallace, P.J., Volcanic SO<sub>2</sub> emissions and the abundance and distribution of exsolved gas in magma bodies, *Journal of Volcanology and Geothermal Research*, 108, 85-106, 2001.
- Williams, H. The great eruption of Cosiguina, Nicaragua, *University of California Publications in Geological Science*, 29, 21-46, 1952.
- Yalcin, K., C.P. Wake, and M. Germani, A 100-year record of North Pacific volcanism in an ice core from Eclipse Icefield, Yukon, Canada, *Journal of Geophysical Research*, 108, doi:10.1029/2002JD002449, 2003.
- Zen, M.T., and D. Hadikusumo, Preliminary report on the 1963 eruption of Mt. Agung in Bali (Indonesia), *Bulletin of Volcanology*, 27, 269-300, 1964.
- Zielinski, G.A., P.A. Mayewski, L.D. Meeker, S. Whitlow, M.S. Twickler, M. Morrison, D. Meese, R.B. Alley, and A.J. Gow, Record of volcanism since 7000 B.C. from the GISP2 Greenland ice core and implications for the volcano-climate system, *Science*, 264, 948-952, 1994.
- Zielinski, G.A., Stratospheric loading and optical depth estimates of explosive volcanism over the last 2100 years derived from the GISP2 Greenland ice core, *Journal of Geophysical Research*, 100, 20,937- 20,955, 1995.

## CHAPTER VIII

### CONCLUSIONS

The Arctic represents a key region for global change research due to the sensitivity of the Arctic to climate change, climate feedbacks making change in the Arctic a precursor to change elsewhere, and the wealth of paleoenvironmental records available from the region. Although numerous ice cores have been recovered from Greenland and the eastern Canadian Arctic, the growing suite of ice cores from the St. Elias Mountains represents a shift in the focus for glaciochemical research to include the North Pacific sector of the Arctic. Ice cores from the North Pacific provide records of paleoclimate and paleoenvironmental changes distinct from the North Atlantic region because they are influenced by climate regimes that characterize the North Pacific such as the Pacific Decadal Oscillation and the Pacific/North American pattern. Furthermore, the region is influenced by North Pacific and Asian sources of natural and anthropogenic aerosols, while eastern Arctic ice cores such as those from the Penny Ice Cap and south (20D) and central (GISP2) Greenland are influenced by North Atlantic and North American sources. North Pacific ice cores also contain information on the role of the Pacific Ocean in atmospheric teleconnections and climate dynamics, thereby complementing existing knowledge on the climatic role of the North Atlantic region. Furthermore, the North Pacific climate variability is coupled to the ENSO system and the tropics, allowing investigations of changes in teleconnections between the tropics and mid-to-high latitudes on decadal to millennial time scales using North Pacific ice cores (Moore *et al.*, 2001; Fisher *et al.*, in press).

Regional paleoclimate records such as that from Eclipse are also important for understanding the regional details of climate change and investigating the differences in climate

variability and forcings between disparate regions. A spatial network of multi-variate ice core records from glaciers in different climatic regions provides the framework to investigate variability of climate on both spatial and temporal scales. In addition, the elevation range of 3 to more than 5 km spanned by the St. Elias ice cores provides the opportunity to investigate different moisture and impurity sources and different atmospheric transport pathways. The Eclipse site at 3017 m sees mostly local to regional sources, while the higher elevation King Col (4135) and Mt. Logan (5340 m) sites are influenced by more distant sources of moisture and atmospheric impurities (Holdsworth *et al.*, 1988, 1992; Yalcin *et al.*, 2003, in press; Wake *et al.*, 2004; Fisher *et al.*, in press).

For example, a one thousand year record of forest fire activity developed using the three ice cores available from Eclipse Icefield suggests that the Eclipse site records mostly forest fires in Alaska and the Yukon. Fire activity in these regions responds to both anthropogenic influences, such as the Klondike Gold Rush, and natural climate variability, such as the warm and dry conditions prevalent during the Medieval Warm Period. The Eclipse forest fire record bears little resemblance to the forest fire record developed from the Mt. Logan Northwest Col ice core (Whitlow *et al.*, 1994). In fact, the Eclipse forest fire record correlates better with the record from 20D, south Greenland, than it does with the Mt. Logan record. It appears that the Mt. Logan ice core samples forest fires burning in Siberia, while the Eclipse site records forest fires burning in nearby regions of Alaska and the Yukon.

The Eclipse site also records a larger number of moderate volcanic eruptions in Alaska, the Aleutian Islands, and Kamchatka than does the Mt. Logan site. Eruptions elsewhere in the Northern Hemisphere extra-tropics, specifically Iceland, Japan and the Kurile Islands, are more important sources of volcanic  $\text{SO}_4^{2-}$  signals at 5340 m on Mount Logan (39% of signals) than at 3017 m on Eclipse Icefield (15% of signals), even though the ice core sites are separated by only 45 km. Mount Logan, at 5 km elevation, is suitably located to sample the upper troposphere but misses plumes confined to the lower troposphere, and hence records a greater proportion of

signals from eruption clouds traveling at higher altitudes. Meanwhile, Eclipse Icefield at 3 km elevation, is suitably located to sample the lower troposphere, and hence records a greater proportion of signals from moderate eruptions carried in the lower troposphere. Tephrochronological evidence from the Eclipse ice core also documents eruptions in Alaska, Kamchatka, and Iceland. There is no convincing evidence from the Eclipse ice cores for the preservation of tephra at this site from more distant eruptions in the tropics. Recovery of dacitic tephra from the 1809 horizon in the Eclipse ice core with a chemical composition distinct from andesitic 1809 tephra found in Antarctic ice cores therefore indicates a second eruption in the Northern Hemisphere, most likely in Alaska or Kamchatka, at this time.

Aerosol and snowpit sampling at King Col (4135 m) also demonstrates the importance of more distant sources at higher elevations in the St. Elias, especially Asian sources. Backwards trajectories for select aerosol concentration peaks document the transport of Asian dust and anthropogenic emissions to King Col at discrete times during the sampling period. Likewise, the 2001 Asian dust plume is clearly recorded in snowpits from King Col while there is no clear signature from this event at Eclipse. Most of the dust at lower elevation sites in the St. Elias is apparently derived from local loess deposits while Asian dust is predominate at King Col and higher elevations (Zdanowicz *et al.*, 2004). Trends in anthropogenic sulfate and nitrate deposition and analysis of sea level pressure fields associated with high sulfate and nitrate deposition at Eclipse suggest transport over the pole from central Europe and the Ural Mountain regions as the source of anthropogenic sulfate and nitrate at lower elevation sites in the St. Elias, rather than trans-Pacific transport from East Asia (Yalcin and Wake, 2001, Wake *et al.*, 2002). These trends at Eclipse are distinctly different from anthropogenic sulfate and nitrate trends observed in ice cores from Greenland as well as the Penny Ice Cap in the eastern Canadian Arctic (Goto-Azuma and Koerner, 2001). Furthermore, no anthropogenic increase in sulfate and nitrate is discernible in ice cores from the summit plateau of Mt. Logan (Mayewski *et al.*, 1993).

This work also provides a detailed investigation of the variability in preserved glaciochemical signals using multiple ice cores records from a single mountain glacier site. Comparison of forest fire signals in the Eclipse ice cores with the record of annual area burned in Alaska and the Yukon demonstrates that 80% of high fire years in Alaska and 79% of high fire years in the Yukon are identifiable as  $\text{NH}_4^+$  concentration residuals in at least one core from Eclipse Icefield, although any individual core only records between 33 and 67% of these events. Although there are several moderately large ( $\text{VEI} \geq 4$ ) eruptions recorded in only one of the three available cores from Eclipse Icefield, the use of multiple records provides signals in at least one core from all known VEI 4 eruptions in Alaska and Kamchatka since the 1820's. Comparison of volcanic  $\text{SO}_4^{2-}$  fluxes for individual eruptions demonstrates a high degree of reproducibility for the largest sulfur producing eruptions such as Katmai 1912. Likewise, volcanic sulfate fluxes from some moderate eruptions vary by as little as 20% between the three cores, while others vary by as much as factor of three. These results are encouraging because they demonstrate the reproducibility of atmospheric  $\text{SO}_4^{2-}$  loading from volcanic eruptions as reconstructed from ice cores, particularly for the larger eruptions. However, calculations of sulfate loading for smaller eruptions should be treated with caution.

Spatial variability in snow chemistry was also investigated using snowpit samples from Eclipse and replicate fresh and surface snow samples from King Col. Species present as coarse mode particles ( $\text{Na}^+$ ,  $\text{Cl}^-$ ,  $\text{Ca}^{2+}$ ,  $\text{Mg}^{2+}$ ) display more spatial variability than do species present mainly in accumulation mode aerosols ( $\text{SO}_4^{2-}$ ,  $\text{NH}_4^+$ ) or in the gas phase ( $\text{NO}_3^-$ ) due to the spotty nature of coarse particle deposition, in agreement with the results of other studies (e.g., Dibb and Jaffrezo, 1997). Spatial variability in snow chemistry appears to be linked to the physical state of the species being deposited. The large amount of signal common to all four snowpits is encouraging for the use of ice cores from Eclipse Icefield in paleoclimatic reconstructions. Since sulfate has the highest amount of signal common to all four snowpits (73- 83%), reconstructions of both anthropogenic sulfate deposition and the atmospheric effects of volcanic eruptions in the

North Pacific from the Eclipse ice cores are particularly robust. A similar pattern of variability is evident when annually averaged ice core data from Eclipse is considered (Wake *et al.*, 2004). A single ice core from Eclipse Icefield provides a record that is 68% to 74% signal on annual time scales for stable isotopes, accumulation, and sulfate; but contains somewhat less signal (57-63%) for dust and sea salt species.

### **Suggestions for Future Research**

Comparison of recent snow chemistry at Eclipse Icefield and King Col demonstrate significant differences in snow chemistry between the two sites (Chapter IV). For example, inputs of sea salt and dust at Eclipse are greater by factors of two to five, respectively, and the average  $\text{Cl}^-/\text{Na}^+$  micro-equivalent ratio in snow at Eclipse (1.37) more closely approaches the seawater ratio than King Col snow (2.56). While the spring aerosol at King Col has been characterized by a short sampling period, such a study has not yet been carried out at Eclipse Icefield. Considering the relative ease of access to Eclipse Icefield, and the expected differences in aerosol chemistry with elevation in the St. Elias Mountains, a campaign to collect simultaneous aerosol and snow samples over a multi-week period at Eclipse Icefield is recommended. At the same time, meteorological data should be collected to investigate the relationships between snow chemistry and local meteorological variables. Ideally, a second team would perform contemporaneous sampling at King Col. Such a program would provide the information needed to characterize the aerosol at Eclipse Icefield, examine the relationships between aerosol and snow chemistry on an event basis, and compare aerosol concentrations and source regions at Eclipse Icefield to those at King Col. This information would improve the interpretation of the glaciochemical records from Eclipse Icefield, and add to our understanding of vertical gradients in aerosol and precipitation chemistry in the St. Elias Mountains.

Eclipse Icefield provides a record of forest fire frequency in Alaska and the Yukon over the last several hundred years. Comparison of the Eclipse record with the existing record from

Mount Logan demonstrates that Mount Logan samples forest fire plumes from a different region, possibly Siberia. Analysis of the new record from Prospector-Russell Col for forest fire signatures and comparison to records of Siberian forest fires provided by remote sensing technologies since 1980 could demonstrate whether Siberia is in fact the source region of forest fire signals preserved at Mount Logan. Unfortunately, there is insufficient overlap between the existing Northwest Col record and remotely sensed data for such an analysis. Furthermore, trace gas measurements on the Northwest Col demonstrate anomalous CO<sub>2</sub> increases that are related to biomass burning (Holdsworth *et al.*, 1996). This data should be made available to the modeling community to investigate the role of boreal forest fires in the global carbon cycle over last several hundred years. Existing efforts have focused on the effects of boreal forest fires since 1990, and have demonstrated that forest fires in the boreal forest are important players in the global carbon cycle (e.g., French *et al.*, 2003). No modeling studies have examined the role of boreal forest fires in the global carbon cycle over longer time periods. The Mount Logan trace gas record (Dibb *et al.*, 1993) provides the data needed to constrain model simulations back to 1690 for such an investigation.

St. Elias ice cores record a large number of volcanic eruptions in Alaska and Kamchatka. However, the ability to confidently attribute volcanic signals to specific eruptions is hampered because few eruptions from this region are documented in the historical record prior to the 20<sup>th</sup> century. Tephrochronological evidence provides an important tool to conclusively link an ice core signal to an eruption from a specific volcano. However, many volcanoes produce tephra with similar major oxide distributions. Therefore, I suggest that future ice core tephrochronological work include determination of trace and rare earth element composition of volcanic glass shards via ICP-MS. These elements are very sensitive to petrogenic process of magma generation, providing clearer discrimination of source volcanoes than is possible from major oxide data alone (e.g., Basile *et al.*, 2001). In fact, if such analyses are performed on the Antarctic tephra provided by the bipolar 1809 volcanic eruption, it should be possible to pinpoint

the volcanic arc responsible for this eruption of global concern, and potentially even the source volcano.

In sampling the Clean Simon portion of the Eclipse Core 2 ice core using the University of Maine's fractional collector system,  $\text{NO}_3^-$  data was contaminated by the acid used to wash bottles for trace metal sample collection. In addition, the  $\text{Ca}^{2+}$  data was affected by co-elution of a second, unidentified species (possibly Ni or Al). When trace metal records are to be developed from future sites, I suggest that a minimum of two cores be drilled: one core for major ions, stable isotopes, radionuclides, etc, and the other core dedicated to trace element analyses because different protocols are required for major ion and trace metal sampling of ice cores. This would be a worthwhile endeavor because trace element analyses are a valuable addition to the wealth of environmental information available from ice cores. They provide the data needed to investigate crustal inputs and provenance (Al, Fe, rare earths), relate nutrient input to ocean productivity (Fe), and develop depositional records of anthropogenic contaminants (Zn, Hg, Pb, As, Cu, Cd).

Finally, these findings illustrate that the Eclipse site samples a distinct air mass with different source regions and transport histories, resulting in a glaciochemical record complementary to, yet distinct from, those available from nearby King Col and Mt. Logan. Continued, joint investigations of the glaciochemical time series developed from these sites and other ice cores already collected (e.g., Bona-Churchill, Wrangell, Kamchatka) as well as those that may be collected in the future (e.g., Denali) will enable a more detailed understanding of the environmental history of this geographically complex and climatologically important region. In particular, the different source regions sampled at different elevations could be robustly investigated through joint analysis of glaciochemical time series and atmospheric pressure patterns provided by the NCEP reanalysis products. This would allow a climatology of source regions for different species to be developed for each site and investigation of how these have changed over time.



## LIST OF REFERENCES

- Adams, J.B., M.E. Mann, and C.M. Ammann, Proxy evidence for an El Nino-like response to volcanic forcing, *Nature*, 426, 274-278, 2003.
- Alexander, B., J. Savarino, K.J. Kreutz, and M.H. Thiemens, Impact of pre-industrial biomass burning emissions on the oxidation pathways of tropospheric sulfur and nitrogen, *Journal of Geophysical Research*, 109, D08303, doi: 10.1029/2003JD004218, 2004.
- Alley, R.B., D. Meese, C.A. Shuman, A.J. Gow, K. Taylor, P. Grootes, M. Ram, E.D. Waddington, J.W.C. White, P.A. Mayewski, and G.A. Zielinski, Abrupt accumulation increase at the Younger Dryas termination in the GISP2 ice core, *Nature*, 362, 527-529, 1993
- Alley, R.B., Resolved: the Arctic controls global climate change, in *Modeling the Arctic system: a workshop report on the state of modeling in the Arctic system science program*, p. 90, 1997.
- Angell, J.K., and J. Korshover, Surface temperature changes following the six major volcanic episodes between 1780 and 1980, *Journal of Climate and Applied Meteorology*, 24, 937-951, 1985.
- Angell, J.K., Impact of El Nino on the delineation of tropospheric cooling due to volcanic eruptions, *Journal of Geophysical Research*, 93, 3697-3704, 1988.
- Arendt, A., K. Echelmeyer, W. Harrison, C. Lingle and V. Valentine, Rapid wastage of Alaska glaciers and their contribution to rising sea level, *Science*, 297, 382-386, 2002.
- Baltensperger, U., M. Schwikowski, H.W. Gaggeler, and D.T. Jost, The scavenging of atmospheric constituents by alpine snow, in *Precipitation Scavenging and Atmosphere-Surface Exchange*, edited by S.E. Schwartz and W.G.N. Slinn, pp. 483-493, Hemisphere, Washington, 1992.
- Baltensperger, U., H.W. Gaggeler, D.T. Jost, M. Lugauer, M. Schwikowski, and E. Weingartner, Aerosol Climatology at the high alpine site Jungfraujoch, Switzerland, *Journal of Geophysical Research*, 102, 19,707-19,715, 1997.
- Barclay, D.J., P.E. Calkin, G.C. Wiles, A 1119-year tree-ring-width chronology from western Prince William Sound, southern Alaska, *The Holocene*, 9, 79- 84, 1999.
- Barrie, L.A., D.A. Fisher, and R.M. Koerner, Twentieth century trends in Arctic air pollution revealed by conductivity and acidity observations in snow and ice in the Canadian high Arctic, *Atmospheric Environment*, 19, 2055- 2063, 1985.
- Barrie, L.A., and M.J. Barrie, Chemical components of lower tropospheric aerosol in the high Arctic: six years of observations, *Journal of Atmospheric Chemistry*, 11, 211-226, 1990.

- Bassett, M., and J.H. Seinfeld, Atmospheric equilibrium model of sulfate and nitrate aerosols, *Atmospheric Environment*, 17, 2237-2252, 1983.
- Basile, I., J.R. Petit, S. Touron, F.E. Grousset, and N. Barkov, Volcanic layers in Antarctic (Vostok) ice cores: Source identification and atmospheric implications, *Journal of Geophysical Research*, 106, 31,915-31,931, 2001.
- Beget, J.E., S.D. Stihler, D.B. Stone, A 500 year long record of tephra falls from Redoubt Volcano and other volcanoes in upper Cook Inlet, Alaska, *Journal of Volcanology and Geothermal Research*, 62, 55- 67, 1994.
- Belkin, H.E., C.R. J. Kilburn, and B. de Vito, Sampling and major element chemistry of the recent (A.D. 1631-1944) Vesuvius activity, *Journal of Volcanology and Geothermal Research*, 568, 273-290, 1993.
- Belkin, I.M., S. Levitus, J. Antonov, and S.A. Malmberg, Great salinity anomalies in the North Atlantic, *Progress in Oceanography*, 41, 1-68, 1998.
- Belousov, A., Deposits of the 30 March 1956 directed blast at Bezymianny volcano, Kamchatka, Russia, *Bulletin of Volcanology*, 57, 649-662, 1996.
- Benjey, W.G., the effects of forest-fire smoke on insolation in the St. Elias Mountains, in *Icefield Ranges Research Project, Scientific Results, vol. 4*, edited by V. Bushnell and M.G. Marcus, pp. 129-131, American Geographic Society, New York, and Arctic Institute of North America, Montreal, 1974.
- Bergin, M.H., J.L. Jaffrezo, C.I. Davidson, J.E. Dibb, S.N. Pandis, R. Hillamo, W. Maenhaut, H.D. Kuhns, and T. Makela, The contributions of snow, fog, and dry deposition to the summer flux of anions and cations at Summit, Greenland, *Journal of Geophysical Research*, 100, 16,275-16,288, 1995.
- Blake, E, Wake, C. and Gerasimoff, M., The ECLIPSE drill: a field portable intermediate-depth ice-coring drill, *Journal of Glaciology*, 44, 175-178, 1998.
- Bluth, G.J.S., C.C. Schnetzler, D.A. Krueger, and L.S. Walter, The contribution of explosive volcanism to global sulfur dioxide concentrations, *Nature*, 366, 327- 330, 1993.
- Boenisch G., J. Blindheim, J.L. Bullister, P. Schlosser, and D.W.R. Wallace, Long term trends of temperature, salinity, density, and transient tracers in the Greenland Sea, *Journal of Geophysical Research*, 102, 18,553-18,571, 1997.
- Bonaccorso, A., S. Calvari, M. Coltelli, C. Del Negro, and S. Falsaperla, Mt. Etna: Volcanic Laboratory, *Geophysical Monograph Series, vol. 143*, 369 pp., American Geophysical Union, Washington, D.C., 2004.
- Borys, R.D., D. Del Vecchio, J.L. Jaffrezo, J.E. Dibb, and D.L. Mitchell, Field observations, measurements, and preliminary results from a study of wet deposition processes influencing snow and ice chemistry at Summit, Greenland, in *Precipitation Scavenging and Atmosphere-Surface Exchange Processes*, vol. 3, edited by S.E. Schwarz and W.G.N. Slinn, pp. 1693-1702, Hemisphere, Washington, D.C. , 1992.

- Bradley, R.S., The explosive volcanic eruption record in northern hemisphere and continental temperature records, *Climatic Change*, 12, 221-243, 1988.
- Bradley, R.S., M.K. Hughes, and H.F. Diaz, Climate in Medieval time, *Science*, 302, 404-405, 2003.
- Braitseva, O.A., I.V. Melekestev, V.V. Ponomareva, V. Kirianov, The caldera-forming eruption of Ksudach volcano about cal. A. D. 240: the greatest explosive event of our era in Kamchatka, Russia, *Journal of Volcanology and Geothermal Research*, 70, 49- 65, 1996.
- Briffa, K.R., P.D. Jones, and F.H. Schweingruber, Tree- ring reconstructions of summer temperature patterns across western North America since 1600, *Journal of Climate*, 5, 735-754, 1992.
- Briffa, K.R., P.D. Jones, and F.H. Schweingruber, Summer temperatures across northern North America: regional reconstructions from 1760 using tree-ring densities, *Journal of Geophysical Research*, 99, 25,835-25,844, 1994.
- Briffa, K.R., P.D. Jones, F.H. Schweingruber, and T.J. Osborn, Influence of volcanic eruptions on Northern Hemisphere temperature over the past 600 years, *Nature*, 393, 450-454, 1998.
- Broecker, W.S., Thermohaline circulation, the Achilles heel of our climate system: Will man-made CO<sub>2</sub> upset the current balance? *Science*, 278, 1339-1342, 1997.
- Brown, R.D., Northern Hemisphere snow cover variability and change, 1915-1997, *Journal of Climate*, 13, 2339-2355, 2000.
- Bulletin of the Global Volcanism Network*, v. 26, n. 4, 2001.
- Bursik, M., I. Melekestsev and O. Braitseva, Most recent fall deposits of Ksudach volcano, Kamchatka, Russia, *Geophysical Research Letters*, 20, 1815- 1818, 1993.
- Caldcleugh, A. Some account of the volcanic eruption of Coseguina in the Bay of Fonseca, commonly called the Bay of Conchagua, on the western coast of Central America, *Philosophical Transactions of the Royal Society of London*, 126, 27-30, 1836.
- Calkin, P.E., G.C. Wiles, and D.J. Barclay, Holocene coastal glaciation of Alaska, *Quaternary Science Reviews*, 20, 449- 461, 2001.
- Calvert, J.K., A. Lazrus, G.L. Kok, B.G. Heikes, J.H. Walega, J. Lind, and C.A. Cantrell, Chemical mechanisms of acid generation in the troposphere, *Nature*, 317, 27-35, 1985.
- Carn, S.A. The Lamongan volcanic field, East Java, Indonesia: physical volcanology, historic activity and hazards, *Journal of Volcanology and Geothermal Research*, 95, 81-108, 2000.
- Carn, S.A., and D.M. Pyle, Petrology and geochemistry of the Lamongan Volcanic Field, East Java, Indonesia: Primitive arc magmas in an extensional tectonic setting? *Journal of Petrology*, 42, 1643-1683, 2001.

- Carrico, C.M., M.H. Bergin, A.B. Shrestha, J.E. Dibb, L. Gomes, and J.M. Harris, The importance of carbon and mineral dust to seasonal aerosol properties in the Nepal Himalaya, *Atmospheric Environment*, 37, 2811-2824.
- Casertano, L., General characteristics of active Andean Volcanoes and a summary of their activities during recent centuries, *Bulletin of the Seismological Society of America*, 53, 1415-1433, 1962.
- Cavalieri, D.J., P. Gloersen, C.L. Parkinson, J.C. Comiso, and H.J. Zwally, Observed hemispheric asymmetry in global sea- ice changes, *Science*, 278, 1104- 1106, 1997.
- Cavalieri, D.J., C.L. Parkinson, and K.Y. Vinnikov, 30-year satellite record reveals contrasting Arctic and Antarctic decadal sea-ice variability, *Geophysical Research Letters*, 30, 1970, doi: 10.1029/2003GL018031, 2003.
- Castellano, E., S. Becagli, J. Jouzel,, A. Migliori, M. Severi, J.P. Steffensen, R. Traversi, and R. Udisti, Volcanic eruption frequency over the last 45 ky as recorded in the EPICA-Dome C ice core (East Antarctica) and its relationship with climatic changes, *Global and Planetary Change*, 42, 195-205, 2004.
- Chapman, W. L., and J.E. Walsh, Recent variations of sea ice and air temperature in the high latitudes, *Bulletin of the American Meteorological Society*, 74, 33-47, 1993.
- Chenoweth, M., Two major volcanic cooling episodes derived from global marine air temperature, AD 1807-1827, *Geophysical Research Letters*, 28, 2963-2966, 2001.
- Clarke, G.C., G.M. Cross, and C.S. Benson, Radar imaging of glaciocvolcanic stratigraphy Mount Wrangell Caldera, Alaska: Interpretation model and results, *Journal of Geophysical Research*, 94, 7237-7249, 1989.
- Clausen, H.B., and C.U. Hammer, The Laki and Tambora eruptions as revealed in Greenland ice cores from 11 locations, *Annals of Glaciology*, 10, 16-22, 1988.
- Clausen, H.B., C.U. Hammer, C.S. Hvidberg, D. Dahl- Jensen, J.P. Steffensen, J. Kipfstuhl, and M. Legrand, A comparison of the volcanic records over the past 4000 years from the Greenland Ice Core Project and Dye 3 Greenland ice cores, *Journal of Geophysical Research*, 102, 26, 707- 26, 723, 1997.
- Cole, P.D., G. Queiroz, N. Wallenstein, J.L. Gaspar, A.M. Duncan, and J.E. Guest, An historic subplinian/phreatomagmatic eruption: the 1630 AD eruption of Furnas volcano, Sao Miguel, Azores, *Journal of Volcanology and Geothermal Research*, 69, 117-135, 1995.
- Cole-Dai, J., E. Mosley-Thompson, and L. Thompson, Ice core evidence for an explosive tropical eruption 6 years preceding Tambora, *Journal of Geophysical Research*, 96, 17,361-17,366, 1991.
- Cole-Dai, J., E. Mosley-Thompson, and L. Thompson, Annually resolved southern hemisphere volcanic history from two Antarctic ice cores, *Journal of Geophysical Research*, 102, 16,761-16,771, 1997.

- Cole-Dai, J., and E. Mosley-Thompson, The Pinatubo eruption in South Pole snow and its potential value to ice core paleovolcanic records, *Annals of Glaciology*, 29, 99-105, 1999.
- Cole-Dai, J., E. Mosley-Thompson, S. Wight, and L. Thompson, A 4100-year record of explosive volcanism from an East Antarctic ice core, *Journal of Geophysical Research*, 105, 24,341-24,441, 2000.
- Coombs, M.L., J.C. Eichelberger, and M.J. Rutherford, Magma storage and mixing conditions for the 1953-1974 eruptions of Southwest Trident volcano, Katmai National Park, Alaska, *Contributions to Mineralogy and Petrology*, 140, 99-118, 2000.
- Crowley, T.J., T.R. Quinn, F.W. Taylor, C. Henin, and P. Joannot, Evidence for a volcanic cooling signal in a 335-year coral record from New Caledonia, *Paleoceanography*, 12, 633-639, 1997.
- Crowley, T.J., and T.S. Lowery, How warm was the Medieval Warm Period? *Ambio*, 29, 51-54, 2000.
- Crutzen, P.J., and M.O. Andreae, Forest fire in the tropics: impact on atmospheric chemistry and biogeochemical cycles, *Science*, 250, 1669-1678, 1990.
- Curry, J.A., J.L. Schramm, and E.E. Ebert, Sea ice-albedo climate feedback mechanism, *Journal of Climate*, 8, 240-247, 1995.
- D'Arrigo, R.D. and G.C. Jacoby, Secular trends in high northern latitude temperature reconstructions based on tree rings, *Climatic Change*, 25, 163-177, 1993.
- D'Arrigo, R.D., and G.C. Jacoby, Northern North American tree-ring evidence for regional temperature changes after major volcanic events, *Climatic Change*, 41, 1-15, 1999.
- D'Arrigo, R., E. Mashig, D. Frank, G. Jacoby, and R. Wilson, Reconstructed warm season temperatures for Nome, Seward Peninsula, Alaska, *Geophysical Research Letters*, 31, L09202, doi: 10.10129/2004GL019756, 2004.
- Dansgaard, W., S.J. Johnsen, H.B. Clausen, and N. Gundestrup, Stable isotope glaciology, *Meddelelser om Gronland Bd*, 197, N2, 1-53, 1973.
- Dansgaard, W., and H. Oeschger, Past environmental long-term records from the Arctic, in *The Environmental Record in Glaciers and Ice Sheets*, edited by H. Oeschger and C.C. Langway, pp. 287- 317, Wiley, New York, 1989.
- Dansgaard, W., S.J. Johnsen, H.B. Clausen, D. Dahl-Jensen, N.S. Gundestrup, C.U. Hammer, C.S. Hvidberg, J.P. Steffensen, A.E. Sveinbjörnsdóttir, J. Jouzel, and G. Bond, Evidence for general instability of past climate from a 250-kyr ice-core record, *Nature*, 364, 218-220, 1993.
- Davi, N.K., G.C. Jacoby, and G.C. Wiles, Boreal temperature variability inferred from maximum latewood density and tree-ring width data, Wrangell Mountain region, Alaska, *Quaternary Research*, 60, 252-262, 2003.

- Davidson, C.I., S. Santhanam, R.C. Fortmann, and M.P. Olson, Atmospheric transport and deposition of trace elements onto the Greenland Ice Sheet, *Atmospheric Environment*, 19, 2065-2081, 1985.
- Davidson, C.I., J.R. Harrington, M.J. Stephenson, F.P. Boscoe, and R.E. Gandley, Seasonal variations in sulfate, nitrate, and chloride in the Greenland Ice Sheet: relation to atmospheric concentrations, *Atmospheric Environment*, 23, 2483-2491, 1989.
- Davidson, C.I., J.L. Jaffrezo, B.W. Mosher, J.E. Dibb, R.D. Borys, B.A. Bodhaine, R.A. Rasmussen, C.F. Boutron, F.M. Ducroz, M. Cahier, J. Ducret, J.L. Colin, N. Z. Heidam, K. Kemp, and R. Hillamo, Chemical Constituents in the air and snow at Dye 3, Greenland II. Analysis of episodes in April 1989, *Atmospheric Environment*, 27, 2723-2737, 1993.
- De Angelis, M., L. Fehrenbach, C. Jehanno, and M. Maurette, Micrometer-sized volcanic glasses in polar ice and snows, *Nature*, 317, 52-54, 1985.
- De Bell, L.J., M. Vozella, R.W. Talbot, and J.E. Dibb, Asian dust storm events of spring 2001 and associated pollutants observed in New England by the AIRMAP monitoring network, *Journal of Geophysical Research*, 109, 1304, doi: 10. 1029/2003JD003733, 2004.
- de Hoog, J.C.M., B.E. Taylor, and M.J. van Bergen, Sulfur isotope systematics of basaltic lavas from Indonesia: implications for the sulfur cycle in subduction zones, *Earth and Planetary Science Letters*, 189, 237-252, 2001.
- de Silva, S.L., and P.W. Francis, *Volcanoes of the Central Andes*, Springer-Verlag, Berlin, 1991.
- de Silva, S.L., and G.A. Zielinski, Global influence of the AD 1600 eruption of Huaynaputina, Peru, *Nature*, 393, 455-458, 1998.
- Delmas, R.J., M. Legrand, A. Aristarian, and F. Zanolini, Volcanic deposits in Antarctic snow and ice, *Journal of Geophysical Research*, 90, 12, 091- 12, 920, 1985.
- Delmas, R.J., S. Kirchner, J.M. Palais, and J.R. Petit, 1000 years of explosive volcanism recorded at the South Pole, *Tellus*, 44, 335- 350, 1992.
- Devine, J.D., H. Sigurdsson, and A.N. Davis, Estimates sulfur and chlorine yield to the atmosphere from volcanic eruptions and potential climatic effects, *Journal of Geophysical Research*, 89, 6309-6325, 1984.
- Dibb, J.E., The Chernobyl reference horizon (?) in the Greenland Ice Sheet, *Geophysical Research Letters*, 16, 987- 990, 1989.
- Dibb, J.E., R.A. Rasmussen, P.A. Mayewski, and G. Holdsworth, Northern Hemisphere concentrations of methane and nitrous oxide since 1800: results from the Mt. Logan and 20D ice cores, *Chemosphere*, 27, 2413-2423, 1993.
- Dibb, J.E., Overview of field data on the deposition of aerosol-associated species to the surface snow of polar glaciers, particularly recent work in Greenland; in *Processes of Chemical Exchange between the Atmosphere and Polar Snow*, NATO ASI Series, vol. 43, edited by E.W. Wolff and R. C. Bales, pp. 249-274, Springer, New York, 1996.

- Dibb, J.E., R.W. Talbot, S.I. Whitlow, M.C. Shipham, J. Winterle, J. McConnell, and R. Bales, Forest fire signatures in the atmosphere and snow at Summit, Greenland: An event on 5 August, 1994, *Atmospheric Environment*, 30, 553-561, 1996.
- Dibb, J.E., and J.L. Jaffrezo, Air-snow investigations at Summit, Greenland: An overview; *Journal of Geophysical Research*, 102, 26,795-26,807, 1997.
- Dibb, J.E., M. Arsenault, M.C. Peterson and R.E. Honrath, Fast nitrogen oxide photochemistry in Summit, Greenland snow, *Atmospheric Environment*, 36, 2501- 2511, 2002.
- Draxler, R.R., and G.D. Hess, Description of the HYSPLIT-4 modeling system, *NOAA Technical Memo, ERLARL-224*, 24 pp., 1997.
- Dunbar, N.W., G.A. Zielinski, and D.T. Voisins, Tephra layers in the Siple Dome and Taylor Dome ice cores, Antarctica: Sources and correlations, *Journal of Geophysical Research*, 108, 2374, doi:10.1029/2002JD0020256, 2003.
- Etheridge, D.M., G.I. Pearman and P.J. Fraser, Changes in tropospheric methane between 1841 and 1978 from a high accumulation rate Antarctic ice core, *Tellus*, 44, 282- 294, 1992.
- Feldman, L.H., *Mountains of Fire, Lands that Shake: Earthquakes and Volcanic Eruptions in the Historic Past of Central America (1505-1899)*, 295 pp., Labyrinthos, Culven City, California, 1993.
- Feuillard, M., C.J. Allegre, G. Brandeis, R. Gaulon, J.L. Le Mouel, J.C. Mercier, J.P. Pozzi, and M.P. Semet, The 1975-1977 crisis of La Soufrière de Guadeloupe: A still-born magmatic eruption, *Journal of Volcanology and Geothermal Research*, 16, 317-334, 1983.
- Fiacco, R.J., T. Thordarsson, M.S. Germani, S. Self, J.M. Palias, S. Whitlow, and P.M. Grootes, Atmospheric aerosol loading and transport due to the 1783-84 Laki eruption in Iceland as interpreted from ash particles and acidity in the GISP2 ice core, *Quaternary Research*, 42, 231- 240, 1994.
- Fierstein, J., and W. Hildreth, Ejecta dispersal and dynamics of the 1912 eruption at Novarupta, Katmai National Park, Alaska, *Eos, Transactions, American Geophysical Union*, 67, 1246, 1986.
- Fierstein, J., and W. Hildreth, The Plinian eruptions of 1912 at Novarupta, Katmai National Park, Alaska, *Bulletin of Volcanology*, 54, 646- 684, 1992.
- Fischer, H., D. Wagenbauch, and J. Kipfstuhl, Sulfate and nitrate firn concentrations on the Greenland ice sheet 2. Temporal anthropogenic deposition changes, *Journal of Geophysical Research*, 103, 21935- 21942, 1998.
- Fisher, D.A., R.M. Koerner, W.S.B. Paterson, W. Dansgaard, N. Gundestrup, and N. Reeh, Effect of wind scouring on climatic records from ice core oxygen isotope profiles, *Nature*, 301, 205-209, 1983.

- Fisher, D., High-resolution multiproxy climatic records from ice cores, tree rings, corals, and documentary sources using eigenvector techniques and maps: assessment of recovered signal and errors, *The Holocene*, 12, 401-419, 2002.
- Fisher, D.A., J. Bourgeois, M. Demuth, R. Koerner, M. Parnandi, J. Sekerka, C. Zdanowicz, J. Zheng, C. Wake, K. Yalcin, P. Mayewski, K. Kreutz, E. Osterberg, D. Dahl-Jensen, K. Goto-Azuma, G. Holdsworth, E. Steig, S. Rupper, and M. Wasckiewicz, Mount Logan ice cores: The water cycle of the North Pacific in the Holocene, *Eos, Transactions, American Geophysical Union*, 8, (47), Fall Meeting Supplement, Abstract PP23C- 07, 2004.
- Fisher, R.V., and H.U. Schminke, *Pyroclastic Rocks*, Springer-Verlag, Berlin, 1984.
- Flannigan, M.D., and J.B. Harrington, A study of the relation of meteorological variables to monthly provincial area burned by wildfire in Canada (1953-1980), *Journal of Applied Meteorology*, 27, 441-452, 1988.
- Forland, E.J., and I. Hanssen-Bauer, Increased precipitation in the Norwegian Arctic: True or false? *Climatic Change*, 46, 485-509, 2000.
- French, N.H.F., E.S. Kasischke, and D.G. Williams, Variability in the emission of carbon-based trace gases from wildfire in the Alaskan boreal forest, *Journal of Geophysical Research*, 108, 8151, doi: 10.1029/2001JD000480, 2003.
- Fritzsche, D., F. Wilhelms, L.M. Savatyugin, J.F. Pinglot, H. Meyer, H.W. Hubberten, and H. Miller, A new deep ice core from Akademii Nauk ice cap, Sernaya Zemlya, Eurasian Arctic: First results, *Annals of Glaciology*, 35, 25-28, 2002.
- Fuhrer, K., A. Neftel, M. Anclin, T. Staffelbach, and M. Legrand, High-resolution ammonium record covering a complete glacial-interglacial cycle, *Journal of Geophysical Research*, 101, 4147-4164, 1996.
- Fuhrer, K., and M. Legrand, Continental biogenic species in the Greenland Ice Core Project ice core: Tracing back the biomass history of the North American continent, *Journal of Geophysical Research*, 102, 26,735- 26,745, 1997.
- Galindo, D.J., On the eruption of the volcano of Cosiguina, in Nicaragua, 17<sup>th</sup> January, 1835, *Journal of the Royal Geographic Society of London*, 5, 387-392, 1835.
- Gard, E.E., M.J. Kleemna, D.S. Gross, L.S. Hughes, J.O. Allen, B.D. Morrical, D.P. Fergenson, T. Dienes, M.E. Galli, R.J. Johnson, G.R. Cass, and K. A. Prather, Direct observation of heterogeneous chemistry in the atmosphere, *Science*, 279, 1184-1186, 1998.
- Gerlach, T.M., H.R. Westrich, T.J. Casadevall, and D.L. Finnegan, Vapor saturation and accumulation in magmas of the 1989-1990 eruption of Redoubt Volcano, Alaska, *Journal of Volcanology and Geothermal Research*, 62, 317-337, 1994.
- Germani, M.S. and P.R. Buseck, Evaluation of automated scanning electron microscopy for atmospheric particle analysis, *Analytical Chemistry*, 63, 2232-2237, 1991.



- Gillett, N.P., M.R. Allen, R.E. McDonald, C.A. Senior, D.T. Shindell, and G.A. Schmidt, How linear is the Arctic Oscillation response to greenhouse gases? *Journal of Geophysical Research*, 107, 10.1029/2001JD000589, 2002.
- Gillett, N.P., A.J. Weaver, F.W. Zwiers, and M.D. Flannigan, Detecting the effect of climate change on Canadian forest fires, *Geophysical Research Letters*, 31, L18211, doi: 10.1029/2004GL020876, 2004.
- Gonzalez-Ferran, O., *Volcanes de Chile*, Instituto Geografica Militar, Santiago, Chile, 1995.
- Gonzalez, M. B., J.R. Ramirez, and C. Navarro, Summary of the historical eruptive activity of Volcán de Colima, Mexico, 1519-2000, *Journal of Volcanology and Geothermal Research*, 117, 21-26, 2002.
- Goto-Azuma, K., S. Kohshima, T. Kameda, S. Takahashi, O. Watanbe, Y. Fujii, and J. O. Hagen, An ice-core chemistry record from Snofjellaafonna, northwestern Spitsbergen, *Annals of Glaciology*, 21, 213- 218, 1995.
- Goto-Azuma, K., R.M. Koerner, M. Nakawo, and A. Kudo, Snow chemistry of Agassiz Ice Cap, Ellesmere Island, Canada, *Journal of Glaciology*, 43, 199-206, 1997.
- Goto-Azuma, K., and R.M. Koerner, Ice core studies of anthropogenic sulfate and nitrate trends in the Arctic, *Journal of Geophysical Research*, 106, 4959- 4969, 2001.
- Goto-Azuma, K., T. Shiraiwa, S. Matoba, T. Segawa, S. Kanamori, Y. Fujii, and T. Yamasaki, An overview of the Japanese glaciological studies on Mt. Logan, Yukon, Canada in 2002, *Bulletin of Glaciological Research*, 20, 65-72, 2003.
- Graf, H.F., J. Feichter, and B. Langmann, Volcanic sulfur emissions: Estimates of source strength and its contribution to the global sulfate distribution, *Journal of Geophysical Research*, 102, 10,727-10,738, 1997.
- Gregor, D.J., A.J. Peters, C. Teixeira, N. Jones, and C. Spencer, The historical residue trend of PCBs in the Agassiz Ice Cap, Ellesmere Island, Canada, *Science of the Total Environment*, 160/161, 117-126, 1995
- Griggs, R.F., *The Valley of Ten Thousand Smokes (Alaska)*, National Geographic Society, Washington, D.C., 340 pp, 1922.
- Groisman, P.Y., Possible regional climate consequences of the Pinatubo eruption, *Geophysical Research Letters*, 19, 1603-1606, 1992.
- Groisman, P.Y., B. Sun, R.S. Vose, J.H. Lawrimore, P.H. Whitfield, E. Forland, I. Hanssen-Bauer, M.C. Serreze, V.N. Razuvaev, and G.V. Alekseev, Contemporary changes in high latitudes of the northern hemisphere: daily time resolution, in *Proceedings of the 14<sup>th</sup> AMS Symposium of on Global Change and Climate Variations*, 10pp., 2003.
- Gronvold, K., N. Oskarsson, S. Johnsen, H.B. Clausen, C.U. Hammer, G. Bond, and E. Bard, Ash layers from Iceland in the Greenland GRIP ice core correlated with oceanic and land sediments, *Earth and Planetary Science Letters*, 135, 149-155, 1995.

- Grumet, N., C.P. Wake, P.A. Mayewski, G.A. Zielinski, S.I. Whitlow, R.M. Koerner, D.A. Fisher, and J.M. Woollett, Variability of sea-ice extent in Baffin Bay over the last millennium, *Climatic Change*, 49, 129- 145, 2001.
- Hallett, D.J., R.W. Mathewes, and R.C. Walker, A 1000-year record of forest fires, drought, and lake-level change in southeastern British Columbia, Canada, *The Holocene*, 13, 751-761, 2003.
- Hameed, S. and I. Pittalwala, The North Pacific Oscillation: Observations compared with simulations in a general circulation model, *Climate Dynamics*, 6, 113-122, 1991.
- Hammer, C.U., Past volcanism revealed by Greenland ice sheet impurities, *Nature*, 270, 482-486, 1977.
- Hammer, C.U., H.B. Clausen, and W. Dansgaard, Greenland ice sheet evidence of postglacial volcanism and its climatic impact, *Nature*, 288, 230- 235, 1980.
- Hammer, C.U., Traces of Icelandic eruptions in the Greenland ice sheet, *Jokull*, 34, 51- 65, 1984.
- Hammer, C.U., P.A. Mayewski, D. Peel, and M. Stuiver, Greenland Summit ice cores; Greenland Ice Sheet Project 2 (GISP2); Greenland Ice Core Program (GRIP), *Journal of Geophysical Research*, 102, 26,315-26,886, 1997.
- Hansen, B., W.R. Turrell, and S. Osterhus, Decreasing overflow from the Nordic seas into the Atlantic Ocean through the Faroe Bank Channel since 1950, *Nature*, 411, 927- 930, 2001.
- Harrington, C. R., *The Year Without a Summer? World Climate in 1816*, 576 pp., Canadian Museum of Nature, Ottawa, 1992.
- Henning, S., E. Weingartner, M. Schwikowski, H.W. Gaggeler, R. Gehrig, K.P. Hinz, A. Trimborn, B. Spengler, and U. Baltensperger, Seasonal variation of water-soluble ions of the aerosol at the high alpine site Jungfraujoch (3580 m asl), *Journal of Geophysical Research*, 108, 4030, doi:10.1029/2002JD002439, 2003.
- Herron, M.M., Impurity sources of F<sup>-</sup>, Cl<sup>-</sup>, NO<sub>3</sub><sup>-</sup>, and SO<sub>4</sub><sup>2-</sup> in Greenland and Antarctic precipitation, *Journal of Geophysical Research*, 87, 3052- 3060, 1982.
- Hess, J.C., C.A. Scott, G.L. Hufford, and M.D. Fleming, El Nino and its impact of fire weather conditions in Alaska. *International Journal of Wildland Fire*, 10, 1-13, 2001.
- Heyerdahl, E.K., L.B. Brubaker, and J.K. Agee, Annual and decadal climate forcing of historical fire regimes in the interior Pacific Northwest, USA, *The Holocene*, 12, 597-604, 2002.
- Hildreth, W., New perspectives on the eruption of 1912 Valley of Ten Thousand Smokes, Katmai National Park, Alaska, *Bulletin of Volcanology*, 49, 680- 693, 1987.
- Hildreth, W., and J. Fierstein, Katmai volcanic cluster and the great eruption of 1912, *Geological Society of America Bulletin*, 112, 1594-1620, 2000.

- Hildreth, W., J. Fierstein, M. Lanphere, and D.F. Siems, Trident Volcano: Four contiguous stratocones adjacent to Katmai Pass, Alaska Peninsula, U.S. *Geological Survey Professional Paper*, 1678, 2003.
- Hind, W.C., *Aerosol Technology*, John Wiley, New York, 1999.
- Holdsworth, G., M. Pourchet, F.A. Prantl, and D.P. Meyerhof, Radioactivity levels in a firn core from the Yukon, Canada, *Atmospheric Environment*, 18, 461- 466, 1984.
- Holdsworth, G. and E. Peake, Acid content of snow at a mid- troposphere sampling site on Mt. Logan, Yukon, Canada, *Annals of Glaciology*, 7, 153- 159, 1985.
- Holdsworth, G., H.R. Krouse, and E. Peake, Trace acid content of shallow snow and ice cores from mountain sites in western Canada, *Annals of Glaciology*, 13, 57- 62, 1988.
- Holdsworth, G., H.R. Krouse, M. Nosal, M.J. Spencer, and P.A. Mayewski, Analysis of a 290-year net accumulation time series from Mt. Logan, Yukon, *IAHS Publication 183*, 71-79, 1989.
- Holdsworth, G., S. Fogarasi, and H.R. Krouse, Variation of the stable isotopes of water with altitude in the Saint Elias mountains of Canada, *Journal of Geophysical Research*, 96, 7483-7494, 1991.
- Holdsworth, G., H.R. Krouse, and M. Nosal, Ice core climate signals from Mount Logan, Yukon AD 1700-1987, in *Climate Since AD 1500*, edited by R.S. Bradley and P.D. Jones, pp. 483-504, Routledge, New York, 1992.
- Holdsworth, G., K. Higuchi, G.A. Zielinski, P.A. Mayewski, M. Wahlen, B. Deck, P. Chylek, B. Johnson, and P. Damaino, Historical biomass burning: late 19<sup>th</sup> century pioneer agriculture revolution in northern hemisphere ice core data and its atmospheric interpretation, *Journal of Geophysical Research*, 101, 23,317- 23,334, 1996.
- Holdsworth, G., and H.R. Krouse, Altitudinal variation of the stable isotopes of snow in regions of high relief, *Journal of Glaciology*, 48, 31-41, 2002.
- Houghton, J.T., G.J. Jenkins, and J.J. Ephraums, editors, *Climate Change; the IPCC scientific assessment*, 365 pp., 1990.
- Hu, F.S., E. Ito, T.A. Brown, B.B. Curry, and D.R. Engstrom, Pronounced climatic variations in Alaska during the last two millennia, *Proceedings of the National Academy of Sciences* 98, 10,552-10,556, 2001.
- Hughes, M. K., and H.F. Diaz, Was there a 'Medieval Warm Period', and of so, where and when? *Climatic Change*, 26, 109-142, 1994.
- Hunt, J.B., and P.G. Hill, Tephra geochemistry: a discussion of some persistent analytical problems, *The Holocene*, 3, 271-278, 1993.
- Huntington, H., and G. Weller, editors, *Impacts of a Warming Arctic: the Arctic Climate Impact Assessment*, Cambridge University Press, 2005.

- Hurrell, J.W., and H. van Loon, Decadal variations in climate associated with the North Atlantic Oscillation, *Climatic Change*, 36, 301-326, 1997.
- Ingrin, J., and J.P. Poirier, Transmission electron microscopy of ejects from the XVIIIth century eruption of the Soufrière, Guadeloupe; microscopic evidence for magma mixing, *Journal of Volcanology and Geothermal Research*, 28, 161-174, 1986.
- Ivanov, B.V., V.I. Gorelchik, V.N. Andreev, A.M. Maksimov, V.V. Stepanov, and A.M. Chrikov, The 1972-1974 eruption of Kliuchevskoi Volcano, Kamchatka, *Bulletin of Volcanology*, 44, 1-10, 1981.
- Jacoby, G.C. and R. D'Arrigo, Tree ring width and density evidence of climatic and potential forest change in Alaska, *Global Biogeochemical Cycles*, 9, 227-234, 1995.
- Jacoby, G.C., D'Arrigo, and B. Luckman, Millennial and near-millennial scale dendroclimatic studies in northern North America, in *Climatic Variations and Forcing Mechanisms of the last 2000 years*, NATO ASI Series, Vol. 141, edited by P.D. Jones, R.S. Bradley, and J. Jouzel, pp. 67-84, Springer-Verlag, Berlin, 1996.
- Jacoby, G.C., K.W. Workman, and R.D. D'Arrigo, Laki eruption of 1783, tree rings, and disaster for northwest Alaska Inuit, *Quaternary Science Reviews*, 18, 1365-1371, 1999.
- Jaenicke, R., Physical aspects of the atmospheric aerosol, in *Aerosols and Their Climatic Effects*, edited by H.E. Gerber and A. Deepack, pp. 7-34, Deepack, Hampton, 1984.
- Jaffe, D.A., B. Cerundolo, and J. Kelley, The influence of Redoubt Volcano emissions on snow chemistry, *Journal of Volcanology and Geothermal Research*, 62, 359-367, 1994.
- Jaffrezo, J.L., and C.I. Davidson, The Dye 3 Gas and Aerosol Sampling Program: an overview, *Atmospheric Environment*, 27A, 2703-2707, 1993.
- Jaffrezo, J.L., J.E. Dibb, R. C. Bales, and A. Neftel, Current status of atmospheric studies at Summit (Greenland) and implications for future research, in *Ice Core Studies of Global Biogeochemical Cycles*, NATO ASI Series 1, vol. 30, edited by R.J. Delmas, pp. 427-458, Springer-Verlag, New York, 1995.
- Jensen, J., K. Adare, and R. Shearer, *Canadian Arctic Contaminants Assessment Report*, Department of Indian and Northern Affairs, Ottawa, 1997.
- Jones, P.D., K.R. Briffa, and F.H. Schweingruber, Tree-ring evidence of the widespread effects of explosive volcanic eruptions, *Geophysical Research Letters*, 22, 1333-1336, 1995.
- Jones, P. D., T.J. Osborn, and K.R. Briffa, The evolution of climate over the last millennium. *Science*, 292, 662-667, 2001.
- Jones, P.D., A. Morberg, T.J. Osborn, and K.R. Briffa, Surface climate response to explosive volcanic eruptions seen in long European temperature records and mid-to-high latitude tree-ring density around the Northern Hemisphere, in *Volcanism and the Earth's Atmosphere*, *Geophysical Monograph Series*, 139, edited by A. Robock, and C. Oppenheimer, pp. 239-254, American Geophysical Union, Washington, D.C., 2004.

- Jordan, C.E., J.E. Dibb, B.E. Anderson, and H.E. Fuelberg, Uptake of nitrate and sulfate on dust aerosols during TRACE-P, *Journal of Geophysical Research*, 108, 8817, doi: 10.1029/2002JD003101, 2003.
- Juhle, W., and H.W. Coulter, The Mount Spurr eruption, July 9, 1953, *Eos, Transactions, American Geophysical Union*, 36, 199-202, 1955.
- Kang, S., P.A. Mayewski, Y. Yan, D. Qin, T. Yao, and J. Ren, Dust records from three ice cores: relationships to spring atmospheric circulation over the Northern Hemisphere, *Atmospheric Environment*, 37, 4823-4835, 2003.
- Kanamori, S., T. Shiraiwa, K. Goto-Azuma, C.S. Benson, and R. Naruse, Seasonal variations in density profiles and densification process at Mts. Logan and Wrangell, *Eos Transactions, American Geophysical Union*, 85 (47), Fall Meeting Supplement, Abstract PP21A- 1367, 2004.
- Kasischke, E.S., D. Williams, and D. Barry, Analysis of the patterns of large fires in the boreal forest region of Alaska, *International Journal of Wildland Fire*, 11, 131-144, 2002.
- Kasischke, E.S., E. Hyer, P. Novelli, L.P. Bruhwiler, N.H.F. French, A.I. Sukhinin, J.H. Hewson, and B.J. Stocks, Influences of boreal fire emissions on Northern Hemisphere atmospheric carbon dioxide and carbon monoxide, *Global Biogeochemical Cycles*, 19, GB1012, doi: 10.1029/2004GB002300, 2005.
- Keen, R.A., Volcanic aerosols and lunar eclipses, *Science*, 222, 1011-1013, 1983.
- Keenan, D.J., Volcanic ash retrieved from the GRIP ice core is not from Thera, *Geochemistry Geophysics Geosystems*, 4, 1097, doi: 10.1029/2003GC000608, 2003.
- Keene, W.C., A.P. Pszenny, J.N. Galloway, and M.E. Hawley, Sea-salt corrections and interpretation of constituent ratios in marine precipitation, *Journal of Geophysical Research*, 91, 6647- 6658, 1986.
- Kelly, P.M., P.D. Jones, and J. Pengqun, The spatial response of the climate system to explosive volcanic eruptions, *International Journal of Climatology*, 16, 537-550, 1996.
- Kirchner, I., G.L. Stenchikov, H.F. Graf, A. Robock, and J.C. Antuna, Climate model simulation of winter warming and summer cooling following the 1991 Mount Pinatubo volcanic eruption, *Journal of Geophysical Research*, 104, 19,039-19,055, 1999.
- Koerner, R.M., and D.A. Fisher, Acid snow in the Canadian high Arctic, *Nature*, 295, 137- 140, 1982.
- Koerner, R.M., and L. Lundgaard, Glaciers and global warming, *Geographie physique et Quaternaire*, 49, 429-434, 1995.
- Koerner, R.M., D.A. Fisher, and K. Goto-Azuma, A 100 year record of ion chemistry from Agassiz Ice Cap, northern Ellesmere Island, NWT, Canada, *Atmospheric Environment*, 33, 347- 357, 1999.

- Kohno, M., and Y. Fujii, Past 220-year bipolar volcanic signals: remarks on common features of their source eruptions, *Annals of Glaciology*, 35, 217-223, 2002.
- Korovin, G.N., Analysis of the distribution of forest fires in Russia, in *Fire in Ecosystems of Boreal Eurasia*, edited by J.G. Goldammer and V.V. Furyaev, pp. 112-118, Kluwer Academic Publishers, Dordrecht, The Netherlands, 1996.
- Kotlyakov, V.M., S.M. Arkipov, K.A. Anderson, and O.V. Nagornov, Deep drilling of glaciers in the Eurasian Arctic as a source of paleoclimate records, *Quaternary Science Reviews*, 23, 1371-1390, 2004.
- Krueger, A. J., L.S. Walter, P.K. Bhartia, C.C. Schnetzler, N.A. Krotkov, I. Sprod, and G.J.S. Bluth, Volcanic sulfur dioxide measurements from the total ozone mapping spectrometer, *Journal of Geophysical Research*, 100, 14057-17076, 1995.
- Krueger, A.J., C.C. Schnetzler, and L.S. Walter, The December 1981 eruption of Nyamuragira Volcano (Zaire), and the origin of the "mystery cloud" of early 1982, *Journal of Geophysical Research*, 101, 15,191-15,196, 1996.
- Kreutz, K.J., P.A. Mayewski, L.D. Meeker, M.S. Twickler, S.I. Whitlow, and I.I. Pittalwala, Bipolar changes in atmospheric circulation during the Little Ice Age, *Science*, 277, 1294-1296, 1997.
- Kreutz, K.J., P.A. Mayewski, M.S. Twickler, S.I. Whitlow, J.W.C. White, C.A. Shuman, C.F. Raymond, H. Conway, and J.R. McConnell, Seasonal variations of glaciochemical, isotopic, and stratigraphic properties in Siple Dome (Antarctica) surface snow, *Annals of Glaciology*, 29, 38-44, 1999.
- Kreutz, K.J., P.A. Mayewski, L.D. Meeker, M.S. Twickler, and S.I. Whitlow, The effect of spatial and temporal accumulation rate variability in West Antarctica on soluble ion deposition, *Geophysical Research Letters*, 27, 2517-2520, 2000.
- Lacis, A., J. Hansen, and M. Sato, Climate forcing by stratospheric aerosols, *Geophysical Research Letters*, 19, 1607-1610, 1992.
- Laj, P., S. Drummey, M. Spencer, J.M. Palais, and H. Sigurdsson, Depletion of H<sub>2</sub>O<sub>2</sub> in a Greenland ice core: implications for oxidation of volcanic SO<sub>2</sub>, *Nature*, 346, 45-48, 1990.
- LaMarche, V.C., and K.K. Hirschboeck, Frost rings in trees as records of major volcanic eruptions, *Nature*, 307, 121-126, 1984.
- Lamb, H., Volcanic dust in the atmosphere with a chronology and assessment of its meteorological significance, *Philosophical Transactions of the Royal Society of London*, 266, 425- 533, 1970.
- Langway, C.C., K. Osada, H.B. Clausen, C.U. Hammer, and H. Shoji, A 10-century comparison of prominent bipolar volcanic events in ice cores, *Journal of Geophysical Research*, 100, 16,241- 16,247, 1995.
- Larsen, C.P.S., Spatial and temporal variations in boreal forest fire frequency in northern Alberta, *Journal of Biogeography*, 24, 663-673, 1997.

- Larsen, G., A. Dugmore, and A. Newton, Geochemistry of historical age silicic tephra in Iceland, *The Holocene*, 9, 463-471, 1999.
- Leathers, D. J., B. Yarnal and M.A. Palecki, The Pacific/North American teleconnection pattern and United States climate. Part I: Regional temperature and precipitation associations, *Journal of Climate*, 4, 517-528, 1991.
- LeBas, M.J., R.W. Maitre, A. Strickeisen, and B. Zanettin, A chemical classification of volcanic rocks based on the total alkali-silica diagram, *Journal of Petrology*, 27, 745-750, 1986.
- Lefer, B.L., R.W. Talbot, R.C. Harriss, J.D. Bradshaw, S.T. Sandholm, J.O. Olson, G.W. Sachse, J. Collins, M.A. Shipman, D.R. Blake, K.I. Klemm, K. Gorzelska, and J. Barrick, Enhancement of acidic gases in biomass-burning impacted air masses over Canada, *Journal of Geophysical Research*, 99, 1721-1737, 1994.
- Legrand, M., and R. J. Delmas, A 220 year continuous record of volcanic H<sub>2</sub>SO<sub>4</sub> in the Antarctic ice sheet, *Nature*, 327, 671- 676, 1987.
- Legrand, M.R., and R.J. Delmas, Formation of HCl in the Antarctic atmosphere, *Journal of Geophysical Research*, 93, 7153-7168, 1988.
- Legrand, M.R., and S. Kirchner, Origins and variations of nitrate in south polar precipitation, *Journal of Geophysical Research*, 95, 3493-3507, 1990.
- Legrand M., M. De Angelis, T. Staffelbach, Z. Neftel, and B. Stauffer, Large perturbations of ammonia and organic acids content in the Summit- Greenland ice core: fingerprint from forest fires?, *Geophysical Research Letters*, 19, 473-475, 1992.
- Legrand, M., and M. De Angelis, Light carboxylic acids in Greenland ice: a record of past forest fires and vegetative emissions from the boreal zone, *Journal of Geophysical Research*, 101, 4129-4145, 1996.
- Legrand, M., and P.A. Mayewski, Glaciochemistry of polar ice cores: a review, *Reviews of Geophysics*, 35, 219- 243, 1997.
- Levine, J.S., editor, *Global Biomass Burning: Atmospheric, Climatic, and Biospheric Implications*, MIT Press, Cambridge, Mass., 1991.
- Luckman, B.H., Developing a proxy climate record for the last 300 years in the Canadian Rockies - some problems and opportunities, *Climatic Change*, 36, 455-476, 1997.
- Luckman, B.H., K.R. Briffa, P.D. Jones, and F.H. Schweingruber, Tree-ring based reconstruction of summer temperatures at the Columbia Icefield, Alberta, Canada, A.D. 1073-1983, *The Holocene*, 7, 375-389, 1997.
- Lugauer, M., U. Baltensperger, M. Furger, H.W. Gaggeler, D.T. Jost, M. Schwikowski, and H. Wanner, Aerosol transport to the high Alpine sites Jungfraujoch (3454 m asl) and Colle Gnifetti (4452 m asl), *Tellus*, 50B, 76-92, 1998.

- Luhr, J.E., and W.G. Melson, Mineral and glass compositions in June 15, 1991, pumices: Evidence for dynamic disequilibria in the dacite of Mount Pinatubo, in *Fire and Mud: Eruptions and Lahars of Mount Pinatubo, Philippines*, edited by C.G. Newhall and R.S. Punongbayan, pp. 733-750, U.S. Geological Survey, Seattle, 1996.
- Luhr, J.F., Petrology and geochemistry of the 1991 and 1998-1999 lava flows from Volcán de Colima, Mexico: implications for the end of the current eruptive cycle, *Journal of Volcanology and Geothermal Research*, 117, 169-194, 2002.
- Lynch, J.A., J.S. Clark, N.H. Bigelow, M.E. Edwards, and B.P. Finney, Geographic and temporal variations in fire history in boreal ecosystems of Alaska, *Journal of Geophysical Research*, 107, 8152, doi: 10.1029/2001JD000332, 2003.
- Lynch, J.A., J.L. Hollis, and F.S. Hu, Climatic and landscape controls of the boreal forest fire regime: Holocene records from Alaska, *Journal of Ecology*, 92, 477-489, 2004.
- Lyons, W.B., P.A. Mayewski, M.J. Spencer, and M.S. Twickler, A northern hemisphere volcanic chemistry record (1869-1984) and climatic implications using a south Greenland ice core, *Annals of Glaciology*, 14, 176- 182, 1990.
- Machida, T., T. Nakazawa, Y. Fujii, S. Aoke, and O. Watanabe, Increase in atmospheric nitrous oxide concentrations during the last 250 years, *Geophysical Research Letters*, 22, 2921-2924, 1995.
- Manabe, S., R.J. Stouffer, M.J. Spelman, and K. Bryan, Transient response of a coupled ocean-atmosphere model to gradual changes of atmospheric CO<sub>2</sub>. Part I: Annual mean response, *Journal of Climate*, 4, 785- 818, 1991.
- Mann, M. E., R.S. Bradley, and M.K. Hughes, Northern Hemisphere temperatures during the past millennium: inferences, uncertainties, and limitations, *Geophysical Research Letters*, 26, 759-762, 1999.
- Mantua, N.J., S.R. Hare, Y. Zhang, and J.M. Wallace, A Pacific interdecadal climate oscillation with impact on salmon production, *Bulletin of the American Meteorological Society*, 78, 1069-1079, 1997.
- Mashiotta, T.A., L.G. Thompson, and M.E. Davis, The White River Ash: New evidence from the Bona-Churchill ice core record, *Eos Transactions, American Geophysical Union*, 85 (47), Fall Meeting Supplement, Abstract PP21A-1369, 2004.
- Mass, C.F., and D.A. Portman, Major volcanic eruptions and climate: A critical evaluation, *Journal of Climate*, 2, 566-593, 1989.
- Matthews, A., *The Night of Purnama*, 200 pp., Jonathan Cape, London, 1965.
- Mayewski, P.A., W.B. Lyons, M.J. Spencer, M. Twickler, W. Dansgaard, B. Koci, C.I. Davidson, and R.E. Hornrath, Sulfate and nitrate concentrations from a south Greenland ice core, *Science*, 232, 975- 977, 1986.
- Mayewski, P.A., M.J. Spencer, M.S. Twickler, and S. Whitlow, A glaciochemical survey of the Summit region, Greenland, *Annals of Glaciology*, 14, 186-190, 1990.



- Mayewski, P.A., W.B. Lyons, M.J. Spencer, C.F. Buck, and S. Whitlow, An ice-core record of atmospheric response to anthropogenic sulfate and nitrate, *Nature*, 346, 554- 556, 1990.
- Mayewski P.A., L.D. Meeker, M.C. Morrison, M.S. Twickler, S. Whitlow, K.K. Ferland, D.A. Meese, M.R. Legrand, and J.P. Steffensen, Greenland ice core "signal" characteristics: an expanded view of climate change, *Journal of Geophysical Research*, 98, 12,839- 12,847, 1993a
- Mayewski, P.A., L.D. Meeker, S. Whitlow, M.S. Twickler, M.C. Morrison, R.B. Alley, P. Bloomfield, and K. Taylor, The atmosphere during the Younger Dryas, *Science*, 261, 195- 197, 1993b.
- Mayewski, P.A., G. Holdsworth, M.J. Spencer, S. Whitlow, M. Twickler, M.C. Morrison, K.K. Ferland, and L.D. Meeker, Ice-core sulfate from three northern hemisphere sites: origin and temperature forcing implications, *Atmospheric Environment*, 27A, 2915- 2919, 1993c.
- Mayewski, P.A., L.D. Meeker, S. Whitlow, M.S. Twickler, M.C. Morrison, P.M. Grootes, G.C. Bond, R.B. Alley, D.A. Meese, and T. Gow, Changes in atmospheric circulation and ocean ice cover over the North Atlantic region over the last 41,000 years, *Science*, 263, 1747- 1751, 1994.
- McCormick, P.M., P.H. Wang, and L.R. Poole, Stratospheric aerosols and clouds, in *Aerosol-Cloud-Climate Interactions*, edited by P. V. Hobbs, pp. 205- 220, Academic, San Diego, Calif., 1993.
- Meeker, L.D., P.A. Mayewski, and P. Bloomfield, A new approach to glaciochemical time series analysis, in *Ice Core Studies of Global Biogeochemical Cycles, NATO ASI Series, Vol I 30*, edited by R. J. Delmas, pp. 384- 400, Springer-Verlag, Berlin, 1995.
- Meeker, L.D., P.A. Mayewski, M.S. Twickler, S.I. Whitlow, and D.A. Meese, A 110,000 year history of change in continental biogenic emissions and related atmospheric circulation inferred from the Greenland Ice Sheet Project 2 ice core, *Journal of Geophysical Research*, 102, 26489-26505, 1997.
- Melekestsev, I.V., O.A. Braitseva, V.V. Ponomareva, and L.D. Sulerzhitskiy, Holocene catastrophic caldera-forming eruptions of Ksudach Volcano, Kamchatka, *Volcanology and Seismology*, 17, 395-422, 1996.
- Miklius, A., M.J.F. Flower, J.P.P. Huijsmans, S.M. Mukasa, and P. Castillo, Geochemistry of lavas from Taal Volcano, Southwestern Luzon, Philippines: evidence for multiple magma supply systems and mantle source heterogeneity, *Journal of Petrology*, 32, 593-627, 1991.
- Miller, T.P., R.G. McGimsey, D.H. Richter, J.R. Riehle, C.J. Nye, M.E. Yount, and J.A. Dumoulin, *Catalog of the Historically Active Volcanoes of Alaska*, U.S. Geological Survey Open-File Report 98-582, 104 pp, 1998.
- Miyashiro, A., Volcanic rock series in island arcs and active continental margins, *American Journal of Science*, 274, 321-355, 1974.

- Monaghan, M.C. and G. Holdsworth, The origin of non-sea-salt sulfate in the Mt. Logan ice core, *Nature*, 343, 245- 248, 1990.
- Monzier, M., C. Robin, and J. Eissen, Kuwae: the forgotten caldera, *Journal of Volcanology and Geothermal Research*, 59, 207-218, 1994.
- Moore, J.C., H. Narita, and N. Maeno, A continuous 770-year record of volcanic activity from East Antarctica, *Journal of Geophysical Research*, 98, 17,353- 17,359, 1991.
- Moore, G., G. Holdsworth, and K. Alverson, Extra-tropical response to ENSO 1736-1985 as expressed in an ice core from the St. Elias mountain range in northwestern North America, *Geophysical Research Letters*, 28, 3457-3460, 2001.
- Moore, G.W.K., G. Holdsworth, and K. Alverson, Climate change in the North Pacific over the past three centuries, *Nature*, 240, 401-403, 2002.
- Moritz, R.E., C.M. Bitz, and E.J. Steig, Dynamics of recent climate change in the Arctic, *Science*, 297, 1497-1501, 2002.
- Morrice, M.G., P.A. Jezek, J.B. Gill, D.J. Whitford, and M. Monoarfa, An introduction to the Sangihe Arc: Volcanism accompanying arc-arc collision in the Molucca Sea, Indonesia, *Journal of Volcanology and Geothermal Research*, 19, 135-165, 1983.
- Mosley-Thompson, E., J.R. McConnell, R.C. Bales, Z. Li, P.N. Lin, K. Steffen, L.G. Thompson, R. Edwards, and D. Bathke, Local to regional-scale variability of annual net accumulation on the Greenland ice sheet from PARCA cores, *Journal of Geophysical Research*, 106, 33,839-33,851, 2001.
- Mosley-Thompson, E., T.A. Mashiotta, and L. Thompson, High-resolution ice core records of late Holocene volcanism: current and future contributions from the Greenland PARCA cores, in *Volcanism and the Earth's Atmosphere, Geophysical Monograph Series, vol. 139*, edited by A. Robock, and C. Oppenheimer, pp. 153-164, American Geophysical Union, Washington, D.C., 2003.
- Muller, E.H., W. Juhle, and H.W. Coulter, Current volcanic activity in Katmai National Monument, *Science*, 119, 319-321, 1954.
- Murphy, A., *A glaciochemical record from the Devon Ice Cap and late Holocene reconstruction of past sea-ice extent in the North Water Polynya, eastern Canadian Arctic*, M.S. thesis, University of New Hampshire, Durham, 2000.
- Neftel, A., J. Beer, H. Oeschger, F. Zurcher, and R.C. Finkel, Sulphate and nitrate concentrations in snow from South Greenland 1895- 1978, *Nature*, 314, 611- 613, 1985.
- Nelson, F.E., Geocryology: (Un) frozen in time, *Science*, 299, 1673-1675, 2003.
- Neumann van Padang, M., Changes in the top of Mount Ruang (Indonesia), *Geologie en Mijnbouw*, 21, 113-118, 1959.

- Newhall, C.G., and S. Self, The volcanic explosivity index (VEI): an estimate of explosive magnitude for historical volcanism, *Journal of Geophysical Research*, 87, 1231- 1238, 1982.
- O'Brien, S.R., P.A. Mayewski, L.D. Meeker, D.A. Meese, M.S. Twickler, and S.I. Whitlow, Complexity of Holocene climate as reconstructed from a Greenland ice core, *Science*, 270, 1962-1964, 1995.
- Olivier, S., M. Schwikowski, S. Brutsch, S. Eyrikh, H.W. Gaggeler, M. Luthi, T. Papina, M. Saurer, U. Schotterer, L. Tobler, and E. Vogel, Glaciochemical investigation of an ice core from Belukha Glacier, Siberian Altai, *Geophysical Research Letters*, 30, 2019, doi:10.1029/2003GL018290, 2003.
- Oppenheimer, C., Ice core and paleoclimate evidence for the timing and nature of the great mid-thirteenth century volcanic eruption, *International Journal of Climatology*, 23, 417-426, 2003.
- Palais, J. and H. Sigurdsson, Petrologic evidence of volatile emissions from major historic and prehistoric volcanic eruptions, in *Understanding Climate Change, American Geophysical Union, Geophysical Monograph*, 52, edited by A. Berger, pp. 31- 53, 1989.
- Palais, J.M., S. Kirchner, and R.J. Delmas, Identification of some global volcanic horizons by major element analysis of fine ash in Antarctic ice, *Annals of Glaciology*, 14, 216-220, 1990.
- Palais, J.M. K. Taylor, P.A. Mayewski, and P.M. Grootes, Volcanic ash from the 1362 A.D. Oraefajokull eruption (Iceland) in the Greenland ice sheet, *Geophysical Research Letters*, 18, 1241-1244, 1991.
- Palais, J.M., M.S. Germani, and G.A. Zielinski, Inter-hemispheric transport of volcanic ash from a 1259 A.D. volcanic eruption to the Greenland and Antarctic ice sheets, *Geophysical Research Letters*, 19, 801-804, 1992.
- Palmer, A.S., T.D.S. van Ommen, M.A.J. Curran, V. Morgan, J.M. Souney, and P.A. Mayewski, High precision dating of volcanic events (A.D. 1301-1995) using ice cores from Law Dome, Antarctica, *Journal of Geophysical Research*, 106, 28,089- 28,095, 2001.
- Palmer, A.S., V.I. Morgan, M.A.J. Curran, T.D. Van Ommen, and P.A. Mayewski, Antarctic volcanic flux ratios from Law Dome ice cores, *Annals of Glaciology*, 35, 329-332, 2002.
- Pang, K.D., Climatic impact of the mid-fifteenth century Kuwae Caldera formation, as reconstructed from historical and proxy data, *Eos, Transactions, American Geophysical Union*, 74, 106, 1993.
- Peixoto, J.P., and A.H. Oort, *Physics of Climate*, American Institute of Physics, New York, 1992.
- Penner, J.E., R.E. Dickinson, and C.A. O'Neill, Effects of aerosol from biomass burning on the global radiation budget, *Science*, 256, 1432-1434, 1992.

- Peters, A.J., D.J. Gregor, C.F. Teixeira, N.P. Jones, and C. Spencer, The recent depositional trend of polycyclic aromatic hydrocarbons and elemental hydrocarbons to the Agassiz Ice Cap, Ellesmere Island, Canada, *Science of the Total Environment*, 160/161, 167- 179, 1995.
- Pitkanen, A., and P. Huttunen, A 1300-year forest fire history at a site in eastern Finland based on charcoal and pollen records in laminated lake sediments, *The Holocene*, 9, 311-320, 1999.
- Portman, D.A., and D.S. Gutzler, Explosive volcanic eruptions, the El Nino-Southern Oscillation, and U.S. climate variability, *Journal of Climate*, 9, 17-33, 1996.
- Pyle, D.M., P.D. Beattie, and G.J.S. Bluth, Sulfur emissions to the stratosphere from explosive volcanic eruptions, *Bulletin of Volcanology*, 57, 663-671, 1996.
- Quinn, W.H., A study of Southern Oscillation-related climatic activity for A.D. 622-1990 incorporating Nile River flood data, in *El Nino: Historical and Paleoclimatic Aspects of the Southern Oscillation*, edited by H.F. Diaz and V. Markgraf, pp. 119-149, Cambridge University Press, New York, 1992.
- Raffles, T. S., *The History of Java*, Black, Parbury, and Allen, London, 1817.
- Rahn, K.A., Relative importance of North America and Eurasia as sources of Arctic aerosol, *Atmospheric Environment*, 15, 1447- 1455, 1981a.
- Rahn, K.A., The Mn/V ratio as a tracer of large-scale sources of pollution aerosol for the Arctic, *Atmospheric Environment*, 15, 1457- 1464, 1981b.
- Rampino, M.R., and S. Self, Historic eruptions of Tambora (1815), Krakatau (1883) and Agung (1963), their stratospheric aerosols and climatic impact, *Quaternary Research*, 18, 127-143, 1982.
- Rampino, M.R., and S. Self, Sulfur rich volcanic eruptions and stratospheric aerosols, *Nature*, 310, 677- 679, 1984.
- Richter, D.H., J.G. Smith, M.A. Lanphere, G.B. Dalrymple, B.L. Reed, and N. Shew, Age and progression of volcanism, Wrangell Volcanic Field, Alaska, *Bulletin of Volcanology*, 53, 29-44, 1990.
- Richter, D.H., S.J. Preece, R.G. McGimsey, and J.A. Westgate, Mount Churchill, Alaska, source of the late Holocene White River Ash, *Canadian Journal of Earth Sciences*, 32, 741-748, 1995.
- Riehle, J.R., A reconnaissance of the major Holocene tephra deposits in the upper Cook Inlet region, Alaska, *Journal of Volcanology and Geothermal Research*, 26, 37-74, 1985.
- Rind, D., R. Healy, C. Parkinson, D. Matinson., The role of sea ice in 2 x CO<sub>2</sub> model sensitivity, Part I: The total influence of sea ice thickness and extent, *Journal of Climate*, 8, 449-463, 1995.

- Robertson, A., J. Overpeck, D. Rind, E. Mosley-Thompson, G.A. Zielinski, J. Lean, D. Koch, J., Penner, I. Tegen, and R. Healy, Hypothesized climate forcing time series for the last 500 years, *Journal of Geophysical Research*, 106, 14,783-14,803, 2001.
- Robin, C., M. Monzier, and J.P. Eissen, Formation of the mid-fifteenth century Kuwae caldera (Vanuatu) by an initial hydroclastic and subsequent ignimbritic eruption, *Bulletin of Volcanology*, 56, 170-183, 1994.
- Robock, A., and C. Mass, The Mount St. Helens volcanic eruption of May 18 1980: Large short term surface temperature effects, *Science*, 216, 628-630, 1982.
- Robock, A., and J. Mao, Winter warming from large volcanic eruptions, *Geophysical Research Letters*, 12, 2405- 2408, 1992.
- Robock, A., And J. Mao, The volcanic signal in surface temperature observations, *Journal of Climate*, 8, 1086-1103, 1995.
- Robock, A., and M.P. Free, Ice cores as an index of global volcanism from 1850 to the present, *Journal of Geophysical Research*, 100, 11,549- 11,567, 1995.
- Robock, A., Volcanic eruptions and climate, *Reviews of Geophysics*, 38, 191-219, 2000.
- Robock, A., Blowin' in the wind: Research priorities for climate effects of volcanic eruptions, *EOS, Transactions, American Geophysical Union*, 83, 472, 2002.
- Robock, A., The climatic aftermath, *Science*, 295, 1242-1244, 2002.
- Rogers, J.C., The North Pacific Oscillation, *Journal of Climatology*, 1, 39-57, 1981.
- Rolandi, G., A.M. Barrella, and A. Borrelli, The 1631 eruption of Vesuvius, *Journal of Volcanology and Geothermal Research*, 58, 183-201, 1993.
- Rothrock, D.A., Y. Yu, and G.A. Maykut, Thinning of the Arctic sea-ice cover, *Geophysical Research Letters*, 26, 3469-3472, 1999.
- Rudolph, W.E., Licancabur: mountain of the Atacamenos, *Geography Review*, 45, 151-171, 1955.
- Rupper, S., E.J. Steig, and G. Roe, The relationship between snow accumulation at Mt. Logan Yukon, Canada, and climate variability in the North Pacific, *Journal of Climate* 17, 4724-4739, 2004.
- Sato, M., J.E. Hansen, M.P. McCormick, and J.B. Pollack, Stratospheric aerosol optical depths, 1850-1990, *Journal of Geophysical Research*, 98, 22, 987- 22,994, 1993.
- Savarino, J., and M. Legrand, High northern latitude forest fires and vegetation emissions over the last millennium inferred from the chemistry of a central Greenland ice core, *Journal of Geophysical Research*, 103, 8267-8279, 1998.
- Scaillet, B., J. Luhr, and M.R. Carroll, Petrological and volcanological constraints on volcanic sulfur emissions to the atmosphere, in *Volcanism and the Earth's Atmosphere*,

*Geophysical Monograph Series, vol. 139*, edited by A. Robock and C. Oppenheimer, pp. 11-40, American Geophysical Union, Washington, D.C., 2003.

- Self, S., M.R. Rampino, and J.J. Barbera, The possible effects of large 19<sup>th</sup> and 20<sup>th</sup> century volcanic eruptions on zonal and hemispheric surface temperatures, *Journal of Volcanology and Geothermal Research*, 11, 41- 60, 1981.
- Self, S., M.R. Rampino, and M.J. Carr, A reappraisal of the 1835 eruption of Cosiguina and its atmospheric impact, *Bulletin of Volcanology*, 52, 57- 65, 1989.
- Self, S., and A.J. King, Petrology and sulfur and chlorine emissions of the 1963 eruption of Gunung Agung, Bali, Indonesia, *Bulletin of Volcanology*, 58, 263-285, 1996.
- Self, S., M.R. Rampino, J. Zhao, and M.G. Katz, Volcanic aerosol perturbations and strong El Nino events: No general correlation, *Geophysical Research Letters*, 24, 1247-1250, 1997.
- Seinfeld, J.H., and S.N. Pandis, *Atmospheric Chemistry and Physics: from Air Pollution to Climate Change*, John Wiley, New York, 1998.
- Shapiro, M.A., R.C. Schnell, F.P. Parungo, S.J. Oltmans, and B.A. Bodhaine, El Chichon volcanic debris in an Arctic tropopause fold, *Geophysical Research Letters*, 11, 412- 424, 1984.
- Shiraiwa, T., Y.D. Muravyev, and S. Yamaguchi, Stratigraphic features of firn as proxy climate signals at the summit ice cap of Ushkovsky Volcano, Kamchatka, Russia, *Arctic and Alpine Research*, 29, 414-421, 1997.
- Shiklomanov, I.A., A.I. Shiklomanov, R.B. Lammers, B.J. Peterson, and C.J. Vorismarty, The dynamics of river inflow to the Arctic Ocean, in *The Freshwater Budget of the Arctic Ocean*, edited by E.L. Lewis, E.P. Jones, P. Lemke, T.D. Prowse, and P. Wadhams, pp. 281-296, Kluwer Academic Publishers, 2000.
- Shindell, D.T., R.L. Miller, G.A. Schmidt, and L. Pandolfo, Simulation of recent northern winter climate trends by greenhouse gas forcing, *Nature*, 399, 452-455, 1999.
- Shindell, D.T., G.A. Schmidt, R.L. Miller, and D. Rind, Northern Hemisphere winter climate response to greenhouse gas, ozone, solar, and volcanic forcing, *Journal of Geophysical Research*, 106, 7193-7210, 2001.
- Shindell, D.T., G.A. Schmidt, M.E. Mann, and G. Faluvegi, Dynamic winter climate response to large tropical volcanic eruptions since 1600, *Journal of Geophysical Research*, 109, D05104, doi:10.1029/2003JD004151, 2004.
- Shrestha, A.B., C.P. Wake, and J.E. Dibb, Chemical composition of aerosol and snow in the high Himalaya during the summer monsoon season, *Atmospheric Environment*, 31, 2815-2826, 1997.
- Shrestha, A.B., C.P. Wake, J.E. Dibb, P.A. Mayewski, S.I. Whitlow, G.R. Carmichael, and M. Ferm, Seasonal variations in aerosol concentrations and compositions in the Nepal Himalaya, *Atmospheric Environment*, 34, 3349-3363, 2000.

- Shrestha, A.B., C. P. Wake, J.E. Dibb, and S.I. Whitlow, Aerosol and precipitation chemistry at a remote Himalayan site in Nepal, *Aerosol Science and Technology*, 36, 441-456, 2002.
- Sigurdsson, H., Evidence of volcanic loading of the atmosphere and climate response, *Paleo*, 89, 277- 289, 1990.
- Simkin, T., and L. Siebert, *Volcanoes of the World*, 2<sup>nd</sup> ed., Geoscience, Tucson, AZ, 1994.
- Silvente, E., and M. Legrand, Ammonium to sulfate ratio in aerosol and snow of Greenland and Antarctic regions, *Geophysical Research Letters*, 20, 687-690, 1993.
- Skinner, W.R., B.J. Stocks, D.L. Martell, B. Bonsal, and A. Shabbar, The associated between circulation anomalies in the mid-troposphere and area burned by wildfire in Canada, *Theoretical and Applied Climatology*, 63, 989-105, 1999.
- Skinner, W.R., M.D. Flannigan, B.J. Stocks, B.M. Wotton, J.B. Todd, J.A. Mason, K.A. Logan, and E.M. Bosch, A 500 hPa synoptic wildland fire Climatology for large Canadian forest fires, 195t9-1996, *Theoretical and Applied Climatology*, 63, 89-105, 2002.
- Slater, J.F., J.E. Dibb, B.D. Keim, and J.D. W. Kahl, Relationships between synoptic-scale transport and interannual variability of inorganic cations in surface snow at Summit, Greenland: 1992-96, *Journal of Geophysical Research*, 106, 20,897-20,912, 2001.
- Slater, J.F., and J.E. Dibb, Relationships between surface and column aerosol radiative properties and air mass transport at a rural New England site, *Journal of Geophysical Research*, 109, D01303, doi: 10.1029/2003JD003406, 2004.
- Staudacher, T., P. Bachelery, M. P. Semet, and J. L. Cheminee, Piton de la Fournaise, *Bulletin of the Global Volcanism Network*, 23, 2-4, 1998.
- Stelling, P., J. Beget, C. Nye, J. Gardner, J.D. Devine, and R.M. George, Geology and petrology of ejecta from the 1999 eruption of Shishaldin Volcano, Alaska, *Bulletin of Volcanology*, 64, 548-561, 2002.
- Stenchikov, G., A. Robock, V. Ramaswamy, M.D. Schwarzkopf, K. Hamilton, and S. Ramachandran, Arctic Oscillation response to the 1991 Mount Pinatubo eruption: Effects of volcanic aerosols and ozone depletion, *Journal of Geophysical Research*, 107, 4803, doi: 10.1029/2002JD002090, 2002.
- Stenni, B., R. Caprioli, L. Cimmino, C. Cremisini, O. Flora, R. Gragnani, A. Longinelli, V. Maggi, and S. Torcini, 200 years of isotope and chemical records in a firn core from Hercules Neve, northern Victoria Land, Antarctica, *Annals of Glaciology*, 29, 106-112, 1999.
- Stenni, B., M. Proposito, R. Gragnani, O. Flora, J. Jouzel, S. Falourd, and M. Frezzotti, Eight centuries of volcanic signal and climate change at Talos Dome, East Antarctica, *Journal of Geophysical Research*, 107, 10.1029/2000JD000317, 2002.
- Stocks, B.J., The extent and impact of forest fires in northern circumpolar countries, in *Global Biomass Burning: Atmospheric, Climatic, and Biospheric Implications*, edited by J.S. Levine, pp. 197-202, MIT Press, Cambridge, Mass., 1991.

- Stocks, B.J., M.A. Fosberg, T.J. Lynham, L. Mearns, B.M. Wotton, Q. Yang, J.Z. Jin, K. Lawrence, G.R. Hartley, J.A. Mason, and D.W. McKenney, Climate change and forest fire potential in Russian and Canadian boreal forests, *Climatic Change*, 38, 1-13, 1998.
- Stocks, B.J., J.A. Mason, J.B. Todd, E.M. Bosch, B.M. Wotton, B.D. Amiro, M.D. Flannigan, K.G. Hirsch, K.A. Logan, D.L. Martell, and W.R. Skinner, Large forest fires in Canada, 1959-1997, *Journal of Geophysical Research*, 107, 8149, doi: 10.1029/2001JD000484, 2002.
- Stothers, R.B., The mystery cloud of AD 536, *Nature*, 307,344-345, 1984.
- Stothers, R.B., Major optical depth perturbations to the stratosphere from volcanic eruptions: Pyrheliometric period, 1881-1960, *Journal of Geophysical Research*, 101, 3901-3920, 1996.
- Stothers, R.B., Climatic and demographic consequences of the massive volcanic eruption of 1258, *Climatic Change*, 45, 361-374, 2000.
- Sukhinin, A.I., N.H.F. French, E.S. Kasischke, J.H. Hewson, A.J. Soja, I.A. Csiszar, E. Hyer, T. Loboda, S.G. Conrad, V.I. Romasko, E.A. Pavlichenko, S.I. Miskiv, and O.A. Slinkin, AVHRR-based mapping of fires in eastern Russia: New products for fire management and carbon cycle studies, *Remote Sensing of the Environment*, 93, 546-564, 2004.
- Sun, J., D. Qin, P.A. Mayewski, J.E. Dibb, S. Whitlow, Z. Li, and Q. Yang, Soluble species in aerosol and snow and their relationship at Glacier 1, Tien Shan, China, *Journal of Geophysical Research*, 103, 28,021- 28,028, 1998.
- Sun, J., M. Zhang, and L. Tungsheng, Spatial and temporal characteristics of dust storms in China and its surrounding regions, 1960-1999: Relations to source area and climate, *Journal of Geophysical Research*, 106, 18-055-18,066, 2001.
- Swanson, S.E., C.J. Nye, T.P. Miller, and V.F. Avery, Geochemistry of the 1989-1990 eruption of Redoubt Volcano: Part II. Evidence from mineral and glass chemistry, *Journal of Volcanology and Geothermal Research*, 62, 453-468, 1994.
- Swanson, S.E., M.L. Harbin, and J.R. Riehle, Use of volcanic glass from ash as a monitoring tool: An example from the 1992 eruptions of Crater Peak vent, Mount Spurr volcano, Alaska, in *The 1992 eruptions of Crater Peak vent, Mount Spurr volcano, Alaska*, edited by T. Keith, U.S. Geological Survey Bulletin, 2139, pp. 129-137, 1995.
- Swetnam, T.W., Fire history and climate change in giant sequoia groves, *Science*, 262, 885-889, 1993.
- Talbot, R.W., A.S. Vijgen, and R.C. Harris, Soluble species in the Arctic summer troposphere: acidic gases, aerosols, and precipitation, *Journal of Geophysical Research*, 97, 16531-16544, 1992.
- Taylor, K.C., P.A. Mayewski, M.S. Twickler, and S.I. Whitlow, Biomass burning recorded in the GISP2 ice core: a record from eastern Canada? *The Holocene*, 6, 1-6, 1996.



- Taylor, S.W., and G. Thandi, *Development and Analysis of a Provincial Natural Disturbance Database*, FRBC Final Report, Project PAR02003-19, 22 pp., 2002.
- Taylor- Barge, B, The summer climate of the St. Elias mountain region, *Arctic Institute of North America Research Paper Number 53*, 1969.
- Thompson, D.W.J., and J.M. Wallace, The Arctic Oscillation signature in wintertime geopotential heights and temperature fields, *Geophysical Research Letters*, 25, 1297-1300, 1998.
- Thompson, L.G., E. Mosley- Thompson, V. Zagorodnov, M.E. Davis, T.A. Mashiotta, and P. Lin, 1500 years of annual climate and environmental variability as recorded in Bona-Churchill (Alaska) ice cores, *Eos Transactions, American Geophysical Union*, 85 (47), Fall Meeting Supplement, Abstract PP23C-05, 2004.
- Thorarinsson, S., and L. Saedmundsson, Volcanic activity in historical time, *Jokull*, 29, 29-32, 1979.
- Thorpe, R.S., and P. W. Francis, Variations in Andean andesite compositions and their petrogenic significance, *Tectonophysics*, 57, 53-70, 1979.
- Toom-Sauntry, D., and L.A. Barrie, Chemical composition of snowfall in the high Arctic: 1990-1994, *Atmospheric Environment*, 36, 2683-2693, 2002.
- Turner, S., F. McDermott, C. Hawkesworth, P. Kepezhinskas, A U-Series study of lavas from Kamchatka and the Aleutians: Constraints on source composition and melting processes, *Contributions to Mineralogy and Petrology*, 133, 217-234, 1998.
- Ulbrich, U., and M. Christoph, A shift of the North Atlantic Oscillation and increasing storm track activity over Europe due to anthropogenic greenhouse gas forcing, *Climate Dynamics*, 15, 551- 559, 1999.
- Voight, B., E.K. Constantine, S. Siswoidjyo, and R. Torely, Historical eruptions of Merapi Volcano, Central Java, Indonesia, 1768-1998, *Journal of Volcanology and Geothermal Research*, 100, 69-138, 2000.
- Volz, F.E., Distribution of turbidity after the 1912 Katmai eruption in Alaska, *Journal of Geophysical Research*, 80, 2643- 2648, 1975.
- Volynets, O.N., V.V. Ponomareva, O.A. Braitseva, I.V. Melekestsev, C.H. Chen, Holocene eruptive history of Ksudach volcanic massif, South Kamchatka: evolution of a large magmatic chamber, *Journal of Volcanology and Geothermal Research*, 91, 23-42, 1999.
- Wake, C.P., J.E. Dibb, P.A. Mayewski, L. Zhongquin, and X. Zichu, The chemical composition of aerosols over the eastern Himalayas and Tibetan Plateau during low dust periods, *Atmospheric Environment*, 28, 675-704, 1994.
- Wake, C., Yalcin, K. and Gundestrup, N., The climate signal recorded in the oxygen isotope, accumulation, and major ion time-series from the Eclipse Ice Core, Yukon, *Annals of Glaciology* 35, 416-422, 2002.

- Wake, C.P., P.A. Mayewski, and S. Kang, Climatic interpretation of the gradient in glaciochemical signals across the crest of the Himalaya, in *Earth Paleoenvironments: Records preserved in Mid- and Low-Latitude Glaciers*, edited by L.D. Cecil et al., pp. 81-94, Kluwer Academic Publishers, 2004.
- Wake, C.P., K. Yalcin, and K.J. Kreutz, Signal-to-noise ratios and climate records from the Eclipse Icefield ice cores, *Eos Transactions, American Geophysical Union*, 85 (47), Fall Meeting Supplement, Abstract PP21A-1364, 2004.
- Wallace, J.M., and D.S. Gutzler, Teleconnections in the geopotential height field during the Northern Hemisphere winter, *Monthly Weather Review*, 109, 784-812, 1981.
- Wallace, P.J., Volcanic SO<sub>2</sub> emissions and the abundance and distribution of exsolved gas in magma bodies, *Journal of Volcanology and Geothermal Research*, 108, 85-106, 2001.
- Walsh, J.E., W.L. Chapman, and T.L. Shy, Recent decrease of sea level pressure in the Central Arctic, *Journal of Climate*, 9, 480-488, 1996.
- Weber, M.G., and B.J. Stocks, Forest fires and sustainability in the boreal forests of Canada, *Ambio*, 27, 545-550, 1998.
- White, J.W.C., D. Gorodetzky, E.R. Cook, and L.K. Barlow, Frequency analysis of an annually resolved, 700 year paleoclimate record from the GISP2 ice core, in *Climatic Variations and Forcing Mechanisms of the last 2000 years, NATO ASI Series, Vol. I 41* edited by P.D. Jones, R.S. Bradley, and J. Jouzel, pp. 193-213, Springer Verlag, Berlin.
- Whiteman, D.C., Observations of thermally developed winds systems in mountainous terrain, in *Atmospheric Processes Over Complex Terrain, Meteorological Monographs vol. 23*, edited by W. Blumen, pp. 5-42, American Meteorological Society, Boston, 1990.
- Whitlow, S., P.A. Mayewski, J.E. Dibb, A comparison of major chemical species seasonal concentration and accumulation at the South Pole and Summit, Greenland, *Atmospheric Environment*, 26A, 2045-2054, 1992.
- Whitlow, S., P. Mayewski, J. Dibb, G. Holdsworth, and M. Twickler, An ice-core-based record of biomass burning in the Arctic and Subarctic, 1750-1980, *Tellus*, 46B, 234-242, 1994.
- Wigley, T.M.L., Global-mean temperature and sea level consequences of greenhouse gas concentration stabilization, *Geophysical Research Letters*, 22, 45-48, 1995.
- Wiles, G.C., R. D'Arrigo, and G.C. Jacoby, Temperature changes along the Gulf of Alaska and the Pacific Northwest coast modeled from coastal tree rings, *Canadian Journal of Forestry Research*, 26, 474-481, 1996.
- Wiles, G.C. and Calkin, P.E., Late Holocene, high-resolution glacial chronologies and climate, Kenai Mountains, Alaska, *American Geological Society Bulletin*, 106, 281-303, 1998.
- Wiles, G.C., D.J. Barclay, and P.E. Calkin, Tree-ring-dated 'Little Ice Age' histories of maritime glaciers from Western Prince William Sound, Alaska, *The Holocene*, 9, 163-173, 1999.

- Wiles, G.C., G.C. Jacoby, N.K. Davi, and R.P. McAllister, Late Holocene glacier fluctuations in the Wrangell Mountains, Alaska, *Geological Society of America Bulletin*, 114, 896-908, 2002.
- Wiles, G.C., R.D. D'Arrigo, R. Villalba, P.E. Calkin, and D.J. Barclay, Century-scale solar variability and Alaskan temperature change over the past millennium, *Geophysical Research Letters*, 31, doi: 10.1029/2004GL020050, 2004.
- Williams, H. The great eruption of Cosiguina, Nicaragua, *University of California Publications in Geological Science*, 29, 21-46, 1952.
- Wotton, B.M., and M.D. Flannigan, Length of the fire season in a changing climate, *Forestry Chronicle*, 69, 187-192, 1993.
- Yalcin, K., *Anthropogenic and volcanic signals in an ice core from Eclipse Icefield, Yukon, Canada*, M.S. thesis, University of New Hampshire, Durham, 2001.
- Yalcin, K., and C. Wake, Anthropogenic signals recorded in an ice core from Eclipse Icefield, Yukon, Canada, *Geophysical Research Letters*, 28, 4487-4490, 2001.
- Yalcin, K., C.P. Wake, and M. Germani, A 100-year record of North Pacific volcanism in an ice core from Eclipse Icefield, Yukon, Canada, *Journal of Geophysical Research*, 108, doi: 10.1029/2002JD002449, 2003.
- Yalcin, K., C.P. Wake, K.J. Kreutz, and S.I. Whitlow, Forest fire signals recorded in ice cores from Eclipse Icefield, Yukon, Canada, *Eos Transactions, American Geophysical Union*, 85 (47), Fall Meeting Supplement, Abstract PP23C-06, 2004.
- Yalcin, K., C.P. Wake, K.J. Kreutz, and S.I. Whitlow, Seasonal and spatial variability in snow chemistry at Eclipse Icefield, Yukon, Canada, *Annals of Glaciology*, in review.
- Yalcin, K., C.P. Wake, K.J. Kreutz, M.S. Germani, and S.I. Whitlow, Ice core evidence for a second volcanic eruption around 1809 in the Northern Hemisphere, in preparation.
- Yang, Q., P.A. Mayewski, S. Whitlow, M. Twickler, M. Morrison, R. Talbot, J. Dibb, and E. Linder, Global perspective of nitrate flux in ice cores, *Journal of Geophysical Research*, 100, 5113-5121, 1995.
- Yang, Q, P.A. Mayewski, E. Linder, S. Whitlow, and M. Twickler, Chemical species spatial distribution and relationship to elevation and snow accumulation rate over the Greenland ice sheet, *Journal of Geophysical Research*, 101, 18,629-18,637, 1996.
- Zdanowicz, C.M., G.A. Zielinski, and M.S. Germani, Mount Mazama eruption: Calendrical age verified and atmospheric impact assessed, *Geology*, 27, 621-624, 1999.
- Zdanowicz C., Y. Amelin, I. Girard, G. Hall, J. Percival, J. Vaive, P. Biscaye, and A. Bory, Trans-Pacific transport of Asian desert dust: characterization of fallout in the St. Elias Mountains, Yukon, Canada, *Eos Transactions, American Geophysical Union*, 85(17), Joint Assembly Supplement, Abstract A23C-06, 2004.

- Zen, M. T., and D. Hadikusumo, Preliminary report on the 1963 eruption of Mt. Agung in Bali (Indonesia), *Bulletin of Volcanology*, 27, 269-300, 1964.
- Zheng, J., Ice core testing on the Devon Ice Cap, Poster at CAPE workshop in Iceland, 2000.
- Zielinski, G.A., P.A. Mayewski, L.D. Meeker, S. Whitlow, M.S. Twickler, M. Morrison, D. Meese, R.B. Alley, and A.J. Gow, Record of volcanism since 7000 B.C. from the GISP2 Greenland ice core and implications for the volcano-climate system, *Science*, 264, 948-952, 1994.
- Zielinski, G.A., M.S. Germani, G. Larsen, M. Baille, S. Whitlow, M.S. Twickler, and K. Taylor, Evidence of the Eldgja (Iceland) eruption in the GISP2 Greenland ice core: relationship to eruption processes and climatic conditions in the tenth century, *The Holocene*, 5, 129-140, 1995a.
- Zielinski, G.A., Stratospheric loading and optical depth estimates of explosive volcanism over the last 2100 years derived from the GISP2 Greenland ice core, *Journal of Geophysical Research*, 100, 20,937- 20,955, 1995b.
- Zielinski, G.A., P.A. Mayewski, L.D. Meeker, S. Whitlow, and M. Twickler, A 110,000 year record of explosive volcanism from the GISP2 (Greenland) ice core, *Quaternary Research*, 45, 109-118, 1996.
- Zielinski, G.A., J.E. Dibb, Q. Yang, P.A. Mayewski, S. Whitlow, M.S. Twickler, and M.S. Germani, Assessment of the record of the 1982 El Chichon eruption as preserved in Greenland snow, *Journal of Geophysical Research*, 102, 30,031-30,045, 1997.
- Zielinski, G., Use of paleo-records in determining variability within the volcano- climate system, *Quaternary Science Reviews*, 19, 417-438, 2000.